Development of a framework for the regional vulnerability assessment of RC buildings: an automatic tool based on typological-mechanical modelling and non linear time history

Politecnico di Bari

LIBERATORIA PER L'ARCHIVIAZIONE DELLA TESI DI DOTTORATO

Al Magnifico Rettore
del Politecnico di Bari

Il/la sottoscritto/a CIAMPOLI Pier Luigi nato a Foggia (FG) il 06/01/1987

residente a Foggia (FG) in via M. Bisceglia, 11 e-mail pierluigi.ciampoli@poliba.it

iscritto al 3° anno di Corso di Dottorato di Ricerca in "Rischio e Sviluppo Ambientale, Territoriale e Edilizio" ciclo XXXIII

ed essendo stato ammesso a sostenere l'esame finale con la prevista discussione della tesi dal titolo:

Development of a framework for the regional vulnerability assessment of RC buildings: an automatic tool based on typological-mechanical modelling and non linear time history analyses

DICHIARA

1) di essere consapevole che, ai sensi del D.P.R. n. 445 del 28.12.2000, le dichiarazioni mendaci, la falsità negli atti e l'uso di atti falsi sono puniti ai sensi del codice penale e delle Leggi speciali in materia, e che nel caso ricorressero dette ipotesi, decade fin dall'inizio e senza necessità di nessuna formalità dai benefici conseguenti al provvedimento emanato sulla base di tali dichiarazioni;
2) di essere iscritto al Corso di Dottorato di ricerca "Rischio e Sviluppo Ambientale, Territoriale e Edilizio ciclo XXXIII, corso attivato ai sensi del "*Regolamento dei Corsi di Dottorato di ricerca del Politecnico di Bari"*, emanato con D.R. n.286 del 01.07.2013;
3) di essere pienamente a conoscenza delle disposizioni contenute nel predetto Regolamento in merito alla procedura di deposito, pubblicazione e autoarchiviazione della tesi di dottorato nell'Archivio Istituzionale ad accesso aperto alla letteratura scientifica;
4) di essere consapevole che attraverso l'autoarchiviazione delle tesi nell'Archivio Istituzionale ad accesso aperto alla letteratura scientifica del Politecnico di Bari (IRIS-POLIBA), l'Ateneo archivierà e renderà consultabile in rete (nel rispetto della Policy di Ateneo di cui al D.R. 642 del 13.11.2015) il testo completo della tesi di dottorato, fatta salva la possibilità di sottoscrizione di apposite licenze per le relative condizioni di utilizzo (di cui al sito http://www.creativecommons.it/Licenze), e fatte salve, altresì, le eventuali esigenze di "embargo", legate a strette considerazioni sulla tutelabilità e sfruttamento industriale/commerciale dei contenuti della tesi, da rappresentarsi mediante compilazione e sottoscrizione del modulo in calce (Richiesta di embargo);
5) che la tesi da depositare in IRIS-POLIBA, in formato digitale (PDF/A) sarà del tutto identica a quelle **consegnate**/inviate/da inviarsi ai componenti della commissione per l'esame finale e a qualsiasi altra copia depositata presso gli Uffici del Politecnico di Bari in forma cartacea o digitale, ovvero a quella da discutere in sede di esame finale, a quella da depositare, a cura dell'Ateneo, presso le Biblioteche Nazionali Centrali di Roma e Firenze e presso tutti gli Uffici competenti per legge al momento del deposito stesso, e che di conseguenza va esclusa qualsiasi responsabilità del Politecnico di Bari per quanto riguarda eventuali errori, imprecisioni o omissioni nei contenuti della tesi;
6) che il contenuto e l'organizzazione della tesi è opera originale realizzata dal sottoscritto e non compromette in alcun modo i diritti di terzi, ivi compresi quelli relativi alla sicurezza dei dati personali; che pertanto il Politecnico di Bari ed i suoi funzionari sono in ogni caso esenti da responsabilità di qualsivoglia natura: civile, amministrativa e penale e saranno dal sottoscritto tenuti indenni da qualsiasi richiesta o rivendicazione da parte di terzi;
7) che il contenuto della tesi non infrange in alcun modo il diritto d'Autore né gli obblighi connessi alla salvaguardia di diritti morali od economici di altri autori o di altri aventi diritto, sia per testi, immagini, foto, tabelle, o altre parti di cui la tesi è composta.

Luogo e data Bari, 01/03/2021 Firma 

Il/La sottoscritto, con l'autoarchiviazione della propria tesi di dottorato nell'Archivio Istituzionale ad accesso aperto del Politecnico di Bari (POLIBA-IRIS), pur mantenendo su di essa tutti i diritti d'autore, morali ed economici, ai sensi della normativa vigente (Legge 633/1941 e ss.mm.ii.),

CONCEDE

- al Politecnico di Bari il permesso di trasferire l'opera su qualsiasi supporto e di convertirla in qualsiasi formato al fine di una corretta conservazione nel tempo. Il Politecnico di Bari garantisce che non verrà effettuata alcuna modifica al contenuto e alla struttura dell'opera.
- al Politecnico di Bari la possibilità di riprodurre l'opera in più di una copia per fini di sicurezza, back-up e conservazione.

Luogo e data Bari, 01/03/2021 Firma 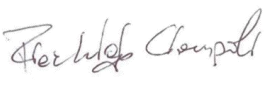

D.R.R.S

POLITECNICO DI BARI

01

2020

PhD Program in Environmental and Building Risk and Development

Coordinator: Prof. Michele Mossa

XXXIII CYCLE
ICAR/09 - Structural Engineering

DICATECh
Department of Civil, Environmental, Building Engineering and Chemistry

Development of a framework for the regional vulnerability assessment of RC buildings: an automatic tool based on typological-mechanical modelling and non linear time history analyses

Prof.ssa Giuseppina Uva
DICATECh
Politecnico di Bari

Prof. Francesco Maddalena
DMMM
Politecnico di Bari

Prof. Giuseppe Maria Coclite
DMMM
Politecnico di Bari

Pier Luigi Ciampoli

D.R.R.S

POLITECNICO DI BARI

01

2020

Dottorato di Ricerca in Rischio e Sviluppo Ambientale, Territoriale e Edilizio

Coordinatore: Prof. Michele Mossa

XXXIII CYCLE
ICAR/09 - Ingegneria Strutturale

DICATECh
Dipartimento di Ingegneria Civile, Ambientale, del Territorio, Edile e di Chimica

Sviluppo di un framework per la valutazione della vulnerabilità sismica regionale di edifici in c.a.: un tool automatico basato su una modellazione tipologico-meccanica e su analisi dinamiche non lineari

Prof.ssa Giuseppina Uva
DICATECh
Politecnico di Bari

Prof. Francesco Maddalena
DMMM
Politecnico di Bari

Prof. Giuseppe Maria Coclite
DMMM
Politecnico di Bari

Pier Luigi Ciampoli

EXTENDED ABSTRACT (en)

In the present work an all comprehensive framework for the seismic vulnerability assessment of existing Reinforced Concrete buildings at a regional scale is proposed and developed.

Proposed approach belongs to the typological-mechanical class of strategies, and draws inspiration from several of the existing approaches belonging to the same class, borrowing what are considered the best characteristics of each existing proposal. The main goal of this proposal is attempting to tighten the gap between the deepening level, and hence reliability of results, between the individual building and the regional scale, within an all comprehensive framework.

It is worth highlighting that it is *infeasible* the use of deepened methods for the regional scale as it is common for individual buildings.

The issue of feasibility is due to two main reasons:

- it is impossible to reach a sufficient knowledge level for the whole building stock in a region, as on the contrary it can be made for a single building;
- deepened analyses (as non-linear dynamic that will be here used) require a cumbersome effort in terms of computational cost, to a point that it could be considered *uneconomical*.

For the first issue, a deepened statistical framework will be used for all unknown parameters, thus with the help of real data in order to calibrate parameters values for better adherence to the building stock under analysis. An increased variability of results is clearly expected, while the error introduced by the statistical procedure will be reduced as much as possible by increasing the number of analysis runs.

The second issue is probably the reason why most of the researchers, engaged in regional scale vulnerability assessment, resort to various degrees of simplifications. In the development of the proposed procedure this issue is assumed to be not critical:

computational cost is considered not crucial, while the development of a working tool will represent the proof of its feasibility.

One of the desired features of the proposed approach is its agility, *i.e.* the ability to be easily modified when needed (as soon as the modification does not regard the core characteristics of the implemented method). The procedure will be developed in order to be organized in modules, according to an object-oriented programming philosophy.

It is worth highlighting that, for its agility, the proposed procedure will not be indissolubly connected with any of the cited modules, neither with assumptions and simplifications that will be used in order to retrieve some example results and test the feasibility of the idea: the procedure is completely open to modifications and enhancements. Also the meaning of *enhancing the procedure* is blurry: depending on the underlying needs, a given edit could represent an improvement or a worsening.

For two crucial elements of the procedure a novel solution will be presented: the *beam model* and the *time integration strategy*. On the other hand, in other modules simplifications will be introduced, postponing further insights to future developments.

Regarding the first element, a novel beam model will be proposed in order to get rid of some mathematical incongruity of existing models. Once presented, the model will be then used into the procedure in order to more effectively model the behaviour of structural elements.

About the time integration strategy, a novel approach in this field will be proposed. For instance, the exactness of the solution provided by this approach will be discussed, together with its uniqueness.

Once the proposed framework will be implemented into a tool, some example applications will be presented, in order to assess its reliability and clarify its feasibility.

Keywords: Earthquake Vulnerability, Risk Assessment, Regional Scale, Existing Buildings, Fragility Curves

EXTENDED ABSTRACT (it)

Nel presente lavoro, un nuovo framework finalizzato alla valutazione della vulnerabilità sismica di edifici esistenti in calcestruzzo armato verrà proposto e implementato.

Il suddetto approccio si colloca nella famiglia dei metodi tipologico-meccanici, traendo ispirazione dagli approcci esistenti nel tentativo di ereditarne gli aspetti di pregio. L'obiettivo dell'approccio proposto va ricercato nel tentativo di ridurre le differenze in termini di livello di approfondimento delle analisi (e dunque di affidabilità del risultato) tra la scala del singolo edificio e quella a livello regionale.

Si vuole sottolineare come il maggiore ostacolo nell'applicare i metodi approfonditi usati per le singole strutture alla scala regionale è rappresentato dal problema della *fattibilità*:

- è impossibile raggiungere lo stesso livello conoscitivo quando la scala di analisi passa dal singolo edificio a un intero patrimonio edilizio;
- con il livello di approfondimento delle analisi aumenta anche l'impegno computazionale, a un punto tale da rischiare di diventare non economico.

Con riferimento al primo problema citato, si utilizzerà un approccio statistico nel valutare i parametri ignoti, con l'ausilio di dati reali per la loro calibrazione. Naturalmente, ci si aspetta una maggiore variabilità dei risultati rispetto al caso del singolo edificio, ma l'errore introdotto dalle procedure statistiche utilizzate verrà ridotto aumentando il numero delle analisi.

Il secondo problema è probabilmente la ragione principale per cui gli approcci esistenti fanno uso di intense approssimazioni. Nella procedura proposta, il problema dell'impegno computazionale non sarà ritenuto prioritario, e lo sviluppo di un tool ne rappresenterà la prova della sua fattibilità.

Una delle caratteristiche di cui si vuole dotare la procedura proposta (e la sua implementazione) è la sua agilità, cioè l'abilità di essere facilmente modificabile (a patto

che la modifica non riguardi il nucleo della procedura stessa). Per questo motivo l'implementazione della procedura sarà organizzata in moduli, seguendo una filosofia di programmazione orientata agli oggetti.

Va sottolineato che, per effetto della succitata agilità, la procedura non è vincolata alle modalità di implementazione di alcuno dei suoi moduli, nè alle ipotesi e alle simplificazioni che verranno di volta in volta precisate, il cui obiettivo è di permettere di testare la fattibilità dell'idea fondante della procedura: quest'ultima resta totalmente aperta a modifiche e migliorie. Oltretutto, il significato di *miglioria* è in questo caso fumosa: a seconda delle necessità, una modifica può rappresentare un miglioramento o un peggioramento della procedura.

Mentre in altri moduli verranno introdotte delle semplificazioni (rimandando a futuri sviluppi ulteriori approfondimenti), per due elementi cruciali per la procedura una soluzione innovativa verrà proposta. Tali elementi sono il *modello di trave* e la *procedura di integrazione numerica*.

Riguardo il primo elemento citato, un nuovo modello di trave verrà proposto con l'obiettivo di superare alcune incongruenze matematiche dei modelli esistenti. Dopo una breve presentazione, verrà utilizzato per predire in maniera più efficace il comportamento degli elementi strutturali.

Con riferimento alla strategia di integrazione numerica, un nuovo approccio verrà proposto, e se ne discuterà l'esattezza e unicità della soluzione.

Una volta implementata la procedura in un tool opportuno, alcune applicazioni verranno presentate al fine di valutare l'affidabilità dei risultati e discutere la fattibilità dell'idea fondante.

Keywords: Vulnerabilità Sismica, Valutazione del Rischio, Scala Regionale, Edifici Esistenti, Curve di Fragilità

Contents

Part I

Introduction

An earthquake achieves what the law promises but does not in practice maintain - the equality of all men.

Ignazio Silone - Emergency Exit

1. SIGNIFICANCE OF THE PROBLEM

Earthquakes pose a prominent threat both to human life and activities. In those current times of pandemic emergency we do not have to forget about how disastrous can be those events.

In Pesaresi et al. (2017) it is stated that, amongst other natural disasters, *"Earthquake is the hazard that accounts for the highest number of exposed population. The number of people living in seismic areas has increased by 93% in 40 years (from 1.4 billion in 1975 to 2.7 billion in 2005)."* and, moreover, *"Half billion people, one fourth of the potentially exposed population in 2015, lives in areas falling within the most dangerous classes"*.

The outstanding threat posed by natural disasters is widely known. In this context, European Parliament recognized that *"In view of the significant increase in the number and severity of natural [...] disasters in recent years [...], an integrated approach to disaster management is increasingly important"* (see EU1313, Preamble) and addressed the need to *"develop risk assessments at national or appropriate sub-national level"* (EU1313, art. 6(a)).

At this point, it is important to define what is intended with ***risk***. In Eq. 1.1 its definition is symbolically presented: Risk (R) comes from ($=$) a combination (x) between Hazard (H), Vulnerability (V) and Exposure (E) (as example references see Antofie et al., 2018; Thywissen, 2006).

$$R = HxVxE \tag{1.1}$$

The main problem in assessing earthquake-related risk is due to its tight connection to the built environment that is stricken. A wide set of influencing conditions are to be included in order to effectively assess earthquake risk, most of them posing a burdening challenge in its evaluation at large scale:

1. Macro-scale seismic hazard, whose characterization is mostly related to the presence of seismic sources in the surroundings and their features; this level is the easiest to be assessed at large scale, considering that few elements (*i.e.* faults) affect wide areas.
2. Local modifications of earthquake characteristics (and, therefore, seismic hazard) due to site-related phenomena, whose importance was clear in some past events (as a limited example in technical literature see Monaco et al., 2009; Pischiutta et al., 2010; Faccioli et al., 2015); at this level the effect is still on hazard, but at a smaller scale. In fact, we can see effects from sub-regional (*e.g.* due to geological characteristics) to sub-municipality scale (*e.g.* due to topography).
3. Response of existing buildings to the event. This level is related to the vulnerability of the built environment that is under study, and is usually the most cumbersome level to be analysed because a lot of elements with not correlated vulnerabilities (buildings) are present in the considered area. Moreover, it is practically impossible to derive a thorough knowledge of vulnerability of all buildings in an area, because a lot of expensive and time consuming activities are needed just for a single building (*e.g.* a complete survey, some materials testing, structural analyses).

From what said, it is clear that the most challenging obstacle for a large scale earthquake risk assessment is represented by existing buildings vulnerability assessment. Moreover, it must be noted that it is not easy to simply extend the vulnerability assessment of a given building to a wider set of *similar* buildings, because this similarity should have to be over a wide set of parameters that influence the seismic response of a structure (*e.g.* structural configuration as in Arnold et al. (1981) and Carniel et al. (2001), infills configuration and characteristics as in Aiello et al. (2017a) other than materials characteristics and construction period amongst others), whose relative importance is not fully understood.

2. OBJECTIVES

In the context of large scale seismic risk assessment, an effective procedure with poor data on existing buildings assumes a paramount importance.

Until now, most of the methods for the seismic vulnerability assessment of existing building are based on derivation of empirical fragility curves from observational data (*e.g.* see Sabetta et al. (1998), Kim (2018), and Del Gaudio et al. (2020)). However, the difficulty of properly generalize structural responses to earthquake has been already cited.

Only few existing methods use a mechanical approach, which could overcome the generalization problem. However, each method has some limitation, *i.e.* do not take into account some parameters that have influence over building seismic vulnerability:

- only some of the available methods take into account the uncertainty of input earthquake through non-linear dynamic analyses (Singhal et al., 1996; Masi, 2003);
- in order to simplify the procedure, most of existing methods assume that the analysed structure is equivalent to a Single Degree of Freedom (SDoF) system (Calvi, 1999; Crowley, Pinho, and Bommer, 2004);
- only few authors considered the presence of infills (Crowley, Pinho, and Bommer, 2004; Del Gaudio, 2015);

Main object of the present work is to give a valid alternative to existing methods for seismic vulnerability assessment, incorporating best characteristics of each approach and globally enhancing the quality of the assessment with improved evaluations in a thorough statistical context.

3. THESIS OUTLINE

After this introductory part, the present dissertation will be divided into three parts.

The Part II will be devoted to the presentation and description of the proposed framework and its implementation through the **EX:MIRIAM** tool.

Chapter 4 will contain a brief description of the main features that a procedure for the seismic vulnerability assessment at large scale needs to have.

In Chapter 5 a critical overview of the state of the art on available methods for seismic vulnerability assessment at large scale will be presented.

In Chapter 6 the proposed approach will be described in general, with particular attention to the succession of steps needed for the procedure. However, details on single steps will be discussed in the subsequent chapters.

Chapter 7 will contain all of the details for the preparatory steps of region-wide data. Cited data are those related to hazard and building stock: with reference to the hazard, steps needed to describe the seismic hazard inside the regional area in order to identify homogeneous sub-regional areas in terms of hazard characteristics will be described; on the other hand, a description of the criteria for the clustering of buildings into homogeneous typologies will be discussed.

The Chapter 8 will be focused on the data needed for the subsequent analyses: ground motions, material mechanical characteristics data, load data. For all of those data the statistical approach used will be explained in detail, and how those data will be used in subsequent steps will also be stated. A section will be also added in order to discuss the use of a simulated design for the definition of some quantities (Section 8.5).

In Chapter 9 all of the issues related to the structural modelling will be deepened. Within this chapter a novel beam model will be introduced (Section 9.1), and its features and characteristics will be discussed. In the same chapter constitutive laws for both structural (columns) and non-structural (infills) elements will be presented, as a

simplified modelling will be used.

In Chapter 10 a novel strategy for the solution of a time integration problem will be developed, its characteristics discussed and its mathematical features studied.

Chapter 11 will be devoted to the description of the several available analysis methodologies, and the details of the chosen one will be discussed. Still in the same chapter, a discussion about the limit states attainment threshold will be presented.

Chapter 12 will finally contain the post-processing steps, which are needed in order to provide synthetic but significant output data.

Once the framework is fully defined, in Part III two applications will be presented.

In Chapter 13 an all comprehensive application to the Puglia region will be described. As an output, fragility curves for buildings clusters for each considered limit state will be provided.

In Chapter 14 an insight of obtained results will be made through their application to an example case study, represented by the urban area of the Bovino municipality.

Part IV will be used to draw conclusions (Chapter 15) and to discuss future developments for the procedure (Chapter 16).

Part II

Proposal of a mechanical approach for the regional-scale seismic vulnerability assessment: the EX:MIRIAM tool

Choose always the way that seems the best, however rough it may be. Custom will render it easy and agreeable.

Pythagoras - Ethical Sentences from Stobaeus

4. INTRODUCTION

A large-scale seismic vulnerability assessment needs a set of steps whose implementation requires to take into account some aspects:

Feasibility a given procedure must be usable, or it would be useless; as an example, proposing a complete in-depth analysis of each building in the studied area would give exactly the results that ideally we want to reach; however, time and resources needed for those operations make this option absolutely unattainable.

Accuracy this term refers to the ability of the procedure to provide unbiased *exact* results; accuracy would be maximized through in-depth analyses, and get worse as more simplifications are introduced in the procedure.

Reliability with this term it is intended the capability of the procedure to provide results with low dispersion; for instance, high dispersions would indicate non usable results, because there would be too much uncertainty over a given result; however, maximum reliability can be reached only knowing every influencing parameter value, while it is lowered by assumptions on those values and by clustering.

5. STATE OF THE ART OF REGIONAL SEISMIC RISK ASSESSMENT PROCEDURES

In the last decades, several approaches were proposed in order to solve the issue of assessing the seismic risk at large scales. It is indeed clear that, while at individual building scale the solutions are at a more advanced level both in terms of usage and of acceptance in academic research, at a larger scale none of the proposed approaches can be considered as *almost universally* accepted.

As a demonstration of what asserted, for individual buildings there exist several standardized procedures, both in regulations for simplified practice-oriented assessment (*e.g.* NTC2018 and EC8-3:2005) and in reports for more deepened evaluations (*e.g.* CNR DT 212:2013). However, those procedures cannot be straightforwardly transformed into large scale approaches given that different issues are to be faced (*e.g.* different sources of uncertainty, the impossibility of a deepened knowledge up to a certain point, the variability of buildings characteristics, etc), and this condition is sometimes clearly stated in cited documents (*e.g.* in EC8-3:2005 4.1 2(P)).

Procedures proposed in technical literature regarding this issue are usually divided into the following categories, on the basis of the strategy used for the assessment (see Calvi et al. (2006) and Del Gaudio (2015)):

Empirical within this type of approach seismic risk is assessed through observation made on past earthquakes effects on the built environment, also with the help of notable experts judgement.

Analytical/Mechanical in this strategy analytical and/or mechanical procedures are used in order to predict the response of structures under study to seismic action, so that seismic risk can be assessed.

5.1 Empirical methods

First developments of seismic risk assessment on building stock can be dated back at least to the early 1970s, and at time the first methods to be proposed were empirical (*i.e.* based on observational data).

As a first attempt to foresee damages on structures due to earthquakes, in Medvedev et al. (1969) a table describing expected damage in qualitative shape (from 1 - slight damage to 5 - total collapse, with indications on how many buildings, from single/few - <5% to most >75%) was presented (reissued in Fig. 5.1). Input data of this table were:

- *Intensity grade*, given as a macroseismic intensity, based on observed effects (*e.g.* if noticeable by people, effects on hanging objects, damages) rather than on measured data.
- *Type of structure*, being all of the structures divided into 3 categories: A - rural structures, in field-stone; B - ordinary brick buildings, half timbered structures, or in natural hewn stone; C - reinforced buildings, well-built wooden structures.

Intensity grade	Types of structures		
	A	B	C
Y	Single - 1		
YI	Single - 2 Many - 1	Single -1	
YII	Single - 4 Many - 3	Many -2	Many - 1
YIII	Single - 5 Many - 4	Single - 4 Many - 3	Single - 3 Many - 2
IX	Many - 5	Single - 5 Many - 4	Single - 4 Many - 3
X	Most - 5	Many - 5	Single - 5 Many - 4

Fig. 5.1 – Expected damages on structures as in Medvedev et al. (1969)

Table presented in Fig. 5.1 can be defined as a ***Damage Probability Matrix*** (DPM): while it is not presented an explicit probability measurement, there is still the qualitative

indication of how many buildings are expected to suffer a given damage level.

First seismic risk assessment procedures used a similar approach, and DPMs were gradually enhanced in order to give an explicit indication of the probability that a given building could suffer a certain damage level: as an example, in Whitman (1973) explicit percentages of expected damage on buildings were presented on the basis of observational data on 1600 buildings damaged from the 1971 San Fernando earthquake.

In Scawthorn et al. (1981), on the basis of observed damages in Sendai City after the 1978 Miyagiken-oki earthquake, a correlation between damage ratio and spectral displacement (as the best fit found from authors amongst all intensity-related parameters) together with number of storeys was computed

On the basis of the observed damages due to the 1980 Irpinia earthquake, in Braga et al. (1982) the first European version of DPM was proposed, and subsequently enhanced in Di Pasquale et al. (2005) and Dolce et al. (2003), mainly in terms of considered vulnerability classes in which the existing building stock is organized. In Fig. 5.2 one of the DPMs proposed in Dolce et al. (2003) is presented.

Table IVb. Damage Probability Matrix for buildings of vulnerability class B.

Intensity	Damage grade					
	0	1	2	3	4	5
VI	0.360	0.408	0.185	0.042	0.005	0.000
VII	0.188	0.373	0.296	0.117	0.023	0.002
VIII	0.031	0.155	0.312	0.313	0.157	0.032
IX	0.002	0.022	0.114	0.293	0.376	0.193
X	0.000	0.001	0.017	0.111	0.372	0.498

Fig. 5.2 – DPM for vulnerability class B (medium vulnerability) as per Dolce et al. (2003)

In Benedetti et al. (1984) and thereafter in GNDT (1993), an approach based on a ***Vulnerability Index*** (VI) was proposed. For instance, said index was computed from a field survey form, where *scores* were assigned to a set of parameters (*e.g.* plan and elevation configuration, type of foundation), each having a given weight as from its importance over the structural response. This index can be then used to define a vulnerability function fitted on damages observed in past earthquakes (as in Guagenti et al. (1989)).

In order to develop the DPMs given in ATC-13:1985, the first (and probably the most important) expert judgement-based method was developed: more than 50 senior earthquake engineering experts were asked to estimate average, lower- and upper-bound of damage factors (expressed in terms ratio of loss to replacement cost) under various seismic intensities for 36 building classes. Weighting those esteems on the basis of experts' experience and confidence level, assuming a lognormal distribution for damage factors, DPMs were developed for each possible couple of intensity level and building class. This same procedure were also used in several subsequent works, *e.g.* in Cardona et al. (1997) for the city of Bogotá, in Fäh et al. (2001) for the city of Basel, in Veneziano et al. (2002) for the city of New Madrid.

In Grünthal (1998) the ***EMS98*** macroseismic scale was proposed, where an implicit definition of a DPM is given. However, information has been argued to be incomplete (not every possible combination of damage level and seismic intensity is covered in terms of percentage of buildings) and vague (only qualitative description of proportion of buildings). Those limitations (as arised in Del Gaudio (2015) and Calvi et al. (2006) amongst others) where overcome in Giovinazzi et al. (2004), where obtained DPMs were also related to a VI, so that *damage grade* μ_D could be assessed directly from the VI value V_I and macroseismic intensity I through Eq. 5.1

$$\mu_D = 2.5 \left[1 + tanh \left(\frac{I + 6.25 \cdot V_I - 13.1}{2.3} \right) \right] \tag{5.1}$$

In Sabetta et al. (1998), starting from damages on nearly 47'677 buildings observed after two events in Italy (Abruzzo and Irpinia earthquakes), mean damage was computed (whose definition is given according to MSK macroseismic scale from Medvedev et al. (1969)). As a result, continuous functions of mean expected damage against several ground motions parameters were proposed (for instance, Peak Ground Acceleration PGA, Expected Peak Acceleration EPA and Arias Intensity AI were taken into account).

In Kappos et al. (1998) data from observed damages after the 1978 Thessaloniki were combined with results of non-linear dynamic analyses on 6 *representative* structural models in order to provide DPMs in terms of cost of repair. This approach, however, can not be described as *fully empirical*, and should be addressed to as a *hybrid*

methodology.

In Orsini (1999) an attempt to overcome the problem of the use of a non-continuous intensity parameter (as for macroseismic scales) was made, for instance using the ***Parameterless Seismic Intensity*** scale (PSI) by Spence et al. (1991). The basis of the method is the hypothesis that the intensity at which a structure exceedes a given damage threshold is distributed according to a Gaussian distribution: after assessing the value of PSI for 41 municipalities hit by 1980 Irpinia earthquake, based on data on 50'000 apartments, the author proposed continuous vulnerability curves depending on the PSI value.

In Rota et al. (2008), a total of 91'000 buildings surveyed after being damaged as an effect of several earthquakes (Irpinia 1980, Abruzzo 1984, Umbria-Marche 1997, Pollino 1998 and Molise 2002) were divided into 23 typologies based on structural typology, material, regularity, number of floors. For each of those typologies, DPMs were extracted and fragility curves were fitted, in both cases using PGA and Housner Intensity (HI) as intensity measures.

5.1.1 Screening methods

Amongst empirical procedures, some methods were proposed in order to assess a *prioritisation scale* rather than a prediction on expected damage.

In Japan the so called ***Japanese Seismic Index Method*** is used at least from 1970s (JBDPA, 1990). According to this method, a *seismic performance index* I_S is calculated for each storey and in every frame direction within the building following Eq. 5.2

$$I_S = E_0 S_D T \tag{5.2}$$

where: E_0 = sub-index regarding the basic structural performance $= C \cdot F$ being C an ultimate strength index and F a ductility-related one

S_D = sub-index about the structural design of the building, that takes into account irregolarities on masses and/or stiffness

T = sub-index that takes into account the time-dependent deterioration of the building, to be defined on the basis of a field survey

Cited index is to be compared to a limit value I_{S0} computed through Eq. 5.3.

$$I_{S0} = E_S Z G U \tag{5.3}$$

where: E_S = a value depending on the degree of the screening deepening

Z = zone-related index

G = index that takes into account the ground-building interaction

U = usage index, that works as an importance factor

If $I_S > I_{S0}$ the structure is assumed to have low vulnerability; if $I_S << I_{S0}$ the structure is labelled as highly vulnerable so that a retrofitting is considered necessary; if I_S is only slightly lower than I_{S0} a more detailed assessment is needed.

The method was subsequently adapted for Turkish buildings on the basis of results of PushOver analyses (PO) on 12 buildings from Zeytinburnu, Istanbul in the work of Ozdemir et al. (2005).

In Hassan et al. (1997) an evaluation method was proposed as in Fig. 5.3 on the basis of two simple geometrical parameters: a *wall index*, equal to the ratio (in %) between cross sectional area of walls in a given direction over the total floor area (infills walls areas are taken as $\frac{1}{10}$ of their value); a *column index*, equal to the ratio (in %) between column total area above base and total floor area.

In Yakut (2004) a *Capacity Index* is computed from orientation, size and material properties (visually inspected) of the lateral load-bearing system, so that a classification of buildings in low/high risk category can be defined.

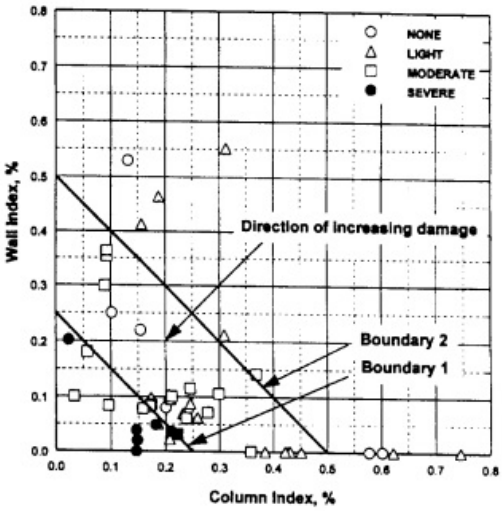

Fig. 5.3 – Evaluation method as proposed in Hassan et al. (1997)

In Grant et al. (2006) a screening procedure was proposed: the design PGA at the time of construction, assuming a perfect code compliance of the building, is considered to be the building capacity. Once the demand PGA is computed, it is possible to define a *PGA deficiency*, that can be used as an indicator of the building vulnerability. This approach is considered to be *conservative*: as an example, for buildings designed without any seismic prescription a null capacity is assumed. However, in a vulnerability assessment framework conservativeness is not a desired feature, while a prediction on seismic response as reliable as possible is desired.

In Ozcebe et al. (2006) a vulnerability index was defined starting from 8 vulnerability-related parameters, subsequently used for the vulnerability assessment of the existing buildings stock in Istanbul.

5.2 Analytical and mechanical methods

In Kunnath et al. (1996) a single building, assumed to be representative of low-rise buildings in Memphis area, was subjected to five ground motions representative of five seismic intensities (PGA ranging from $0.1g$ to $0.5g$). In order to identify the severity of

the effects on the structure, authors used a ***Damage Index*** DI depending on both the maximum experienced deformation and the dissipated hysteretic energy, normalized to a maximum value of 1 if ultimate capacity is reached. Results of analyses indicated that the structure could withstand the earthquake with $PGA = 0.1g$ with repairable damages (Damage index $DI = 0.08$), while for $PGA = 0.2g$ or more the structure experienced collapse ($DI > 1$).

In Singhal et al. (1998) a Bayesian approach is used in order to take into account the existence of *measurement errors* (*i.e.* errors due to the uncertainty on model parameters) and *statistical errors* (*i.e.* errors due to the use of a finite data set), while *errors of ignorance and simplification* (*i.e.* errors due to the incomplete knowledge of the physical phenomenon) are recognized to be practically impossible to be computed and then neglected. Using a global damage index based on the Park and Ang model (Park et al., 1984), through a Monte Carlo approach, correcting predictions on the basis of observed damages from 1994 Northridge earthquake, fragility curves were proposed for low- mid- and high-rise RC buildings.

In Ordaz et al. (1998) a correlation between damage level and maximum interstorey drift and between the latter and the spectral acceleration is presented. This latter correlation was defined through a simplified model based on the analogy between the building and a cantilever beam subjected to flexural and shear deformations. Some coefficients were used in order to take into account several influencing parameters (*e.g.* height of the structure, ratio between elastic and inelastic demand, irregularities both in plan and in elevation).

In Calvi (1999) a methodology was proposed and then developed in subsequent researches (Pinho et al., 2002; Crowley, Pinho, and Bommer, 2004; Crowley, Pinho, Bommer, and Bird, 2006): the ***DBELA*** methodology (Displacement-Based Earthquake Loss Assessment). Within this procedure, a displacement shape is assumed for each limit state, and then a displacement capacity is computed through local thresholds. Possible variations of both capacity and period of vibration of the equivalent SDoF model are then computed, and then in a period-displacement plane rectangles can be defined from the position of the single capacity-period point. A uniform probability function is

assumed over rectangles, in order to represent the variability of the capacity. Representing seismic demand through a displacement spectrum, it is then possible to directly compare it with the capacity as a function of the period: as in Fig. 5.4, the ratio between the rectangle area below the demand displacement spectrum and the total rectangle area represents the expected proportion of the building exceeding the considered limit state.

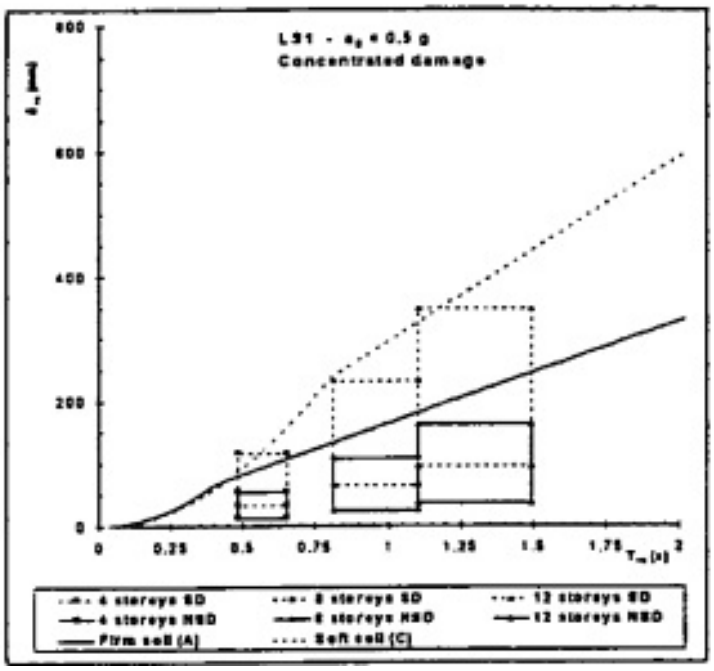

Fig. 5.4 – Comparison between seismic demand and capacity according to the DBELA procedure in Calvi (1999)

In the work of Masi (2003) a single structure, considered as representative of the most widespread structural type in Italy, was analysed through non-linear dynamic analyses after a simulated design step. The same building was studied in three configurations: bare frame, totally infilled and pilotis. Each of those configurations was subjected to a set of both artificial and natural accelerograms, in order to compute the damage degree L_D defined according to the European Macroseismic Scale EMS-98 (Grünthal, 1998), and then define a vulnerability class according to the cited reference.

In Dumova-Jovanoska (2004) several representative RC buildings of the Skopje region were modelled and subjected to 240 synthetic earthquake records. Results were organized in order to produce damage-intensity relations (in terms of vulnerability curves and DPMs) assuming a normal distribution for damage (defined through the damage index by Park et al. (1984) model).

In Rossetto et al. (2005) a population of 25 buildings generated from a single one from material parameters variation was subjected to adaptive PushOver analyses, based on 30 accelerograms, and the performance point was found through the Capacity Spectrum approach (Fajfar, 1999). Computed performance point was then correlated to a damage state with a damage scale calibrated on observational data, thus leading to the definition of analytical displacement-based vulnerability curves, that showed good correlation with post-earthquake damage statistics (as reported in Del Gaudio (2015)).

In the procedure proposed in Cosenza et al. (2005), a building class is defined in terms of construction year and number of floors. For each class, several buildings are generated on the basis of the statistical distribution of both geometrical and mechanical parameters of the building. Three failure mechanisms (Fig. 5.5) were then analysed in order to assess the *collapse mechanism* as the one having the lower strength. Through a Monte Carlo simulation the probability of having a capacity lower than an assigned value was computed. However, authors did not provide vulnerability curves nor any other information about the probability of reaching a given limit state and/or damage level with respect to a varying seismic demand measure: only cumulative distributions of capacity parameters were given.

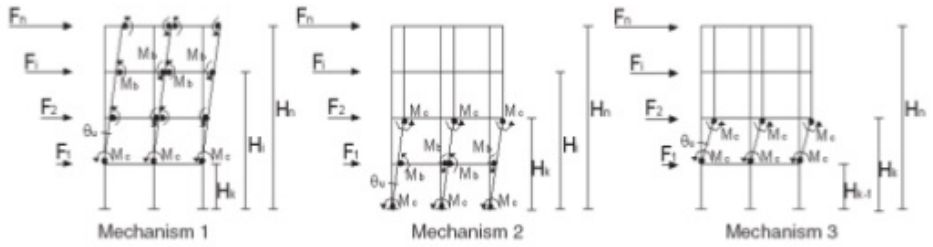

Fig. 5.5 – Considered mechanism in the approach proposed in Cosenza et al. (2005)

Within the ***HAZUS*** approach (Kircher et al., 2006) a total of 36 structural typologies

are considered, and for each a predefined bi-linear capacity curve is provided both in terms of yield/collapse points and of damage levels thresholds. Using Capacity Spectrum Method (Fajfar, 1999) the demand related to a fixed intensity level is computed, and peak response displacement and acceleration are defined from the intersection between demand spectrum and capacity spectrum. The performance point provides the displacement input into the limit state vulnerability curves to give the probability of being in a given damage band.

In Iervolino, Manfredi, et al. (2007) a procedure was developed using Static PushOver analyses. Assuming as random variables both geometrical and mechanical characteristics of the analysed building class, upper and lower bounds were determined and a *scanning step* was fixed, so that every possible combination of parameters could be taken into account. For each analysis, period T, strength C_S and displacement capacity C_d for the equivalent SDoF structure were computed. Using the Capacity Spectrum approach (Fajfar, 1999), an estimate of the failure probability is given as ratio between number of structures for which threshold is exceeded over the total number of analysed structures.

The ***SP-BELA*** procedure (Simplified Pushover-Based Earthquake Loss Assessment) was proposed in Borzi, Pinho, et al. (2008). This methodology consisted in the definition of a mechanism-based simplified PushOver curve with a procedure similar to the one proposed in Cosenza et al. (2005), from which a base shear capacity for the building stock is defined and analysed with a framework similar to the one used for DBELA procedure. A Monte Carlo approach together with a Latin Hypercube sampling procedure are used for deriving vulnerability curves for a class of buildings and for each limit state. While in Borzi, Crowley, et al. (2008) an attempt was made in order to include the effect of infills, it is not fully clear how authors took into account the presence of brittle elements in a mechanism-based procedure.

In the work by Verderame, Ricci, Del Gaudio, et al. (2013) pushover analyses are performed on simplified structural models. A Monte Carlo approach is used in order to take into account uncertainties related to both seismic demand and capacity. Presence of infills is considered, both in terms of influence on the global response and of suffered

damage. Results are given in terms of *Damage States* defined according to the EMS-98 Macroseismic scale (Grünthal, 1998), and both fragility curves and annual failure probabilities are computed.

In El-Betar (2018) a rapid visual screening (RVS) procedure is performed on two structures, each representing the two most common types of structures in Egypt: a pre-seismic-code structure and a more modern one. According to FEMA P-154, when the *score* given by RVS procedure does not fulfil a *safety* criterion, further analyses are performed (for instance, pushover analyses).

5.3 Advantages and drawbacks of each strategy

Not including the features of single procedures cited in previous sections, each have some advantages and disadvantages common with other methodologies that share the general strategy (*i.e.* empirical or analytical/mechanical).

5.3.1 Empirical approaches

Empirical methodologies were the first to be developed as it is clearly easier to be implemented, especially considering that damage data are usually collected also for other reasons (*e.g.* structure usability assessment, rebuilding issues), and the use of macroseismic scale as intensity measure was in the past very effective for regional scale risk assessment considering that hazard maps were usually defined through this parameter.

The use of a macroseismic intensity scale can bring to inconsistencies to the results: those scales are defined through observed damages on buildings, so that the earthquake intensity measured through one of those scales as a matter of fact is influenced by the vulnerability of the hit built environment. Hence, correlating observed damages with macroseismic intensity brings to the theoretical inconsistency: the vulnerability of buildings, intended as the likelihood of a structure to suffer a given damage level under a given seismic intensity, is included in the measure of the intensity, because intensity is measured through observed damages. Thus, macroseismic intensity scale

is not an effective intensity measure for the regional scale seismic risk assessment purpose, while only few authors used other measures within an empirical approach (*e.g.* Scawthorn et al. (1981) and Rota et al. (2008)).

From a contemporary point of view, hazard is no more represented through macroseismic intensity scales. Two possibilities are possible: if a methodology using macroseismic intensity is selected, the problem of transforming the macroseismic intensity into other modern measure of intensity arises (usually hazard is represented in terms of PGA/spectra); if a procedure using directly a quantitative measure of intensity is developed, the problem of matching a value for the chosen intensity measure with each damaged building arises, considering that intensity measures (*e.g.* PGA) are not available continuously in the hit area (and usually wide areas are uncovered).

The use of observed damage data, while from a point of view is a strong point, on the other hand gives to the methodologies an outstanding limit: data are available only for some conditions in terms of each of influencing parameters (*e.g.* intensity, built environment characteristics) corresponding to actual situations where a strong earthquake hit. While strong earthquake (luckily) infrequently occur in densely populated areas, it is expected a shortage of data for high intensity (and then damages). In order to overcome this problem, data collected from areas with very different conditions have to be used (*e.g.* as in Rota et al. (2008)), thus limiting the validity of results in a way or the other.

An attempt to overcome some of cited disadvantages comes from *indirect* methods. Within those methods several experts are usually involved so that their prestigious judgement grant reliability (*e.g.* ATC-13:1985 and GNDT (1993)). However, uncertainties on the esteems are not taken into account, there is still the risk of inconsistencies, and the relative importance of some building characteristics is implicitly and unconsciously taken into account while an explicit assessment is maybe needed.

5.3.2 Analytical/Mechanical approaches

Analytical/Mechanical methods were mainly developed in order to overcome the limitations of empirical approaches. Within those methods a physical significance of the

procedure can be achieved, thus allowing sensitivity analyses on the relative importance of structures characteristics. Moreover, results can be given also for building stocks that were never hit by a strong earthquake, for which empirical data are not available, both in terms of structural characteristics and of hazard. Those methods are straightforwardly suitable for parametric studies, and stand in a position of advantage for the use in definition and/or calibration of urban planning, retrofitting, insurance and other similar policies or initiative.

The main disadvantage of those procedures is represented by the intense computational effort needed. Moreover, several other modelling-related sources of uncertainty need to be taken into account, and in general the need of explicitly modelling the behaviour of representative buildings can eventually be a cumbersome effort.

In general, the use of this strategy needs a more detailed knowledge of the existing building stock, given that the issue of selecting a *statistically significant* set of models to be analysed needs to be extended to in-depth characteristics of the built environment.

Results obtained, however, need to be validated through observed damage data, in order to assess the reliability of the procedure in terms of its ability to predict the effects of a earthquake. In some cases, hybrid approaches were used, *e.g.* calibrating results on data, in order to overcome this issue.

Some methods use one or few models to represent wide building classes (*e.g.* Kunnath et al. (1996) and Masi (2003)): in this case the issue of extending those results to the whole class arises, and hence it has to be assessed the reliability of this hypothesis.

The explicit modelling of a given set of structures requires all of the influencing factors to be taken into account, or unreliable results would be provided. As an example, the influence of infills is only addressed in few proposed methodologies (*e.g.* in Masi (2003) and Crowley, Pinho, and Bommer (2004)), while it is generally recognized its outstanding importance.

Another modelling-related source of uncertainty is represented by the simplification made in some approaches (*e.g.* in Calvi (1999)) to consider an equivalent SDoF structure in place of the actual analysed structure: this simplification brings to an higher uncertainty in the results, being clear that every simplification is connected to this trade-

off.

While different procedures use different analyses, it is important to assess the uncertainty related to each of those analysis typologies. One does not have to think that the use of a more *advanced* analysis (*e.g.* dynamic rather than static non-linear analysis) brings to a reduced uncertainty. Deepened analyses need more parameters to be included into the model: as an example, the use of dynamic analyses requires the explicit definition of hysteretic behaviour of elements, that is not needed in static analyses, and both hypotheses on this behaviour and its parameters definition introduce a source of uncertainty in the analysis (for an insight on those issues refer to Bradley (2013)).

6. BRIEF OVERVIEW OF THE PROPOSED PROCEDURE

In this work, the ***EX:MIRIAM*** tool is presented (**EX**isting buildings: a **M**atlab **I**mplementation of a new **RI**sk **A**ssessment **M**ethodology). In this tool, a mechanical procedure for the large-scale seismic vulnerability assessment of existing RC residential buildings is implemented, whose general structure in synthetically depicted in Fig. 6.1.

1. First module (see Chapter 7) is about ***Preparatory Steps on Regional Data***. It is aimed at some preliminary steps for general purpose data analysis. It is worth highlighting that the outputs of this module are not strictly tied to the proposed procedure, so that other approaches can be used to define needed data, as well as other procedures can use it.
   1*a*) Within ***Reference Hazard Analysis*** step, analysis on hazard characteristics is carried on. The aim of this step is to define sub-areas with homogeneous hazard characteristics, so that subsequent analyses can be run overcoming the problem of the strict connection between hazard definition and exact geographic location.
   1*b*) In ***Buildings Clustering*** step, a collection of homogeneous clusters of buildings is defined. As a result, a handful of building typologies (with statistically varying parameters) can describe the set of existing buildings in the analysed region. This way, subsequent analyses can get rid of the tight bond between the structural model under analysis and a single existing building.
2. Second module (see Chapter 8) concerns the ***Initialization of Input Data for the Structural Analyses***. Steps of this module are aimed at the definition of all of the data needed for structural analyses.
   2*a*) The ***Ground Motion Selection*** step is about the complete definition of the hazard for analysed cluster and for each considered intensity level.

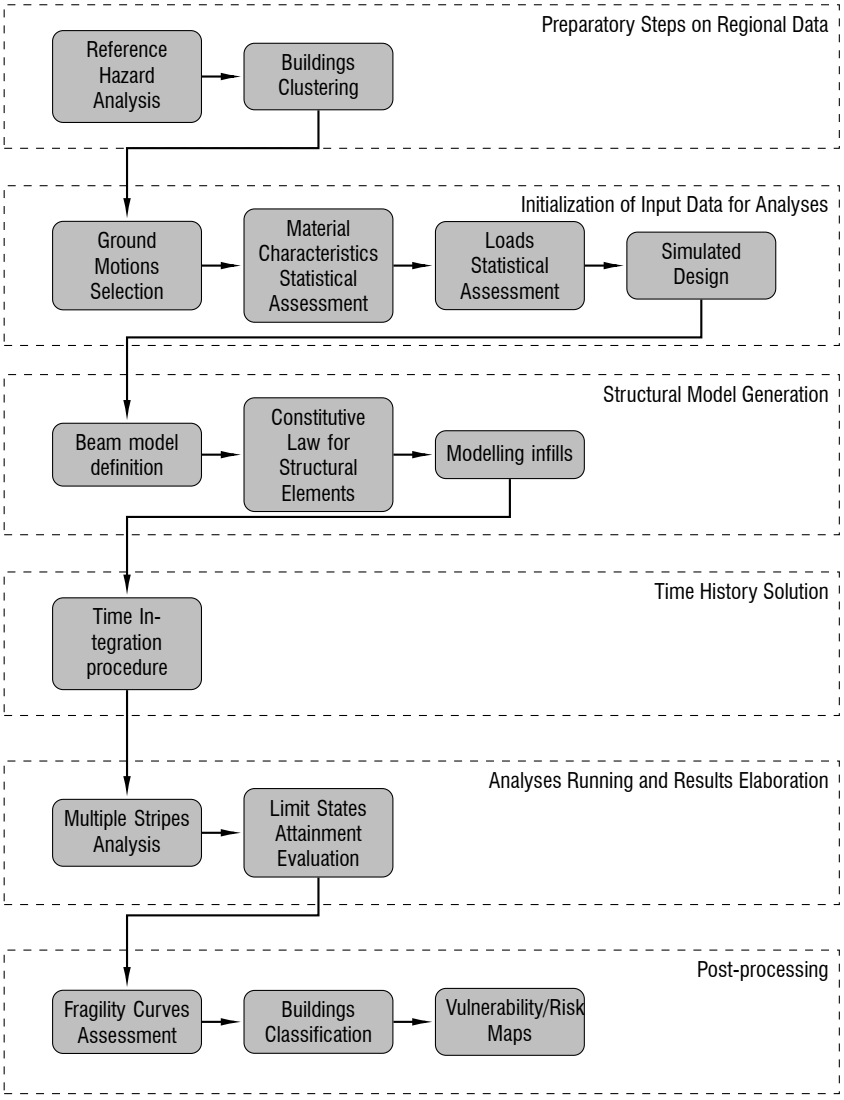

Fig. 6.1 – Synthetic flow chart of procedure steps

Given that the proposed procedure uses non-linear dynamic analyses for its scope, it is clear that a set of ground motions is needed.

2*b*) In the ***Materials Characteristics Statistical Assessment*** step, statistical evaluations on material characteristics are performed. It is indeed clear the impossibility of knowing mechanical characteristics of materials for all of the existing buildings in a given region. However, some statistical analyses

can be carried on starting from available datasets of those characteristics.

2*c*) With the ***Load Statistical Assessment*** step, a statistical description of loads acting on the structure is achieved. Actually, it must be noted that loads have a paramount importance in structural behaviour: statistical assessment is a better description of real conditions than the fixed-value approach usually given in standards.

2*d*) Starting from some of the data collected in previous steps, in the ***Simulated Design*** step remaining data needed for the definition of a structural model are *deterministically* defined. Here, the approach is deterministic rather than probabilistic because some data can be unequivocally defined given the regulations requirements for design in the construction period.

3. Third module ***Structural Model Generation*** (see Chapter 9) covers any step needed to actually generate structural models starting from data collected in the previous module.

3*a*) The first step in this module is the ***Beam Model Definition***, by which the initial elastic behaviour of single structural elements can be fully assessed.

3*b*) In order to assess the post-elastic behaviour of elements, a complete ***Constitutive Law for Structural Elements*** has to be defined, including hysteretic behaviour.

3*c*) Given the characteristics of the proposed procedure, a ***Modelling Infills*** step is needed, in which an opportune model for including their influence over the global structural behaviour is set up.

4. Fourth module (see Chapter 10) is about the ***Time History Solution***: given the model defined in previous module, a solution strategy of the transient non-linear dynamic analysis has to be defined.

4*a*) The ***Time Integration Procedure*** step regards the approach to be used in order to solve the non-linear dynamic analysis problem.

5. Fifth module (see Chapter 11) concerns ***Analyses Running and Results Elaboration***.

5*a*) The ***Multiple Stripes Analysis*** step is aimed at the description of the be-

haviour of the structural model under analysis under increasing seismic action intensity through the Multiple Stripes approach.

5*b*) Once one analysis is completed, a ***Limit States Attainment Evaluation*** step is needed, through the definition of opportune thresholds for each considered limit state.

6. In the sixth module (see Chapter 12), ***Post-Processing*** steps are collected, so that synthetic but significant informations can be given about obtained results.

6*a*) As a first step, a ***Fragility Curves Assessment*** is needed in order to compare the behaviour of different building typologies subjected to seismic actions.

6*b*) In order to effectively compare buildings vulnerability, a ***Buildings Classification*** step is needed: single buildings are to be classified on the basis of their typology and local conditions, so that a comprehensive information on its vulnerability and/or risk can be given.

6*c*) ***Vulnerability/Risk Maps*** are then drawn so that a simple but significant representation of the vulnerability and/or risk distribution in the area under study can be given.

7. PREPARATORY STEPS ON REGIONAL DATA

The proposed procedure has to be preceded by some preparatory activities, needed in order to collect necessary information for subsequent steps.

7.1 Reference Hazard Analysis

The first problem to be solved is related to the reference hazard in the area under study. With ***Reference Hazard*** here is intended the characteristics of the hazard in a given place without considering local modifications, under the hypothesis of rigid and plain ground conditions.

According to the consulted references listed in Chapter 5, this problem was never faced by existing methods.

In general, apart from local conditions (*e.g.* topography and soil conditions), the hazard is still not homogeneous over a given area. Moreover, assuming that the analysed area is *wide*, differences in the reference hazard become significant.

As an example, considering the reference hazard in Italy, local regulations (see NTC2008 Annexes A-B, recalled in NTC2018 §3.2) give in-depth information over hazard on 10751 points that define a reference grid (depicted in Fig. 7.1).

Obviously, considering a wider area the hazard of individual points is a lot more different with respect to others. For regional scale assessments, however, the area is clearly wide. For this reason a problem arises: what hazard is to be considered?

National regulations NTC2018 give for every point of the reference grid for 9 values of the return period (30, 50, 72, 101, 140, 201, 475, 975 and 2475 years) a set of values for a_g, F_0 and T_C^* from which it is possible to derive a spectrum from equations

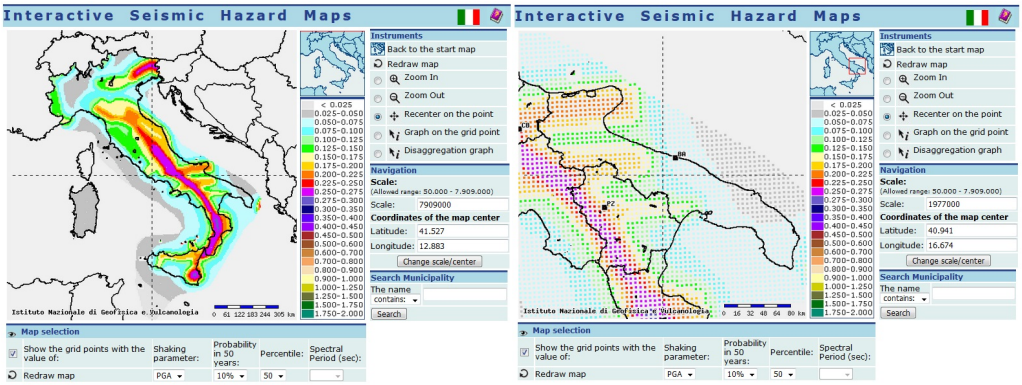

(a) Hazard map for Italy

(b) Hazard map zoomed

Fig. 7.1 – Values of a_g (expected Peak Ground Acceleration) with an exceedence probability of 10% in 50 years from *Interactive Seismic Hazard Maps* n.d. based on Meletti et al., 2007

3.2.2 in NTC2018, that for convenience are reported in Eq. 7.1.

$$0 \leq T < T_B \rightarrow S_e(T) = a_g \cdot S \cdot \eta \cdot F_0 \left[\frac{T}{T_B} + \frac{1}{\eta F_0} \left(1 - \frac{T}{T_B} \right) \right] \tag{7.1a}$$

$$T_B \leq T < T_C \rightarrow S_e(T) = a_g \cdot S \cdot \eta \cdot F_0 \tag{7.1b}$$

$$T_C \leq T < T_D \rightarrow S_e(T) = a_g \cdot S \cdot \eta \cdot F_0 \left[\frac{T_C}{T} \right] \tag{7.1c}$$

$$T_D \leq T \rightarrow S_e(T) = a_g \cdot S \cdot \eta \cdot F_0 \left[\frac{T_C T_D}{T^2} \right] \tag{7.1d}$$

where:

$S_e(T)$ is the spectral acceleration for the period T;

T_C is the period from which constant velocity branch in spectrum starts, and is equal to $T_C = C_C \cdot T_C^*$;

T_B is the period that corresponds to the start of the constant acceleration section of the spectrum, and its value is $T_B = T_C/3$;

T_D corresponds to the start of constant displacement part in the spectrum, and its value is determined from $T_D = 4,0 \frac{a_g}{g} + 1,6$;

S is a factor that takes into account both topographic and soil conditions, being $S = S_S S_T$;

η is a factor for viscous damping not equal to 5%;

S_S and C_C are values that depend mainly on soil category (other than from $\frac{a_g}{g}$ and F_0 the first, from T_C^* the latter);

S_T is a factor that depends on topographic conditions.

Hence, for each of the 10751 cited points of the reference grid, spectra for the 9 values of return period are defined. Moreover, the same national regulation NTC2018 provides a method to interpolate spatially (Eq. 7.2) and with reference to return period (Eq. 7.3), recalling Annex A of NTC2008.

Spatial interpolation of a generic parameter p (that can be a_g, T_C^* or F_0) considers the four vertexes of the reference grid's elementary cell in which is included the point under analysis. Calling p_i the value of p in the i-th vertex (for $i = 1...4$) and d_i the distance between the i-th vertex and the analysed point, the value of p in that point is given by Eq. 7.2.

$$p_i = \frac{\sum_{i=1}^{4} \frac{p_i}{d_i}}{\sum_{i=1}^{4} \frac{1}{d_i}} \tag{7.2}$$

Interpolation for values at a return period T_R not included in the 9 values given by the regulation starts from the nearest return periods T_{R1} and T_{R2}, for which the generic parameters p has respectively values p_1 and p_2, and is made through Eq. 7.3.

$$log(p_i) = log(p_1) + log\left(\frac{p_2}{p_1}\right) \cdot log\left(\frac{T_R}{T_{R1}}\right) \cdot \left[log\left(\frac{T_{R2}}{T_{R1}}\right)\right]^{-1} \tag{7.3}$$

Extrapolations, however, are never permitted.

The problem here is to find a reasonable equilibrium between two extrema:

- Considering the *true* hazard for each point, *i.e.* using spectra given by spatial interpolation for the point where each building in the analysed area is located; this solution, however, would give absolute reliable and accurate results, but is practically infeasible because analyses would have to be made for each building.

- Considering a fixed hazard for all the analysed area, for example using some averaged spectra for subsequent analyses; this solution, that is surely feasible, would give excessively unreliable and inaccurate results, because for buildings in areas with hazard very different from the fixed one the results would have an excessive error.

A solution is to find *homogeneous* subareas in terms of hazard inside the analysed area.

In this work, homogeneity is defined as follows: a point can be considered included in a homogeneous area if spectra associated have values that are never a given percentage different from *central reference* spectra of the homogeneous area. This evaluation is made over ranges of a_g and T as in Eq. 7.4.

$$a_g = [0.2; 0.4; 0.6; 0.8; 1.0; 1.5; 2.0; 2.5]g \tag{7.4a}$$

$$T = [0.1; 0.2; 0.3; 0.4; 0.5; 0.6; 0.7]s \tag{7.4b}$$

Practically, the value of the return period T_R associated to the given value of a_g is found from inverse formulation of Eq. 7.3, and then values of F_0 and T_C^* for that T_R are found from Eq. 7.3 in its original shape. With this procedure, spectra with fixed a_g can be defined.

It is clear that, from now on, return period is not involved. This is because, in this step, what is interesting is the hazard *characteristics*, and not the hazard itself[1].

Having in mind what is the main goal (assessing the seismic vulnerability of *existing residential buildings*), it appears clear that most of the elements of interests (buildings) are concentrated into urban areas. For this reason the points under consideration are

[1] To be clear: if two places have exactly the same spectra but with different return period, still belong to the same homogeneous area; this is because those homogeneous areas are needed for the assessment of fragility curves, that are independent from the hazard itself (that is to be included in successive steps for risk analyses): it only describes how a given building responds to earthquakes of increasing intensity (measured in this work in terms of a_g), without taking into account how much those earthquakes are frequent.

the municipalities city halls inside the area under analysis[2].

The ***Central Reference Spectra*** (CRS) cited before as a reference for a homogeneous area need to be defined. A simple solution could be using an averaged spectrum for a given value of a_g between the spectra of all the points. However, in this work another solution is adopted, and its reason is defined through an example intentionally simple and extreme.

Consider that an homogeneous area includes only two cities. City A has $B_A = 10'000$ buildings under analysis while city B only $B_B = 1'000$. Consider that the CRS can be described by a single number, *e.g.* spectral acceleration S at a given T and for a fixed a_g, and that for city A this value is 0.9 while for city B is 1.1. Running analyses with the average value (1) would give a homogeneous error for all 11'000 buildings equal to 10%. However, in order to reduce the global error, it is reasonable to take a value closer to 0.9 (that is the true value for most of the buildings under analysis). For this reason, this value is weighted as in Eq. 7.5.

$$S_{ref} = \frac{S_A \cdot B_A + S_B \cdot B_B}{B_A + B_B} = \frac{0.9 \cdot 10'000 + 1.1 \cdot 1'000}{10'000 + 1'000} = 0.918 \tag{7.5}$$

With this solution, the reference value would be 0.918, so that for 10'000 buildings the error is 2% while for 1'000 is 20%. The Sum of Squared Errors (SSE) in this case is 36.36, while for the previous case it was 110.

Out of the example, in the procedure, this weighting is applied to every spectral value found for the ranges in Eq. 7.4. Moreover, seen that it is not easy to know how many residential buildings are inside a municipality, the weighting is made over the population (assuming that there is a perfect correlation between the two).

In conclusion, it must be noted that the whole process is intensively iterative, and is tightly connected to the starting point. In fact, once a municipality is added to a homogeneous area, its CRS changes and could happen that some municipalities previously included do not meet anymore homogeneity condition.

[2]This assumption corresponds to the simplification to collapse the hazard of all buildings into the hazard of the point where the city hall of its municipality is located. However, this simplification does not introduce a huge error, considering that a urban area does not have an extent so that significant variations of the hazard occur.

7.2 Buildings clustering

In order to effectively assess the seismic vulnerability of a huge number of buildings, it is convenient to organize those buildings into homogeneous clusters.

Within this context, some rapid surveys in the area under study are needed so that recurrent building typologies can be identified. However, some tools are very useful for accomplishing this task.

One of those tools is surely the service *StreetView* by *Google Maps* (n.d.), that can straightforwardly replace at least partly the survey step. In fact, according to the rapidity of surveys required by a large scale approach, there is no need to collect in-depth data, so that a virtual survey can be at least a partial solution.

Another useful tool is given by National Civil Protection (DPC - Dipartimento della Protezione Civile), that funded a research in the context of ReLUIS (*"Rete dei Laboratori Universitari di Ingegneria Sismica"*, *Network of Seismic Earthquake Universitary Laboratories*) 2014-2016 projects named *"Inventario delle tipologie strutturali ed edilizie esistenti"* (*Inventory of existing structural and architectural typologies*). This tool is the ***CARTIS form*** (Fig. 7.2), together with the methodology that is behind the form aimed at typologies assessment. A description of the form and of its goals is given in Zuccaro et al. (2015), and its usefulness is demonstrated by its use in various large-scale assessments as in Uva, Leggieri, et al. (2019), Olivito et al. (2019), Polese, d'Aragona, et al. (2019), and Polese, Di Ludovico, et al. (2020).

Another important source of information is given by the last national census (*15° Censimento Generale della Popolazione e delle Abitazioni* 2011), whose aggregate data can be downloaded from the site of ISTAT (*"Istituto Nazionale di Statistica"*, *National Institute of Statistics*). Cited data comprise some that can be very useful in the context of building clustering (and not only), *e.g.* construction year range, number of floors, structural typology.

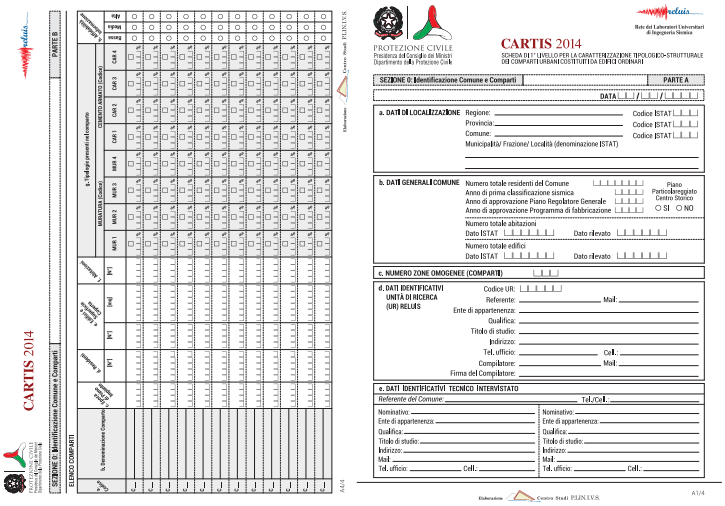

(a) CARTIS Section 0: Identification of Municipality and General Information

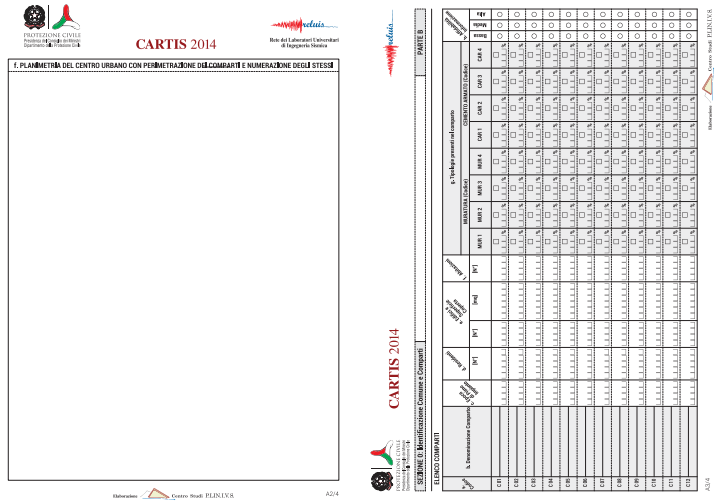

(b) CARTIS Section 0: Identification of Municipality and Compartments

Fig. 7.2 – Cartis Form

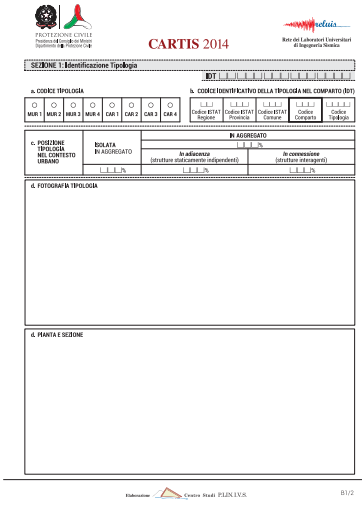

(c) CARTIS Section 1: Identification of Building Typology

(d) CARTIS Section 2: General Characteristics of Building Typology

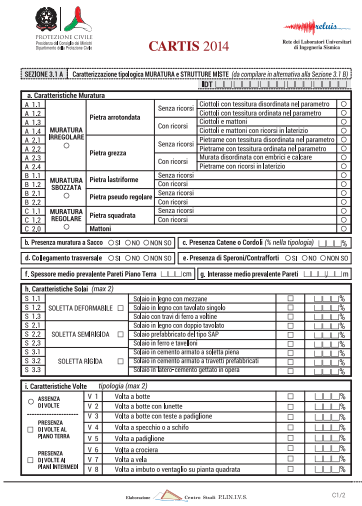

(e) CARTIS Section 3: Characteristics for Masonry Buildings

(f) CARTIS Section 3: Characteristics for Masonry Buildings (contd.)

Fig. 7.2 – Cartis Form

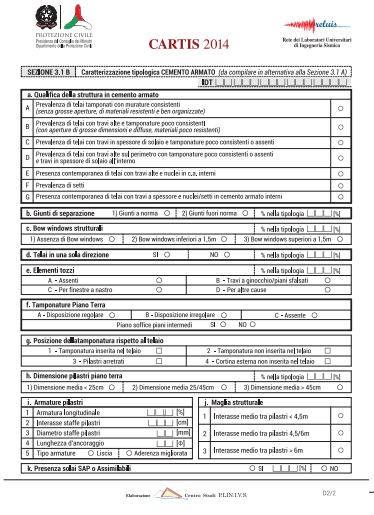

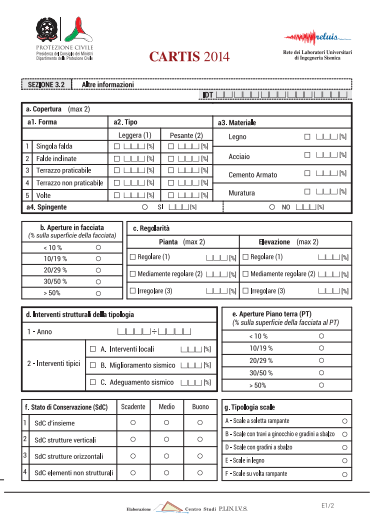

(g) CARTIS Section 3: Characteristics for RC Buildings

(h) CARTIS Section 3: Other Informations

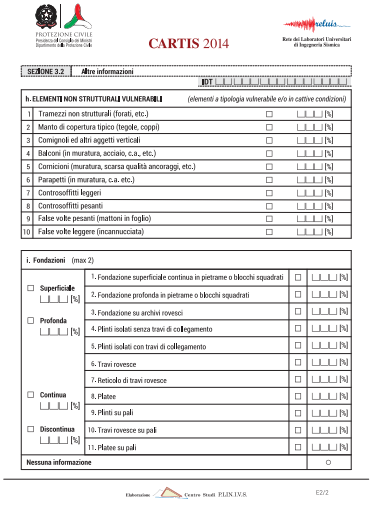

(i) CARTIS Section 3: Other Informations (contd.)

Fig. 7.2 – Cartis Form

7.2.1 The SOCRATES tool for collecting buildings informations

Together with the CARTIS form, that gives an important contribution to the problem of building clustering, another tool was developed. This tool is the ***SOCRATES online form*** (**S**ite-based **O**rganised **C**ollection of data for **R**isk **A**ssessment of a **T**erritory's **E**xisting **S**tructures), whose features are synthetically presented in Fig. 7.3.

As per Fig. 7.3a, the first step is the selection of a municipality (so far only municipalities in Puglia region are implemented). Once a municipality is selected, elements representing the contours of existing buildings of the municipality are loaded onto the map, which are taken from *CTR maps* (*"Carte Tecniche Regionali"*, Regional Technical maps) downloadable from *SIT Puglia* (n.d.).

Selecting one of the buildings in the municipality, the form changes (see Fig. 7.3b and Fig. 7.3c) in order to let the user to insert a set of data about the building itself. Some subsections of the form are initially hidden, and only appear when a condition is met (*e.g.* some information that only has sense for RC buildings appear only if selected structural typology is RC building, as in Fig. 7.3d).

An overview of input data of **SOCRATES** form is given in Tab. 7.1, where also dependencies are shown.

Tab. 7.1 – An overview of **SOCRATES** input data

Input data	Brief description	Notes
Construction year	Estimated construction year of the building	
Main use	*e.g.* residential, commercial, productive, strategic, etc	
Utilization	Percentage of building use (in percentage)	
Dangerous contents	Presence of dangerous elements for public health and/or environment	Visible only if *main use* is productive, strategic, storage or other
Structural system	*e.g.* Masonry, RC, steel	
Main use variation	Changes in the main use of the building	
Originary use	If its use changed, previous main use	Visible only if *Main Use Variation* is checked
Superelevation	Presence of superelevation (subsequent to original construction)	
Added structures	Added structural bodies (after original construction)	
Structural adjustments	Structural global adjustments on the building	

Continued on next page

Tab. 7.1 – continued from previous page

Input data	Brief description	Notes
Local adjustments	Structural *local* adjustments (*e.g.* only for a limited number of structural elements)	
Adjacency	Structural connection with surroundings structures	
Structural joints	Adequate structural joints with surrounding structures	Visible only if *Adjacency* is set to "with joints"
Topography	Topographic position (*e.g.* in plain or on a slope)	
Distance from street	Distance of building contour from the nearest street	
Shape	Plan shape (*e.g.* rectangular, L-shaped, C-shaped)	
Floors	Number of floors	
Underground Floors	Number of underground floors	
Storey height	Average height of typical storey	
First storey height	Height of the first storey	
Offset between floors	Presence of offset between floors	
Smaller last floor	Presence of last floor with smaller covered area	
Last floor surface	Covered area of last floor	Visible only if *Smaller last floor* is checked
Geometric details	*e.g.* average distance between structural elements, number of structural elements in a facade, etc	Visible only if *Shape* is set
Slab constructive typology	*e.g.* solid concrete, hollow slab, concrete-brick combo, etc	
Slab thickness	Average thickness of slabs	
Slabs structural orientation	Structural orientation of slabs (for 1-direction typologies)	Hidden if *Slab constructive technology* is set to "vaults"
Vault typologies	Typology of vaults	Visible only if *Slab constructive technology* is set to "vaults"
Roof typology	*e.g.* plain or pitched	
Roof structural material	*e.g.* RC, masonry, etc	
Roof details	*e.g.* insulation, typical roof, etc	
Infill thickness	Average infills thickness	
Infill structural typology	Infills connection with structural elements	Hidden if *Structural system* is set to "Masonry"
Opening percentage	Average openings percentage over infills surface	
1st floor openings percentage	Average openings percentage at 1st level	
Infill insulation	Information on insulation in infills	
Stairs structural typology	*e.g.* hanging steps, on a valut, independent etc	
Stairs structural material	*e.g.* RC, wood, etc	Hidden if *Stairs structural typology* is set to "independent"
Stairs position	Stairs position with respect to symmetry over building shape	Hidden if *Stairs structural typology* is set to "independent"
Elevator	Presence of a elevator	
Elevator position	Elevator position with respect to symmetry over building shape	Visible only if *Elevator* is checked
Non-structural elements	*e.g.* window bands, chimneys, balconies	

Continued on next page

Tab. 7.1 – continued from previous page

Input data	Brief description	Notes
Damage and deterioration	Visible damages and deterioration entity and extent	
Foundation system	Foundation system typology	
Masonry typology	Structural masonry typology	Visible only if *Structural system* is set to "Masonry" or "Mixed RC-Masonry"
Hollow walls	Masonry with internal cavity, eventually filled with worse material	Visible only if *Structural system* is set to "Masonry" or "Mixed RC-Masonry"
Aligned openings	Check if exist continuity of structural masonry from foundation to roof	Visible only if *Structural system* is set to "Masonry" or "Mixed RC-Masonry"
Masonry general information	*e.g.* lodges, masonry toothing, etc	Visible only if *Structural system* is set to "Masonry" or "Mixed RC-Masonry"
RC structural typology	*e.g.* framed, with shear walls, mixed	Visible only if *Structural system* is set to "RC" or "Mixed RC-Masonry"
Shear walls thickness	Average thickness of shear walls	Visible only if *Structural system* is set to "RC" or "Mixed RC-Masonry" and *RC structural typology* is not set to "framed"
Shear walls length	Average length of shear walls	Visible only if *Structural system* is set to "RC" or "Mixed RC-Masonry" and *RC structural typology* is not set to "framed"
Rebars typology	*i.e.* smooth or corrugated	Visible only if *Structural system* is set to "RC" or "Mixed RC-Masonry"
Column width	Average RC column width	Visible only if *Structural system* is set to "RC" or "Mixed RC-Masonry" and *RC structural typology* is not set to "shear walls"
Deep beam height	Average RC deep beam height	Visible only if *Structural system* is set to "RC" or "Mixed RC-Masonry"
Flat beam width	Average RC flat beam width	Visible only if *Structural system* is set to "RC" or "Mixed RC-Masonry"

It is worth highlighting some features of input data presented in Tab. 7.1. As one can see, most of input data of the CARTIS form (Fig. 7.2) are here collected. Some more data, however, are added.

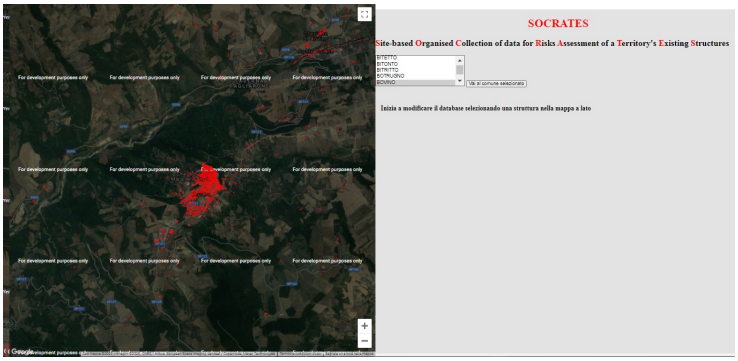

(a) SOCRATES Municipality selection page

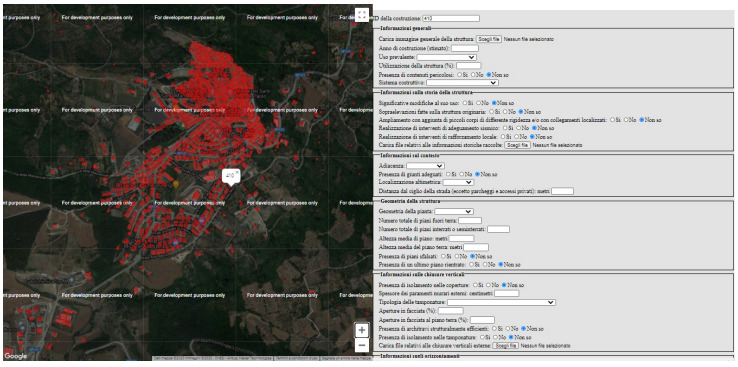

(b) Individual building characteristics form

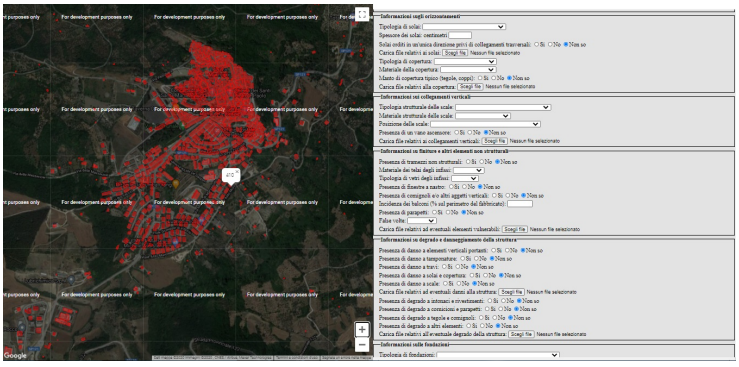

(c) Individual building characteristics form (contd.)

Fig. 7.3 – The **SOCRATES** online form: an overview of its features

As it is clear looking at data in Tab. 7.1, with **SOCRATES** form it is possible to collect data that are not strictly related to seismic vulnerability assessment(*e.g.* insulation data, distance from street). The reason behind this choice is to be found in a simple

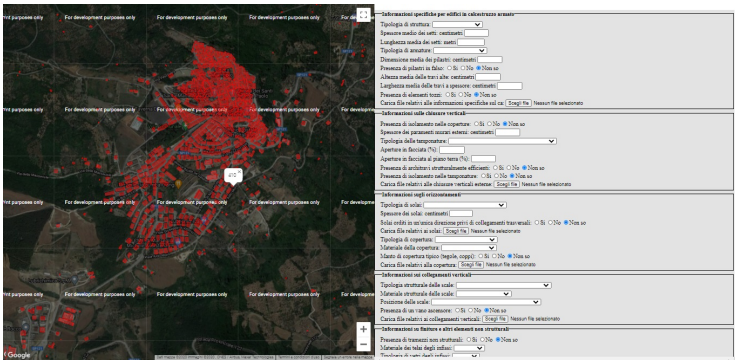

(d) Individual RC building characteristics form

Fig. 7.3 – The **SOCRATES** online form: an overview of its features

consideration: once a survey is made, there is the possibility to collect a lot of other information without further effort, that anyway can be useful to other researchers or for future developments. For instance, insulation information was added thinking at energetic assessments; distance from street was added as it can be useful for eventual deepening of seismic risk assessment over urban ways of communication (that undoubtedly play a fundamental role in emergency management).

Other data included in the **SOCRATES** form and that need further explaining are those about steel rebars: in Tab. 7.1 it can be seen the presence of the *Rebar typology* field, intended to collect the information about the reinforcing bars being smooth or ribbed. This information could appear unachievable in a rapid screening context as the one assumed here, and this is true most of the time. However, sometimes the deterioration of structural elements surfaces reaches such a degree that reinforcing rebars are exposed and visible (see Fig. 7.4). In those cases, cited field could be filled: it is not rational neglecting a valuable information as that on rebars typology, relevant especially in regional analyses.

It is worth highlighting that this tool, while developed together with the proposed approach that is the subject of the present work, is not tightly connected with it: given the absolute generality of the **SOCRATES** tool, in fact, it can be used for a wide range of applications, *i.e.* whenever regional data need to be retrieved through rapid surveys. This ductility of the procedure, hence, has been developed on purpose: it appears to be

Fig. 7.4 – Examples of highly corroded existing columns, so that reinforcement bars are exposed (from Iovino et al. (2014))

more rational the standardization of data collecting within a single tool, so that a single survey can be useful for a wider range of applications.

The not-necessary connection of the **SOCRATES** tool with the rest of the procedure has also another consequence: if the **SOCRATES** tool can be used within other approaches, the proposed approach can be used with other data collecting tools, being sufficient that it provides needed data for the procedure.

8. INITIALIZATION OF INPUT DATA FOR THE STRUCTURAL ANALYSES

Once preprocessing steps are ended, it is necessary to organize input data in a consistent statistical framework. Assuming that a given building cluster and homogeneous hazard area are selected, following steps are needed.

8.1 Ground Motion Selection

One of needed steps for the preparation of input data is the ground motion selection, on the basis of the seismic hazard defined in Section 7.1.

The reason of this step is to be found in the necessity to perform non-linear dynamic analyses, aiming at including seismic input uncertainty into the assessment.

Several ground motion databases are today available, *e.g.* the European Strong Motion (ESM) database (Lanzano et al., 2019), or the PEER NGA-West2 database (Ancheta et al., 2013). However, a problem arises in how to collect a representative set of accelerograms coherently with the seismic hazard of the area under study. Several researchers faced this problem, and general review of available approaches together with an in-depth analysis of some critical issues in selection and manipulation of ground motions can be found in Iervolino and Manfredi (2008) and Katsanos et al. (2010) amongst other works.

In this context, several works were made proposing tools for ground motion selection, *e.g.* REXEL by Sgobba et al. (2019), GCIM Ground Motion Selection Software by Bradley (2010), DGML by Youngs et al. (2007) and OPENSIGNAL by Cimellaro et al. (2015).

Amongst all tools developed for ground motion selection, in this work the Conditional Spectrum ground motion selection software by Baker and Lee (2018) is used. Beyond its clear importance in the present time research, one of the main reasons for

this selection is the availability of the source code of the software. In fact, in order to introduce a ground selection tool in the **EX:MIRIAM** procedure, it must be as much customizable and automatable as possible (and those, indeed, are features clearly possessed by an open-source tool).

For instance, the tool had to be modified in order to switch from a scenario-based selection (as for original tool, see Baker and Lee (2018)) to a fixed spectrum one.

8.2 Materials characteristics statistical analysis

In order to effectively assess the seismic vulnerability of a given building cluster, it is necessary to identify how materials characteristics are probabilistically distributed. In fact, the evaluation of this parameter at a building level would need extensive in-site tests on structural elements, and this is indeed not coherent with present work purpose.

With respect to steel characteristics, a useful study is available from Verderame, Ricci, Esposito, et al. (2011). In cited work, a population of 10'331 results of tests on steel for RC structures between 1950 and 1980 is scanned. As a result, distribution of both steel classes used in that period and of mechanical characteristics is given (see Fig. 8.1).

Obviously, the use of that results implies that homogeneity of underlying data with what would be found in the area under investigation is assumed. It must be noted that data used from authors come from tests made by laboratory of University of Naples *Federico II*, so that data can be assumed representative of an area around Naples.

For concrete characteristics a similar work does not exist, so other evaluations have to be made. A help in this effort is given by a database of concrete tests made by private laboratories, available at *DICATECh* department of Polytechnic University of Bari.

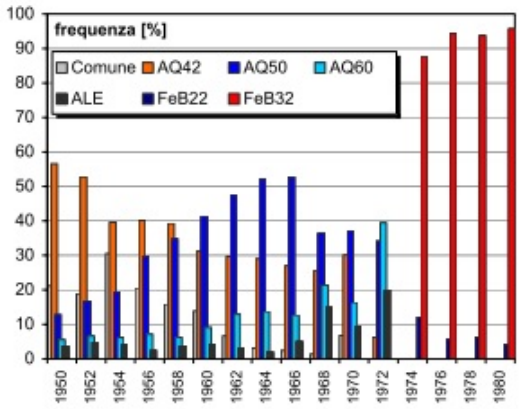

Fig. 8.1 – Steel classes usage between 1950 and 1980 (from Verderame, Ricci, Esposito, et al. (2011))

8.3 Load statistical assessment

In the statistical framework of this work, also loads have to be treated statistically.

8.3.1 Permanent loads assessment

Given that permanent loads have low variability, their values are taken as respective expected values. Indeed structural elements, finishes, infills usually are not strongly modified in a residential building.

For this reason, given its typology, loads for each of the elements previously cited can be uniquely defined.

8.3.2 Variable loads assessment

Considering that only residential buildings are here considered, the load distribution to be determined is the one for *residential use areas*, classified as *category A* in NTC2018 art.3.1.4. This category is further divided into 2 subcategories: the first (here referred to as *A1*) for proper residential areas, the second (*A2*) for areas likely to be crowded (*e.g.* common areas as stairs, balconies, etc).

Tab. 8.1 – Characteristic and expected values of distributed loads for residential areas

Load category	**Characteristic value** (95th percentile) $[kN/m^2]$	**Expected value** (50th percentile) $[kN/m^2]$
A1	2.00	0.60
A2	4.00	1.20

For each category, NTC2018 gives the characteristic (95th percentile) value of the distributed load (in table 3.1.II) and the factor ψ_{2j} that, multiplied with characteristic value of the load q_{kj}, gives the expected value for that load $q_{mj} = \psi_{2j} \cdot q_{kj}$.

For the category under analysis, $\psi_{2j} = 0.3$. Both characteristic and expected values for distributed load are summarized in Tab. 8.1.

Supposing that loads values during time distribute according to a log-normal distribution, it is possible to infer load distribution characteristics through some statistical assessments.

In particular, in a normal distribution the relation in Eq. 8.1 between expected and characteristic values through standard deviation exist.

$$V_m = V_k - 1.64\sigma \tag{8.1}$$

Considering that *logarithms* of load values are assumed to be normally distributed, in Eq. 8.2 the same relation is expressed.

$$log\left(q_{mj}\right) = log\left(q_{kj}\right) - 1.64\sigma \tag{8.2}$$

Being known from Tab. 8.1 values of both q_{mj} and q_{kj}, it is possible to evaluate standard deviations of logarithms for both categories A1 and A2 as in Eq. 8.3.

$$\begin{aligned} \sigma_{A1} = & \quad \frac{log(2.00) - log(0.60)}{1.64} = \quad 0.734 \\ \sigma_{A2} = & \quad \frac{log(4.00) - log(1.20)}{1.64} = \quad 0.734 \end{aligned} \tag{8.3}$$

8.3.3 Mass eccentricity statistical assessment

Another parameter to take into account is the eccentricity of masses due to cited loads. In fact, while those loads are usually modelled as uniformly distributed over floor areas, in reality uniform distribution is not perfectly achieved, bringing to accidental eccentricity of loads with respect to the geometrical floor center.

In NTC2018 art.7.2.6 for design purposes this accidental eccentricity is required to be considered at least 5 % of the building plan dimension measured perpendicularly with respect to assumed direction of seismic action.

Assuming that, as for much of the design provisions, given value is a characteristic one (95th percentile), given that accidental eccentricity can be considered normally distributed with mean 0, standard deviation of its distribution can be computed through Eq. 8.1 as in Eq. 8.4.

$$\sigma_e = \frac{5-0}{1.64} = 3.05\% \tag{8.4}$$

8.4 Input data usage for structural analyses

Once the statistical representation of input data is assessed, it is necessary to translate this information into a set of structural analyses in order to evaluate the statistical distribution of structural response of given building typology under seismic actions.

In present work, a *Monte Carlo approach* is used. For instance, a value is defined for each of the data described in previous sections from their statistical distribution, so that a ***realization*** (*i.e.* a *virtual* possible building belonging to the building cluster under analysis) is defined.

Structural analyses are then run on models of those realizations: if a *sufficiently numerous* realizations are analysed, results can be assumed to be statistically representative of the population of buildings under analysis.

In particular:

- General data of the building realization is defined through its cluster limits on those

data (from Section 7.2, *i.e.* construction year, geometrical features), assuming a uniform distribution amongst cited limits given the unavailability of data on their statistical distribution.

- Mechanical characteristics of materials (Section 8.2) and loads (Section 8.3) are defined selecting a randomly generated value according to their statistical distributions.
- A ground motion from those defined in Section 8.1 is randomly selected in order to be applied to the building realization.

8.5 Simulated design

Starting from data selected according to Section 8.4, some other needed data can be defined within a deterministic approach rather than a probabilistic one as made until now.

Having in mind the design standard procedure at the time of building realization construction, it is possible to simulate its design in order to assess some data: it is not rational to treat in a statistical way those data (*e.g.* elements dimensions and rebars) that is possible to define deterministically with sufficient reliability.

From those premises, it is clear the necessity of a review of standard design procedures of the past, with reference to both regulations and manuals. In this context a paramount importance has the history of seismic-related provisions, both regarding the classification of seismic hazard of the area under study and the law requirements for seismic detailing.

8.5.1 Overview of past regulations in Italy

For the purposes of the present work, it can be assumed that the significant part of structural regulations history start with the XX century (while first seismic regulations can be traced back at least to XVII century), under the more than probable assumption that no residential RC existing buildings are traced farer from that date.

D.M. 10/01/1907 can be considered as the first structural regulation in Italy. In fact, for the first time it was required that a structural design made by an engineer was at the basis of the construction phase (Annex B art.1). However, those prescription were only valid for public structures. It was fixed a minimum tested compressive strength for concrete of $150kg/cm^2$ (art.7). Tested tensile strength of reinforcement steel was limited to be between 36 and $45kg/mm^2$ (art.8). For design purposes, variable load was prescribed to be incremented of 25% (art.22); ratio between Young modulus of reinforcing steel and concrete was fixed in $n = 10$ being the latter $E_c = 200t/cm^2$ (art.23); admissible stresses were fixed to be $\frac{1}{5}$ of tested strength for concrete in compression, $1000kg/cm^2$ for reinforcing steel under compression or tension and $800kg/cm^2$ in shear related computations (art.27).

An important event in history of italian seismic regulation is for sure the 1908 Messina earthquake. As a consequence of that event, R.D. 18/04/1909 was emitted, which contained prescriptions on structural requirements of building in hit areas. Prescriptions, however, were not always fully indicated: as an example, in art.24 were prescribed an increase of vertical load and the application of horizontal accelerations to masses, without numerical data.

Subsequent regulations gave further details for design purposes. As an example, in D.L. 05/11/1916 art.229 for design of buildings in municipalities hit by 1908 Messina earthquake, an increase of 50% on both permanent and variable loads was prescribed. Horizontal (F_h) forces had to be applied to each floor, whose value was a given fraction of total weight of said floor (W_i): $F_h = \frac{1}{8}W_i$ for first floor, $F_h = \frac{1}{6}W_i$ for all of other floors. Those prescription were valid for municipalities directly hit by previously cited earthquake, in the provinces of Messina, Reggio Calabria and Catanzaro.

In R.D. 23/10/1924 art.28 design parameters were confirmed, while it is explicitly stated that the increase of vertical loads and horizontal forces did not have to be considered as acting together, but as two separate load patterns.

In R.D. 13/03/1927 municipalities in national territory were divided into two categories: 1st category collecting high seismic hazard areas, and 2nd category for moderate seismic hazard areas. However, most of the national territory was still assumed

to be not seismic at all. As per art.28, for 1st category the increase of 50% of vertical loads was confirmed, while for 2nd category it was set to $\frac{1}{3}$. For 1st category was also confirmed the ratio between horizontal force and weight of a given floor ($\frac{1}{8}$ for 1st floor, $\frac{1}{6}$ for others), while for 2nd category this value was set to $\frac{1}{10}$ for the 1st floor and $\frac{1}{8}$ for others. A minimum dimension of column was set to 30x30cm. Increase in vertical load and horizontal forces were confirmed as two separate load patterns.

In R.D. 03/04/1930 art.31 confirms what prescribed by previous standards, while it was clearly stated that reduced ratio between horizontal force and floor weight is valid not only for 1st floor but also eventual underground floors.

In R.D. 29/07/1933 some general provisions are given. In art.13 a minimum value for tested compressive strength of concrete was set in $450kg/cm^2$, while for strengths higher than $600kg/cm^2$ the concrete had to be labelled as *high resistance*. For design purposes, admissible compressive stress was set in art.17 as the minimum between $\frac{1}{4}$ of tested strength and $40kg/cm^2$ (for mainly compressed elements) or $50kg/cm^2$ (elements under bending action), while for high resistance concrete those limit values were respectively $50kg/cm^2$ and $65kg/cm^2$. Tensile strength of steel for reinforcing bars was set to be between 38 and $50kg/mm^2$ in art.16, while for design purposes in art.18 admissible tensile stress was set to $1200kg/cm^2$. As per art.20 variable loads had to be increased by 25%. Ratio between Young modulus of reinforcing steel and concrete was set to be $n = 10$ in art.21, being the latter $E_c = 200t/cm^2$. In art.29 maximum reinforcement ratios were given: 1% of column minimum required area $A_{c,req}$ for column gross area $A_c < 1600cm^2$,0.7% of $A_{c,req}$ for $A_c > 6400cm^2$, linearly interpolated for other values.

In art.30 of R.D. 25/03/1935 design parameters are modified. For instance, the increase in vertical loading was reduced from 50% to 40% for 1st category and from $\frac{1}{3}$ to 25% for 2nd. Also ratios between horizontal forces and floor weights were reduced, and uniformed with respect to the floor level, becoming 0.10 for 1st category and 0.07 for 2nd. When computing floor weight, however, a reduction on variable load was introduced: for instance, it was reduced up to $\frac{1}{3}$ of its value, but with the limitation that the global load could not be less than $\frac{2}{3}$ of the global load with maximum value of variable

load.

In R.D. 22/11/1937 art.5 admissible tensile strength of reinforcing steel was increased to $1400kg/cm^2$ from $1200kg/cm^2$ of R.D. 29/07/1933 for *ferro omogeneo*, and a new steel class was introduced (*acciaio semiduro*) with admissible tensile strength of $2000kg/cm^2$. In art.31 the vertical load was augmented by 40% but assuming variable load reduced by $\frac{1}{3}$ in 1st category, by 25% again with $\frac{1}{3}$ of variable load for 2nd category; in both cases total load could not be less than the untouched total load. Horizontal forces were still computed as a ratio of floor weight, whose value were computed considering $\frac{1}{3}$ of variable load, while limitations on this value were dropped. For 1st category cited ratio was kept equal to the previous provision (0.10), while for 2nd category was reduced from 0.07 to 0.05.

R.D. 16/11/1939 n.2228 in art.4 gave higher limitations on tested concrete strength ($> 500kg/cm^2$ instead of 450 in R.D. 29/07/1933 for Portland concrete, $> 680kg/cm^2$ instead of 600 for high resistance concrete).

In R.D. 16/11/1939 n.2229 a comprehensive set of prescriptions were given for RC structures. In art.17 tested tensile strength of reinforcing steel was limited to be between 42 and $50kg/mm^2$ for *acciaio dolce* (increased from $38 \div 50$ range in R.D. 29/07/1933 for *ferro omogeneo*) with yielding stress $> 23kg/mm^2$, between 50 and $60kg/mm^2$ with yielding $> 27kg/mm^2$ for *acciaio semiduro*, between 60 and $70kg/mm^2$ with yielding at $> 31kg/mm^2$ for the newly defined *acciaio duro*. In art.18 admissible stresses for concrete were given, being $35kg/cm^2$ for uniform compression and $40kg/cm^2$ for bending (respectively increased to 45 and $50kg/cm^2$ for high resistance concrete). In art.19 admissible stress for reinforcing steel was set, confirming the values given in R.D. 22/11/1937 ($1400kg/cm^2$ for *acciaio dolce* and $2000kg/cm^2$ for *acciaio semiduro*, extended also to *acciaio duro*). In art.22 ratio between concrete and reinforcing steel Young modulus were confirmed to be $n = 10$ for Portland concrete (R.D. 29/07/1933), and $n = 8$ for high resistance concrete. Art.30 modified reinforcing limits for columns previously set in R.D. 29/07/1933: 0.8% of minimum required area for $A_c < 2000cm^2$, 0.5% for $A_c > 8000cm^2$ with linear interpolation for other values.

C.M. 23/05/1957, while not mandatory in case law, introduced the use of ribbed

bars. Reinforcement steel classes were renamed in *Aq.42* (*acciaio dolce*), *Aq.50* (*acciaio semiduro*) and *Aq.60* (*acciaio duro*), where numbers were minimum ultimate tensile strength in kg/mm^2. Admissible stresses were fixed to be the minimum between 14, 16 or $18kg/mm^2$ for the three steel classes and 50% of yielding stress. For ribbed bars admissible tensile stress was limited to be at most the minimum between 40% of ultimate strength, 50% of yielding stress and $22kg/cm^2$.

In L. 25/11/1962 for structures in non-seismic areas was fixed an inferior limit for variable loads (set to $200kg/m^2$ in art.4). For both 1st and 2nd category the previously prescribed increase of vertical loads for modelling vertical seismic action was excluded; ratio between horizontal forces and floor weight was again increased to 0.07 for 2nd category (being still 0.10 for 1st), keeping the reduction of variable loads to $\frac{1}{3}$ of its value for this computation.

D.M. 30/05/1972 represented a major modification in structural design procedure. In art.2.3 concrete were organized in classes (150, 200, 250, 300, 400, 500) based on characteristic compressive strength R_{bk} in kg/cm^2, and admissible stress was fixed in $\sigma_c = 60 + \frac{R_{bk}-150}{4}$ (reduced by 30% in uniformly compressed sections). Art.2.5 set prescriptions on reinforcement steel: two classes of steel for smooth bars were defined (*FeB22* and *FeB32*) from their characteristic yielding stress 22 and $32kg/mm^2$, with admissible stress of 12 and $16kg/mm^2$ respectively; for ribbed bars three classes were defined (*A38*, *A41* and *FeB44*), again with the number representing yielding stress, having admissible stress of 22, 24 and $26kg/cm^2$ respectively. Ribbed bars had to be used only with concrete having $R_{bk} > 250kg/cm^2$. Ratio between Young modulus of materials were fixed in $n = 10$, while also the value $n = 15$ were accepted (art.2.6). Young modulus of concrete was fixed in $E_c = 18'000\sqrt{R_{bk}}$ (in kg/cm^2, art.2.10). Limitations in reinforcement ratio of columns included also a maximum limit and it was no more dependent on A_c: it had to be at least the maximum between 0.6% of minimum required area and 0.3% of effective area, with a maximum of 5% of minimum required area (art.2.12).

In D.M. 03/03/1975 the dynamic characteristic of earthquake was introduced via a response spectrum dynamic analysis (art.B.6). A static analysis, however, was still

possible (art.C.6.1) with the application of a system of horizontal forces $F_h = K_h \cdot W_i$, being $K_h = C \cdot R \cdot \epsilon \cdot \beta \cdot \gamma_i$, $C = \frac{S-2}{100}$, $S \geq 2$ seismicity index, R a *response coefficient* being $R = \frac{2}{3}\frac{0.862}{T_0}$ if fundamental period of structure $T_0 > 0.8s$ or $R = 1$ otherwise, ϵ coefficient for soil influence (usually $= 1$), β structural coefficient (usually $= 1$), $\gamma_i = h_i \frac{\sum W_j}{\sum W_j h_j}$ coefficient for force distribution, W_i floor weight (computed reducing variable loads with a factor of 0.33). Fundamental period of structure could be computed in a simplified way through equation $T_0 = 0.1\frac{H}{\sqrt{B}}$ (H height and B minimum dimension in plan, both in m). Vertical forces due to earthquake were no more considered except in some particular cases (art.C.6.1.3). The seismicity index S, that was meant to be an indirect measure of seismic hazard, was fixed to be $S = 12$ for 1st category and $S = 9$ for 2nd.

D.M. 16/06/1976 confirmed most of the provisions given in the previous technical standard D.M. 30/05/1972 (*e.g.* admissible stress of concrete, its division in classes, etc). With respect to D.M. 30/05/1972, steel for reinforcement bars were modified: while steel for smooth bars were keep unchanged, for ribbed bars a class were dropped (*A41*) and one renamed (from *A38* to *FeB38k*). Other steel classes were only renamed by adding *k* (*e.g.* from *FeB22* to *FeB22k*). The limitation on the use of concrete of at least $R_{bk} = 250kg/cm^2$ with ribbed bars was dropped.

In D.M. 26/03/1980 all previous prescriptions on materials were confirmed. In art.3.1.1 only the homogeneization ratio $n = 15$ was kept, so that the value of $n = 10$ was no more usable. Limitations on concrete reinforcement ratio were increased: reinforcement area could be at least the maximum between 0.3% of effective concrete area and 0.8% of the minimum required concrete area, and no more than 6% of effective area. Subsequent regulations(*i.e.* D.M. 01/04/1983, D.M. 27/07/1985, D.M. 14/02/1992), at least for prescriptions of interest for present work, did not include novelties.

D.M. 19/06/1984 introduced an *importance factor*, at least equal to $I = 1.1$, to be applied to earthquake equivalent forces. The response coefficient was defined to be $R = \frac{0.862}{T_0^{2/3}}$. All other prescriptions from previous standard D.M. 03/03/1975 were recalled.

In D.M. 24/01/1986 the minimum value of importance factor was set to $I = 1$, while all other prescriptions were confirmed.

In 1996 D.M. 09/01/1996 and D.M. 16/01/1996 overcome all previous prescriptions. However, for present work purposes, years subsequent to those regulations are considered to be outside the period of interest.

8.5.2 Summary of past regulations for design

In order to complete the insight on past design practices, a comprehensive summary of cited rules is presented in Tab. 8.2 and Tab. 8.3.

Regarding variable loads, while L. 25/11/1962 set as mandatory a value of $200kg/m^2$, oldest manuals agree setting a value between 150 and $180kg/m^2$ for residential buildings (see *e.g.* Colombo (1890), Colombo (1895) and Barro (1934)). However, the use of a value of $200kg/m^2$ can be traced back at least to 1950s (RDB (1956)).

Tab. 8.2 – Summary of past design practices

Year	Concrete	Steel $[kg/mm^2]$	Column reinforcement
1909	$\sigma_c = \frac{1}{5}\sigma_{c,28}$ $E_c = 200t/cm^2$	$36 \leq f_{s,u} \leq 45$ $\sigma_s = 10$ $n = 10$	-
1933	**Portland**: $\sigma_c = min\left(\frac{1}{4}\sigma_{c,28}; 50\right)$ **High res.**: $\sigma_c = min\left(\frac{1}{4}\sigma_{c,28}; 65\right)$ Uniform compression: limited to 40 and 50 respectively $E_c = 200t/cm^2$	$38 \leq f_{s,u} \leq 45$ $\sigma_s = 12$ $n = 10$	$A_c < 0.16m^2 : 1\%A_{c,req}$ $A_c > 0.64m^2 : 0.7\%A_{c,req}$ otherwise: linear interpolation
1937		ferro omogeneo: $\sigma_s = 14$ acciaio semiduro: $\sigma_s = 20$	
1939	**Portland**: $\sigma_c = min\left(75 + \frac{\sigma_{c,28}-225}{9}; 40\right)$ **High res.**: $\sigma_c = min\left(75 + \frac{\sigma_{c,28}-225}{9}; 50\right)$ Uniform compression: limited to 35 and 50 respectively $E_c = 200t/cm^2$	**Acciaio dolce**: $\sigma_s = 14$ $42 \leq f_{s,u} \leq 50$ $f_y > 22$ **Acciaio semiduro**: $\sigma_s = 20$ $50 \leq f_{s,u} \leq 60$ $f_y > 27$ **Acciaio duro**: $\sigma_s = 20$ $60 \leq f_{s,u} \leq 70$ $f_y > 31$	$A_c < 0.20m^2 : 0.8\%A_{c,req}$ $A_c > 0.80m^2 : 0.5\%A_{c,req}$ otherwise: linear interpolation

Continued on next page

Year	Concrete	Steel $[kg/mm^2]$	Column reinforcement
1957		Acciaio dolce → **Aq.42** $\sigma_s = min\,(50\%f_y, 14)$ Acciaio semiduro → **Aq.50** $\sigma_s = min\,(50\%f_y, 16)$ Acciaio duro → **Aq.60** $\sigma_s = min\,(50\%f_y, 18)$ Ribbed bars: $\sigma_{s,max} = 40\%f_{s,u}$	
1972	Classes: 150, 200, 250, 300, 400, 500 $\sigma_c = 60 + \frac{R_{bk}-150}{4}$ $E_c = 1800\sqrt{R_{bk}}$	**FeB22** (smooth bars): $f_y = 22$ $\sigma_s = 12$ **FeB32** (smooth bars): $f_y = 32$ $\sigma_s = 16$ **A38** (ribbed bars): $f_y = 38$ $\sigma_s = 22$ **A41** (ribbed bars): $f_y = 41$ $\sigma_s = 24$ **FeB44** (ribbed bars): $f_y = 44$ $\sigma_s = 26$ $n = 10$ or 15	$A_s > 0.6\%A_{c,req}$ $A_s > 0.3\%A_c$ $A_s < 5\%A_{c,req}$
1976		FeB22 → **FeB22k** FeB32 → **FeB32k** A38 → **FeB38k** FeB44 → **FeB44k**	
1980		$n = 15$	$A_s > 0.8\%A_{c,req}$ $A_s > 0.3\%A_c$ $A_s < 6\%A_{c,req}$

Tab. 8.3 – Summary of past design practices in seismic areas

Year	Vertical forces	Seismic masses	Horizontal forces
1916	50% on both Q and G	W_i calculated from effective values of loads	$\frac{1}{8}W_i$ (1st floor) $\frac{1}{6}W_i$ (other floors)
1927	**cat.I**: 50% **cat.II**: $\frac{1}{3}$		**cat. I**: $\frac{1}{8}W_i$ (1st floor) $\frac{1}{6}W_i$ (other floors) **cat. II**: $\frac{1}{10}W_i$ (1st floor) $\frac{1}{8}W_i$ (other floors)
1935	**cat.I**: 40% **cat.II**: 25%	Reduction on variable load: $Q_{red} = \frac{1}{3}Q$ being $(Q_{red} + G) > \frac{2}{3}(Q + G)$	**cat. I**: $0.10W_i$ **cat. II**: $0.07W_i$

Continued on next page

Year	Vertical forces	Seismic masses	Horizontal forces
1937	**cat.I**: 40 % **cat.II**: 25 % Computed using $Q_{red} = \frac{1}{3}Q$ being $F_v \geq (Q + G)$	Reduction on variable load: $Q_{red} = \frac{1}{3}Q$	**cat. I**: $0.10W_i$ **cat. II**: $0.05W_i$
1962	$F_v = 0$ except for particular structural conditions		**cat. I**: $0.10W_i$ **cat. II**: $0.07W_i$
1975			$F_h = c \cdot R \cdot \epsilon \cdot \beta \cdot \gamma_i$
1975			$F_h = c \cdot R \cdot \epsilon \cdot \beta \cdot \gamma_i \cdot I$

9. GENERATION OF THE STRUCTURAL MODELS

In order to lay the foundation for structural analyses, in accordance with specific peculiarities of the proposed procedure, a complete structural model need to be assembled.

It is clear that, while maximum adherence to reality is appreciated, what is subjected to analyses is as a matter of fact just a *model*, not the reality itself (see Magritte et al. (1977)). For this reason, assumptions and modelling choices have to be made in model construction step.

Cited assumptions are clearly tightly connected to the typology of analyses that are intended to be run: for instance, the modelling approach has to be inherently different if non-linear dynamic analyses are made (as in the present work and in Masi (2003)) rather than static (as *e.g.* in Crowley, Pinho, and Bommer (2004) and in a previous proposal in Aiello et al. (2017b)), at least because in latter case there is no need to model hysteresis behaviour.

In present work, the following major hypotheses are made:

1. Analyzed buildings can be modelled with a *shear-type* behaviour, thus have rigid floors, and the whole behaviour is controlled by vertical structural elements (*i.e.* beam do not participate in a decisive manner in global response).

2. Vertical seismic action have no significant influence over global behaviour, so that it can be excluded from analyses.

3. Structural elements do not fail with brittle shear mechanism. This hypothesis could appear non reasonable, especially looking at works that demonstrate brittle shear mechanism to be the main failure cause in existing buildings (see *e.g.* Kato et al. (2011) and Del Zoppo et al. (2016)). Paradoxically, the undoubted importance of shear brittle mechanism in existing buildings behaviour is part of the reason of its exclusion from the structural model: while every single building un-

der analysis suffers shear deficiencies, usually shear failure happens at quite low seismic intensities; most of the buildings would result in immediate "collapse", losing the information about relative inter-buildings vulnerability. In conclusion, it is assumed that shear deficiencies are already solved as a pre-condition for vulnerability assessment.

9.1 Proposal of a beam model for effective stiffness evaluation

9.1.1 State of the art of beam modelling

In structural analysis, the choice of an appropriate beam model is of paramount importance. While this issue is addressed from long time, although several models have been developed by researchers at the moment a globally accepted solution does not exist.

First attempts in explaining the behaviour of a *beam* can be traced back to Leonardo da Vinci: in Fig. 9.1 the *folio 84* of *Codex Madrid I* is depicted. The written part can be translated as follows (from Ballarini (2003)):

"Of bending of the springs: If a straight spring is bent, it is necessary that its convex part become thinner and its concave part, thicker. This modification is pyramidal, and consequently, there will never be a change in the middle of the spring. You shall discover, if you consider all of the aforementioned modifications, that by taking part 'ab' in the middle of its length and then bending the spring in a way that the two parallel lines, 'a' and 'b' touch a the bottom, the distance between the parallel lines has grown as much at the top as it has diminished at the bottom. Therefore, the center of its height has become much like a balance for the sides. And the ends of those lines draw as close at the bottom as much as they draw away at the top. From this you will understand why the center of the height of the parallels never increases in 'ab' nor diminishes in the bent spring at 'co.'"

As a demonstration of how those intuitions were outstandingly advanced for the period (*Codex Madrid I* was written in late XV century), the first complete beam theory is the one by Euler-Bernoulli (second half of XVIII century), which is usually referred to as the *classical* beam theory. This theory is based on the assumption of the conservation

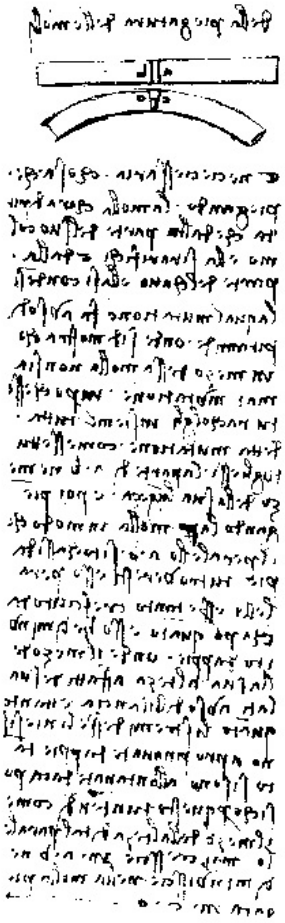

Fig. 9.1 – da Vinci's discussion of the deformation of a beam/spring (image taken from Ballarini (2003))

of planarity and orthogonality of the cross section. Although, those assumption bring to an underestimation of deflections induced by static loads and conversely overestimates natural frequencies (Sayyad, 2011).

In Timoshenko (1921) a new model was proposed including the assumption of non-orthogonally deformation of the plane cross-section with respect to the longitudinal axis. As a result, the distribution of shear stresses and deformations is evaluated from the model as a constant value through the element thickness.

In order to more correctly predict the deformation energy, a *shear correction factor*

χ must be included, whose value is applied as a multiplicative factor to the element area and is usually set $\chi = \frac{5}{6}$. Although, various authors have proposed different values for χ: in Cowper (1966) the Eq. 9.2 was proposed, afterwards modified from Kaneko (1975) as per Eq. 9.1; in Stephen (1980) the Eq. 9.3 was proposed; in Gruttmann et al. (2001) several values of χ are charted for various values of the Poisson ratio ν and the length-to-height ratio L/b.

$$\chi = \frac{5(1+\nu)}{6+5\nu} \tag{9.1}$$

$$\chi = \frac{10(1+\nu)}{12+11\nu} \tag{9.2}$$

$$\chi = \frac{5(1+\nu)^2}{6+11\nu+\nu^2\left(5-\left(\frac{b}{h}\right)^4+\frac{90\left(\frac{b}{h}\right)^5\sum_{n=1}^{\infty}\left(\frac{tanhn\pi\frac{b}{h}}{n^5}\right)}{\pi^5}\right)} \tag{9.3}$$

After the proposal of the *Timoshenko-Ehrenfest*, several other authors gave their contribution on this issue, thus creating a well-established research field aimed at the definition of alternative models able to overcome the limitations of cited theories.

An absolute reference amongst those models is represented by the one proposed in Reddy (1984), because it is possible to derive every other polynomial-shaped model (*e.g.* Ambartsumian (1958), Kaczkowski (1968), Panc (1975), Reissner (1975), Shi et al. (1998), and Eisenberger (2003)) simply by multiplying with a constant its function ϕ (that in this context does not have the meaning of a rotation as in the classical *Timoshenko-Ehrenfest* model).

Similarly, all of the trigonometric models (Vlasov, 1966; Touratier, 1991; Shimpi et al., 2001; Zenkour, 2013) can be reduced to the model of Levy (1877).

In Levinson (1981), Murty (1984), and Heyliger et al. (1988) higher order models assuming a parabolic pattern for shear stress through the cross section were proposed.

A model based on hyperbolic form of the axial displacements was developed in Ghugal et al. (2009) starting from the original proposal in Soldatos (1992).

Exponential models in Karama et al. (2003) and Aydogdu (2009) complete the family of the *homogeneous models* available in the technical literature. Other models, that for various reasons can not be included in any of the previously defined categories, can be found in Kant, Owen, et al. (1982), Kant and Gupta (1988), Vasil'Ev et al. (1992), Mantari et al. (2012), Thai et al. (2012), Neves et al. (2013), and Sayyad and Ghugal (2017a).

Other than the shape of the displacement fields, here used as categorization criterion in order to efficiently show the various available beam models, another important parameter for the classification of beam models is the number of unknown functions used to define the displacement fields. From a comprehensive survey amongst proposed models, it has been observed that most use two unknown functions as in the *Timoshenko-Ehrenfest* model (Sayyad and Ghugal, 2017b).

Although so much models have been proposed in the past, all of them fail at fulfilling equilibrium conditions inside the beam domain.

9.1.2 General presentation of the model

In order to effectively represent stiffness of structural members, a novel beam model is implemented. While further details and in-depth analysis of its effectiveness can be found in Ciampoli et al. (2020), a general purpose presentation of the model is here introduced.

Hypotheses of the model are as follows:

1. Beam's material is elastic, linear, homogeneous and isotropic.
2. The beam is subjected to volume forces ρ acting along z axis, thus being a gravity-like load (see Fig. 9.2).
3. Excluding the two terminal sections, beam boundaries are not subjected to any external loading.
4. Cross section of the beam (assumed rectangular), in deformed configuration, does not remain plane.
5. Small displacements hypothesis stands.

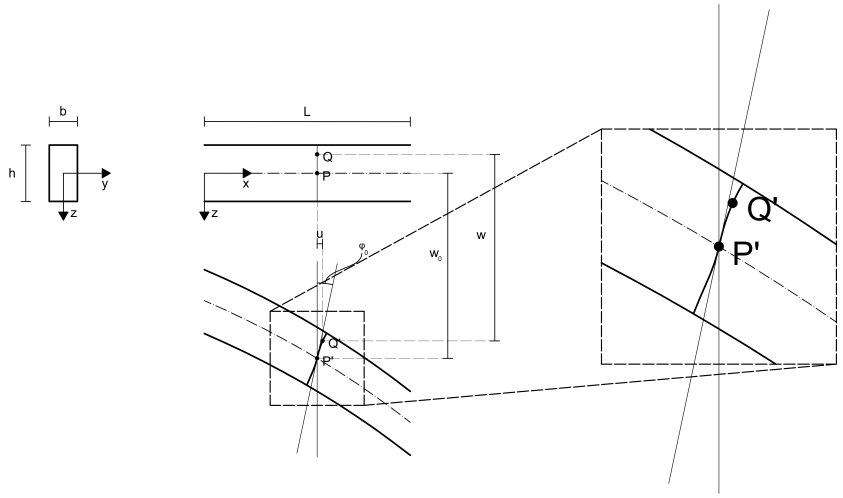

Fig. 9.2 – Geometry, reference system, deformed and undeformed configurations according to the proposed model

With explicit reference to nomenclature used in Fig. 9.2, the model kinematic is described through Eq. 9.4.

$$u(x,z) = z^3\beta_1(x) - z\phi_0(x) \tag{9.4a}$$

$$w(x,z) = \alpha_2(x)z^4 + \alpha_1(x)z^2 + w_0(x) \tag{9.4b}$$

In Eq. 9.4: $u(x,z)$ and $w(x,z)$ are the displacements respectively in y and z directions of a generic point Q of the cross section; $w_0(x)$ is the displacement in y direction of the point P' belonging to the baricentric axis, while $\phi_0(x)$ is the rotation around z axis; $\alpha_1(x)$, $\alpha_2(x)$ and $\beta_1(x)$ are functions of the abscissa x. (see Fig. 9.2 for reference)

The strain field of the beam is defined through the non-null strains given in Eq. 9.5.

$$\epsilon_x = z^3\beta_1'(x) - z\phi_0'(x) \tag{9.5a}$$

$$\epsilon_z = 4\alpha_2(x)z^3 + 2\alpha_1(x)z \tag{9.5b}$$

$$\gamma_{xz} = \alpha_2'(x)z^4 + \left(3\beta_1(x) + \alpha_1'(x)\right)z^2 - \phi_0(x) + w_0'(x) \tag{9.5c}$$

From Eq. 9.5, using constitutive law for linear elastic materials, stress field can be defined as in Eq. 9.6.

$$\sigma_x = \frac{E\left(4\nu\alpha_2(x) + (1-\nu)\beta_1'(x)\right)z^3}{\nu(2\nu-3)+1} + \\ + \frac{E\left(2\nu\alpha_1(x) + (\nu-1)\phi_0'(x)\right)z}{\nu(2\nu-3)+1} \tag{9.6a}$$

$$\sigma_z = -\frac{E\left(4(\nu-1)\alpha_2(x) - \nu\beta_1'(x)\right)z^3}{\nu(2\nu-3)+1} + \\ - \frac{E\left(2(\nu-1)\alpha_1(x) + \nu\phi_0'(x)\right)z}{\nu(2\nu-3)+1} \tag{9.6b}$$

$$\tau_{xz} = \frac{E\alpha_2'(x)z^4}{2(\nu+1)} + \frac{E\left(3\beta_1(x) + \alpha_1'(x)\right)z^2}{2(\nu+1)} + \\ + \frac{E\left(w_0'(x) - \phi_0(x)\right)}{2(\nu+1)} \tag{9.6c}$$

9.1.3 Indefinite equilibrium conditions and virtual work principle

Taking into account stresses in Eq. 9.6, non-trivial indefinite equilibrium conditions are defined from Eq. 9.7.

$$\frac{\delta\sigma_x}{\delta x} + \frac{\delta\tau_{xz}}{dz} = 0 \tag{9.7a}$$

$$\frac{\delta\tau_{xz}}{\delta x} + \frac{\delta\sigma_z}{\delta z} = -\rho(x) \tag{9.7b}$$

Substituting Eq. 9.6 in Eq. 9.7, Eq. 9.8 arise.

$$\left(2(4\nu^2-\nu+1)\alpha_2'(x) + (1-\nu^2)\beta_1''(x)\right)z^3 + \\ + \left((6\nu^2-9\nu+3)\beta_1(x) + (4\nu^2-\nu+1)\alpha_1'(x) + (\nu^2-1)\phi_0''(x)\right)z = 0 \tag{9.8a}$$

$$\left(-\frac{2(\nu^2-1)}{(2\nu^2-3\nu+1)}\alpha_1(x)+\frac{(-4\nu^2+\nu-1)}{2(2\nu^2-3\nu+1)}\phi_0'(x)+\frac{1}{2}w_0''(x)\right)+$$
$$+\left(-\frac{12\left(\nu^2-1\right)}{(2\nu^2-3\nu+1)}\alpha_2(x)+\frac{3(4\nu^2-\nu+1)}{2(2\nu^2-3\nu+1)}\beta_1'(x)+\frac{1}{2}\alpha_1''(x)\right)z^2+$$
$$+\alpha_2''(x)z^4=-\frac{2(\nu+1)}{E}\rho(x) \tag{9.8b}$$

Given that Eq. 9.8 must be fulfilled in every point of the beam, each of those equation must be true independently from the value of z. For this reason, Eq. 9.8 can be split with regard to different powers of z into Eq. 9.9, and then dependencies between variables can be assessed in Eq. 9.10.

$$\frac{E}{2(\nu+1)}\alpha_2''(x)=0 \tag{9.9a}$$
$$2(4\nu^2-\nu+1)\alpha_2'(x)+(1-\nu^2)\beta_1''(x)=0 \tag{9.9b}$$
$$-\frac{12\left(\nu^2-1\right)}{(2\nu^2-3\nu+1)}\alpha_2(x)+\frac{3(4\nu^2-\nu+1)}{2(2\nu^2-3\nu+1)}\beta_1'(x)+\frac{1}{2}\alpha_1''(x)=0 \tag{9.9c}$$
$$3(2\nu^2-3\nu+1)\beta_1(x)+(\nu(4\nu-1)+1)\alpha_1'(x)+\left(\nu^2-1\right)\phi_0''(x)=0 \tag{9.9d}$$
$$-\frac{2\left(\nu^2-1\right)}{(2\nu^2-3\nu+1)}\alpha_1(x)+\frac{\left(-4\nu^2+\nu-1\right)}{2(2\nu^2-3\nu+1)}\phi_0'(x)+\frac{1}{2}w_0''(x)=-\rho(x) \tag{9.9e}$$

from Eq. 9.9e $\alpha_1(x)=$

$$=\frac{(\nu-1)(\nu+1)(2\nu-1)}{2E\left(\nu^2-1\right)}\rho(x)+$$
$$+\frac{\left(-4\nu^2+\nu-1\right)}{4\left(\nu^2-1\right)}\phi_0'(x)+$$
$$+\frac{(\nu(2\nu-3)+1)}{4\left(\nu^2-1\right)}w_0''(x) \tag{9.10a}$$

from Eq. 9.9d $\beta_1(x) =$

$$
\begin{aligned}
&= \frac{\left(4\nu^2 - \nu + 1\right)}{6E(\nu - 1)} \rho'(x) + \\
&+ \frac{(3\nu + 1)\left(2\nu^2 - \nu + 3\right)}{12(\nu - 1)^2(\nu + 1)} \phi_0''(x) + \\
&- \frac{\left(4\nu^2 - \nu + 1\right)}{12(\nu - 1)(\nu + 1)} {w_0}^{(3)}(x)
\end{aligned}
\tag{9.10b}
$$

from Eq. 9.9c $\alpha_2(x) =$

$$
\begin{aligned}
&= - \frac{\nu\left(3\nu^2 - 2\nu + 1\right)}{12E(\nu - 1)^2} \rho''(x) + \\
&+ \frac{\left(\nu^2 + 1\right)\left(4\nu^2 - \nu + 1\right)}{24(\nu - 1)^3(\nu + 1)} {\phi_0}^{(3)}(x) + \\
&- \frac{\nu\left(3\nu^2 - 2\nu + 1\right)}{24(\nu - 1)^2(\nu + 1)} {w_0}^{(4)}(x)
\end{aligned}
\tag{9.10c}
$$

Both Eq. 9.9b and Eq. 9.9a give limitations on solution, namely those given in Eq. 9.11.

$$
\begin{aligned}
{\phi_0}^{(4)}(x) &= \\
&= \frac{2(\nu - 1)(\nu + 1)\left(\nu^2 + 1\right)\left(4\nu^2 - \nu + 1\right)}{E\left(\nu^2 + \nu + 2\right)\left(5\nu^3 - 3\nu^2 + 5\nu + 1\right)} \rho^{(3)}(x) + \\
&+ \frac{(\nu - 1)\left(\nu^2 + 1\right)\left(4\nu^2 - \nu + 1\right)}{\left(\nu^2 + \nu + 2\right)\left(5\nu^3 - 3\nu^2 + 5\nu + 1\right)} {w_0}^{(5)}(x)
\end{aligned}
\tag{9.11a}
$$

$$
\begin{aligned}
{w_0}^{(5)}(x) &= \\
&= \frac{\left(\nu^2 + \nu + 2\right)\left(5\nu^3 - 3\nu^2 + 5\nu + 1\right)}{(\nu - 1)\left(\nu^2 + 1\right)\left(4\nu^2 - \nu + 1\right)} {\phi_0}^{(4)}(x) + \\
&- \frac{2(\nu + 1)\rho^{(3)}(x)}{E}
\end{aligned}
\tag{9.11b}
$$

$$\phi_0{}^{(5)}(x) = 0 \tag{9.11c}$$

From condition Eq. 9.11c, assuming $\rho(x)$ as a constant value p_0, given Eq. 9.11b, it is possible to rewrite field functions as in Eq. 9.12.

$$\phi_0(x) = c_4 x^4 + c_3 x^3 + c_2 x^2 + c_1 x + c_0 \tag{9.12a}$$

$$\begin{aligned} w_0(x) = {} & c_9 x^4 + c_8 x^3 + c_7 x^2 + c_6 x + c_5 + \\ & + \frac{\left(\nu^2+\nu+2\right)\left(5\nu^3-3\nu^2+5\nu+1\right)}{5(\nu-1)\left(\nu^2+1\right)\left(4\nu^2-\nu+1\right)} c_4 \end{aligned} \tag{9.12b}$$

With the definition of field variables in Eq. 9.12, from which it is possible to derive all of the other quantities needed for the definition of the displacements field through Eq. 9.10, all of the indefinite equilibrium conditions are fulfilled.

Another condition to be fulfilled is represented by the virtual work principle. Assuming as stress/forces system the actual system and as strains/displacements an arbitrary one, the formal definition of the principle can be expressed as in Eq. 9.13.

$$L_i = \int_V \sum_{i,j=x,y,z} \sigma_{ij}\epsilon_{ij} dV = \int_V \sum_{i=x,y,z} \rho_i s_i dV = L_e \tag{9.13}$$

In order to fulfill this principle, equalities in Eq. 9.14 must hold.

$$c_4 = 0 \tag{9.14a}$$

$$c_9 = \frac{c_3}{4} \tag{9.14b}$$

$$c_8 = \frac{c_2}{3} \tag{9.14c}$$

$$c_7 = \frac{c_1}{2} - \frac{3(1+\nu)\rho}{2E} \tag{9.14d}$$

$$c_3 = \frac{2(1-\nu)^2\rho}{Eh^2} \tag{9.14e}$$

$$c_2 = \frac{2(1-\nu)^2(c_0 - c_6)}{h^2(1+\nu)} \tag{9.14f}$$

9.1.4 Plain stress and strain conditions

At this point it is worth highlighting a feature of the model: as it has been defined in Eq. 9.4 it clearly describes a plane strain condition (given that displacement in y transversal direction is assumed to be identically null).

However, both generally and especially for this work's aims, a plain strain condition does not represent accurately the beam behaviour. A plain strain condition, in fact, accurately models a situation where the beam is restrained at its lateral boundaries. Considering that for the proposed procedure this model is to be applied to columns assumed to not be restrained at its external faces, it is clear that the plain strain condition is not a suitable modelling choice.

A more accurate representation of the real behaviour of the beam would be the plain stress condition: if boundary faces are not restrained (*i.e.* σ_y can be considered null), with a reasonable error it can be assumed that σ_y is null in every point of the beam section.

Transformation of the model in order to achieve a plane stress condition is achieved through construction science methods, namely substituting mechanical characteristics of the material E and ν with those given in Eq. 9.15, where E_D and ν_D are related to the plain strain condition and E_T ν_T to the plain stress condition.

$$E_T = \frac{E_D}{(1+\nu_D)(1-\nu_D)} \tag{9.15a}$$

$$\nu_T = \frac{\nu_D}{1-\nu_D} \tag{9.15b}$$

9.1.5 Practical-use-related results of the model

Using Eq. 9.15 some useful quantities found until now can be rewritten as in Eq. 9.16

$$w_0(x) = \frac{p_0 x^4}{2h^2(2\nu_T E_T + E_T)} + \frac{2\left(c_0 - c_6\right)x^3}{3h^2\left(2\nu_T^2 + 3\nu_T + 1\right)} + \\ + \frac{\left(E_T c_1 - 3(\nu_T + 1)p_0\right)x^2}{2E_T} + c_6 x + c_5 \tag{9.16a}$$

$$\phi_0(x) = \frac{2p_0 x^3}{E_T h^2(2\nu_T + 1)} + \\ + \frac{\left(2E_T c_0 - 2E_T c_6\right)x^2}{E_T h^2(\nu_T + 1)(2\nu_T + 1)} + c_1 x + c_0 \tag{9.16b}$$

$$\sigma_x = -\frac{6zp_0 x^2}{h^2} + \frac{z\left(8E_T c_6 - 8E_T c_0\right)x}{2h^2(\nu_T + 1)} + \\ - E_T(2\nu_T + 1)zc_1 + \left(\frac{4(2\nu_T(\nu_T + 1) + 1)z^3}{h^2} + \frac{\nu_T z}{2}\right)p_0 \tag{9.16c}$$

$$M = -\frac{1}{12}bE_T(2\nu_T + 1)c_1 h^3 + \frac{1}{120}b(3\nu_T + 2)(4\nu_T + 3)p_0 h^3 + \\ + \frac{bx\left(40E_T c_6 - 40E_T c_0\right)h}{120(\nu_T + 1)} - \frac{1}{2}bx^2 p_0 h \tag{9.16d}$$

$$\tau_{xz} = -\frac{\left(h^2 - 4z^2\right)\left(E_T c_0 - E_T c_6\right)}{2h^2(\nu_T + 1)} + \\ - \frac{3x\left(h^2 - 4z^2\right)p_0}{2h^2} \tag{9.16e}$$

$$V = \frac{bE_T h\left(c_6 - c_0\right)}{3(\nu_T + 1)} - bhxp_0 \tag{9.16f}$$

From Eq. 9.16, with simple transformations, it can be demonstrated that conditions in Eq. 9.17 stand.

$$\left(w_0'(x) - \phi_0(x)\right) = \frac{3(1+\nu_T)}{E_T bh} V = \frac{V}{G\frac{2}{3}A} \tag{9.17a}$$

$$w_0''(x) = -\frac{M}{EJ(1+2\nu)} - \frac{48\nu^2 + 73\nu + 24}{10E(1+2\nu)} p_0 \tag{9.17b}$$

It is interesting to look at the distribution of stress τ_{xz} along the height of the section, starting from its definition in Eq. 9.16e (rewritten Eq. 9.18a for clarity).

$$\begin{aligned}\tau_{xz} = &-\frac{\left(h^2 - 4z^2\right) E_T \left(c_0 - c_6\right)}{2h^2(\nu_T + 1)} + \\ &- \frac{3x\left(h^2 - 4z^2\right) p_0}{2h^2} = \\ &= \frac{3\left(h^2 - 4z^2\right)}{2bh^3}\left(\frac{E_T bh(c_6 - c_0)}{3(\nu_T + 1)} - bhxp_0\right)\end{aligned} \tag{9.18a}$$

from Eq. 9.16f:

$$\tau_{xz} = \frac{3\left(h^2 - 4z^2\right)}{2bh^3} V$$

for rectangular sections $J = \frac{bh^3}{12}$:

$$\tau_{xz} = \frac{h^2 - 4z^2}{8}\frac{V}{J}$$

with simple transformations:

$$\tau_{xz} = \frac{\left(\frac{z}{2} + \frac{h}{4}\right)\left(\frac{h}{2} - z\right) b}{b}\frac{V}{J} \tag{9.18b}$$

Using the scheme in Fig. 9.3, it is clear that the numerator of the first fraction in Eq. 9.18 represents the static momentum of the highlighted area. So Eq. 9.19 can be finally written.

$$\tau_{xz} = \frac{VS}{Jb} \tag{9.19}$$

It is worth recalling that Eq. 9.19 is exactly what in shear theory of Jourawsky is

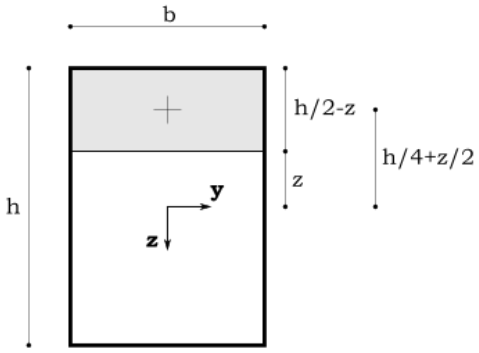

Fig. 9.3 – Simple scheme for assessing quantities in Eq. 9.18

presented as the average shear stress of the chord.

9.1.6 Stiffness evaluation for the problem under analysis

As stated in hypothesis 1 at page 63, in this work it is assumed that the structure behaves accordingly to a shear-type pattern (see Fig. 9.4). Starting from this hypothesis, stiffness evaluation using the proposed beam model can be done.

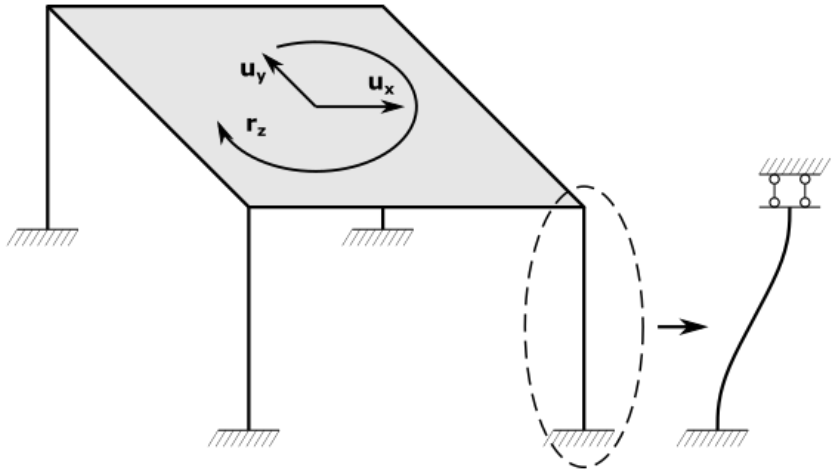

Fig. 9.4 – Scheme for the evaluation of structural members stiffness

In order to get the stiffness of a structural member with the proposed beam model, starting from Eq. 9.20, the solution procedure is presented in Eq. 9.21. [1]

$$M = X - F(l - x) \tag{9.20a}$$

$$V = F \tag{9.20b}$$

from (9.20) and (9.16f):

$$V = \frac{EA}{3(1+\nu)}(c_6 - c_0) \rightarrow$$

$$\rightarrow (c_6 - c_0) = \frac{3(1+\nu)}{EA}F \tag{9.21a}$$

from (9.20) and (9.16d):

$$M = EJ(1+2\nu)c_1 + \frac{EA}{3(1+\nu)}x(c_6 - c_0) =$$

$$= X - F(L - x) \rightarrow$$

$$\rightarrow c_1 = \frac{FL - X}{EJ(1+2\nu)} \tag{9.21b}$$

from boundary conditions:

$$w_0(x=0) = 0 \rightarrow c_5 = 0$$

$$\phi_0(x=0) = 0 \rightarrow c_0 = 0$$

$$\phi_0(x=L) = 0 \rightarrow X = \frac{FL}{2} \tag{9.21c}$$

setting $w_0(x = L) = 1$ and rearranging:

$$K = F|_{w_0(x=L)=1} =$$

$$= \frac{1+2\nu}{1+3(1+2\nu)^2\left(\frac{h}{L}\right)^2}\frac{12EJ}{l^3} \tag{9.21d}$$

[1] It is worth highlighting that a perfectly equivalent approach is possible in order to compute the (same) solution, namely using (9.17).

9.2 Non-linear constitutive model of structural elements

Given the need of modelling the non-linear behaviour of structural elements, an hysteretic model must be defined so that an effective prediction of the response can be made.

While different hysteresis models are available in technical literature (see *e.g.* Clough (1966), Takeda et al. (1970), Bouc (1971), Otani (1974), Mander (1983), and Ibarra et al. (2005)), there is no widely accepted procedure to accurately model RC structural elements, especially if interaction between various stress characteristics is intended to be included.

To be exact, all actions on an element should have to be included in modelling (moments, shear and axial forces), because all interact and intervene in the global non-linear behaviour.

From modelling hypotheses given in page 63, however, it is possible to simplify this issue: from hypothesis 3 effect of shear forces on global behaviour is dropped because sufficient shear strength is assumed; from hypothesis 2 seismic action do not produce a *direct* effect on axial actions through a vertical component, while from shear-type hypothesis 1 the turning of rigid floors around horizontal axes is assumed negligible so that axial forces variations due to this action is neglected too.

As a result, only bi-axial interaction between bending moments is to be taken into account. In computation of behaviour, however, axial force is to be included, but as a constant action equal to that given by static loads.

It must be noted that the global behaviour of a given element (*i.e.* column, due to hypothesis 1) is modelled, so that force-displacement interaction are in the following considered as it foresees what displacement would be experienced by the top of a column when subjected to a force acting in the same point, without any section-level consideration (*i.e.* plastic hinges formation).

However, following considerations can be made:

- given hypothesis 1, at both ends of a column the same bending moment is experienced;

- variation of axial force between top and bottom ends is assumed negligible, so that resisting moments at both end sections can be computed with the same axial force level;
- same rebar patterns are assumed for each column section, as it is expected to happen in structures under analysis.

For those reasons, response modifications are assumed to happen symmetrically along the column. As a result, starting from a lumped plasticity approach, the global response of the whole element can be computed conveniently modifying the moment-rotation law of end sections.

For instance, from the static scheme (see Fig. 9.4 and Eq. 9.20) the bending moment M acting on both end sections due to an external force F is $M = \frac{FL}{2}$, while from Fig. 9.5 the chord rotation θ of each end section due to the deflection Δ of column top end is $\theta = \frac{\Delta}{L}$. Hence, knowing the behaviour of end sections plastic hinges, it is possible to derive the global element law $F - \Delta$ by using Eq. 9.22.

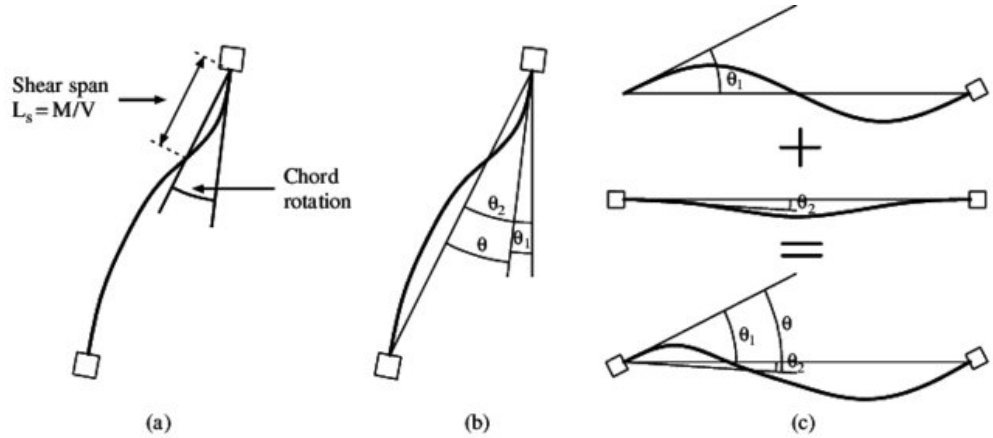

Fig. 9.5 – Definition of chord rotation, from Mpampatsikos et al. (2008)

$$F = \frac{2M}{L} \tag{9.22a}$$

$$\Delta = \theta L \tag{9.22b}$$

9.2.1 Unidirectional backbone curves

As a first step, unidirectional behaviour is to be assessed. Namely, a tri-linear backbone curve is assumed, where discontinuity points are represented by conventional events of cracking (***Cr***), yielding (***Y***) and collapse (***C***) as in Fig. 9.6.

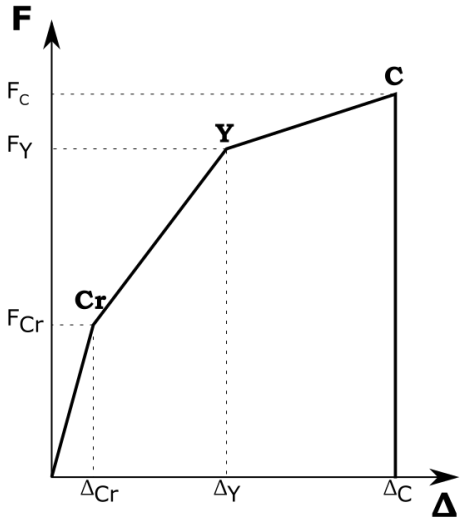

Fig. 9.6 – Constitutive law backbone curve scheme

It is hence necessary the definition of opportune values for the three $F - \Delta$ couples (at cracking, yielding and collapse).

For ***cracking***, linear elastic behaviour is assumed for the whole section, so that concrete reacts both in tension and compression (with the same stiffness). Section analysis is performed in order to compute the value of M_{Cr} for which, given the axial force level, a point experiences its limit stress.

For instance, while different limit stresses are checked (yielding of steel both in tension and compression, concrete strength in tension and compression), it is expected that the reaching of concrete tension limit stress always determines the value to be computed. This parameter is computed according to NTC2018 art.11.2.10.2 (Eq. 9.23).

$$f_{cfm} = 1.2 \left(0.3 f_c^{2/3}\right) \tag{9.23}$$

After transforming M_{Cr} into F_{Cr} through Eq. 9.22a, Δ_{Cr} is computed as $\Delta_{Cr} = \frac{F_{Cr}}{K}$ being K the stiffness in Eq. 9.21d. [2]

For ***yielding***, chord rotation θ_Y is computed through C.M. 21/01/2019 art.C8.7.2.3.4, rewritten in Eq. 9.24.

$$\theta_Y = \phi_y \frac{L_v}{3} + 0.0013 \left(1 + 1.5 \frac{h}{L_v}\right) + 0.13 \phi_y \frac{d_b f_y}{\sqrt{f_c}} \tag{9.24}$$

where: $\phi_y =$ yield curvature of end section
$L_v = \frac{M}{V}$ ratio at end section (here $= \frac{L}{2}$)
$h =$ height of the section
$d_b =$ diameter of rebars
$f_y =$ strength at yielding of reinforcing steel [MPa]
$f_c =$ compressive strength of concrete [MPa]

Section analysis is performed taking into account non-linear behaviour of materials (for instance, concrete is assumed to have no stiffness at all in tension). The value of M_Y is found (iteratively) as the value for which, given the axial load level, steel reaches its yielding strain or concrete its compression ultimate strain. Within the said procedure, also yield curvature ϕ_y needed in Eq. 9.24 is computed.

About ***collapse***, chord rotation is computed through EC8-3:2005 A.3.2.2 (almost the same as C.M. 21/01/2019 art.C8.7.2.3.2), rewritten in Eq. 9.25, eventually reduced by a factor of 1.2 if there is no seismic detailing for reinforcements.

$$\theta_C = \frac{1}{\gamma_{el}} 0.016 \left(0.3^{\nu}\right) \left[\frac{max(0.01; \omega')}{max(0.01; \omega')} f_c\right]^{0.225} \left(min\left(9; \frac{L_v}{h}\right)\right)^{0.35} 25^{\left(\alpha \rho_{sx} \frac{f_{yw}}{f_c}\right)} \left(1.25^{100 \rho_d}\right) \tag{9.25}$$

[2] It is worth highlighting that, up to cracking, perfect linear elastic behaviour is assumed, so that it makes sense the use of purely elastic stiffness for evaluation of displacement.

where: γ_{el} = partial factor, $= 1.5$ for *primary* elements

$\nu = \frac{N}{A_c f_c}$ = normalized axial force

$\omega,\ \omega'$ = $\frac{A_s f_y}{A_c f_c}$ mechanical reinforcement ratios, respectively for tension and compression rebars

α = confinement effectiveness ratio

$= \left(1 - \frac{s_h}{2b_0}\right)\left(1 - \frac{s_h}{2h_0}\right)\left(1 - \frac{\sum b_i^2}{6h_0 b_0}\right)$

$b_0,\ h_0$ = dimensions of confined core from centerline of hoops

b_i = centerline spacing of restrained longitudinal bars

s_h = stirrup spacing

$\rho_{sx} = \frac{A_{sx}}{b_w s_h}$ = ratio of transverse steel parallel to loading direction

ρ_d = ratio of diagonal reinforcement

According to C.M. 21/01/2019, $\alpha = 0$ is assumed if transverse reinforcement does not have 135° hoops.

Section analysis is again performed taking into account non-linear behaviour of materials. The value of M_C is once more found as the value for which, given the axial load level, steel or concrete reach its limit strain, while in this case limit strain for steel is its ultimate.

Once all parameters M_i and θ_i (with $i = \{Cr, Y, C\}$) are found, through Eq. 9.22 homologous values for element global behaviour F_i and Δ_i are computed.

9.2.2 Bidirectional assessment of backbone curves limits

Given unidirectional backbone curves, it is now necessary to assess when a limit condition (*i.e.* cracking, yielding or collapse) is reached when forces are applied in both directions.

The approach used in present work is to consider interaction domains as ellipses defined starting from unidirectional values of $\Delta_{i,x}$ and $\Delta_{i,y}$, being i each of limit conditions (*i.e.* $i = \{Cr, Y, C\}$). As it can be seen in Fig. 9.7 limit conditions are defined in terms of displacements rather than forces, while it is straightforwardly possible to redefine schemes with respect to forces.

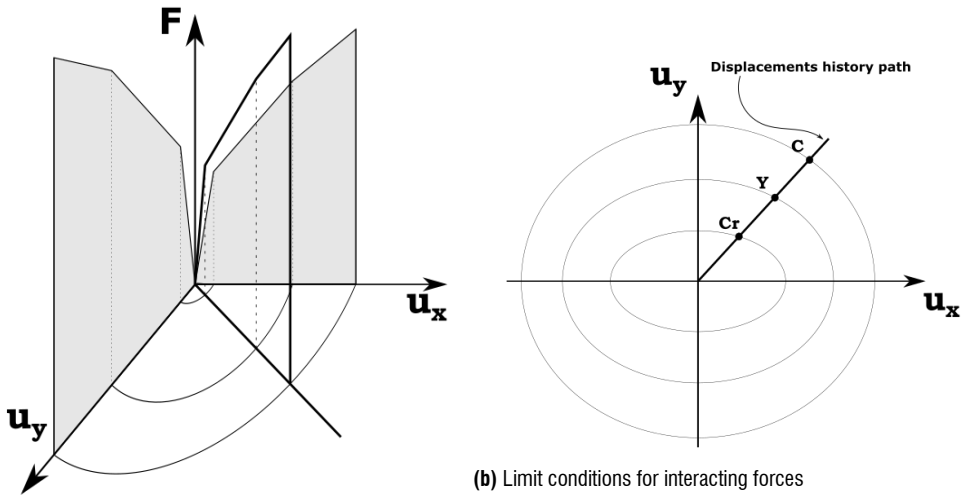

(a) Scheme of biaxial limit conditions assessment

(b) Limit conditions for interacting forces

Fig. 9.7 – Approach used in the present work for interaction assessment

To be clear: if in its displacements history a column reaches a point on the first ellipse in Fig. 9.7b, it means that cracking condition has been reached. The same for other ellipses, for yielding and collapse conditions respectively.

9.2.3 Hysteresis cycle in the monodirectional case

In present work, a simplified Takeda-like model (Takeda et al., 1970) is proposed.

The 1D hysteresis cycle is concisely described in Fig. 9.8, and is defined through the following rules:

1. **Elastic behaviour**: when displacement does not exceed the cracking value Δ_{Cr}, element response is purely elastic with stiffness as given in Eq. 9.21d, as it happens in branch $0-1$ in both Fig. 9.8a and Fig. 9.8b.
2. **Loading post cracking before yielding, as a first increase of this magnitude**: when cracking is exceeded, force-displacement history of the element continues to follow the backbone curve toward yielding point as in $1-2$ branch of Fig. 9.8b. If unloading happens *before* yielding point is reached, the maximum (in module)

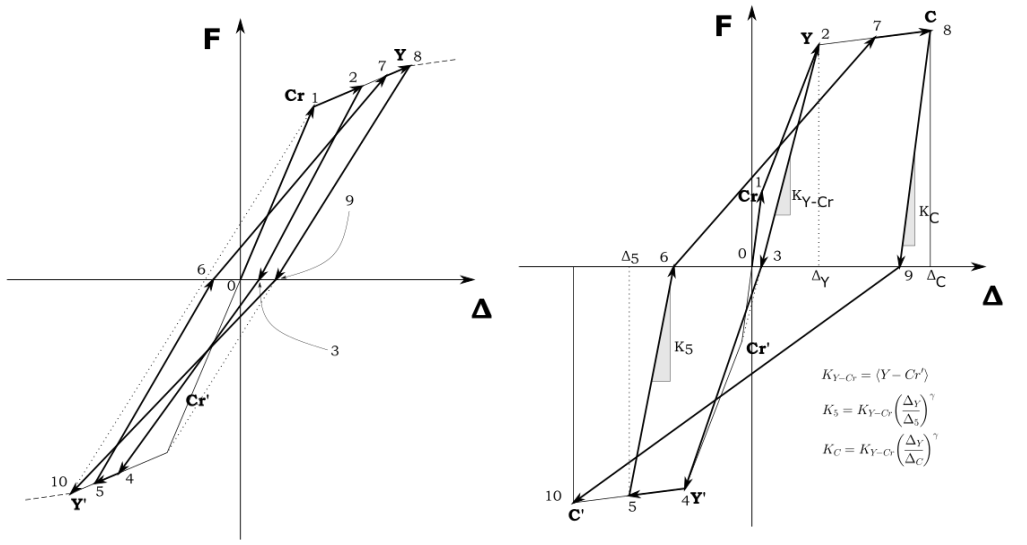

(a) Assumed 1D hysteresis behaviour up to yielding

(b) Assumed 1D hysteresis behaviour after yielding but before collapse

Fig. 9.8 – 1D hysteresis behaviour assumed for the simplified non-linear modelling of structural elements

reached displacement is saved as Δ_M as in branch $1-2$ of Fig. 9.8a (in that case $\Delta_M = \Delta_2$). When unloading happens, rule 5 becomes active. This rule becomes again the active one whenever Δ_M is exceeded as in branches $4-5$ and $7-8$ of Fig. 9.8a.

3. **Loading post yielding before collapse, as a first increase of this magnitude**: whenever yielding is exceeded, the response of the element follows the backbone curve toward collapse point as happens in branches $4-5$ and $7-8$ of Fig. 9.8b. Also in this case, if unloading happens maximum absolute displacement is saved as Δ_M and rule 5 becomes the active one (in Fig. 9.8b point 5 before and then point 8 become points of maximum absolute reached displacement).

4. **Behaviour after collapse**: this rule is defined for taking into account the behaviour after the element collapse. Given the hypotheses of the model, no force at all is retrieved from the element once it is collapsed, both in case of loading or unloading.

5. **Unloading**: as soon as unloading happens, if element has experienced cracking

but not collapse, this rule becomes the active one. A simple stiffness degradation model is used:

- if yielding is not exceeded (*i.e.* $\Delta_M < \Delta_Y$), stiffness is computed as a linear interpolation between elastic stiffness $\langle CrCr' \rangle$ if $\Delta_M = \Delta_{Cr}$, and stiffness defined connecting yielding point to opposite cracking point $\langle YCr' \rangle$ if $\Delta_M = \Delta_Y$. This behaviour can be seen in Fig. 9.8a between points $2-3$, $5-6$ and $8-9$. Analytically, stiffness is defined through Eq. 9.26.

$$K_u = K_{Cr-Cr'} + (K_{Y-Cr'} - K_{Cr-Cr'}) \cdot \frac{\Delta_M - \Delta_{Cr}}{\Delta_Y - \Delta_{Cr}} \tag{9.26}$$

- if yielding is exceeded (*i.e.* $\Delta_M > \Delta_Y$), stiffness is computed through an approach that is straightforwardly inherited from the original Takeda model. However, the original proposal in Takeda et al. (1970) in terms of unloading stiffness was subsequently modified in order to give a parametrization of the general behaviour through the parameter γ, that controls the amount of stiffness degradation. As a result, following subsequent enhancements of the Takeda model, unloading stiffness is defined through Eq. 9.27, where $\gamma = 0.6$ according to Hopper (2009).

$$K_u = K_{Y-Cr'} \cdot \left(\frac{\Delta_Y}{\Delta_M} \right)^{\gamma} \tag{9.27}$$

  This behaviour can be seen in Fig. 9.8b between points $2-3$, $5-6$ and $8-9$.

Whenever a load reversal (*i.e.* a change in force value sign) or a reloading happen, rule 6 becomes active, while if Δ_M is exceeded (both in positive or negative), rule 2 or 3 becomes active depending on wether $\Delta_M < \Delta_Y$ or not.

6. **Reloading**: when reloading or load reversal happen, force-displacement law goes toward the point on the backbone curve with displacement Δ_M, positive or negative depending on the direction in which reloading is happening. For instance, branches $3-4$, $6-7$ and $9-10$ in both Fig. 9.8a and Fig. 9.8b are representative

of this behaviour

9.2.4 Hysteresis cycle in the bidirectional case

Given the general description of assumed hysteretic behaviour of structural elements under monodirectional loading in the previous Section 9.2.3, it is necessary to assess the response of structural elements under biaxial loading.

For instance, it is necessary to slightly modify the global behaviour described in Fig. 9.8 in order to include some specific features of bidirectional behaviour.

In Fig. 9.9 an example of the bidirectional hysteretic behaviour is given, whose details are given in the following highlighting how it can be described in light of rules given in Section 9.2.3 (referred to with a number in parentheses inside Fig. 9.9).

0-1 Within this branch the behaviour is fully elastic in accordance with rule 1. However, the limit point for this behaviour is no more the cracking displacement *as is*: rule 1 is unactivated when *cracking ellipse* is reached, *i.e.* the *locus of points* where cracking happens as defined in Section 9.2.2. For instance, in given example this happens in point 1.

1-2 After cracking is exceeded, rule 2 becomes the active rule for both directions, and according to this rule force-displacement law follows a path toward yielding point (differently from the 1D case, it can be seen that in this case the force-displacement path does not overlap backbone curve, while it still goes toward yielding point).

2-3 If in a direction unloading starts (x direction in this case), its active rule becomes rule 5, with a stiffness $K_{u,2}$ that follows Eq. 9.26 (because yielding is not exceeded) with a slight modification: Δ_M in Eq. 9.26 is computed as $\Delta_{E2,x}$, being this value the x-semiaxis of the maximum reached ellipse (rather than the maximum displacement of the 1D case), and hence Δ_{Cr} and Δ_Y are taken respectively equal to $\Delta_{Cr,x}$ and $\Delta_{Y,x}$. In the y direction there is still loading and, considering that also globally there is loading (*i.e.* the state point $P(\Delta_x, \Delta_y)$ keeps laying on wider ellipses), the active rule is still rule 2 and $F_y - \Delta_y$ path

continues going toward yielding point.

3-4 This branch is very similar to the previous one except for a single significant difference: the element is *globally unloading*, in the sense that subsequent points $P(\Delta_x, \Delta_y)$ lay on smaller ellipses than previous one. In this case, while in x direction rule 5 is still the active one, in y direction rule 6 is active (there is loading but not *as a first increase of this magnitude* as required by rule 2). For this reason, $F_y - \Delta_y$ path goes toward the point on backbone curve having displacement $\Delta_{E3,y}$ (*i.e.* the point relative to the maximum reached ellipse).

4-5 In this branch it can be observed a (negative) reloading in x direction, while in y direction no change happens. For reloading rule 6 is active, and according to this rule the $F_x - \Delta_x$ path must go toward the point on the backbone curve having a displacement equal to the x semi-axis of the maximum reached ellipse. It is worth highlighting that maximum reached ellipse is, for x direction, ellipse E_4: previous maximum reached ellipse while loading for this direction was E_2, but in point 4 there *is* loading in x.

5-6 Along this path, both x and y directions experience unloading: while Δ_x is increasing its value, it is in its negative part of the consitutive law, so it is as a matter of fact an *unloading*. For this reason in both directions rule 5 is active, with stiffness defined through Eq. 9.26. It must be emphasized that Δ_M is computed from ellipse E_4 for x direction ($K_{u,4}$), from E_3 for y direction ($K_{u,3}$).

6-7 While for direction y rule 5 is still active with the same stiffness as before, in x direction a load reversal is happened, so rule 6 is active and $F_x - \Delta_x$ path points toward the point on backbone curve having displacement $\Delta_{E4,x}$.

7-8 While in direction y there is still unloading (so that active rule is still 5), in x direction the previous maximum reached ellipse (E_4) is exceeded. Considering that the element experiences for the first time a loading of this magnitude in this direction, rule 2 conditions are fulfilled: the $F_x - \Delta_x$ path moves toward yielding point.

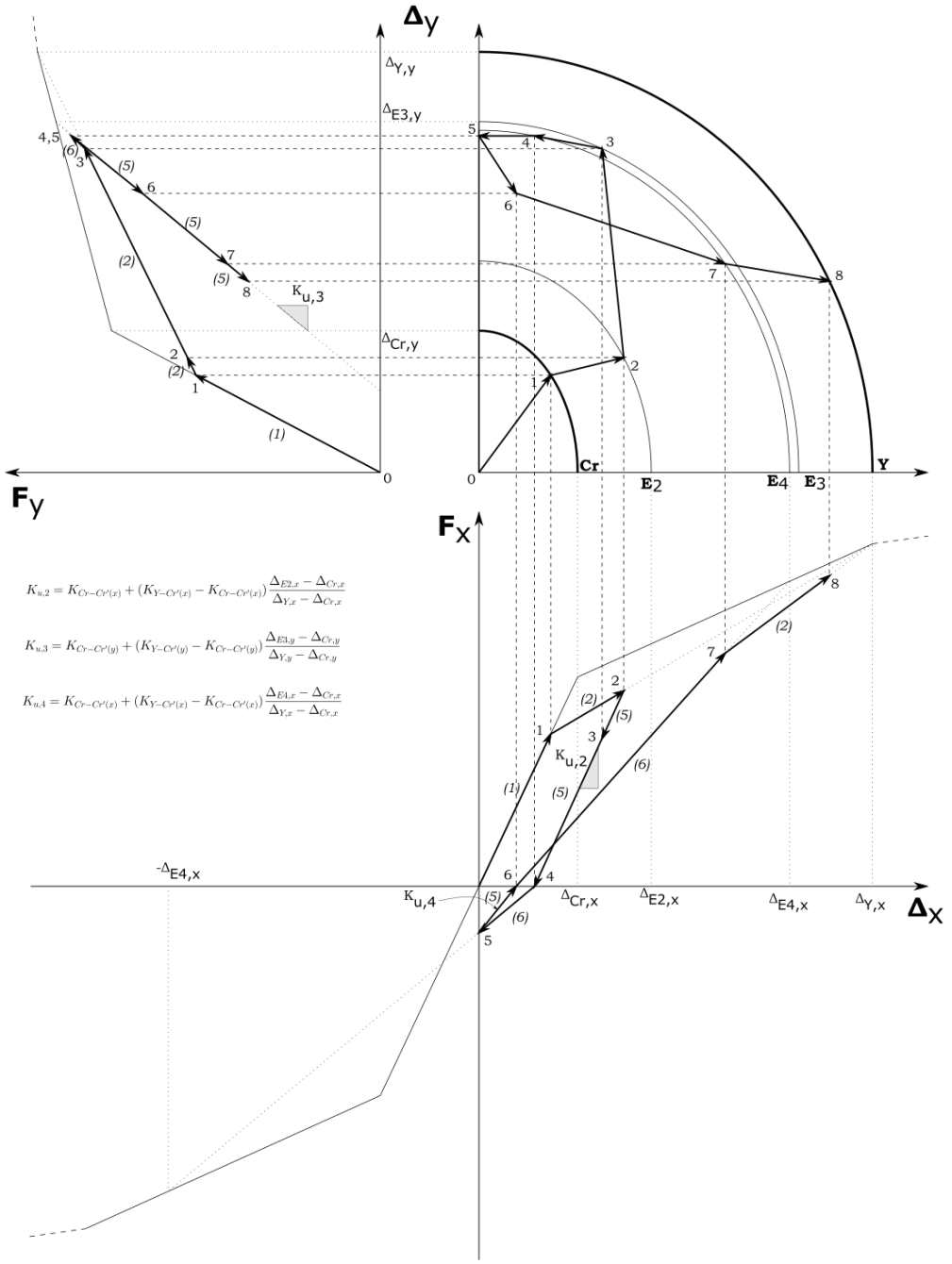

Fig. 9.9 – Assumed 2D hysteresis behaviour (backbone curves are represented only up to yielding for clarity)

9.3 Modelling the infills contribution

In order to get a full model of the structure under analysis, also infills are to be included. In fact, it is clear that most of residential buildings have infills (mainly masonry infills), that usually are not detached from surrounding structural frame (especially in not-so-recent structures).

While masonry infills are clearly non structural elements, and in design are considered only as loads, it is clear that have an outstanding influence over the global behaviour of structures (see *e.g.* Panagiotakos et al. (1996), Murty and Jain (2000), Uva, Porco, et al. (2012), Perrone et al. (2016), and Aiello et al. (2017b)). For this reason it is clear the key role of infills in seismic vulnerability assessments.

For instance, in the present work infills are modelled through a macro-element approach. Moreover, a single global macro-element is defined for each infill, thus including behaviour in both directions. However, behaviour in a direction is independent from the other, so that the cited single macro-element is equivalent to the usual simplified modelling that makes use of two struts (see Polyakov (1956), Smith (1962), Mainstone (1974), and Rodrigues et al. (2010)) as in Fig. 9.10.

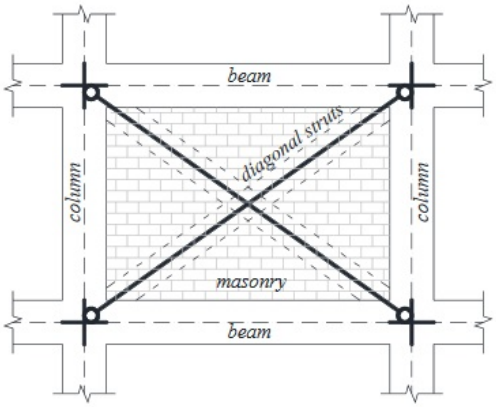

Fig. 9.10 – 2-struts modelling approach (from Lima et al. (2014))

9.3.1 In-plane non-linear behaviour of infills

The in-plane behaviour of infills is here taken into account through a modified version of the model by Panagiotakos et al. (1996), which generic scheme of force-displacement law is presented in Fig. 9.11.

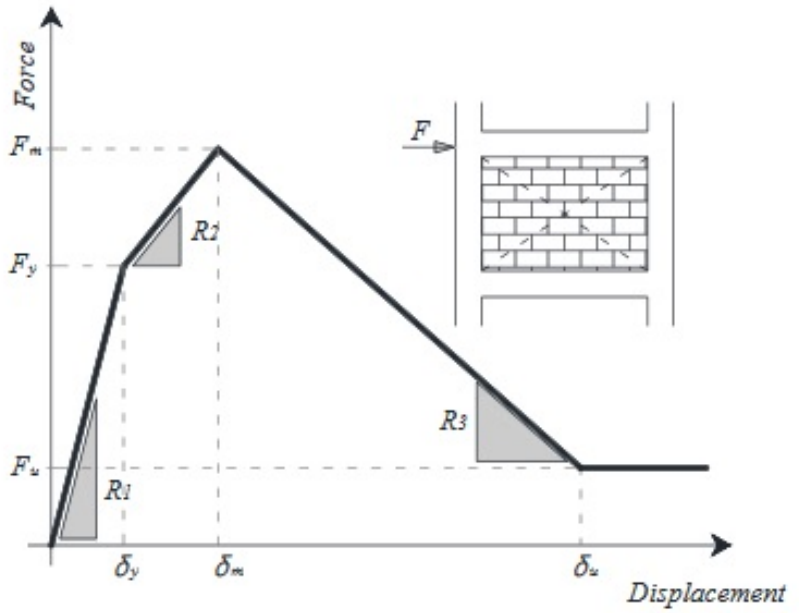

Fig. 9.11 – General scheme of the Panagiotakos-Fardis model (from Lima et al. (2014))

It must be noted that force-displacement law in Fig. 9.11 is to be intended as a horizontal force - horizontal displacement as in Panagiotakos et al. (1996).

In present work, residual force is considered to be null: the use of a non-null value is suggested only in order to guarantee numerical stability in nonlinear analyses (Lima et al., 2014).

Characteristic values for the constitutive law of the infills is derived from several sources. Stiffness in elastic stage (*i.e.* before cracking, R_1 in Fig. 9.11) is computed through Eq. 9.28 according to Panagiotakos et al. (1996).

$$R_1 = \frac{G_m L t}{H} \tag{9.28}$$

where: G_m = shear modulus of masonry
L = length of infill panel
t = thickness of infill

Cracking force (F_y in Fig. 9.11) is computed again according to Panagiotakos et al. (1996) through Eq. 9.29.

$$F_y = \tau \cdot L \cdot t \tag{9.29}$$

where: τ = shear strength of masonry

The maximum strength F_m exhibited by the infill is computed as in Eq. 9.30 according to Panagiotakos et al. (1996).

$$F_m = 1.3 \cdot F_y \tag{9.30}$$

The displacement δ_m at which the maximum strength is exhibited is defined according to NTC2018, that in 7.3.6.1 assumes that a *brittle* infill will fail at a displacement $\delta_m = 0.005 \cdot H$ being H the inter-storey height.

The evaluation of some needed infill parameters is made through following equations:

shear modulus:

$$G_m = 0.4 E_m$$

from EC6-1-1 3.7.3(1)

Young modulus:

$$E_m = 1000 f_m$$

from EC6-1-1 3.7.2(2)

Tab. 9.1 – Reduction factors on strut width for modelling the influence of openings in infills according to several existing models

Reference	Strut width (w)
Al-Chaar (2002)	$1 - 1.6\alpha + 0.6\alpha^2$
Mondal et al. (2008)	$1 - 2.6\alpha$
Asteris et al. (2011)	$1 - 2\alpha^{0.54} + \alpha^{1.14}$
Tasnimi et al. (2011)	$1 - 2\alpha^{0.54} + \alpha^{1.14}$
Mansouri et al. (2013)	$1 - 0.31\alpha$
Cetisli (2015)	$1 - 2\alpha^{0.5\cdot(1+0.4L/H)} + \alpha^{1+0.4L/H}$

In order to take into account the presence of openings in infill, according to the strategy usually adopted in technical literature, a reduction factor RF has been defined to be applied to infill strength.

However, the main issue in the definition of a value for RF is that there exist several proposals in the technical literature, and the variation of provided values is outstanding. This is clearly due to the presence of inherent errors in each model when predicting the strength reduction due to openings, and this can be explained by the absence of a huge amount of experimental data about this issue, thus bringing to an inevitable poor knowledge of the phenomenon and of how its influencing parameters take part in the definition of RF.

Considering this huge source of uncertainty, the only rational strategy for reducing as much as possible the amount of said error is to take as selected value of RF the median of all values predicted by existing models. It is indeed expected that errors in the model are random and not biased, so that a central value can be assumed to be a better estimator than the value provided by one of the models.

In Tab. 9.1 the considered models are listed, where the parameter $\alpha = \frac{A_o}{A_i}$ is the ratio between areas of the opening and of the infill panel.

About hysteresis behaviour of infills, in Fig. 9.12 a *realistic* model is represented.

In present work, behaviour is simplified as in Fig. 9.13. For instance, unloading is supposed to happen with elastic stiffness (*i.e.* no stiffness degradation is assumed) as depicted in the positive quadrant (where stiffness of various branches are indicated recalling the nomenclature used in Fig. 9.11). In the negative quadrant of Fig. 9.13 is depicted an eventual schematic hysteresis cycle:

- during phase *I* in the $0 - Cr$ branch elastic stiffness R_1 holds until one of the

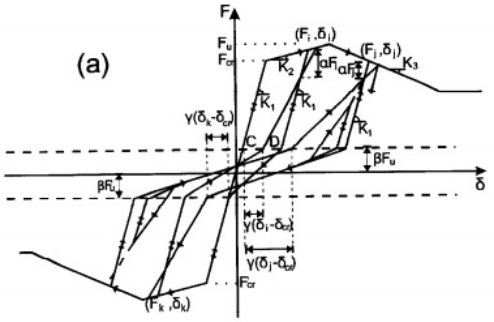

Fig. 9.12 – Hysteresis expected behaviour of infills (from Panagiotakos et al. (1996))

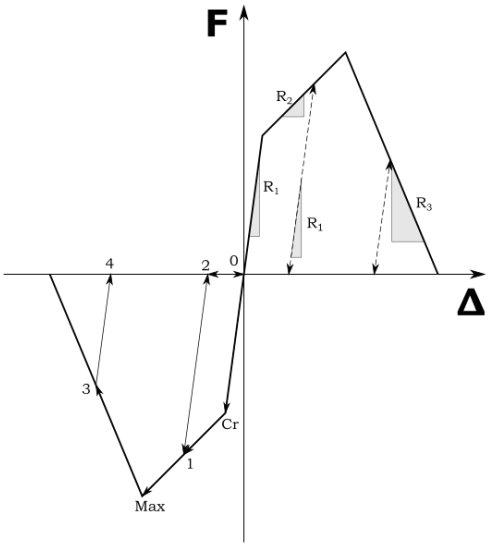

Fig. 9.13 – Assumed hysteresis behaviour of infills

two extrema are exceeded, independently from what happens in between (*i.e.* loading-unloading cycles);

- in phase *II*, after exceeding Cr, diagonal strut behaviour start controlling the infill global behaviour with R_2 stiffness up to the start of eventual unloading (labeled as point 1 in the example in Fig. 9.13);
- during phase *III* unloading happens with elastic stiffness (R_1), up to zero-force point 2; if reloading happens, its stiffness is still R_1;

- once point 2 is surpassed in phase *IV* (going toward 0), it becomes the *activation point* of the strut (remembering that the model assumes that two independent struts act to define the infill global behaviour); in this phase, no force is retrieved by the infill, also if the action is reversed (up to the activation point 2 of the strut);
- when point 2 is again exceeded during phase *V*, reloading happens again with elastic stiffness R_1 toward point 1 on the backbone curve (*i.e.* maximum reached displacement);
- as soon as maximum reached point 1 is exceeded, in phase *VI* the backbone curve is followed until another unloading happens or point of maximum force Max is reached;
- when in phase *VII* the point Max of maximum force is exceeded, the backbone softening branch is followed (with stiffness R_3) until displacement reversal happens or null force is reached;
- in phase *VIII* an unloading is supposed to happen starting from point 3, and again it happens with elastic stiffness R_1 up to point 4;
- in phase *IX*, from newly defined activation point of the strut 4 no force is retrieved at all (both in loading and unloading) up to when point 4 or the activation point of the other strut is exceeded.

9.3.2 Out-of-plane behaviour of infills

In order to get a realistic assessment of the infills response to dynamic actions, also out-of-plane (***OoP***) behaviour must be included. Namely, the infill is assumed to give no further stiffness to the structural system when loaded in OoP direction. However, it can experience collapse due to said loading. Hence, a control is implemented in the procedure in order to check if OoP collapse is reached: if so, the infill is assumed to fall, so that in-plane response no longer exist, and only a given percentage of its mass is kept in further steps of analysis. [3]

[3] After an OoP collapse it is assumed that the infill falls, so that it is no more included in the structure: this is the reason why both in-plane behaviour and mass are dropped (as if the infill no longer exists).

Lateral strength of infill is computed through Eq. 9.32, taken from EC6-1-1 6.3.2(6).

$$q_{lat} = f_m \left(\frac{t}{L}\right)^2 \tag{9.32}$$

This lateral strength is expressed in terms of uniformly distributed action over the lateral surface of the infill panel. However, in-plane damage can reduce lateral strength. Amongst the several studies that face this condition, the model in Ricci et al. (2018) is here used. A reduction factor R, whose value is given by Eq. 9.33 depending on Interstorey Drift Ratio (***IDR***, given in percentage), is hence used on Eq. 9.32.

$$R = \left(1.21 + 0.05min\left(20.4; \frac{H}{t}\right)\right)\left(IDR_{\%}\right)^{-0.89} \tag{9.33}$$

However, a given limited percentage of said mass (10%) is held, under the hypothesis that part of the infill remains attached to surrounding frame.

10. STRATEGY FOR THE TIME HISTORY ANALYSES SOLUTION: PROPOSAL OF AN EXACT APPROACH

10.1 State of the art of the time integration of dynamic problems

One of the open issues in structural dynamics is the definition of an appropriate procedure for the time integration of transient dynamic problems, *i.e.* when a structure is subjected to random external forces/accelerations, especially whenever the nonlinearity of at least a part of the structure is triggered.

The mathematical representation of said problem is presented in Eq. 10.1.

$$[M]\{\ddot{u}(t)\} + [C]\{\dot{u}(t)\} + \{f_r(t, u(t), \dot{u}(t))\} = \{f(t)\} \tag{10.1}$$

where: $[M]\,[C]$ = are respectively mass and damping matrices

$\{u(t)\}$ = is the vector containing the Degrees of Freedom (***DoF***) displacements, while $\{\dot{u}(t)\}$ $\{\ddot{u}(t)\}$ are its first and second derivative with respect to time

$\{f_r(t, u(t), \dot{u}(t))\}$ = is the vector containing restoring forces, equal to $[K]\{u(t)\}$ in the linear case

$\{f(t)\}$ = is the vector containing external forces applied to each DoF

Given the importance of the problem, several authors proposed a lot of time integration schemes.

Early history of those solutions in structural dynamics can be traced back at least to 1950s, when in Newmark (1952) and Newmark (1959) the *Newmark method* was proposed. For instance, within this nomenclature a *family* of methods are included, which are distinguished for the different values of the two free parameters β and γ.

Although it is almost 70 years from its proposal, the Newmark family of methods is

one of the most used, and is still an ever-present reference when a new time integration scheme is developed.

Within this time integration scheme, the solution at the end of a time step is expressed by a Taylor series, whose remainder is approximated by a quadrature formula (Goudreau et al., 1972). The resulting scheme can be described through Eq. 10.2 (in terms of a SDoF system for clarity).

$$ma_{n+1} + cv_{n+1} + kd_{n+1} = f_{n+1} \tag{10.2a}$$

$$v_{n+1} = v_n + (1-\gamma)a_n\Delta t + \gamma a_{n+1}\Delta t \tag{10.2b}$$

$$d_{n+1} = d_n + v_n\Delta t + \left(\frac{1}{2} - \beta\right) a_n(\Delta t)^2 + \beta a_{n+1}(\Delta t)^2 \tag{10.2c}$$

where: m, c, k = Mass, damping and stiffness of the system respectively
f_n = value of the external force at the step n
a_n, v_n, d_n = acceleration, velocity and displacement of the mass at the step n respectively
Δt = time step
β, γ = free parameters of the scheme

Some remarks on the proposed scheme need to be deepened:

- Unless $\gamma = \frac{1}{2}$, a *spurious damping* is introduced, and for instance if $\gamma < \frac{1}{2}$ a *negative damping* results (*i.e.* a self-excited vibration arises from the numerical procedure), while if $\gamma > \frac{1}{2}$ a *positive damping* arises (*i.e.* the numerical procedure brings to a reduction of the response as if an additional damping is set, also if no damping at all was included in the fundamental equation Eq. 10.1). In Newmark (1959) those eventualities are described as unwanted by a time integration scheme, thus $\gamma = \frac{1}{2}$ is set, while following authors proposed their own schemes *from* this feature.
- The generic scheme of the Newmark family has a convergence limit, *i.e.* there exist choices of parameters for which the solution does not converge to the exact

one. In order to keep the error ρ in terms of acceleration less than 1, the time step must fulfil the condition $\frac{\Delta t}{T} < \frac{1}{2\pi}\sqrt{\frac{1}{\beta}}$. The term T is the vibration period of the SDoF, while in the case of MDoF systems author suggested to use the shortest period of vibration.

- The generic scheme of the Newmark family has also a stability limit, *i.e.* there exist choices of parameters for which the solution starts oscillating without bounds. In order to avoid this condition, the condition $\frac{\Delta t}{T} < \frac{1/\pi}{\sqrt{1-4\beta}}$ must hold.
- The free parameter β controls the assumed variation of the acceleration within Δt: $\beta = 1/6$ corresponds to a linear variation of acceleration, $\beta = 1/4$ to a uniform value equal to the average between the extrema of the time step Δt, $\beta = 1/8$ to a step function with a constant value equal to the initial value for the first half of Δt, and equal to the final value for the remaining half.
- The scheme is demonstrated to introduce an error in both amplitude and oscillation period, assessed through a free vibration analysis, that is proportional to $\frac{\Delta t}{T}$.

In Wilson et al. (1972) the *Wilson θ-method* was developed. Within this approach, the mass acceleration is assumed to vary linearly amongst the time interval $[t \quad t+\theta\Delta t]$ being $\theta > 1$ the only free parameter of the scheme. Under this assumption, acceleration velocity and displacements at the end of the time step (*i.e.* at $t + \Delta t$) are computed. While if $\theta \geq 1.37$ the method is unconditionally stable (*i.e.* it is stable for every value of Δt), errors in terms of period elongation and amplitude decay increase with the increase of θ (and, obviously, as Δt increases) as depicted in Fig. 10.1.

In Hilber, Hughes, and Taylor (1977) the Hilber-Hughes-Taylor (HHT) integration scheme was developed slightly modifying the Newmark scheme by adding another parameter α. For instance, the integration scheme can be described in the non-damped case as in Eq. 10.3.

$$ma_{n+1} + (1+\alpha)kd_{n+1} - \alpha kd_n = f_{n+1} \tag{10.3a}$$

$$v_{n+1} = v_n + (1-\gamma)a_n\Delta t + \gamma a_{n+1}\Delta t \tag{10.3b}$$

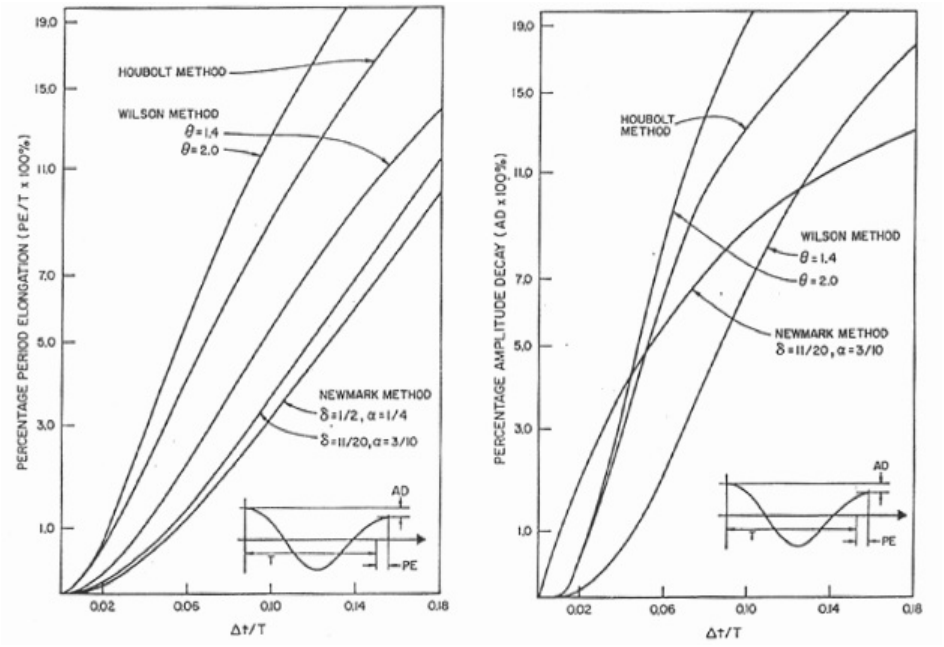

Fig. 10.1 – Error assessment for several time integration schemes (from Bathe and Wilson (1972))

$$d_{n+1} = d_n + v_n \Delta t + \left(\frac{1}{2} - \beta\right) a_n (\Delta t)^2 + \beta a_{n+1} (\Delta t)^2 \tag{10.3c}$$

Authors set some desired requirements for the scheme: unconditional stability, controllable numerical dissipation through a parameter other than Δt, numerical dissipation that does not affect lower modes too strongly.

In order to fulfil said requirements, authors fixed $\beta = (1-\alpha)^2/4$ and $\gamma = 1/2 - \alpha$, so that only α is kept as free parameter. In order to fulfil the unconditional stability, the limitation $-1/2 \leq \alpha \leq 0$ was computed, while for error limitation authors indicated the range $-1/3 \leq \alpha \leq 0$ as the one of practical interest.

It must be noted that if $\alpha = 0$ the scheme reduces to Newmark, because α is the controlling parameter for numerical dissipation.

In Goudreau et al. (1973) an issue of numerical methods was highlighted: the *overshoot*. This phenomenon is clearly depicted in Fig. 10.2, where displacements and velocities provided by several integration schemes for the case of free vibration with

non-null initial conditions are depicted.

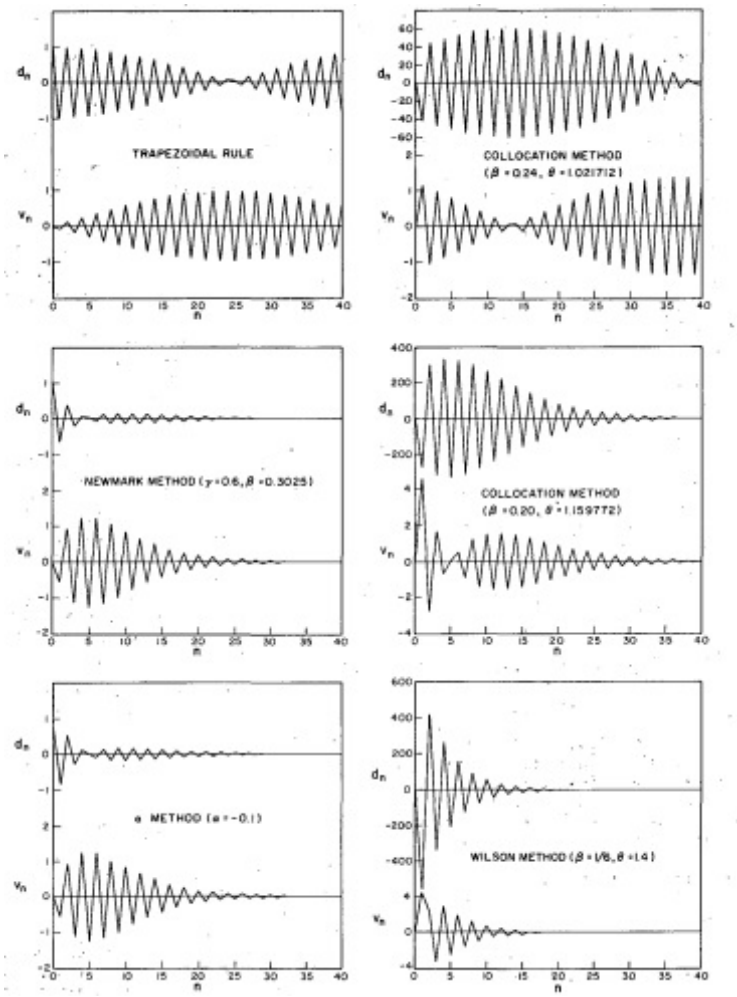

Fig. 10.2 – Overshoot behaviour for several time integration schemes (from Hilber and Hughes (1978))

In order to solve this issue, in Hilber and Hughes (1978) the *collocation scheme* was proposed, that can be sinthetically defined through Eq. 10.4 for the non-damped SDoF case.

$$ma_{n+\theta} + kd_{n+\theta} = f_{n+\theta} \tag{10.4a}$$

$$a_{n+\theta} = (1-\theta)a_n + \theta a_{n+1} \tag{10.4b}$$

$$f_{n+\theta} = (1-\theta) f_n + \theta f_{n+1} \tag{10.4c}$$

$$d_{n+\theta} = d_n + \theta \Delta t v_n + (\theta \Delta t)^2 \left[\left(\frac{1}{2} - \beta \right) a_n + \beta a_{n+\theta} \right] \tag{10.4d}$$

$$v_{n+1} = v_n + (1-\gamma) a_n \Delta t + \gamma a_{n+1} \Delta t \tag{10.4e}$$

$$d_{n+1} = d_n + v_n \Delta t + \left(\frac{1}{2} - \beta \right) a_n (\Delta t)^2 + \beta a_{n+1} (\Delta t)^2 \tag{10.4f}$$

For practical applications, authors suggested the use of $\gamma = \frac{1}{2}$ and several couples (β, θ) are given in order to use the *optimal* scheme.

In Wood et al. (1980) the *Bossak-Newmark* algorithm was presented, whose definition is given in Eq. 10.5.

$$f_{n+1} = (1-\alpha_B) m a_{n+1} + \alpha_B m a_n + c v_{n+1} + (1+\alpha) k d_{n+1} - \alpha k d_n \tag{10.5a}$$

$$v_{n+1} = v_n + (1-\gamma_B) a_n \Delta t + \gamma_B a_{n+1} \Delta t \tag{10.5b}$$

$$d_{n+1} = d_n + v_n \Delta t + \left(\frac{1}{2} - \beta_B \right) a_n (\Delta t)^2 + \beta_B a_{n+1} (\Delta t)^2 \tag{10.5c}$$

Unconditional stability, second order accuracy and positive numerical damping are achieved if $\beta_B > \frac{\gamma_B}{2} > \frac{1}{4}$ and $\alpha_B = \frac{1}{2} - \gamma_B$.

In Bazzi et al. (1982) the ρ*-family of algorithms* was developed, whose definition is given according to the cited reference in Eq. 10.6.

$$\begin{Bmatrix} d_{n+1} \\ \Delta t v_{n+1} \\ (\Delta t)^2 a_{n+1} \end{Bmatrix} = A \begin{Bmatrix} d_n \\ \Delta t v_n \\ (\Delta t)^2 a_n \end{Bmatrix} \tag{10.6}$$

The *amplification matrix* A is given in Eq. 10.7.

$$A = \frac{1}{D} \begin{bmatrix} A_{11} & A_{12} & A_{13} \\ A_{21} & A_{22} & A_{23} \\ A_{31} & A_{32} & A_{33} \end{bmatrix} \tag{10.7}$$

where: $D = 1 + \xi\Omega + \frac{\Omega^2}{2(1+\rho)}$

ξ = damping ratio

$\Omega = \omega\Delta t$

ω = natural frequency of the SDoF system

$$A_{11} = 1 + \xi\Omega - \frac{\rho}{2(1+\rho)}\Omega^2$$
$$A_{12} = 1$$
$$A_{13} = \frac{\rho-1}{2(1+\rho)}$$
$$A_{21} = \Omega^2$$
$$A_{22} = 1 - \xi\Omega - \frac{\omega^2}{2(1+\rho)}$$
$$A_{23} = \frac{1-\rho}{1+\rho}\xi\Omega + \frac{1-\rho}{2(1+\rho)^2}\Omega^2$$
$$A_{31} = -\frac{1}{2}(1+\rho)(1+\rho^2)\Omega^2$$
$$A_{32} = -(1+\rho)(1+\rho^2)\xi\Omega - \frac{1}{2}(1+\rho^2)\Omega^2$$
$$A_{33} = \frac{1}{2}(1-\rho-\rho^2-\rho^3) + (1-\rho-\rho^3)\left(\xi\Omega + \frac{\Omega^2}{2(1+\rho)}\right)$$

The free parameter ρ can have values ranging in the interval $[0, 1]$, thus controlling the numerical damping of the scheme, being $\rho = 1$ the case of no numerical damping that reduces to trapezoidal rule.

In Hoff et al. (1988) a new generalized algorithm was developed so that, using authors' words, *"the numerical dissipation is not associated with disadvantages such as decrease in accuracy, a significant spurious root in the low frequencies, and overshooting"*. Its scheme is described in Eq. 10.8.

$$\begin{aligned}&(\theta_1\eta m + \theta_2\gamma\Delta t c + \theta_3\beta\Delta t^2 k)\Delta a = \\ =&f_n + \theta_0(f_{n+1} - f_n) - ma_n - c(v_n + \theta_1\Delta t a_n) + k(d_n + \theta_1\Delta t v_n + 1/2\theta_2\Delta t^2 a_n)\end{aligned} \tag{10.8a}$$

$$v_{n+1} = v_n + a_n\Delta t + \gamma\Delta a\Delta t \tag{10.8b}$$

$$d_{n+1} = d_n + v_n\Delta t + 1/2 a_n\Delta t^2 + \beta\Delta a\Delta t^2 \tag{10.8c}$$

Amongst the parameters in Eq. 10.8, some were defined from authors in order to

get some desired features (*e.g.* second order accuracy, unconditional stability).

In Chung et al. (1993) the *generalized-α method* was presented, whose constitutive equations are summarized in Eq. 10.9

$$f(t_{n+1-\alpha_f}) = ma_{n+1-\alpha_m} + cv_{n+1-\alpha_f} + kd_{n+1-\alpha_f} \tag{10.9a}$$

$$v_{n+1} = v_n + (1-\gamma)a_n\Delta t + \gamma a_{n+1}\Delta t \tag{10.9b}$$

$$d_{n+1} = d_n + v_n\Delta t + \left(\frac{1}{2} - \beta_B\right) a_n(\Delta t)^2 + \beta_B a_{n+1}(\Delta t)^2 \tag{10.9c}$$

where: $d_{n+1-\alpha_f} = (1-\alpha_f)d_{n+1} + \alpha_f d_n$

$v_{n+1-\alpha_f} = (1-\alpha_f)v_{n+1} + \alpha_f v_n$

$a_{n+1-\alpha_m} = (1-\alpha_m)a_{n+1} + \alpha_m a_n$

$t_{n+1-\alpha_f} = (1-\alpha_f)t_{n+1} + \alpha_f t_n$

$\gamma = \frac{1}{2} - \alpha_m + \alpha_f$ for second-order accuracy

$\alpha_m \leq \alpha_f \leq \frac{1}{2} =$ for unconditional stability

$\beta = \frac{1}{4}(1-\alpha_m+\alpha_f)^2$

Several previous schemes are demonstrate to belong to this family when particular values are given to its parameters.

With Chung et al. (1994) a new time integration scheme was introduced, defined through Eq. 10.10.

$$\begin{bmatrix} 1 & 0 & -\beta_l \\ 0 & 1 & -\gamma_l \\ \alpha_{k_l}\Omega^2 & \alpha_{c_l} 2\xi\Omega^2 & \alpha_{m_l} \end{bmatrix} \begin{Bmatrix} d_{n+1} \\ v_{n+1}\Delta t \\ a_{n+1}\Delta t^2 \end{Bmatrix} =$$

$$= \begin{bmatrix} 1 & 0 & \beta \\ 0 & 1 & \gamma \\ -\alpha_k\Omega^2 & -\alpha_c 2\xi\Omega^2 & -\alpha_m \end{bmatrix} \begin{Bmatrix} d_n \\ v_n\Delta t \\ a_n\Delta t^2 \end{Bmatrix} + \begin{bmatrix} 0 & 0 \\ 0 & 0 \\ \alpha_f & \alpha_{f_l} \end{bmatrix} \begin{Bmatrix} f_n \\ f_{n+1} \end{Bmatrix} \tag{10.10}$$

Authors fixed some of the parameters involved in Eq. 10.10, namely those in Eq. 10.11,

thus resulting in a single-parameter γ_l scheme.

$$\begin{array}{ccc} \alpha_{m_l} = 1 & \alpha_k = 0 & \beta = \gamma \\ \beta_l = \gamma + \gamma_l & \alpha_m = -\frac{1}{2} & \alpha_{k_l} = \frac{1}{2\beta_l} \\ \alpha_c = -\frac{2\beta+\beta_l}{4\beta_l^2} & \alpha_{c_l} = \frac{2\beta+3\beta_l}{4\beta_l^2} & \alpha_{f_l} = \alpha_{k_l} \\ \alpha_f = \alpha_k & & \gamma = \frac{1}{2}\left(\frac{1}{2} - \gamma_l\right) \end{array} \tag{10.11}$$

In ZHAI (1996) the *Zhai algorithm* was developed as depicted in Eq. 10.12 for the case of non-damped systems.

$$f(t_{n+1}) = ma_{n+1} + kd_{n+1} \tag{10.12a}$$

$$v_{n+1} = v_n + (1+\varphi)a_n\Delta t - \varphi a_{n-1}\Delta t \tag{10.12b}$$

$$d_{n+1} = d_n + v_n\Delta t + \left(\frac{1}{2} + \phi\right)a_n(\Delta t)^2 - \phi a_{n-1}(\Delta t)^2 \tag{10.12c}$$

Author suggested fixing both parameters ϕ and φ at 0.5.

In Chang (1999) and Chang and Liao (2005) the *Chang family of methods* was founded. The same author in Chang (2017) discovered an unusual overshooting behaviour of the scheme, subsequently solved in Chang (2018a).

$$f_{n+1} = ma_{n+1} + cv_{n+1} + kd_{n+1} \tag{10.13a}$$

$$v_{n+1} = v_n + \Delta t[(1-\gamma)a_n + \gamma a_{n+1}] \tag{10.13b}$$

$$d_{n+1} = d_n + \beta_1 v_n\Delta t + \beta_2 a_n\Delta t^2 + \beta_3 \tag{10.13c}$$

The Chang family of methods is referred to as a *structure-dependent* integration method because its parameters are defined through structural characteristics as in Eq. 10.14, while usually for others methods parameters are uniquely defined independently from the structure under analysis. In Eq. 10.14 $\Omega_0 = \omega_0\Delta t$ and terms with 0 subscript indicate the initial value.

$$\beta_1 = \frac{1 + 2\gamma\xi\Omega_0}{1 + 2\gamma\xi\Omega_0 + \beta\Omega_0^2} \tag{10.14a}$$

$$\beta_2 = \frac{1/2 - 2(\beta - \gamma/2)\xi\Omega_0}{1 + 2\gamma\xi\Omega_0 + \beta\Omega_0^2} \tag{10.14b}$$

$$\beta_3 = \frac{\beta\Delta t^2(f_{n+1} - f_n)}{m + \gamma\Delta t c_0 + \beta\Delta t^2 k_0} \tag{10.14c}$$

In Bathe and Baig (2005) a composite integration scheme was proposed. After several improvements amongst years (Bathe, 2007; Bathe and Noh, 2012; Noh et al., 2018), the scheme resulted in the ρ_∞-*Bathe method* as described in Noh et al. (2019) and Kwon, Bathe, et al. (2020). It is said to be *composite* because two sub-steps are defined: as described in the Eq. 10.15, in the first sub-step trapezoidal rule is used, while in the second a 3-point Euler backward method is used.

1st sub-step:

$$f(t + \gamma\Delta t) = ma(t + \gamma\Delta t) + cv(t + \gamma\Delta t) + kd(t + \gamma\Delta t) \tag{10.15a}$$

$$u(t + \gamma\Delta t) = u(t) + \frac{\gamma\Delta t}{2}\left(v(t) + v(t + \gamma\Delta t)\right) \tag{10.15b}$$

$$v(t + \gamma\Delta t) = v(t) + \frac{\gamma\Delta t}{2}\left(a(t) + a(t + \gamma\Delta t)\right) \tag{10.15c}$$

2nd sub-step:

$$f(t + \Delta t) = ma(t + \Delta t) + cv(t + \Delta t) + kd(t + \Delta t) \tag{10.15d}$$

$$u(t + \Delta t) = u(t) + \Delta t\left(q_0 v(t) + q_1 v(t + \gamma\Delta t) + q_2 v(t + \Delta t)\right) \tag{10.15e}$$

$$v(t + \Delta t) = v(t) + \Delta t\left(s_0 a(t) + s_1 a(t + \gamma\Delta t) + s_2 a(t + \Delta t)\right) \tag{10.15f}$$

$$\tag{10.15g}$$

Most of the parameters of the scheme are defined in order to provide the model stability and accuracy. For instance, the method is called ρ_∞ because this is explicitly a free parameter of the scheme, hence representing directly the spectral radius of its amplification matrix, that is a direct measurement of the numerical damping.

Starting from the work by Chang (1999), in Chen et al. (2008) the *Chen-Ricles* (CR) family of structure-dependent methods was developed. It was then generalized in Kolay et al. (2014) into the *Kolay-Ricles* (KR) family, and subsequently modified in Chang (2018b) in order to get rid of an observed overshooting behaviour of the method. In its last formulation the method is defined through Eq. 10.16.

$$\begin{aligned}(1-\alpha_3)ma_{n+1} + \alpha_3 ma_n + (1-\alpha_f)c_0 v_{n+1} + \alpha_f c_0 v_n + \\ +(1-\alpha_f)k_{n+1}d_{n+1} + \alpha_f k_n d_n = (1-\alpha_f)f_{n+1} + \alpha_f f_n \end{aligned} \tag{10.16a}$$

$$d_{n+1} = d_n + \Delta t v_n + \alpha_2 \Delta t^2 a_n + p_{n+1} \tag{10.16b}$$

$$v_{n+1} = v_n + \alpha_1 \Delta t a_n \tag{10.16c}$$

where:
$$\begin{aligned}\alpha_1 &= \frac{1}{D} \\ \alpha_2 &= \frac{1}{D}\left(\frac{1}{2}+\gamma\right) \\ \alpha_3 &= \frac{1}{D}\left(\alpha_m + 2\alpha_f\gamma\xi\Omega_0 + \alpha_f\beta\sigma\Omega_0^2\right) \\ D &= 1 + 2\gamma\xi\Omega_0 + \beta\sigma\Omega_0 \\ \alpha_m &= \frac{2\rho_\infty - 1}{\rho_\infty + 1} \\ \alpha_f &= \frac{\rho_\infty}{\rho_\infty + 1} \\ \beta &= \frac{1}{4}\left(1 - \alpha_m + \alpha_f\right)^2 \\ \gamma &= \frac{1}{2} - \alpha_m + \alpha_f\end{aligned}$$

Several other methods have been proposed in recent years, that for sake of brevity are here only cited (Ghassemieh et al., 2008; Yina, 2011; Katsikadelis, 2013; Wen et al., 2014; Gui et al., 2014; Zhang et al., 2015; Kwon and Lee, 2018; Vaiana et al., 2019).

Some methods are defined through an eventually interesting characteristic for the present work: those that are claimed to be *analytical* in several degrees.

In Abassy (2012) the *Piecewise Analytical Method* (PAM) is presented, which consists in a solution strategy that involves Taylor or Padé approximations over a given sub-interval (also if the problem is continuous) up to any wanted degree of precision.

An interesting semi-analytical approach is introduced in Michels et al. (2015) for

the solution of molecular dynamics problems. The molecular dynamics problem to be solved is expressed through Eq. 10.17.

$$[M]\{\ddot{R}(t)\} + [K]\{R(t)\} + G(\{R(t)\}) = 0 \tag{10.17}$$

where: $\{R(t)\}$ = vector containing the position of all nuclei
$[M]$ = the molecules nuclei mass matrix
$[K]\{R(t)\}$ = bonding forces between nuclei vector
$G(\{R(t)\})$ = function regrouping all weaker forces deriving from angle, torsional, Lennard-Jones and Coulomb potentials

With some modifications, geometrically non-linear deformations are split into a rigid rotation and a pure strain parts through a rotation matrix $[Q]$ so that:

$$[K]\{R(t)\} = [Q][K]([Q]^{-1}\{R(t)\} - \{R_0\})$$

where $\{R_0\}$ stores the resting position, with the use of modified coordinates $\{\chi(t)\} = \sqrt{[M]}\{R(t)\}$ Eq. 10.17 can be rewritten as in Eq. 10.18.

$$\{\ddot{\chi}(t)\} + [\Omega]^2\{\chi(t)\} + \Lambda(\{\chi(t)\}) = 0 \tag{10.18}$$

where: $[\Omega]^2 = \sqrt{[M]}[A]\sqrt{[M]}$
$[A] = [M]^{-1}[Q][K][Q]^T$
$\Lambda(\{\chi(t)\}) = \sqrt{[M]}^{-1}\left\{\bar{G}\left(\sqrt{[M]}^{-1}\{\chi(t)\}\right)\right\}$
$\bar{G}(\{R(t)\}) = G(\{R(t)\}) - [Q][K]\{R_0\}$

Eq. 10.18 is then solved by splitting into two 1-degree differential equations (defining $\{v(t)\} = \{\dot{\chi}(t)\}$), and its discrete formulation is written as in Eq. 10.19.

$$\{\chi_{n+1}\} = \cos(\Delta t[\Omega])\{\chi_n\} + [\Omega]^{-1}\sin(\Delta t[\Omega])\{v(t)\}_n + \\ + \frac{1}{2}\Delta t^2\psi(\Delta t[\Omega]) \cdot \Lambda(\phi(\Delta t[\Omega])\{\chi_n\}) \tag{10.19a}$$

$$\{\upsilon(t)\}_{n+1} = -[\Omega]\sin(\Delta t[\Omega])\{\chi_n\} + \cos(\Delta t[\Omega])\{\upsilon(t)\}_n + \\ + \frac{1}{2}\Delta t\left(\psi_0(\Delta t[\Omega])\Lambda(\phi(\Delta t[\Omega])\{\chi\}_n)\right) + \psi_1(\Delta t[\Omega])\cdot\Lambda(\phi(\Delta t[\Omega])\{\chi\}_{n+1}) \tag{10.19b}$$

where: $\psi(\cdot) = (\cdot)^{-1}\sin(\cdot)\psi_1(\cdot)$
$\psi_0(\cdot) = \cos(\cdot)\psi_1(\cdot)$
$\psi(\cdot) = \left[(\cdot)^{-1}\sin(\cdot)\right]^2$
$\phi(\cdot) = (\cdot)^{-1}\sin(\cdot)$

Approximate solution given in Eq. 10.19, however, appears to be a lot problem-specific: the underlying problem, in fact, has *weak non-linearities*, as stated in the reference. It is worth highlighting that the method is named *semi-analytic* because only the non-linear part described by function $\Lambda(.)$ is approximated, while for the remaining part the exact analytical solution is derived.

Other examples involve the solution of a linear elastic continuum, whose definition is much more complicated by the presence of spatial coordinates, so that spatial derivatives and mixed spatial-temporal derivatives are present in the governing equation. This is not the main concern in this work, in which the presence of non-linearity is the main issue, while it is not included in those types of methods. For instance, amongst described methods it is worth highlighting the *distributed transfer function method* (DTFM) first developed in Yang et al. (1991) and used to *"yield closed-form analytical solutions for a variety of static and dynamic problems of structures and flexible mechanical systems"* (YANG, 2007); the semi-analytical method developed in Andersen et al. (2008) and subsequently deeply described in Bucinskas et al. (2017) used for the assessment of Soil-Structure Interaction (SSI).

It is important to not let the algorithms aimed at other scopes be confused with those for *time integration* (the subject here): it can be the case of the *Semi-Analytical Finite Elements Method* (SAFEM), first developed in Wilson (1965). This is a semi-analytical solution that has as target the *spatial integration* inherent to a Finite Elements Analysis (FEA). As an example, in Liu et al. (2017) this method is used in combination with the

Newmark time integration scheme in order to provide a solution to a dynamic problem involving asphalt pavement.

10.1.1 Brief discussion of available time integration schemes

Time integration algorithms can be divided into two categories: explicit and implicit methods. An integration scheme is explicit if the solution at each time step is a function of the available solution from previous time steps only. Otherwise it is said implicit. Both categories have advantages and disadvantages, that are tightly connected to the problem to be solved.

Explicit schemes have the outstanding advantage that do not need the solution of any implicit system and do not need any iteration for each time step. Thus, the computational effort is significantly lowered when compared with implicit schemes, and the implementation is simple. Although, generally those methods are only conditionally stable, so that a limit on usable time steps exists. Advantages and disadvantages of implicit schemes are the converse of those of explicit schemes: more computational effort per single time step, unconditional stability.

Much efforts have been made to develop an unconditionally stable explicit method, in order to combine the virtues of both methods, but whenever an unconditionally stable explicit method have been proposed, it has been showed that the use of large time steps brings to very poor solution due to a significant deterioration in accuracy (Chang and Liao, 2005).

According to Hilber and Hughes (1978), a time integration algorithm is required to possess the following features: unconditional stability at least if applied to linear problems, no more than one set of implicit equations to be solved at each time step, second-order accuracy, controllable numerical dissipation in higher modes response, self-starting. An additional feature that became clearly important with the time is the absence of overshooting behaviour (Chang, 2018a).

However, once a time integration scheme is developed, although it has all of desired features, another main issue is to be faced: in practical use, it is not easy the correct definition of the scheme parameters so that the solution provided is sufficiently accurate,

especially if non-linearities are involved (Zhang et al., 2015). Also if *optimal* sets of parameters values are sometimes provided by authors, there still exist a parameter that is indeed the most influencing one and that can not be defined independently from the analysed problem: the time step Δt.

For instance, the influencing parameter on the solution accuracy (assuming that stability is not involved) is $\frac{\Delta t}{T}$. While for SDoF systems T is unequivocally defined, for MDoF systems it should have to be fixed as the natural period of the higher mode *significantly influencing* the structure response. However, the use of the very last mode could bring to insanely short time steps, thus annihilating the motivations of using a computationally efficient procedure. Another approach could be iteratively reducing T until the solution is observed to stabilize, but the same drawbacks are involved.

It is widely known that computer performances steadily increase over time, and this can be observed in Fig. 10.3. It is author's opinion that the attention to the computational efficiency can be misleading: the relative importance between efficiency and accuracy is expected to tilt the balance in favour of the latter. Hence, an accuracy-focused approach disregarding computational efficiency is desired. Moreover, said approach would be significantly more desirable if the issue of selecting opportune values for scheme parameters is solved, *e.g.* with a procedure that do not include any parameter and do not need the selection of a time step either.

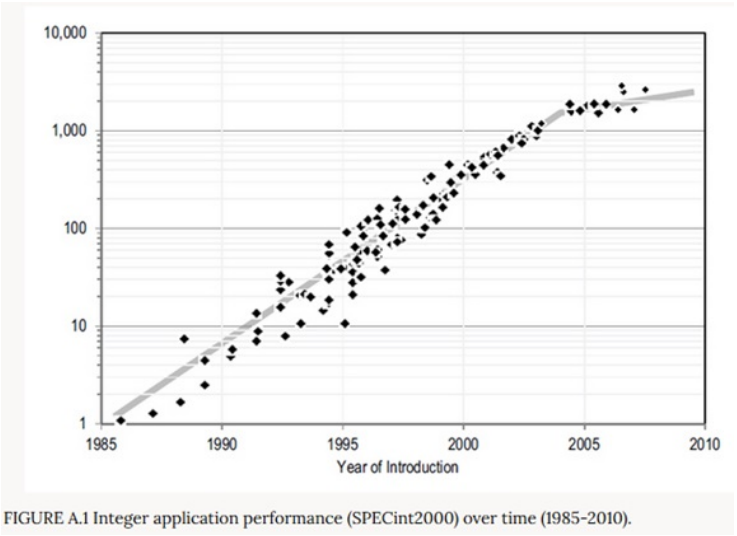

Fig. 10.3 – Computers performance over time (from Fuller et al. (2011))

10.2 Description of the novel time integration approach

Given the necessity required from the proposed procedure to run non-linear dynamic analyses, an adequate and accurate solution strategy has to be implemented.

For this purpose, a novel procedure for the exact evaluation of structural response is proposed. In the following, a description of the approach is presented.

The problem to be solved can be mathematically expressed with Eq. 10.20.

$$[M]\{\ddot{u}(t)\} + [C]\{\dot{u}(t)\} + [K]\{u(t)\} = \{f(t)\} \tag{10.20}$$

where:

- $[M]$ $[C]$ $[K]$ are respectively mass, damping and stiffness matrices;
- $\{u(t)\}$ is the vector containing the Degrees of Freedom (***DoF***) displacements, while $\{\dot{u}(t)\}$ $\{\ddot{u}(t)\}$ are its first and second derivative with respect to time;
- $\{f(t)\}$ is the vector containing external forces applied to each DoF.

In the present case, $\{f(t)\}$ is represented by the effect of a ground-level acceleration, so that it can be expressed as $\{f(t)\} = -[M]\{\ddot{u}_g(t)\}$, being clear that usually ac-

celerograms are defined through a discrete sequence of acceleration values measured in instants at fixed time step Δt. Moreover, being necessary to include non-linearity into the solution process, it makes no sense to speak about a *stiffness* (that is expected to vary during the analysis), and it is better to replace the term $[K]\{u(t)\}$ with a general term $\{F_r(p_r)\}$ representing non-linear restoring force. Here is represented a generic dependency of F_r to some parameters p_r, that usually include $\{u(t)\}$ and $\{\ddot{u}(t)\}$, but in general a wider set of parameters is involved (*e.g.* maximum reached displacement). Hence, Eq. 10.20 is transformed into Eq. 10.21.

$$[M]\{\ddot{u}(t)\} + [C]\{\dot{u}(t)\} + \{F_r(p_r)\} = -[M]\{\ddot{u}_g(t)\} \tag{10.21}$$

At this point an hypothesis has to be made: restoring forces of each element of the model has to be describable with a piecewise linear law with respect to displacement $u_i(t)$. If so, restoring forces can be represented as $F_r = k \cdot u + F_0$, and hence assembling for the MDoF problem Eq. 10.22 is defined.

$$[M]\{\ddot{u}(t)\} + [C]\{\dot{u}(t)\} + [K]\{u(t)\} + \{F_0\} = -[M]\{\ddot{u}_g(t)\} \tag{10.22}$$

Without any loss of generality, for clarity the problem is treated as a SDoF problem, given that every evaluation will be still valid for the MDoF system. In fact, through modal analysis, MDoF system response can be split into the sum of several SDoF systems responses.

So, for SDoF system the problem is defined through Eq. 10.23.

$$m\ddot{u}(t) + c\dot{u}(t) + ku(t) + F_0 = -m\ddot{u}_g(t) \tag{10.23}$$

Whereas piecewise linear law must exist between restoring force and displacement, Eq. 10.24 is the formal representation of the globally nonlinear - locally linear characteristic of $F_r - u$ law.

$$F_r = k \cdot u + F_0 \quad \text{where } \{k, F_0\} = \begin{cases} \{k_1, F_{0,1}\} & \text{if condition } C_1(p_r) \\ \{k_2, F_{0,2}\} & \text{if condition } C_2(p_r) \\ \{k_3, F_{0,3}\} & \text{if condition } C_3(p_r) \\ \vdots & \\ \{k_n, F_{0,n}\} & \text{if condition } C_n(p_r) \end{cases} \tag{10.24}$$

It is strictly needed that, for each possible set of values of parameters p_r, it is possible to define a finite value for F_r through $\{k_n, F_{0,n}\}$.

Moreover, conditions C_i are mutually exclusive. An exception to latter rule is represented by boundary sets:

- in the transition from a condition to another by continuously varying parameters p_r values there exists a *single set*[1] of those values valid for both conditions;
- from previous point follows that every transition from a condition $C_i(p_r)$ to another features an overlapping set of values common to both conditions;
- each condition has at least an overlapping set of values with other conditions[2].

As an usual scenario for structural dynamic problems, it is assumed that displacement u_0 and velocity v_0 are fixed at a given initial instant t_0.

Moreover, input accelerogram $\ddot{u}_g(t)$ has to be at least piecewise continuous. Usually ground motions are recorded so that acceleration values are provided at discrete time steps. Hence, some hypothesis has to be made in order to step from a discrete to a piecewise continuous representation of $\ddot{u}_g(t)$. For instance, in the present work a linear variation is assumed in the interval between two subsequent sampled values, so that Eq. 10.25 can be written.

[1] It cannot be an interval of any of the parameters p_r.

[2] If not, this would mean that there exist no possible transition from this condition to any other, so that current condition is the only possible, bringing to a linear elastic behaviour. Hence, this requirement is only needed for nonlinear behaviours, for which multiple conditions need to be defined. However, in the approach development nonlinearities are assumed to exist and thus given hypothesis is postulated to be true.

$$\ddot{u}_g(t) = f_1 + f_2 t \tag{10.25}$$

Finally, the problem Eq. 10.23 can be rewritten as in Eq. 10.26.

$$\begin{cases} m\ddot{u}(t) + c\dot{u}(t) + ku(t) + F_0 = -m(f_1 + f_2 t) \\ u(t = t_0) = u_0 \\ \dot{u}(t = t_0) = v_0 \\ t \geq t_0 \end{cases} \qquad \{k, F_0\} = \begin{cases} \{k_1, F_{0,1}\} & \text{if } C_1(p_r) \\ \{k_2, F_{0,2}\} & \text{if } C_2(p_r) \\ \vdots & \\ \{k_n, F_{0,n}\} & \text{if } C_n(p_r) \end{cases} \tag{10.26}$$

Call C_I the condition valid both in t_0 and in its positive neighbourhood t_0^+ as in Eq. 10.27. [3]

$$C_I = \{C \in \{C_i\} \mid C(t_0), C(t_0^+)\} \tag{10.27}$$

Define the time t_I, as in its formal definition in Eq. 10.28, to be the first instant after the starting one t_0 for which: condition C_I is fulfilled in t_I but not in t_I^+ *OR* function defining external action changes (*i.e.* t_I is one of the discrete instants in which $\ddot{u}_g(t)$ is defined in the original accelerogram). Moreover, define C_{II} as in Eq. 10.29 to be the condition fulfilled in both t_I and t_I^+. [4]

[3] Usually only the first condition (*i.e.* $C(t_0)$) is needed to be fulfilled. However, it can happen that initial parameter set $p_{r,0}$ at time t_0 is an overlapping set between two conditions. In this case the condition that is met also in subsequent instants is defined as C_I. In the case both conditions are met for a given finite interval Δt, the procedure can start at $t_0 + \Delta t$: given that $u(t) \in p_r$, it is known that $u(t \in \Delta t) = u_0$ because by hypothesis an overlapping set of parameters $p_{r,o}$ does not contain intervals for any of its parameters but only single values; hence, following condition stands:

$$\forall\, p_{r,o} = \{p_r \mid C_i(p_r), C_j(p_r), i \neq j\} \quad \exists\,!\, \bar{u} \in p_{r,o}$$

[4] It can happen that $C_{II} \equiv C_I$ when t_I is defined through condition on $\ddot{u}_g(t)$ rather then from a variation of fulfilled condition.

$$t_I = \min \left[\begin{array}{c} \{\tau \mid \tau > t_0, C_I(\tau), \neg C_I(\tau^+)\} \\ \{\tau \mid \tau > t_0, f_1(\tau^-) \neq f_1(\tau^+) \vee f_2(\tau^-) \neq f_2(\tau^+)\} \end{array} \right] \tag{10.28}$$

$$C_{II} = \left\{ C \in \{C_i\} \mid C_{II}(t_I), C_{II}(t_I^+) \right\} \tag{10.29}$$

Consider Eq. 10.30, that is a sub-problem of Eq. 10.26 in the time interval $\Omega_I = [t_0,\, t_I]$, and its solutions given in Eq. 10.31 depending on the value of k_I.

$$\begin{cases} m\ddot{u}(t) + c\dot{u}(t) + ku(t) + F_0 = -m(f_1 + f_2 t) \\ u(t = t_0) = u_0 \\ \dot{u}(t = t_0) = v_0 \\ t \in \Omega_I \end{cases} \qquad \{k, F_0\} = \{k_I, F_{0,I}\} \tag{10.30}$$

$$\begin{aligned} k_I > 0 \;&\Rightarrow \\ &\Rightarrow\; u_I(t) = e^{-\frac{\kappa}{2}t}\left(C_1 \cos(\omega_D t) + C_2 \sin(\omega_D t)\right) + \\ &\quad - \frac{f_0 + f_1}{\omega^2} - \frac{f_2}{\omega^2} t + \kappa \frac{f_2}{\omega^4} \end{aligned} \tag{10.31a}$$

$$\begin{aligned} k_I = 0 \;&\Rightarrow \\ &\Rightarrow\; u_I(t) = C_1 e^{-\kappa t} + C_2 - \frac{f_1 + f_0}{\kappa} + \frac{f_2}{\kappa^2} t - \frac{f_2}{2\kappa} t^2 \end{aligned} \tag{10.31b}$$

$$\begin{aligned} k_I < 0 \;&\Rightarrow \\ &\Rightarrow\; u_I(t) = C_1 e^{\left(-\kappa - \sqrt{\kappa^2 + 4\omega^2}\right)t/2} + C_2 e^{\left(-\kappa + \sqrt{\kappa^2 + 4\omega^2}\right)t/2} + \\ &+ \kappa \frac{f_2}{\omega^4} + \frac{f_2}{\omega^2} t - \frac{f_1 + f_0}{\omega^2} \end{aligned} \tag{10.31c}$$

where: $\omega = \sqrt{\frac{|k_I|}{m}}$

$\kappa = \frac{c}{m}$ being assumed that $0 < \kappa < 2\omega$

$\omega_D = \frac{\sqrt{4\omega^2 - \kappa^2}}{2}$

$f_0 = \frac{F_0}{m}$

$C_1\ C_2 =$ integration constants, to be computed from initial conditions

Eq. 10.30 can be rewritten as in Eq. 10.32.

$$\begin{cases} \dot{x} = G(t,x) \\ x(t_0) = x_0 \\ t \in \Omega_I \end{cases} \qquad where: \begin{cases} x = \begin{Bmatrix} x_1 \\ x_2 \end{Bmatrix} = \begin{Bmatrix} u \\ \dot{u} \end{Bmatrix} \\ x_0 = \begin{Bmatrix} u_0 \\ v_0 \end{Bmatrix} \\ G(t,x) = \begin{Bmatrix} x_2 \\ -f_1 - f_2 t - \kappa x_2 - \omega^2 x_1 - f_0 \end{Bmatrix} \end{cases} \tag{10.32}$$

Hence, from Eq. 10.32, Eq. 10.33 stands.

$$\delta G(t,x)\delta x_1 = \begin{Bmatrix} 0 \\ -\omega^2 \end{Bmatrix} \tag{10.33a}$$

$$\delta G(t,x)\delta x_2 = \begin{Bmatrix} 1 \\ -\kappa \end{Bmatrix} \tag{10.33b}$$

From Eq. 10.33 function $G(t,x)$ can be said locally Lipschitz-continuous in Ω_I with respect to x. Moreover $G(t,x)$ is also continuous because sum of continuous functions: both $x_1 = u$ and $x_2 = \dot{u}$ are continuous as can be seen in Eq. 10.31, where solutions given to the problem are always continuous; all of the other terms are constant.

Hence, the hypotheses of the Picard-Lindelöf theorem are met, so a solution to the sub-problem in Eq. 10.30 exists and is unique. By calling this solution $u_I(t)$, it can be said that $u_I(t)$ is a local solution of the problem in Eq. 10.26 in Ω_I, and it is unique in the

sense that every solution $u_i(t)$ of Eq. 10.30 in Ω_I or in any subinterval of Ω_I overlaps $u_I(t)$, *i.e.* condition in Eq. 10.34 is fulfilled.

$$u_i(t) = u_I(t) \quad \forall\, t \in \Omega_I \tag{10.34}$$

Knowing $u_I(t)$ from Eq. 10.31 in each instant of Ω_I, the state of the system (*i.e.* all of its parameters values) is known. From an operative perspective it is worth highlighting that only at this step it is possible to know the numeric value of t_I: recalling the definition of t_I (that is the extreme of the Ω_I interval) in Eq. 10.28, it depends on $C_I(p_r)$ and hence on the value of parameters p_r, that are usually not known until this point.

Recalling the definition of condition C_{II} given in Eq. 10.29, it is valid for instants subsequent to t_I and in t_I itself. Hence, it is possible to define Eq. 10.35 (homologous of Eq. 10.30).

$$\begin{cases} m\ddot{u}(t) + c\dot{u}(t) + ku(t) + F_0 = -m(f_1 + f_2 t) \\ u(t = t_I) = u_I \\ \dot{u}(t = t_I) = v_I \\ t \in [t_I \; t_{II}] \end{cases} \qquad \{k, F_0\} = \{k_{II}, F_{0,II}\} \tag{10.35}$$

where: $t_{II} = \min \left[\begin{array}{c} \{\tau \mid \tau > t_0, C_{II}(\tau), \neg C_{II}(\tau^+)\} \\ \{\tau \mid \tau > t_0, f_1(\tau^-) \neq f_1(\tau^+) \vee f_2(\tau^-) \neq f_2(\tau^+)\} \end{array} \right]$

$u_I = u_I(t = t_I)$

$v_I = \dot{u}_I(t = t_I)$

Given that sub-problem in Eq. 10.35 is formally equal to the one in Eq. 10.30, every consideration made for the latter is valid for the first. Extending what found, it is possible to repeat previous steps until an ending time (say t_n) is reached.

In conclusion, a global solution $u(t)$ given from a concatenation of local solution can be defined as in Eq. 10.36.

$$u(t) = \left\{ \begin{array}{cc} u_I(t) & t \in \Omega_I \\ u_{II}(t) & t \in \Omega_{II} \\ \vdots & \\ u_n(t) & t \in \Omega_n \end{array} \right\} \tag{10.36}$$

Given that:

- each local solution $u_i(t)$ is an *exact* solution in its validity interval Ω_i, and it is moreover *unique*;
- time intervals Ω_i when attached assemble a continuous interval Ω that span from initial instant t_0 to the final one t_n;
- in each instant t_i that is common to two subsequent time intervals Ω_i continuity of both $u(t)$ and $\dot{u}(t)$ is granted;

then it is possible to say that $u(t)$ as defined in Eq. 10.36 is the *exact* and therefore *unique* solution to the problem introduced in Eq. 10.26.

10.3 Example application of the procedure

In order to effectively introduce the proposed approach, a simple dynamic example problem is here presented.

For instance, a SDoF non-linear system is analysed: while the proposed example is utterly simple, said simplicity is required for sake of clarity, being understood that the approach can be extended to tougher problems. Due to its simplicity, the problem can be fully described by a simple scheme as in Fig. 10.4a. For the same reason, also the constitutive law of the spring is selected as simple as possible, for instance being non-linear elastic and with a perfectly plastic behaviour beyond its linearity threshold as depicted in Fig. 10.4b.

Given that no hysteretic behaviour is assumed, the restoring force F_r of the spring is only function of the displacment, thus represented as $F_r(u(t))$.

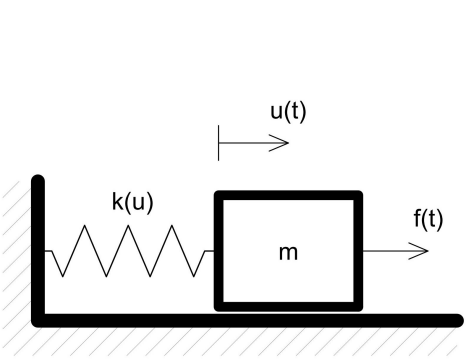

(a) Representative scheme of the problem under analysis

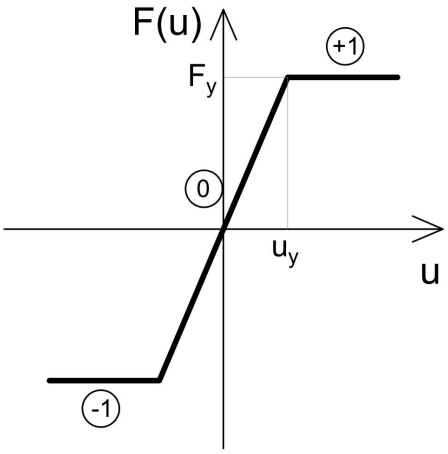

(b) Assumed constitutive law for the spring

Fig. 10.4 – Characteristics of the example problem

From a practical point of view, the proposed procedure can be briefly described with the following steps:

- Identification of the active branch of the constitutive law, *i.e.* the branch that the current response of the spring belongs to on the basis of the initial conditions.
- Definition of the displacement law of the mass, analytically defined from the differential governing equation.
- Calculation of the instant t_I as defined in Eq. 10.28.

10.3.1 Step 1: Definition of the active branch of the constitutive law

In the first step of the procedure, the active branch of the constitutive law must be defined. Naturally, this step is absolutely problem-related, as it depends on the assumed constitutive law. Considering the constitutive law depicted in Fig. 10.4b, said u_0, v_0 respectively initial displacement and velocity, the conditions for the definition of the active branch are defined in Tab. 10.1.

In Tab. 10.1 every single possible condition is taken into account, except the following two cases:

Tab. 10.1 – Conditions for the definition of the active branch of the constitutive law

Alternative conditions	Active branch
$u_0 < u_y$ and $u_0 > -u_y$ $u_0 = u_y$ and $v_0 < 0$ $u_0 = -u_y$ and $v_0 > 0$ $u_0 = u_y$ and $v_0 = 0$ and $f(0^+) < F_y$ $u_0 = -u_y$ and $v_0 = 0$ and $f(0^+) > -F_y$	0
$u_0 < -u_y$ $u_0 = -u_y$ and $v_0 < 0$ $u_0 = -u_y$ and $v_0 = 0$ and $f(0^+) < -F_y$	-1
$u_0 > u_y$ $u_0 = u_y$ and $v_0 > 0$ $u_0 = u_y$ and $v_0 = 0$ and $f(0^+) > F_y$	+1
Conditions are said to be *alternative* because the fulfilment of one criterion is a sufficient condition to define the active branch. $f(0^+)$ stands for the value of the forcing action at $t = 0$ or, if a null value is encountered, in a positive neighbourhood of zero	

$$u_0 = -u_y \text{ and } v_0 = 0 \text{ and } f(0^+) = -F_y$$

$$u_0 = u_y \text{ and } v_0 = 0 \text{ and } f(0^+) = F_y$$

Under any of those two conditions, the system is in equilibrium, so that it is necessary to start the analysis from a further instant.

10.3.2 Step 2: Computation of the mass displacement law

Once the active constitutive law branch is defined, the governing differential equation of the problem has to be solved. Namely, said differential equation has been already presented in Eq. 10.23, thus it is rewritten for the case of general forcing action and non-damped system in Eq. 10.37.

$$m\ddot{u}(t) + ku(t) + F_0 = f(t) \tag{10.37}$$

In Eq. 10.37, both k and F_0 must be defined from constitutive law (according to the definition in Eq. 10.24), and for the constitutive law in Fig. 10.4b are defined according to Eq. 10.38.

Tab. 10.2 – Definition of the associated homogeneous differential equation solution

Case	Equation format	Solution $u_g(t)$
$k > 0$	$m\ddot{u}(t) + ku(t) = 0$	$C_1 \cos(\omega t) + C_2 \sin(\omega t)$
$k = 0$	$m\ddot{u}(t) = 0$	$C_1 + C_2 t$
$k < 0$	$m\ddot{u}(t) + ku(t) = 0$	$C_1 e^{\omega t} + C_2 e^{-\omega t}$

Where:

$\omega = \sqrt{\frac{|k|}{m}}$

$C_1,\ C_2$ integration constants, to be defined from initial conditions

$$F_r = k \cdot u + F_0 \quad \text{where } \{k, F_0\} = \begin{cases} \{k_0 = \frac{F_y}{u_y}, F_{0,0} = 0\} & \text{if active branch: 0} \\ \{k_{-1} = 0, F_{0,-1} = -F_y\} & \text{if active branch: -1} \\ \{k_{+1} = 0, F_{0,+1} = F_y\} & \text{if active branch: +1} \end{cases} \tag{10.38}$$

Given that the problem is described through a non-homogeneous differential equation, its solution $u(t)$ can be found as the sum between the solution of its homogeneous differential equation ($u_g(t)$) and a particular solution of the equation itself ($u_p(t)$) as in Eq. 10.39.

$$u(t) = u_g(t) + u_p(t) \tag{10.39}$$

Regarding the solution of the associated homogeneous differential equation, when values of k and F_0 from Eq. 10.38 are applied, the problem itself changes drastically on the basis of the value of k. Thus, the solution $u_g(t)$ can be computed according to Tab. 10.2.

About the particular solution, an *a-priori* solution obviously can not be defined until the functional shape of the forcing action is assumed. While in the present work a linear increase in forcing action is assumed in Eq. 10.25 in order to represent a recorded accelerogram, in this context of presentation of the procedure with a general example a more general case is needed.

In order to not lose generality in the procedure, it must be noted that every input signal can be approximated by the sum of n harmonic waves as in Eq. 10.40.

Tab. 10.3 – Definition of the particular solution for the harmonic waves

Case	Equation format	Solution $u_p(t)$
$k > 0; \Omega \neq \omega$	$m\ddot{u}(t) + ku(t) = A_{1,n}\cos(\Omega_n t) + A_{2,n}\sin(\Omega_n t)$	$\frac{\bar{A_1}}{\omega^2 - \Omega^2}\cos(\omega t) + \frac{A_2}{\omega^2 - \Omega^2}\sin(\omega t)$
$k > 0; \Omega = \omega$	$m\ddot{u}(t) + ku(t) = A_{1,n}\cos(\Omega_n t) + A_{2,n}\sin(\Omega_n t)$	$\frac{\bar{A_1}}{2\omega} t\sin(\omega t) - \frac{\bar{A_2}}{2\omega} t\cos(\omega t)$
$k = 0$	$m\ddot{u}(t) = A_{1,n}\cos(\Omega_n t) + A_{2,n}\sin(\Omega_n t)$	$-\frac{\bar{A_1}}{\Omega^2}\cos(\Omega t) - \frac{\bar{A_2}}{\Omega^2}\sin(\Omega t)$
$k < 0; \Omega \neq \omega$	$m\ddot{u}(t) + ku(t) = A_{1,n}\cos(\Omega_n t) + A_{2,n}\sin(\Omega_n t)$	$-\frac{\bar{A_1}}{\omega^2 + \Omega^2}\cos(\omega t) - \frac{\bar{A_2}}{\omega^2 + \Omega^2}\sin(\omega t)$
$k < 0; \Omega = \omega$	$m\ddot{u}(t) + ku(t) = A_{1,n}\cos(\Omega_n t) + A_{2,n}\sin(\Omega_n t)$	$-\frac{\bar{A_1}}{2\omega^2}\cos(\omega t) - \frac{\bar{A_2}}{2\omega^2}\sin(\omega t)$

Where:

$$\omega = \sqrt{\frac{|k|}{m}};\ \bar{A_1} = \frac{A_1}{m};\ \bar{A_2} = \frac{A_2}{m}$$

Tab. 10.4 – Definition of the particular solution associated to the term F_0

Case	Equation format	Solution $u_{p,F_0}(t)$
$k > 0$	$m\ddot{u}(t) + ku(t) = F_0$	$-\frac{\bar{F_0}}{\omega^2}$
$k = 0$	$m\ddot{u}(t) + = F_0$	$-\frac{t^2}{2}\bar{F_0}$
$k > 0$	$m\ddot{u}(t) + ku(t) = F_0$	$\frac{\bar{F_0}}{\omega^2}$

Where:

$$\omega = \sqrt{\frac{|k|}{m}};\ \bar{F_0} = \frac{F_0}{m}$$

$$f(t) = \sum_{i=1}^{n} \left(A_{1,n}\cos(\Omega_n t) + A_{2,n}\sin(\Omega_n t)\right) \tag{10.40}$$

Thus, it is possible to define the particular solution of Eq. 10.37 for the single harmonic wave according to Tab. 10.3.

For instance, a particular solution must be found also for the term F_0, which behaves like an external force. [5] Particular solutions associated to the term F_0 are provided in Tab. 10.4.

In conclusion, the solution to Eq. 10.37 can be written as in Eq. 10.41.

[5] It must be noted that, regarding the particular solutions for the non-homogeneous part of the differential equation, it is possible to consider separately each non-homogeneous term, and the particular solution for the general case in Eq. 10.37 (with the assumption in Eq. 10.40) can be found as sum of the particular solutions associated to each term of $f(t)$ plus the one associated to F_0.

Tab. 10.5 – Functions to be passed to the root-finding algorithm in order to find t_I

Active branch	Functions
0	$f(\cdot) = u(t) - u_y$
	$f(\cdot) = u(t) + u_y$
-1	$f(\cdot) = u(t) + u_y$
+1	$f(\cdot) = u(t) - u_y$

$$u(t) = u_g(t) + \sum_{i=1}^{n} u_{p,i}(t) + u_{p,F_0}(t) \tag{10.41}$$

10.3.3 Step 3: Definition of the temporal validity of the solution

As it is now available the displacement law of the mass, it is now necessary to define the limiting instant t_I in which a branch crossing happens and then the solution is no more valid. For instance, this instant is the one defined in Eq. 10.28.

This search is made through a *root-finding algorithm*. [6] Those algorithms are usually designed so that it is found when the input function reaches a null value. In order to use a root-finding algorithm for finding t_I, conditions in Tab. 10.1 have to be redefined in a usable form for those algorithms, *i.e.* limit conditions have to be in the format $f(\cdot) = 0$ and thus functions $f(\cdot)$ need to be defined. For this reason, limit conditions for each branch are defined in Tab. 10.5.

10.3.4 Numerical results

In order to give a comprehensive insight of the procedure, some numerical results for the example in Fig. 10.4 are given. For instance, numerical values for the parameters have to be fixed. Being understood that units are consistent with each other (*e.g.* kg-N-m),

[6] For instance, in the implementation presented in the present work it has been selected the *Brent-Dekker* algorithm for root-finding (Dekker, 1969; Brent, 1976).

the following values are fixed:

- Mass: $m = 1$;
- Limit force for the 0 branch: $F_y = 1000$;
- Limit displacement for the 0 branch: $u_y = 10$;
- Forcing action $f(t) = 500 \cdot \sin(10t)$;
- Initial conditions $u(0) = 0$; $\dot{u}(0) = 0$.

Thus, from previous values, the following characteristics of the system can be calculated:

- Stiffness in the 0 (linear-elastic) branch: $k_0 = \frac{F_y}{u_y} = 100$;
- Natural frequency of the system in the 0 branch: $\omega_0 = \sqrt{\frac{k_0}{m}} = 10$;

Following the previously presented steps, few time intervals are taken into account for a full presentation of the results.

Tab. 10.6 – Numerical results for the example procedure

Time interval I	
Initial conditions:	$u(0) = 0$
	$\dot{u}(0) = 0$
	$u_0 < u_y$ and $u_0 > -u_y$
Step 1:	Active branch: 0
	$k = 100$; $F_0 = 0$
Step 2:	$u_I(t) = 2.5 \cdot \sin(10t) - 25 \cdot t\cos(10t)$
Step 3:	$t_I = 0.5353s$
Final conditions:	$u(t_I) = -10$
	$\dot{u}(t_I) = -107.3075$
Time interval II	
Initial conditions:	$u(0) = -10$
	$\dot{u}(0) = -107.3075$
	$u_0 = -u_y$ and $v_0 < 0$
Step 1:	Active branch: -1
	$k = 0$; $F_0 = -1000$
Step 2:	$u_{II}(t) = -14.0094 + 77.4339 \cdot t + 550 \cdot t^2 - 5 \cdot \sin(10(t + 0.5353))$
Step 3:	$t_{II} = 0.2319s$
Final conditions:	$u(t_I) = -10$

Continued on next page

Tab. 10.6 – continued from previous page

	$\dot{u}(t_I) = 145.3503$
Time interval III	
Initial conditions:	$u(0) = -10$ $\dot{u}(0) = 145.3503$ $u_0 = -u_y$ and $v_0 > 0$
Step 1:	Active branch: 0 $k = 100$; $F_0 = 0$
Step 2:	$u_{III}(t) = -10 \cdot \cos(10t) + 14.989 \sin(10t) - 25 \cdot t \cdot \cos(10(t + 0.76714))$
Step 3:	$t_{III} = 0.1049s$
Final conditions:	$u(t_I) = 10$ $\dot{u}(t_I) = 197.4647$

The procedure is repeated until the target time is reached, thus providing the results depicted in Fig. 10.5.

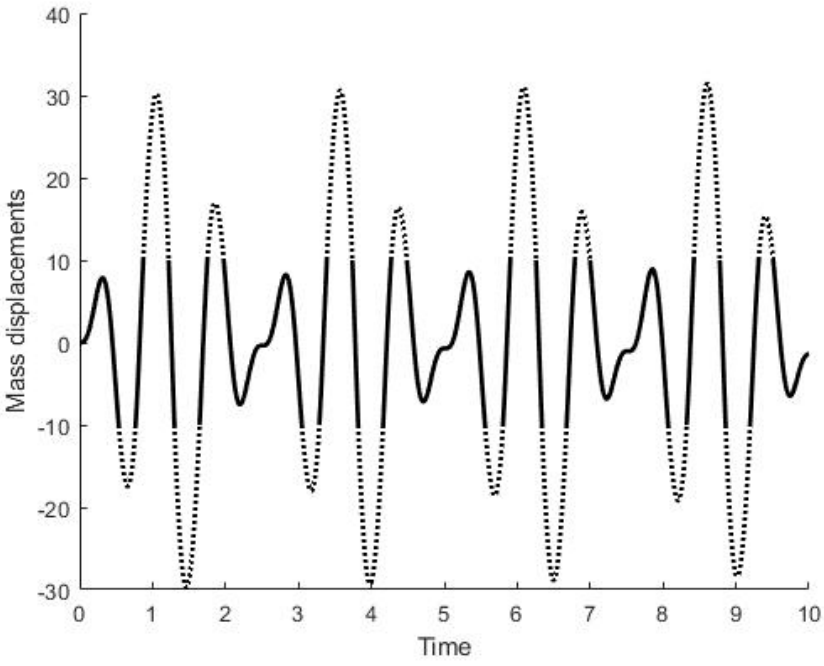

Fig. 10.5 – Total displacement law obtained for the example problem (solid line: 0 branch; dotted line: $+1/-1$ branch)

10.3.5 Comparison of the results with some selected time integration schemes

In order to assess the advantages of the proposed procedure, some selected time integration schemes amongst those presented in Section 10.1 are used for comparison.

Results for other integrations schemes have been obtained by opportunely modifying a MATLAB procedure designed for the solution of SDoF problems with the Newmark scheme (Wong, 2019), in order to use it also for other integration schemes.

The first integration scheme to be used for comparison is the Newmark scheme (Newmark, 1952). In order to ensure some desired characteristics, the following values for the scheme parameters were chosen:

- $\gamma = \frac{1}{2}$ in order to ensure that no numerical damping is included, that is the desired condition of a SDoF problem;
- $\beta = \frac{1}{6}$ corresponding to the assumption of linear variation of the acceleration within the time step, thus enhancing the accuracy, but with the drawback of the conditional stability;
- $\left(\frac{\Delta t}{T}\right)_{stab} = \frac{1/\pi}{\sqrt{1-4\beta}} = 0.551$; $\left(\frac{\Delta t}{T}\right)_{conv} = \frac{1}{2\pi}\sqrt{\frac{1}{\beta}} = 0.389$: limits on time step for stability and convergence respectively.

Results obtained for 3 values of Δt (always fulfilling stability and convergence limits) are depicted in Fig. 10.6.

As expected, the more Δt is reduced, the closer the solution provided by the Newmark scheme gets to the one of the proposed procedure (that is plotted at discrete point so that $\Delta t/T = 0.1$). A closer look to the solution is given in Fig. 10.7.

Looking at both Fig. 10.6 and Fig. 10.7 it is clear the error in terms of amplitude decay and period elongation, as expected from Fig. 10.1 (Bathe and Wilson, 1972).

When looking for other time integration schemes to be used for comparison purposes, a problem arises. Every other scheme is designed so that a controllable numerical dissipation can be introduced in the algorithm with an algorithm-specific parameter, which can be however related to the spectral radius of the amplification matrix in the limit $\omega\Delta t \to \infty$. This quantity ($\rho_\infty$) is a direct measurement of the equivalent damping ratio at high frequency (ξ_∞, Kolay et al. (2014)). Namely, $\rho_\infty = 1$ corresponds to the

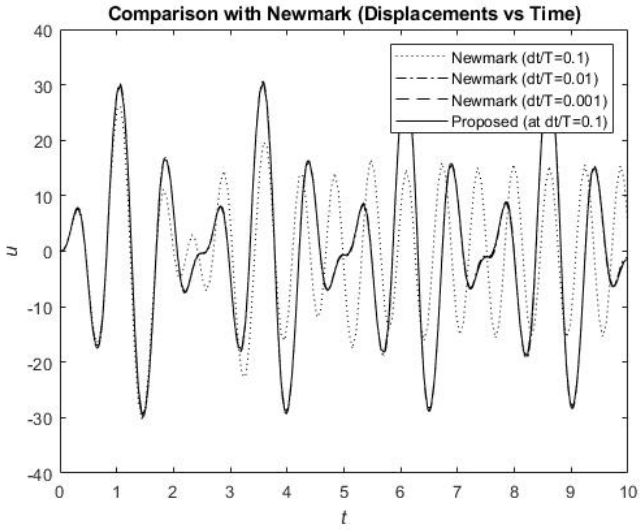

Fig. 10.6 – Comparison of the results with those of the Newmark integration scheme, obtained with 3 values of Δt

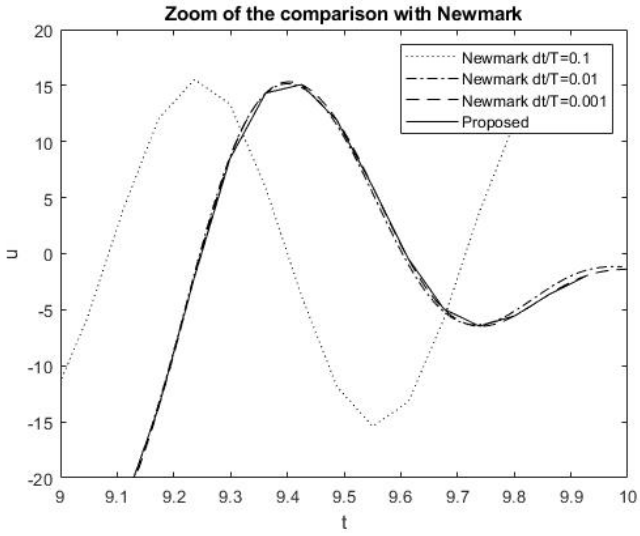

Fig. 10.7 – Detail of the comparison of the results with those of the Newmark integration scheme, obtained with 3 values of Δt

no-numerical-dissipation case (as in Newmark), while $\rho_\infty = 0$ is the *asymptotic dissipation case* (*e.g.* the high-frequency response is annihilated in a single step), whereas

intermediate values provide intermediate behaviours (Chung et al., 1993).

It has been said that the ideal case for a SDoF problem is the non-numerical-dissipation case, given that no higher modes response need to be damped out. However, most of the existing time integration schemes collapse into the Newmark one if $\rho_\infty = 1$ is set (through an opportune choice of the scheme-specific parameters).

With this advice, in the following comparisons with other schemes will be presented assuming the minimum value for ρ_∞, being clear that those results would get closer to those in Fig. 10.6 as ρ_∞ approaches 1.

For the Hilber-Hughes-Taylor (HHT) scheme (Hilber, Hughes, and Taylor, 1977) the ρ_∞-related parameter is α, assumed to have its limit value $\alpha = -\frac{1}{3}$ in Fig. 10.8 so that $\rho_\infty = \frac{1}{2}$ (Chung et al., 1993).

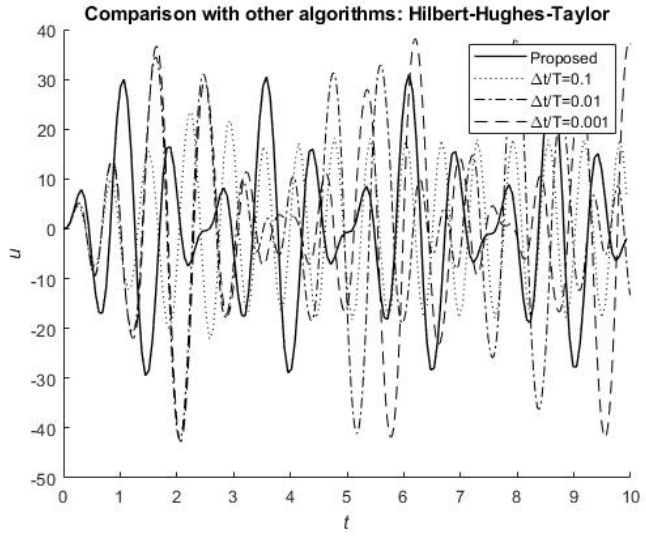

Fig. 10.8 – Comparison of the results with those of the HHT integration scheme (Hilber, Hughes, and Taylor, 1977)

The Wood-Bossak-Zienkiewicz (WBZ) proposal of a time integration scheme (Wood et al., 1980) is used with $\alpha_B = -1$, resulting in $\rho_\infty = 0$ according to Chung et al. (1993). Results are given in Fig. 10.9.

The Hoff-Pahl Θ_1 scheme (HP) in Hoff et al. (1988) is used with $\Theta_1 = 0.95 \rightarrow \rho_\infty = 0.8$, and obtained results are given in Fig. 10.10.

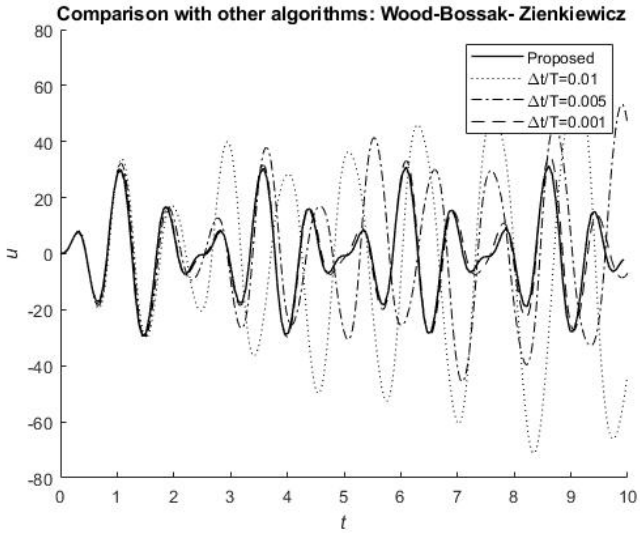

Fig. 10.9 – Comparison of the results with those of the WBZ integration scheme (Wood et al., 1980)

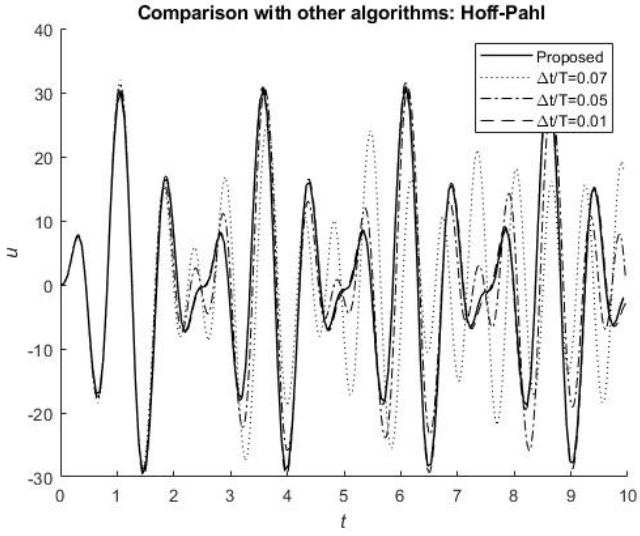

Fig. 10.10 – Comparison of the results with those of the HP integration scheme (Hoff et al., 1988)

The Chung-Hulbert generalized-α scheme (Chung et al., 1993) is used with $\rho_\infty = 0.25$, given that for $\rho_\infty = 0$ it would collapse into the WBZ scheme. Results are syntetized in Fig. 10.11.

One of the few alternatives to the Newmark scheme with no numerical dissipation is

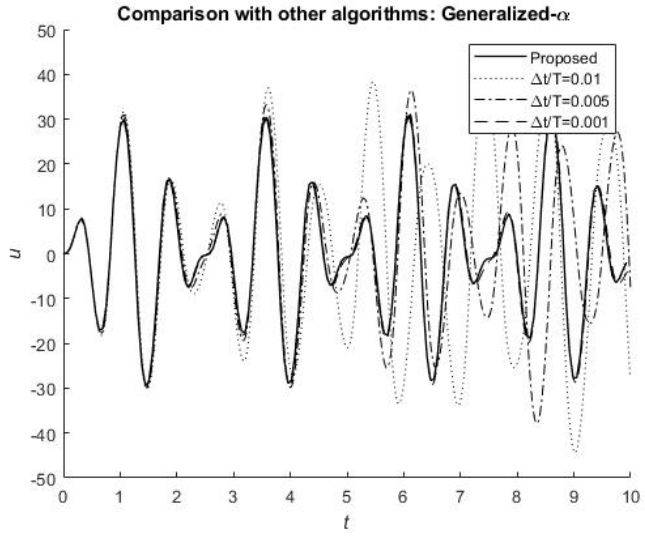

Fig. 10.11 – Comparison of the results with those of the generalized-α integration scheme (Chung et al., 1993)

the Chen-Ricles algorithm (CR) from Chen et al. (2008), whose results are depicted in Fig. 10.12. The algorithmically-dissipative counterparts of this scheme here presented are the Kolay-Ricles (KR) (Kolay et al., 2014) and the Modified Kolay-Ricles (MKR) (Chang, 2018b), for which results are given respectively in Fig. 10.13 (KR, with $\rho_\infty = 1$) and in Fig. 10.14 (MKR, with $\rho_\infty = 0.5$).

From the results provided by the several time integration schemes here used for comparison purposes, the following conclusions can be drawn:

- The results for the HHT scheme in Fig. 10.8 appear to be significantly different from those provided by the proposed scheme, also if the time step is very little. Those differences arise when the system is still in its elastic branch, so that it can be assumed that the problem stands in the scheme itself. However, it must be noted that the extreme value of $\alpha = -1/3$ is usually not recommended.
- WBZ, HP and generalized-α schemes (Wood et al., 1980; Hoff et al., 1988; Chung et al., 1993) give results significantly different from those of the proposed procedure, but getting closer as the time step is reduced. For instance, at the same level of $\Delta t/T = 0.01$ the HP scheme in Fig. 10.10 appear to be the most accurate

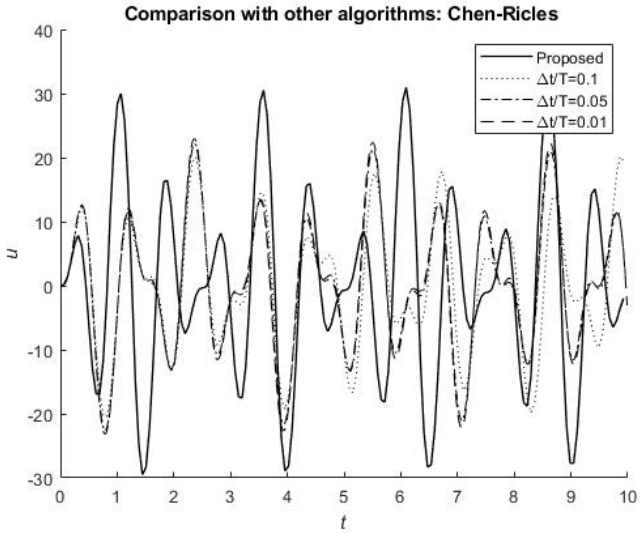

Fig. 10.12 – Comparison of the results with those of the CR integration scheme (Chen et al., 2008)

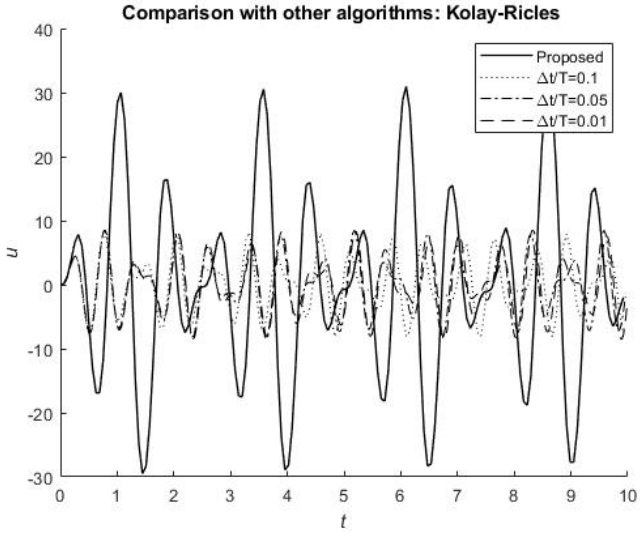

Fig. 10.13 – Comparison of the results with those of the KR integration scheme (Kolay et al., 2014)

with respect to the results in Fig. 10.9 and Fig. 10.11 for the other two schemes. However, it must be noted that it has the advantage of having an higher value of $\rho_\infty = 0.8$, thus closer to the ideal value of 1. Indeed, this comparison is not in its ideal format.

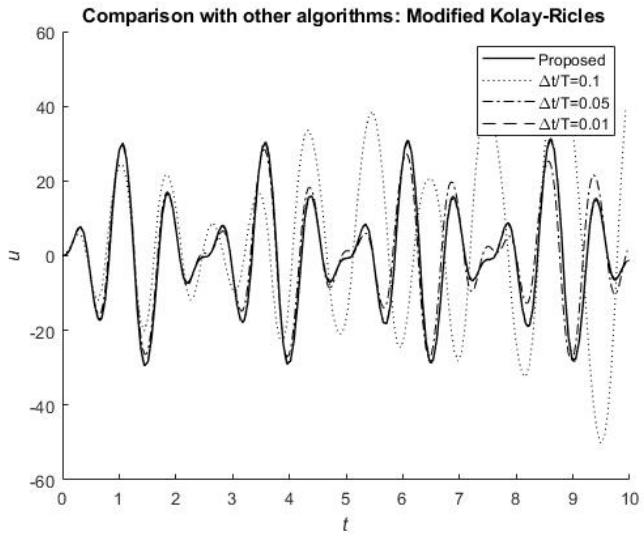

Fig. 10.14 – Comparison of the results with those of the MKR integration scheme (Chang, 2018b)

- CR and KR algorithms (Chen et al., 2008; Kolay et al., 2014) provide results respectively in Fig. 10.12 and Fig. 10.13 that are significantly different from those of the proposed procedure, also when decreasing the time step, namely moving toward a different solution in the limit $\Delta t \to 0$. However, the modified version of said algorithms (MKR, Chang (2018b)) clearly approaches said results as the time step is decreased.

10.4 Conclusive remarks

A novel approach for the solution of structural dynamics problems have been presented, its exactness have been shown together with the uniqueness of the outcome.

In Section 10.3.5 solutions obtained for an example problem with non-linearities involved have been presented. As expected, existing time integration schemes provide solutions that get closer to that obtained from the proposed procedure as parameters are chosen in their *ideal* value.

It has been demonstrated that a non-careful selection of parameters value can bring

to significantly inaccurate results. Moreover, the same care must be given to the time step selection, given its outstanding importance in influencing outcomes. It must be noted that those behaviours have been observed in a rather simple SDoF example, while for complex MDoF structures those evaluations can be significantly harder to be made, and unwanted effects can be unseen.

All of those issues are automatically solved when using the proposed approach, that is one true parameters-free procedure.

11. ANALYSES RUNNING AND RESULTS ELABORATION

As a first aspect to be considered when running analyses, it has to be taken into account the strategy with whom it is intended to solve the problem of assessing the behaviour of the considered structural typology as seismic intensity changes.

Once non-linear dynamic analyses are run, results have to be processed. For instance, *Limit States* and their attainment is to be checked in order to assess significant information over the vulnerability of a given structural typology.

11.1 Limit States Threshold definition

In the first place, it is necessary to define which limit states have to be considered, how are defined and consequently which thresholds for what parameters must be checked in order to assess if a given limit state is attained or not.

While this phase is clearly subsequent to analysis running in the proposed procedure, and hence subsequent to the strategy previously cited for organizing analyses, it is described now because it comes *conceptually* before other steps: while analyses are run *temporally* before limit state attainment definition, and latter need analyses output to be assessed, the analysis strategy need to be based on a rational evaluation of an expected result on limit states attainment. This way, the behaviour of the structural typology under study can be fully described with reference to various expected performance limits under varying seismic intensity.

In present work, limit states in their *general* definition are specified according to EC8-3:2005. In the following, characterization of said limit states is presented directly citing art.2.1(1)P of EC8-3:2005:

Near Collapse (NC) The structure is heavily damaged, with low residual lateral strength and stiffness, although vertical elements are still capable of sustaining vertical

loads. Most non-structural components have collapsed. Large permanent drifts are present. The structure is near collapse and would probably not survive another earthquake, even of moderate intensity.

Significant Damage (SD) The structure is significantly damaged, with some residual strength and stiffness, and vertical elements are capable of sustaining vertical loads. Non-structural components are damaged, although partitions and infills have not failed out-of-plane. Moderate permanent drifts are present. The structure can sustain after-shocks of moderate intensity. The structure is likely to be uneconomic to repair.

Damage Limitation (DL) The structure is only lightly damaged, with structural elements prevented from significant yielding and retaining their strength and stiffness properties. Non-structural components, such as partitions and infills, may show distributed cracking, but the damage could be economically repaired. Permanent drifts are negligible. The structure does not need any repair measures.

Given those definitions, a set of rules for each limit state has been defined.

Nevertheless, definitions of limit states are given so that *general* behaviour of the structure is usually checked, while more commonly *local* thresholds are defined in order to assess the attainment of a given limit state: as a limited set of examples, in the same EC8-3:2005 (and, for instance, also in EC8-1:2004), in NTC2018 and in CNR DT 212:2013 limit states attainment checks are referred to only in terms of a comparison between demands and capacities defined at single section level. It is worth highlighting that this approach was used in a previous realization of proposed procedure (see Aiello et al. (2017a) and Aiello et al. (2017b)).

For this reason, limit states thresholds have been defined with reference to two levels: local, *i.e.* section/element level, for which limit state overcoming is considered to happen when a single element exceeds its capacity at said limit state (straightforwardly following indications in both NTC2018 and EC8-3:2005); global, *i.e.* regarding the overall behaviour of the structure, for which limit state thresholds are defined on the basis of overall response of the structure (where, in absence of guidelines, *reasonable* thresholds are defined in order to fulfill cited definitions of limit states):

Local NC Limit State Limit state is assumed to be attained whereas any structural element reaches its ultimate chord rotation as defined in Eq. 9.25.

Global NC Limit State Given that a condition for this limit state to not be exceeded is that the structure shows *"low residual lateral strength and stiffness"*, an indirect check on variation in stiffness is made: a comparison is made between 1st mode period of undeformed structure ($T_{1,undef}$) against the 1st mode period of damaged one ($T_{1,def}$). If period elongation $\Delta_T = T_{1,def} - T_{1,undef}$ exceedes a given percentage of $T_{1,undef}$, limit state is assumed to be overcome. For instance, in present work said threshold percentage is set to 200 %. [1] Another condition is that *"vertical elements are still capable of sustaining vertical loads"*, assuming that bending damage does not affect vertical loads bearing capacity of columns, recalling hypothesis 1 in page 63 about absence of shear collapse, it follows that the only way cited condition can be overcome is through the activation of a *soft-storey mechanism*. For this reason, eventual activation of a soft-storey mechanism is checked, *i.e.* if all of the columns in a floor reach collapse the limit state is exceeded.

Local SD Limit State Limit state exceeding is assumed to happen whereas any structural element reaches $\frac{3}{4}\theta_C$, being θ_C its ultimate chord rotation as defined in Eq. 9.25. Given that it is needed that *"partitions and infills have not failed out-of-plane"*, the out-of-plane (***OoP***) collapse of infills is also checked with reference to Section 9.3.2.

[1] A 200 % increase in 1st mode period, assuming that the mass is constant, corresponds to a reduction of stiffness to 11.11 % of its original value. In fact, recalling the connection between period T and stiffness K:

$$T_1 = \frac{2\pi}{\omega_1} = 2\pi\sqrt{\frac{M}{K}}$$

calling $\alpha = K_{def}/K_{undef} < 1$ the stiffness reduction factor, it is related with the period elongation as follows:

$$\frac{\Delta T}{T_{1,undef}} = \frac{2\pi\sqrt{\frac{M}{K_{undef}}}\left(\frac{1}{\sqrt{\alpha}} - 1\right)}{2\pi\sqrt{\frac{M}{K_{undef}}}} = \frac{1}{\sqrt{\alpha}} - 1$$

Thus, in order to reach a period elongation of 200 %, a value of $\alpha = 0.111$ is to be selected.

Global SD Limit State As for the local counterpart, also in this case the OoP collapse of infills is checked according to Section 9.3.2. Moreover, this limit state is considered to be exceeded also if more than half of the infills have collapsed (with an in-plane mechanism).

Local DL Limit State Limit state is assumed to be overcome whereas any structural element reaches yielding chord rotation as defined in Eq. 9.24, as it is required the structure to have *"structural elements prevented from significant yielding and retaining their strength and stiffness properties"*. Moreover, it is allowed that in the considered limit state *"Non-structural components, such as partitions and infills, may show distributed cracking"*; although, in-plane (***IP***) collapse is assumed to not be accepted in said definition, so that IP collapse limit as defined in Section 9.3.1 is checked.

Global DL Limit State Recalling that in order to fulfill limit state it is needed that *"Permanent drifts are negligible"*, a check is made on after-analysis deformed condition: whereas a given Interstorey Drift Ratio (***IDR***) is exceeded, the limit state is assumed to be overcome. For instance, in present work this limit is set to 0.5%. Moreover, a check on stiffness is implemented in an indirect fashion, checking the 1st mode period elongation as for other limit states. For instance, with a period elongation more than 40% the limit state is assumed to be exceeded. [2]

It is obvious that limit states are organized in a hierarchical framework: if a threshold for CP Limit state is exceeded, also SD and DL limit states are assumed to be exceeded, given that if the structure is in a near-collapse state (and, then, heavily damaged) it is clearly significantly damaged. The same happens between SD and DL limit states, given that a structure that is significantly damaged can not fulfil the damage limitation required by DL limit state.

[2]The 40% period elongation corresponds to a reduction to 50% of the stiffness. It could appear a rather high reduction of stiffness for a limit state that requires a limitation on damage. However it must be recalled that in FEMA 273 effective stiffness of columns is assumed to be at most 70% of its elastic stiffness, and in FEMA 356 for axially weakly-loaded columns this reduction goes to 50%.

11.2 A strategy for analyses running: the Multiple Stripes Analysis (MSA)

In order to rationally organize analyses to be run, a strategy has to be defined.

In technical literature, three main approaches are available in order to select analyses to be run (see Baker (2013) and Jalayer, Ebrahimian, et al. (2017) as example references):

Incremental Dynamic Analysis (IDA) (see Vamvatsikos et al. (2002), Dolsek (2009)) through this approach, a given set of ground motion are progressively scaled in order to assess the structural behaviour over a wide range of seismic intensities defined through an *Intensity Measure* (***IM***), with respect to a given *Engineering Demand Parameter* (***EDP***). However, record selection is usually fixed in order to match a given condition (*e.g.* response spectrum) at a predetermined seismic intensity, selected to be *significant* over the phenomenon under analysis (*i.e.* limit state exceeding). Moreover, some authors raised a debate about the potential bias introduced in results by an excessive scaling of ground motions (*e.g.* see Baker and Allin Cornell (2006), Du et al. (2019) for further reference), given that for this procedure no limitation can be given to the scale factor to be used on records.

Cloud Analysis (CA) (see Shome et al. (1998) and Jalayer, Ebrahimian, et al. (2017)) according to this approach a set of ground motions is selected in order to match a given scenario, usually in terms of magnitude-distance couple, set from disaggregation data. Usually, fewer analyses are needed for computations, and the scaling issue can be completely solved by using unscaled records. However, records selection is tightly connected to a scenario-related approach, and it is not possible to apply it to a varying hazard characteristics with IM (as in Section 7.1).

Multiple Stripes Analysis (MSA) (see Jalayer and Cornell (2009)) within this approach, a different set of ground motions is selected for each considered IM, thus allowing to differentiate selected records on the basis of intensity level, in order to both harmonise hazard description at the very different considered IMs and control (*i.e. limit*) the scale factor of records. However, a significant further effort is

needed, and various authors proposed some simplifications to make it practically viable (see as an example reference Ruggieri et al. (2020)).

Therefore, a Multiple Stripes Approach is selected to be used in present work.

12. POST-PROCESSING OF RESULTS

As soon as analyses results are available, some post-processing can be made on those data.

12.1 Fragility Curves

An outstandingly important information that can be collected from the results of MSA is the ***Fragility Curve***. Those curves are the graphical representation of the probability that a given limit state is exceeded with the increase of the earthquake intensity.

For instance, results of MSA provide a discrete representation of said curves, given that this analysis typology investigates the structural response in some fixed values of seismic intensity. It is useful, however, to have a synthetic representation of those curves.

Under the assumption that the seismic intensity at which the considered limit state is reached IM_{LS} follows a log-normal distribution, the fragility curve is represented by a cumulative log-normal distribution. In fact, from its definition, the value assumed by the fragility curve in a generic fixed value $I\bar{M}$ is the probability that $IM_{LS} < I\bar{M}$, thus representing the definition of cumulative distribution for IM_{LS}.

Starting from this definition, it is possible to fit a cumulative log-normal distribution on discrete fragility curve data provided by MSA as in Fig. 12.1.

An important parameter of this distribution is represented by the mean μ, which can be easily used to compare the vulnerability of different building clusters.

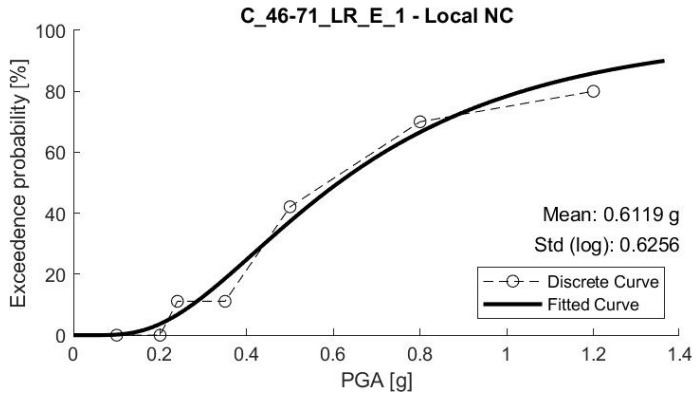

Fig. 12.1 – An example of discrete fragility curve and its fitting with a log-normal cumulative distribution

12.2 Vulnerability and Risk maps

As a scalar representation of the vulnerability is now available for each considered couple buildings cluster - limit state, it is possible to provide a significant, synthetic and readable representation of seismic vulnerability of buildings in a given area through maps.

However, several alternatives are available in order to represent vulnerability on a map.

- The mean μ of the fitted fragility function. This measure is a pure indicator of the building vulnerability.
- The probability p_{LS} of exceeding the considered limit state in a given number of year N. In order to compute this value, the probability distribution of the intensity level p_{IM} needs to be assessed. As this distribution varies spatially, a practical solution that avoids unacceptable errors is its definition at municipality level.
- The expected loss L_{LS} in a given number of year N. Before computing this value, a correlation must be defined between limit-states-related information and *loss*, however it is defined (*e.g.* economic, human lives).

Part III

Application of the procedure

In theory, there is no difference between theory and practice.
In practice, there is.

Benjamin Brewster - The Yale Literary Magazine

13. THE CASE STUDY OF PUGLIA REGION

13.1 Introduction

In order to fully describe the proposed procedure, a case study over the territory of Puglia region is presented.

Puglia is an italian region located at its south-eastern part, with an approximate extension of 19'540 square kilometers, 4 millions inhabitants in 257 municipalities, organized in 6 provinces (Fig. 13.1).

Fig. 13.1 – Provinces of Puglia

13.2 Hazard assessment

13.2.1 Regional Hazard Analysis

According to the procedure presented in Section 7.1, an analysis of homogeneous areas in terms of hazard [1] over the regional territory is performed.

The first step is to calculate hazard parameters at municipalities city halls locations.

An iterative procedure is performed in order to recognize homogeneous groups of municipalities. Cited procedure has an initial threshold for homogeneity assessment of 20 %, but in some cases this highly restricting limit is relaxed in order to retrieve reasonable results. The outcome of said procedure is outlined in Fig. 13.2, that describes the territorial extent of 4 homogeneous areas in terms of seismic hazard for region Puglia, while in Tab. A.1 in Annex A municipalities belonging to each homogeneous area are listed.

Reference spectra for each homogeneous area are then computed, using the weighting criterion through inhabitants explained in Section 7.1, while some example results are presented in Fig. 13.3

Only for a concise comparison of results, computed spectra are then linearised so that each spectrum can be defined from the three parameters that are used for spectra definition in NTC2018, *i.e.* a_g that is fixed for the given spectrum by hypothesis, F_0 and T_C^* are computed through a least squares approach. In Tab. 13.1 parameters for spectra computation for each homogeneous group and for selected values of a_g are listed [2].

[1] It is worth recalling that, in Section 7.1, homogeneity of hazard was defined as follows: a point can be considered included in a homogeneous area if spectra associated have values that are never a given percentage different from *central reference* spectra of the homogeneous area. This evaluation is made over ranges of a_g and T as in Eq. 13.1.

$$a_g = [0.02; 0.04; 0.06; 0.08; 0.10; 0.15; 0.20; 0.25]g \tag{13.1a}$$

$$T = [0.1; 0.2; 0.3; 0.4; 0.5; 0.6; 0.7]s \tag{13.1b}$$

[2] It is worth highlighting a particular feature: looking at Tab. 13.1, for some *extreme* values of a_g, not all groups have parameters values set. This could appear *strange*, but it directly comes from the prohibition given in NTC2018 to extrapolate data. To clarify, in group I there are no parameters for $a_g = 0.02g$ because none of the municipalities has values lower or equal to $0.02g$ for a_g in the range of return

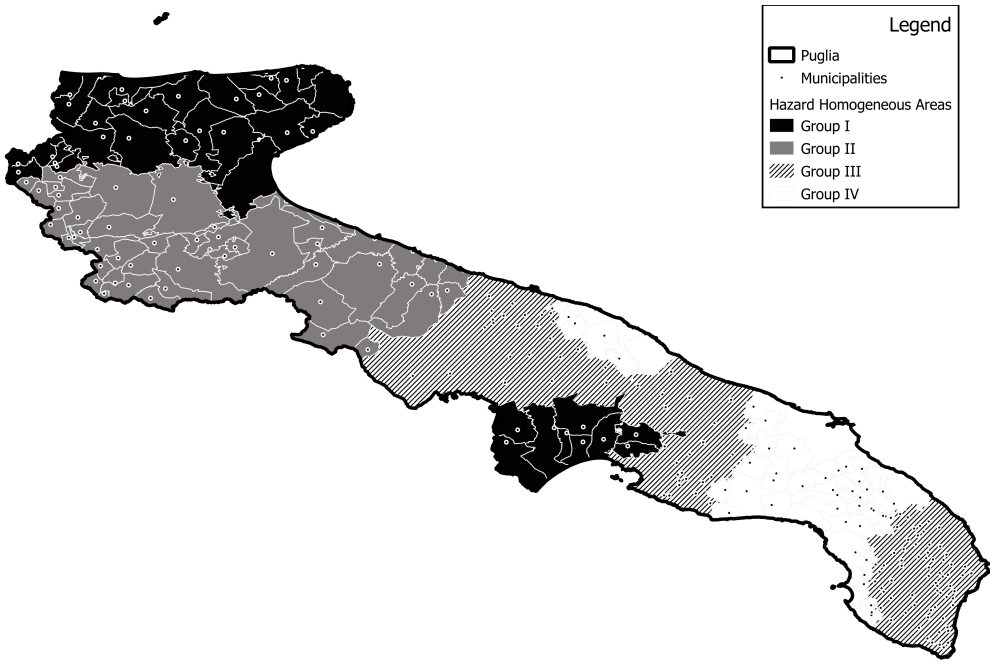

Fig. 13.2 – Hazard homogeneous areas

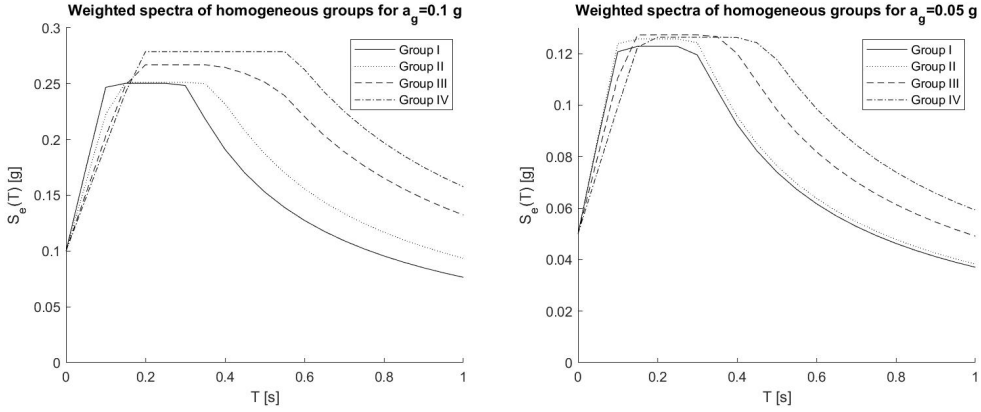

Fig. 13.3 – Example weighted reference spectra for homogeneous areas

periods covered by the cited regulation (*e.g.* those given in (13.1), whose minimum is $T_R = 30yrs$)

Tab. 13.1 – Spectral Parameters for homogeneous groups of municipalities

$a_g[g]$	Group I		Group II		Group III		Group IV	
	F_0	$T_C^*[s]$	F_0	$T_C^*[s]$	F_0	$T_C^*[s]$	F_0	$T_C^*[s]$
0.02					2.401	0.206	2.356	0.218
0.04	2.423	0.296	2.525	0.279	2.504	0.335	2.471	0.392
0.06	2.489	0.290	2.518	0.325	2.606	0.425	2.631	0.515
0.08	2.492	0.301	2.515	0.350	2.642	0.472	2.655	0.567
0.10	2.499	0.306	2.511	0.372	2.653	0.494	2.788	0.565
0.12	2.496	0.312	2.517	0.382	2.631	0.472		
0.14	2.492	0.317	2.530	0.388	2.650	0.506		
0.16	2.481	0.319	2.529	0.393	2.659	0.513		
0.18	2.473	0.321	2.518	0.399	2.664	0.519		
0.20	2.463	0.324	2.490	0.410				
0.22	2.456	0.327	2.472	0.414				
0.24	2.450	0.331	2.442	0.395				
0.26	2.445	0.336	2.420	0.396				
0.28	2.434	0.343	2.393	0.395				
0.30	2.432	0.346	2.374	0.396				

13.2.2 Ground motions selection

In order to consistently represent the seismic hazard using accelerograms starting from its representation in spectral shape, a modified version of the Conditional Spectrum ground motion selection software (***CS_selection***) by Baker and Lee (2018) is used (see Section 8.1 for reference).

This algorithm, originally developed in Jayaram et al. (2011) and then enhanced in Baker and Lee (2018), is designed so that a generic amount of ground motions from a given database is retrieved in order to match a predefined scenario. It has been then modified in order to permit the selection on the basis of a predefined spectrum, whose definition has been presented in Section 13.2.1.

The selection of the maximum allowable scale factor was made having in mind two main issues:

- the need to extend the number of selectable ground motions, in order to have a selection that reflects as much as possible the characteristics of the target spectrum;

- the need to limit the scale factor, considering that earthquake with very different magnitudes have very different characteristics, so that a bias can be introduced in results by scaling (see Du et al. (2019) for further reference).

Considering that usually a wider set of records is available for lower intensities, it is clear that the use of a single maximum scaling factor is not the best solution: the use of a large allowable scale factor would widen the available set of records for higher intensities while introducing an unnecessary strong modification of records for lower intensities, whereas a small maximum scale factor would limit the number of number of selectable records (in some cases to the point that no selectable records are available in the database).

As a result, a starting value for the maximum scale factor of $SF_{max} = 2.0$ is initially selected, and is then increased up to the point where selectable ground motion records are at least five times the number of records to be selected (fixed to $no_{GM} = 30$ in the present work).

It must be noted that, while in the original *CS_selection* no minimum scale factor is introduced, a modification of cited tool is implemented so that $SF_{min} = 1/SF_{max}$.

In order to give a reliable representation of the hazard for the area under analysis, the Engineering Strong Motion Database (***ESM***, Lanzano et al. (2019) and Luzi et al. (2020)) is used. Given that most of the records in cited database comes from events in mediterranean area, it is assumed that local earthquake characteristics are better reflected by using ESM records.

As an example, ground motion selection for group I soil type A topography condition T1 is presented in Fig. 13.4 in terms of resulting spectrum, while in Tab. 13.2 selected ground motion details are given.

Tab. 13.2 – Selected ground motion parameters for group I, A-category soil, T1 topographic condition, for $a_g = 0.50g$

Event	Date	Station	Scale Factor
CENTRAL_ITALY	18-Jan-2017 13:33:37	PCB	1.79
SWITZERLAND	01-Jul-2017 08:10:34	SCOD	3.42
CENTRAL_ITALY	24-Aug-2016 02:33:29	FOC	2.96
IZMIT	17-Aug-1999 00:01:38	ATS	2.31
AEGEAN_SEA	08-Jan-2013 14:16:09	ENZZ	3.49

Continued on next page

Event	Date	Station	Scale Factor
CENTRAL_ITALY	30-Oct-2016 06:40:18	NRC	1.18
CENTRAL_ITALY	30-Oct-2016 06:40:18	T1214	0.99
EMILIA_2ND_SHOCK	29-May-2012 07:00:02	MIR02	2.20
IZMIT	17-Aug-1999 00:01:38	4101	2.53
CENTRAL_ITALY	30-Oct-2016 06:40:18	MZ102	1.29
EMILIA_2ND_SHOCK	29-May-2012 07:00:02	MIR08	2.13
DUZCE	12-Nov-1999 16:57:19	8101	1.07
IZMIT	17-Aug-1999 00:01:38	8101	1.45
L_AQUILA	06-Apr-2009 01:32:40	GSA	3.39
IRPINIA	23-Nov-1980 18:34:53	STR	1.86
CENTRAL_ITALY	30-Oct-2016 06:40:18	AM05	1.93
NORTHWESTERN_BALKAN_PENINSULA	15-Apr-1979 06:19:41	PETO	1.35
L_AQUILA	06-Apr-2009 01:32:40	AQU	1.77
EMILIA_2ND_SHOCK	29-May-2012 07:00:02	MIRE	2.29
IZMIT	17-Aug-1999 00:01:38	CNAK	3.27
CENTRAL_ITALY	26-Oct-2016 19:18:06	MZ04	3.24
CENTRAL_ITALY	24-Aug-2016 01:36:32	NRC	1.36
DUZCE	12-Nov-1999 16:57:19	487	1.71
CENTRAL_ITALY	26-Oct-2016 19:18:06	AM05	2.79
CENTRAL_ITALY	26-Oct-2016 17:10:36	NOR	3.06
EMILIA_2ND_SHOCK	29-May-2012 07:00:02	MOG0	2.47
EMILIA_2ND_SHOCK	29-May-2012 07:00:02	CNT	1.93
EMILIA_2ND_SHOCK	29-May-2012 07:00:02	T0800	1.71
CENTRAL_ITALY	30-Oct-2016 06:40:18	ACC	1.21
EMILIA_2ND_SHOCK	29-May-2012 07:00:02	T0802	1.79

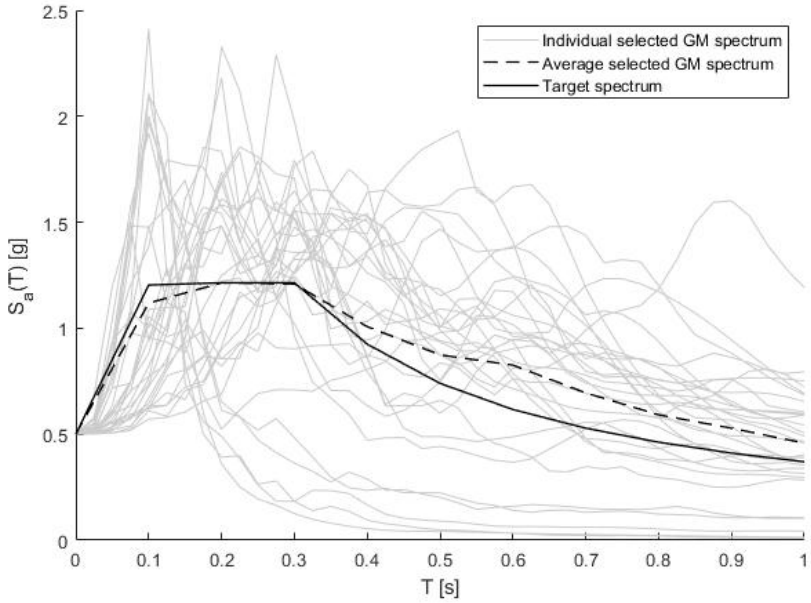

Fig. 13.4 – Spectra of selected ground motion for group I, A-category soil, T1 topographic condition

13.3 Buildings clustering

The buildings clustering is mainly based on data collected through CARTIS form, which was briefly described in Section 7.2.

For instance, the results collected in this section start from the findings in Conte (2018), in which an elaboration of CARTIS data is present. In the cited work, structural typologies identified through CARTIS form in 14 municipalities are analysed, for a total of 90 typologies (see Tab. 13.3).

Tab. 13.3 – Number of RC building typologies identified in CARTIS project

Municipality	RC typologies
Andria	8
Bisceglie	16
Bovino	1
Carlantino	1
Castellaneta	5
Cisternino	29

Continued on next page

Municipality	RC typologies
Erchie	1
Faeto	1
Foggia	15
Locorotondo	4
Minervino Murge	4
Ruvo di Puglia	3
Sant'Agata di Puglia	1
Vico del Gargano	1

Being clear that it is probable that some building typologies are common between different municipalities, cited work examines this classification and joins some typologies that are considered *similar* in a seismic vulnerability assessment framework. As a result, for the part that is interesting for this work, a total of 17 clusters are identified, whose characteristics are presented in Tab. 13.4.

Tab. 13.4 – RC building clusters identified in Conte (2018)

Cluster	Construction year	No. of floors	Plan surface
CA-PUGLIA_ 1	<1945	0-3	0-230
CA-PUGLIA_ 2	<1945	4-6	0-230
CA-PUGLIA_ 3	1946-1971	0-3	0-230
CA-PUGLIA_ 4	1946-1971	4-6	0-230
CA-PUGLIA_ 5	1946-1971	4-6	230-500
CA-PUGLIA_ 6	1972-1981	0-3	0-230
CA-PUGLIA_ 7	1972-1981	4-6	230-500
CA-PUGLIA_ 8	1972-1981	4-6	230-500
CA-PUGLIA_ 9	1982-1996	0-3	0-230
CA-PUGLIA_ 10	1982-1996	0-3	230-500
CA-PUGLIA_ 11	1982-1996	4-6	0-230
CA-PUGLIA_ 12	1982-1996	4-6	230-500
CA-PUGLIA_ 13	1982-1996	7-9	0-230
CA-PUGLIA_ 14	1982-1996	7-9	230-500
CA-PUGLIA_ 15	1997-2008	0-3	0-230
CA-PUGLIA_ 16	1997-2008	4-6	230-500
CA-PUGLIA_ 17	1997-2008	7-9	230-500

The classification in Tab. 13.4, however, is further modified in order to match present work's goals.

As a first modification, all of the building typologies subsequent to 1982 are dropped, considering that starting from this date *modern* structural design is assumed to be used,

also with the help of personal computer widespread usage (see CNR10024:1986 about criteria on technical report preparation for computer-aided designs as a proof).

Another outstanding parameter when considering a building response to earthquake is its shape: while only rectangular buildings are here considered, a structure with a *compact* plan (*i.e.* with almost equal dimensions in the two main directions) usually behaves very differently from a structure with *elongated* plan shape, also if other parameters are kept constant. For this reason, being B and b the dimensions in plan in the two main directions with $B > b$, building classes are further divided in *compact* (if $\frac{B}{b} < 1.5$) and *elongated* (otherwise). This parameter is assumed to be more influencing than the floors surface, thus the latter is dropped in assessing clustering.

The last typological parameter taken into account in the building clustering regards the eventual seismic-related design of structures in the cluster. Seismic category of the municipality where a building is located at the time of its construction is used as criterion for additional subdivision of building clusters.

As a result, building clusters assumed in the present work are those described in Tab. 13.5.

It is worth highlighting that in Tab. 13.5 clusters labelling is modified in order to give an immediate information about the cluster itself, being organized as follows:

- a fixed initial letter *C*, that stands for *cluster*;
- the indication of construction year range;
- the number of floors range, indicated as *LR* (low-rise) for 0-3 floors, *MR* (mid-rise) for 4-6 floors, *HR* (high-rise) for >7 floors;
- the indication of the plan shape, with *C* indicating *compact* shape and *E* the *elongated* one;
- the seismic category of the building municipality at the time of its construction: 0 for uncategorized, 1 for 1st category and 2 for 2nd;
- each item is bounded by an underscore.

Tab. 13.5 – Building clusters assumed in the present work

Cluster	Construction year	No. of floors	Plan shape	Seismic Category
C_<45_LR_C_0	<1945	0-3	compact	0
C_<45_LR_C_1	<1945	0-3	compact	1
C_<45_LR_C_2	<1945	0-3	compact	2
C_<45_LR_E_0	<1945	0-3	elongated	0
C_<45_LR_E_1	<1945	0-3	elongated	1
C_<45_LR_E_2	<1945	0-3	elongated	2
C_<45_MR_C_0	<1945	4-6	compact	0
C_<45_MR_C_1	<1945	4-6	compact	1
C_<45_MR_C_2	<1945	4-6	compact	2
C_<45_MR_E_0	<1945	4-6	elongated	0
C_<45_MR_E_1	<1945	4-6	elongated	1
C_<45_MR_E_2	<1945	4-6	elongated	2
C_46-71_LR_C_0	1946-1971	0-3	compact	0
C_46-71_LR_C_1	1946-1971	0-3	compact	1
C_46-71_LR_C_2	1946-1971	0-3	compact	2
C_46-71_LR_E_0	1946-1971	0-3	elongated	0
C_46-71_LR_E_1	1946-1971	0-3	elongated	1
C_46-71_LR_E_2	1946-1971	0-3	elongated	2
C_46-71_MR_C_0	1946-1971	4-6	compact	0
C_46-71_MR_C_1	1946-1971	4-6	compact	1
C_46-71_MR_C_2	1946-1971	4-6	compact	2
C_46-71_MR_E_0	1946-1971	4-6	elongated	0
C_46-71_MR_E_1	1946-1971	4-6	elongated	1
C_46-71_MR_E_2	1946-1971	4-6	elongated	2
C_72-81_LR_C_0	1972-1981	0-3	compact	0
C_72-81_LR_C_1	1972-1981	0-3	compact	1
C_72-81_LR_C_2	1972-1981	0-3	compact	2
C_72-81_LR_E_0	1972-1981	0-3	elongated	0
C_72-81_LR_E_1	1972-1981	0-3	elongated	1
C_72-81_LR_E_2	1972-1981	0-3	elongated	2
C_72-81_MR_C_0	1972-1981	4-6	compact	0
C_72-81_MR_C_1	1972-1981	4-6	compact	1
C_72-81_MR_C_2	1972-1981	4-6	compact	2
C_72-81_MR_E_0	1972-1981	4-6	elongated	0
C_72-81_MR_E_1	1972-1981	4-6	elongated	1
C_72-81_MR_E_2	1972-1981	4-6	elongated	2

It is clear that, out of the 36 building clusters identified in Tab. 13.5, some could be not significant (*i.e.* few or no buildings belonging to some clusters could be effectively present in the territory). This eventuality arises from the additional parameters added in the clustering process with respect to the clusters given in Tab. 13.4: those clusters

were defined directly from information in the CARTIS form, so their representativeness is assured, while this is not necessarily true for modified clusters in Tab. 13.5.

13.4 Materials characteristics assessment

13.4.1 Reinforcing steel characteristics

According with what said in Section 8.2, characteristics of steel used for reinforcement are defined with reference to results in Verderame, Ricci, Esposito, et al. (2011).

In cited work, an in-depth analysis is performed over reinforcing steel used in 1950-1980 years. Here is assumed that those results are consistent with reinforcing steel used in Puglia during the same period.

As a first result, the ribbed vs smooth bars ratio over years under investigation is analyzed, and results are depicted in Fig. 13.5. Starting from those results, the distribution assumed in this work is given in Tab. 13.6.

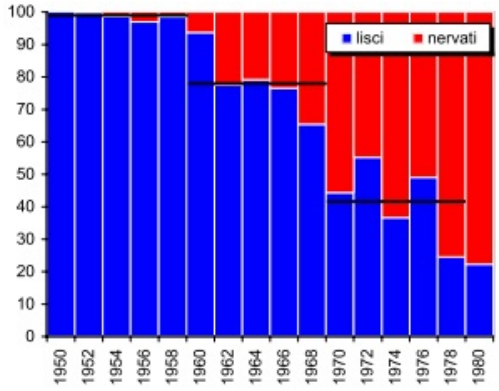

Fig. 13.5 – Distribution of reinforcing steel used over 1950-1980 period range (red:ribbed bars, blue:smooth bars), taken from Verderame, Ricci, Esposito, et al. (2011)

Period	Smooth bars	Ribbed bars
1950-1961	100%	0%
1962-1969	80%	20%
1970-1977	40%	60%
1978-1980	20%	80%

Table 13.6 – Assumed distribution of reinforcing steel used over 1950-1980 period range

Together with those results, in cited work also distribution of used steel classes for smooth bars are given. For instance, steel classes are defined according to regulations

Tab. 13.7 – Steel classes for reinforcement as in regulations active in the period 1950-1980

R.D. 16/11/1939 n.2229 art.17	C.M. 23/05/1957	D.M. 30/05/1972 art.2.5	D.M. 16/06/1976 art.2.5	out-law
Acciaio dolce	Aq42	FeB22	FeB22k	
Acciaio semiduro	Aq50			
Acciaio duro	Aq60	FeB32	FeB32k	
		A38	FeB38k	
		A41		
		FeB44	FeB44k	
				Common
				HEL

active in that period range, and summarized in Tab. 13.7. As stated in Verderame, Ricci, Esposito, et al. (2011), however, some steel classes only changed nomenclature when a new standard was published: in order to clearly distinguish truly different steel classes, in Tab. 13.7 the result of a grouping step is presented.

Still from Verderame, Ricci, Esposito, et al. (2011), some *out-of-law* steel classes are included, in order to represent steel with no coherent characteristics with any *legal* steel class, but that was used in periods when controls on steel were not particularly deepened. With this regard, *Common* and *High Elastic Limit* (HEL) in Tab. 13.7 are two classes directly inherited from analyses in Verderame, Ricci, Esposito, et al. (2011), and include steels for which test resulted in too low (Common class) or too high (HEL class) yielding strength with respect to standard-provided classes.

It is worth highlighting that, starting from D.M. 30/05/1972, steel classes were designated to be used for smooth or ribbed bars (FeB22 and FeB32 for smooth, the others for the latter).

Given that in Verderame, Ricci, Esposito, et al. (2011) only smooth bars were analyzed, in Fig. 13.6 is depicted what found from authors in terms of relative usage percentage for steel classes in smooth bars, while the distribution assumed in this work is given in Tab. 13.8.

Considering that no information is available on distribution of steel classes for ribbed bars, some hypotheses are made:

- For years up to 1972, no distinctions were made between steel classes used for smooth or ribbed bars. For those years, it is assumed that the same distribution of usage of steel classes holds between smooth and ribbed bars.

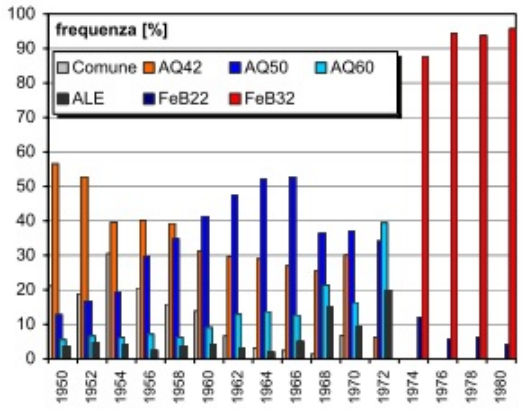

Fig. 13.6 – Distribution of reinforcing steel classes used for smooth bars, taken from Verderame, Ricci, Esposito, et al. (2011)

Period	Steel Classes used
1950-1961	**Common**: 20%
	AQ42/FeB22: 40%
	AQ50: 30%
	AQ60/FeB32: 10%
1962-1971	**AQ42/FeB22**: 30%
	AQ50: 40%
	AQ60/FeB32: 20%
	HEL: 10%
1972-1980	**AQ42/FeB22**: 10%
	AQ60/FeB32: 90%

Table 13.8 – Assumed distribution of reinforcing steel classes used for smooth bars

- From 1972 3 steel classes existed for the use in ribbed bars. However, after only 4 years, in 1976 with D.M. 16/06/1976 class *A41* was dropped. It is here assumed that the reason of this exclusion was due to low usage of this class, so it is here assumed that was not used at all.
- No information at all exists about relative usage importance of A38/FeB38k vs FeB44/FeB44k. For this reason, same percentage of usage is assumed for the two classes.

As a result of said hypotheses, joining also information given in Tab. 13.6 and in Tab. 13.8, the final usage distributions assumed in this work are given in Tab. 13.9.

It is clear from Tab. 13.9 that too much precision is given about years ranges. However, one must always keep in mind what the main goal of those assessments is: collecting data for mechanical analyses of building typologies, for which it is clear that construction year is not certainly defined, but is based on esteems that can be precise over the decade at most, not the year. For this reason it is reasonable to simplify results in Tab. 13.9, and for instance use as period ranges the same of Section 13.3.

An additional hypothesis is made due to lack of knowledge: for structures built before 1945 smooth bars and *common* steel class is assumed as only available setting.

Tab. 13.9 – Assumed distribution of reinforcing steel classes

Period	Steel Classes	Usage percentage
1950-1961	**Common-Smooth**	20%
	AQ42/FeB22-Smooth	40%
	AQ50-Smooth	30%
	AQ60/FeB32-Smooth	10%
1962-1971	**AQ42/FeB22-Smooth**	25%
	AQ42/FeB22-Ribbed	5%
	AQ50-Smooth	30%
	AQ50-Ribbed	10%
	AQ60/FeB32-Smooth	15%
	AQ60/FeB32-Ribbed	5%
	HEL-Smooth	10%
1972-1977	**AQ42/FeB22-Smooth**	5%
	AQ60/FeB32(k)-Smooth	35%
	A38/FeB38k-Ribbed	30%
	FeB44(k)-Ribbed	30%
1978-1980	**AQ60/FeB32(k)-Smooth**	20%
	A38/FeB38k-Ribbed	40%
	FeB44(k)-Ribbed	40%

After all, results can be finally given in Tab. 13.10.

For each of considered steel classes, main mechanical parameters are given in Tab. 13.11.

Tab. 13.10 – Final assumed distribution of reinforcing steel classes

Period	Steel Classes	Usage percentage
<1945	**Common-Smooth**	100%
1946-1971	**Common-Smooth**	20%
	AQ42/FeB22-Smooth	30%
	AQ42/FeB22-Ribbed	10%
	AQ50-Smooth	30%
	AQ60/FeB32-Smooth	10%
1972-1981	**AQ60/FeB32(k)-Smooth**	40%
	A38/FeB38k-Ribbed	30%
	FeB44(k)-Ribbed	30%

Tab. 13.11 – Mechanical parameters of reinforcing steel classes (from previously cited standards)

Steel Class	Yielding strength $f_{y,min}[MPa]$	Ultimate strength $f_{u,min}[MPa]$
Common	280*	380**
AQ42/FeB22(k)	220	340
AQ50	270	500
AQ60/FeB32(k)	320	500
A38/FeB38k	380	460
FeB44(k)	440	550

*: median value based on Verderame, Ricci, Esposito, et al. (2011)
**: value based on median values for f_y and $\frac{f_u}{f_y}$ in Verderame, Ricci, Esposito, et al. (2011)

13.4.2 Concrete mechanical characteristics

For concrete, a comprehensive study on its mechanical parameters over years is not available. However, as already stated in Section 8.2, a database of test results on concrete is available.

While also non-destructive test results are available in the database, only results of destructive tests are here considered. As a result, a total of 1'005 test results are taken into account, so that only tests on *ordinary* structures (mainly residential) are comprised.

Those tests were made on existing buildings, but it is not known the construction year of said structures. For this reason an assumption has to be made: it is assumed that concrete classes usage percentage is constant throughout all considered years.

It must be noted that most of the results refer to tests on buildings in the Bari province (854, 85% of the total). However, homogeneity is assumed for the whole regional territory.

As a first step, the compressive strength resulting from tests is modified in order to take into account a series of boundary conditions that influence the result. For instance, this correction is needed because tested concrete comes from drilling on existing structures, rather than from samples prepared on purpose. Said correction is made according to the formulation given in Masi (2005), then modified in Masi et al. (2019), using Eq. 13.2.

$$f_{c,is} = \left(C_{h/D} \cdot C_{dia} \cdot C_{st} \cdot C_d\right) f_{core} \tag{13.2}$$

where: $f_{c,is}$ = in-situ concrete compressive strength
f_{core} = compressive strength of drilled core (from test)
$C_{h/D}$ = shape factor, depending on height-on-diameter ratio h/D of the drilled core, $C_{h/D} = 2/(1.5 + D/h)$, under the assumption $0.5 \leq h/D \leq 2$
C_{dia} = factor related to the diameter of the drilled core, equal to 1.06 1.00 0.98 for diameters of respectively 50 100 150 mm
C_{st} = factor taking into account eventual presence of steel reinforcement in the drilled core, whose value varies from 1.03 for small diameter bar ($\phi 10$) to 1.13 for wider bars ($\phi 20$)
C_d = correction factor for damage due to drilling, in this work assumed to vary linearly from 1.30 if $f_{core} = 10$ MPa to 1.00 if $f_{core} = 30$ MPa

From this correction, a total of 11 test results are dropped: 4 have diameters less than 50mm, 6 have $h/D > 2$, 1 has $h/D < 0.5$. Other 5 are then excluded due to extreme values (< 5 MPa and a test with $f_{c,is} = 85$ MPa). As a result, a total of 989 data is considered, with the distribution of concrete compressive strength presented in Fig. 13.7.

In this work this distribution is supposed to come from an underlying superposition of various concrete classes, each with its own distribution, each with its own relative importance within global distribution (*i.e.* percentage of occurrence of a given class in the global population). For instance, total distribution is assumed to follow the rule given in Eq. 13.3.

$$\begin{aligned} p[f_c = \bar{f}_c] &= \sum_{i=1}^{n_{classes}} p\left[class = i | f_{c,i} = \bar{f}_c\right] \\ \overset{given}{\rightarrow} & p\left[class = i | f_{c,i} = \bar{f}_c\right] = p[class = i] \cdot p[f_{c,i} = \bar{f}_c] \\ \overset{defining}{\rightarrow} & w_i = p[class = i] \\ & p[f_c = \bar{f}_c] = \sum_{i=1}^{n_{classes}} w_i \cdot p[f_{c,i} = \bar{f}_c] \end{aligned} \tag{13.3}$$

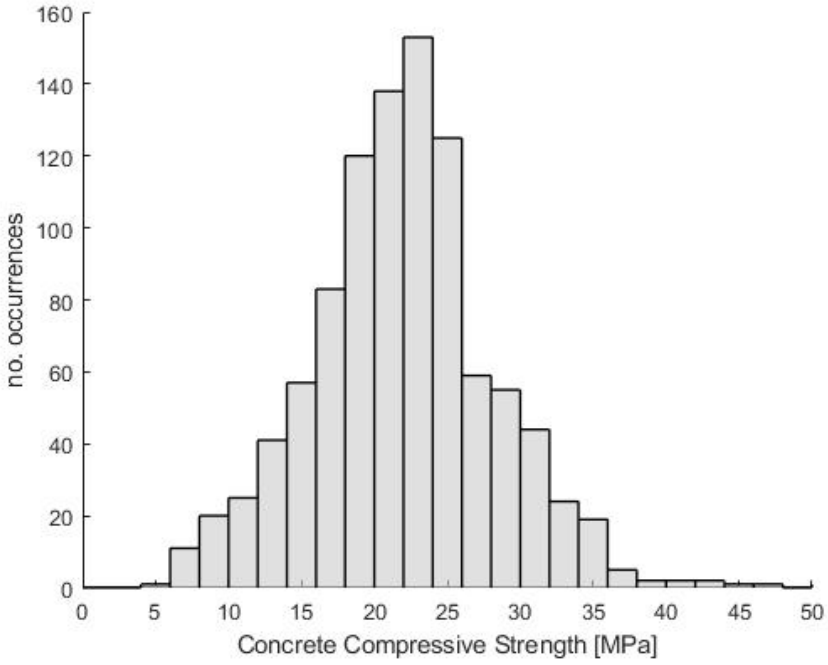

Fig. 13.7 – Concrete compressive strength distribution in the database

where: w_i = *weight* of the ith class over the whole population
$p[f_{c,i} = \bar{f}_c]$ = distribution of compressive strength of concretes belonging to the ith class
$p[f_c = \bar{f}_c]$ = total distribution of compressive strengths

Concrete classes are determined from D.M. 30/05/1972 art.2.3 [3], which introduced a total of 6 concrete classes, identified through characteristic compressive strength after 28 days in kg/cm^2: 150 200 250 300 400 500. Anyway, classes 400 and 500 are supposed to be not used for ordinary residential buildings, because notably deepened preliminary studies and continuous statistical checks were required.

Computation of expected value of concrete compressive strength from characteristic one is made according to Annex I of D.M. 30/05/1972, that actually describes the

[3]Previous standard (*i.e.* R.D. 16/11/1939 n.2229) only indicated minimum requirements for concrete, that was only classified on the basis of its chemical characteristics (*i.e.* due to additives).

procedure to assess characteristic strength from a set of tests (see Eq. 13.4).

$$R'_{bk} = R'_{bm} - k\delta \tag{13.4}$$

Eq. 13.4 stands under the hypothesis of a normal distribution of data: if R'_{bm} is the expected value (mean value of tests in the procedure of D.M. 30/05/1972), R'_{bk} the characteristic value (5th percentile), δ the standard deviation, $k = 1.64$ (in D.M. 30/05/1972 the value of k depends on the number of tests, and $k = 1.64$ stands if 30 or more tests are considered).

Given that concrete classes are identified through characteristic compressive strength, this parameter is assumed to be fixed for each class, while expected value R'_{bm} is evaluated through the (unknown) value of δ.

Characteristic compressive strength R'_{bk}, however, is defined in D.M. 30/05/1972 as the strength of a *cube* of concrete ($h/D = 1$), while database data depicted in Fig. 13.7 are expressed in terms of *cylindrical* strengths (*i.e.* with $h/D = 2$). Transformation of compressive strength between cubic R_b and cylindrical f_b is made through Eq. 13.2, in which only factor $C_{h/D}$ is taken different from 1, bringing to Eq. 13.5. [4]

$$f_b = 0.8 \cdot R_b \tag{13.5}$$

Starting from Eq. 13.3, assuming a lognormal distribution for concrete strength, under the hypothesis that each concrete class shares the same (unknown) standard deviation with all others, Eq. 13.6 stands.

[4]It is worth highlighting that the same transformation, according to NTC2018 art.11.2.10.1, would be made with a factor of 0.83. However, it must be noted that NTC2018 prescription is valid for new, standard-compliant concretes, while equation given in Masi et al. (2019) is specifically valid for existing concrete.

$$
\begin{aligned}
p[f_c = \bar{f}_c] = \quad & w_{150} \cdot p[f_{c,150} = \bar{f}_c] \\
+ \quad & w_{200} \cdot p[f_{c,200} = \bar{f}_c] \\
+ \quad & w_{250} \cdot p[f_{c,250} = \bar{f}_c] \\
+ \quad & w_{300} \cdot p[f_{c,300} = \bar{f}_c]
\end{aligned}
\tag{13.6}
$$

$$
\begin{aligned}
p[log(f_c) = log(\bar{f}_c)] = \quad & w_{150} \cdot N\left(log(.8 \cdot 15) + 1.64 \cdot \delta_{LN}, \delta_{LN}\right) \\
+ \quad & w_{200} \cdot N\left(log(.8 \cdot 20) + 1.64 \cdot \delta_{LN}, \delta_{LN}\right) \\
+ \quad & w_{250} \cdot N\left(log(.8 \cdot 25) + 1.64 \cdot \delta_{LN}, \delta_{LN}\right) \\
+ \quad & w_{300} \cdot N\left(log(.8 \cdot 30) + 1.64 \cdot \delta_{LN}, \delta_{LN}\right)
\end{aligned}
$$

It must be noted that Eq. 13.6 is expressed in terms of logarithms (*e.g.* δ_{LN} is the standard deviation of logarithms) and strengths are given in [MPa]. Moreover, it is clear that sum of weigths w_i (defined as strictly positive) must be exactly 1.

Using a least square approach, unknown parameters of Eq. 13.6 are determined. Results are given in Fig. 13.8 and Tab. 13.12.

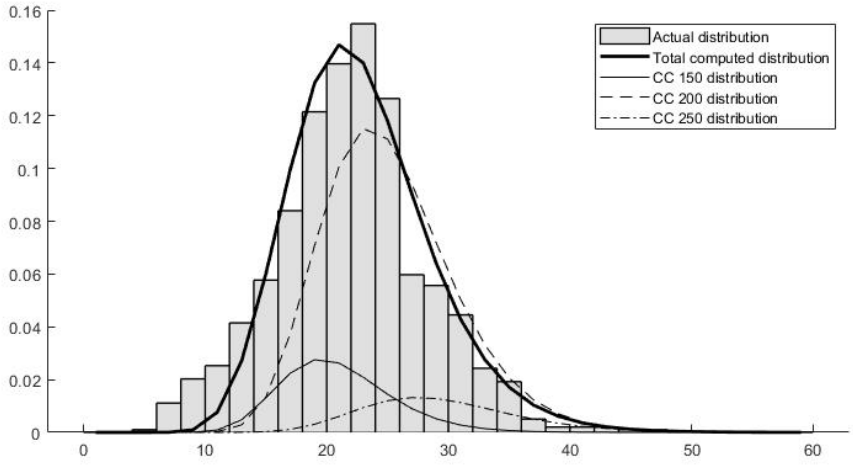

Fig. 13.8 – Distribution of concrete strengths

Tab. 13.12 – Details on concrete classes mechanical parameters and relative weights

Concrete Class	Relative weight w_i [%]	Expected strength [MPa]
CC 150	15	17.03
CC 200	75	22.71
CC 250	10	28.39
CC 300	0	34.07
$\delta_{LN} = 0.2136$		

Young modulus of concrete is defined, according to NTC2018 art.11.2.10.3, using Eq. 13.7.

$$E_{cls} = 22'000 \left(\frac{fcm}{10} \right)^{0.3} \qquad [MPa] \tag{13.7}$$

Within-structure variability of concrete characteristics have been taken into account assuming a Coefficient of Variation (CV) according to Masi et al. (2019), variable with the number of floors as in Eq. 13.8.

$$CV_{\text{within structure}} = \frac{\mu}{\sigma} = 0.0628 \cdot \log\left(n_{\text{floors}}\right) + 0.1979 \tag{13.8}$$

13.4.3 Infills mechanical characteristics

Given that the proposed procedure explicitly takes into account the behaviour of infills, it is clear the necessity to evaluate mechanical characteristics of those elements.

One of the main problem to be faced in this context is the absolute lack of knowledge over infills characteristics and typologies used in existing buildings. An useful source of information, however, is represented by the results in Rossi (1982): in cited work various test results over several brick elements are presented. It is worth highlighting that it can be assumed that tested bricks are representative of elements used in the past, given the year of publication of the cited work.

In Tab. 13.13 results in terms of average compressive strength f_m from Rossi (1982) are summarized.

Starting from Tab. 13.13, assuming that cited brick typologies were used with the same probability, a lognormal distribution of strengths is derived. For instance, an

Tab. 13.13 – Brick masonry compressive strength from Rossi (1982)

Typology	Thickness $[cm]$	Strength $[kPa]$
Tamponamento TV	20	5.33
ISOEDIL	25	6.59
CLIMABLOCK	25	3.91
ISOLATER	25	2.70
QUADRIUNI	25	3.63

expected value of $\mu = 1.441$ (corresponding to 4.225 MPa) and a standard deviation $\sigma = 0.3468$ have been determined, bringing to a probability distribution function depicted in Fig. 13.9.

Again from Tab. 13.13, a fixed thickness of 25cm for infills has been set.

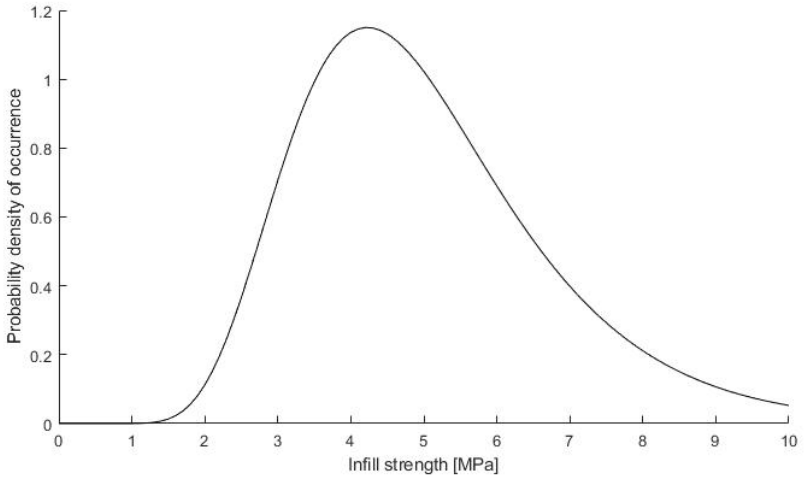

Fig. 13.9 – Probability distribution function of infill strength (based on data from Rossi (1982))

13.5 Loads assessment

While variable loads have been fully described in Section 8.3.2, permanent loads have to be defined through expected typologies used in the buildings under analysis.

In order to evaluate the numerical values to be used for those loads, it is necessary to consider what typologies of elements were used in years under analysis. For instance,

various manuals used in the past have been checked for data collecting.

In order to define the structural loads G_1 due to slabs, its typology must be assessed.

Regarding structural typologies of slabs to be considered, in past manuals a huge set of slab dimensions is taken into account, given that not only residential buildings were designed starting from that information. In order to have a reliable prediction of structural loads, only *recurrent* dimensions were considered, *i.e.* around 25cm of thickness.

In the following, the most probably used floors typologies are discussed on the basis of said past manuals. Description of those typologies, however, is outside the scope of the present work, hence insights can be made referring to documents cited in the following.

Slabs structural typologies found in checked manuals are summarized in Tab. 13.14, with explicit reference to supposed usage.

Tab. 13.14 – Main structural slabs typologies

Typology	Years of main usage (supposed)	Notes
SAP	<1960	Permanent load is assumed $G_1 = 1.75kPa$ based on Protti (1934), CNR - Consiglio Nazionale delle Ricerche (1953), and RDB (1958). Usage years are defined considering that newer manuals than those cited do not include this structural typology
SAPAL and **STIMIP**	-	As SAP typology, those typologies are cited in several manuals (*e.g.* Protti (1934), CNR - Consiglio Nazionale delle Ricerche (1953), and RDB (1958) and, for STIMIP typology, also in RDB (1968)). However, it was uncommon to use those typologies for residential buildings, given that were used for long spans (up to 10m for SAPAL, up to 16m for STIMIP).
VARESE	1945-1970	Main years of usage are taken from LECA (2014), while it is assumed from CNR - Consiglio Nazionale delle Ricerche (1953) $G_1 = 1.8kPa$
EXCELSIOR and **CELERSAP**	>1960	Their usage can be surely tracked back to late 1950s (see RDB (1958)), while those typologies are still used. $G_1 = 3kPa$ and $G_1 = 2kPa$ are respectively assumed for the two typologies, taken from technical details of currently produced elements.
BISAP	>1970	While this typology is still used, its usage can be tracked at least up to late 1960s (see RDB (1968)). $G_1 = 2.8kPa$ is assumed from currently produced elements.

Continued on next page

Typology	Years of main usage (supposed)	Notes
Generic in-situ	Always	This *generic* typology is added in order to take into account the use of a *generic* slab typology, still belonging to hollow slab category. $G_1 = 3kPa$ is assumed.
Other structural typologies have been neglected because only few manuals within the same period of time describe its use, so that a not-so-common usage is assumed		

Starting from Tab. 13.14, in Tab. 13.15 is summarized the assumed distribution of slabs typology (and, hence, G_1 values in Tab. 13.16) for various years ranges. It must be noted that, given that no information is available regarding relative usage of slab typologies, same usage probability is assumed for each typology.

About non-structural loads G_2 acting on floors, in RDB (1958) is given a comprehensive example of a typical floor finishes pack, for which a total value of $G_2 = 1.5kPa$ is given (including the load due to internal partitions). This value is confirmed from specific weights of single elements provided by other checked manuals.

Regarding infills weight, several technical sheets of present-time old-style bricks have been checked, and a specific weight of $8\frac{kN}{m^3}$ has been set.

While the procedure is designed so that additional load can be included in order to model the presence of balconies, those elements were neglected due to the total lack of data on their distribution in the considered building stock.

Tab. 13.15 – Assumed usage of the considered slab typologies

Period	Slab typology	Expected usage	G_1 $[kPa]$
<1960	SAP	33%	1.75
	VARESE	33%	1.80
	Generic	33%	3.00
1960-1970	VARESE	25%	1.80
	CELERSAP	25%	2.00
	EXCELSIOR	25%	3.00
	Generic	25%	3.00
>1970	CELERSAP	25%	2.00
	EXCELSIOR	25%	3.00
	BISAP	25%	2.80
	Generic	25%	3.00

Tab. 13.16 – Assumed usage of structural load values

Period	G_1 $[kPa]$	Expected usage
<1960	1.80	70%
	3.00	30%
1960-1970	2.00	50%
	3.00	50%
>1970	2.00	25%
	3.00	75%

13.6 Overview of structural models generation

In order to effectively present the procedure, it is worth clarifying the whole structural model generation phase in light of definitions given in the previous sections.

The definition of the parameters needed for the generation of the structural models involves several steps, that for convenience of a clear description will be divided into two groups of steps.

1. In the first group of steps, parameters used for the simulated design of the structure are fixed. Thus, values are defined according to the prescriptions and the practices of the construction period.

1*a*) **Definition of the construction year**. Given the years range defined by the building cluster as in Tab. 13.5 (*i.e.* <1945, 1946-1971, 1972-1981), an exact year is randomly extracted assuming a uniform distribution of construction years amongst said ranges. The definition of a fixed construction year is needed given that some prescription changed amongst years in the assumed range.

1*b*) **Selection of number of floors**. Starting from the range of number of floors defined for the considered cluster in Tab. 13.5 (*i.e.* 1-3 for low-rise, 4-6 for mid-rise, >7 for high-rise), the number of floors is set assuming a uniform distribution amongst the range (*i.e.* each number of floors has the same probability to be extracted).

1*c*) **Floors heights definition**. The first floor interstorey height is selected to be 3m or 3.5m with the same probability, while remaining floors have the

fixed height of 3m.

1*d*) **Definition of geometrical features of the structure**. Geometrical features are defined in terms of spans number and lengths. Spans number is picked in the ranges 2-3 and 3-6 for the two directions, and amongst those ranges every value has the same probability to be picked. Spans length are selected in the range 4-6m with a 0.5m step so that each value has the same probability to be selected. Selected geometrical features are dropped if the condition on the plan dimension ratio as in Section 13.3 is not fulfilled: in that case, the selection procedure is re-run.

1*e*) **Definition of the reinforcing steel class**. Starting from the construction year, a reinforcing steel class is extracted according to the distribution given in Tab. 13.10, and mechanical parameters are defined from Tab. 13.11.

1*f*) **Extraction of a concrete class**. A concrete class is then selected according to the usage percentages, cited in Tab. 13.12 as *relative weight*. The only exception is when the construction year is between 1972 and 1976 and the reinforcing steel bars used are ribbed: in said period D.M. 30/05/1972 prescribed the use of concrete class >C250 with ribbed bars, so that concrete class C250 is selected if previously cited conditions are met.

1*g*) **Selection of design loads**. Structural loads used for design are selected according to Tab. 13.16 starting from the construction year. According to Section 13.5, loads for infills are computed assuming a thickness of 25cm and a specific weigth of $8\frac{kN}{m^3}$. Variable loads value is selected according to Section 8.5.2 on the basis of the construction year. For non-structural loads a fixed value of $1.5kPa$ is selected according to Section 13.5.

1*h*) **Definition of active law prescriptions**. Starting from Tab. 8.2 and Tab. 8.3, active law prescriptions for design are defined on the basis of the construction year.

From said parameters, a simulated design is performed. Thus, at this point, a building is completely defined as if existing in reality. This is called a *realization* of the considered cluster.

2. Starting from the previously defined realization, the second group of steps is intended for the definition of the parameters needed for a *realistic* representation of the building.

2*a*) **Reinforcing steel mechanical characteristics**. Starting from the reinforcing steel class defined in step 1*e*), mechanical characteristics are deterministically selected according to Tab. 13.11. This is made under the assumption that steel mechanical characteristics have low dispersion as observed in data from Section 13.4.1.

2*b*) **Concrete mechanical characteristics**. Starting from the concrete class defined in step 1*f*), the concrete expected strength $E[f_c]$ is selected from Tab. 13.12. The value of f_c for the building is then selected from a log-normal distribution having mean $E[f_c]$ and standard deviation of logarithm $\delta_{LN} = 0.2136$ according to Tab. 13.12.

2*c*) **Mechanical characteristics of concrete for each column**. Given the variability of concrete characteristics amongst structural elements belonging to the same structure, its mechanical characteristics are varied amongst columns. Namely, starting from the expected concrete strength for the whole structure f_c as computed in step 2*b*), concrete strength for the generic $_i$th column $f_{c,i}$ is picked according to a log-normal distribution having mean f_c and coefficient of variation dependent from the number of floors (fixed in step 1*b*)) according to Eq. 13.8. Young modulus $E_{c,i}$ is then computed through Eq. 13.7.

2*d*) **Infills mechanical characteristics**. Infills strength is selected according to the distribution depicted in Fig. 13.9. While it is clear that a differentiation for single infill would be needed as made for columns in step 2*c*), unavailability of opportune data brings to the assumption that all of the infills share the same strength.

2*e*) **Loads assessment**. Permanent loads are defined through their value as fixed in step 1*g*). On the other hand, variable loads values are selected from a log-normal distribution as defined in Section 8.3.2 (mean from Tab. 8.1,

standard deviation of logarithms from Tab. 8.3). Moreover, eccentricity of masses are included according to Section 8.3.3 for both directions, namely selecting values of e_x and e_y from a normal distribution with mean $E[e] = 0$ and standard deviation $\sigma_e = 3.05\%$ according to Eq. 8.4. Both values of eccentricities and the value of the variable loads are defined distinctly for each floor.

Starting from the parameters defined in cited steps, the behaviour of all of the structural elements can be defined. Namely, for columns according to Section 9.2, for infills according to Section 9.3.

13.7 Analyses results

Once analyses are run according to Chapter 11, results can be used to build fragility curves for each of the analysed building clusters.

As an example, fragility curves for cluster C_46-71_LR_E_1 are depicted in the following, assuming that the underlying hazard characteristics are those related to a municipality in cluster 1, soil category *A*, topographic condition *T1*.

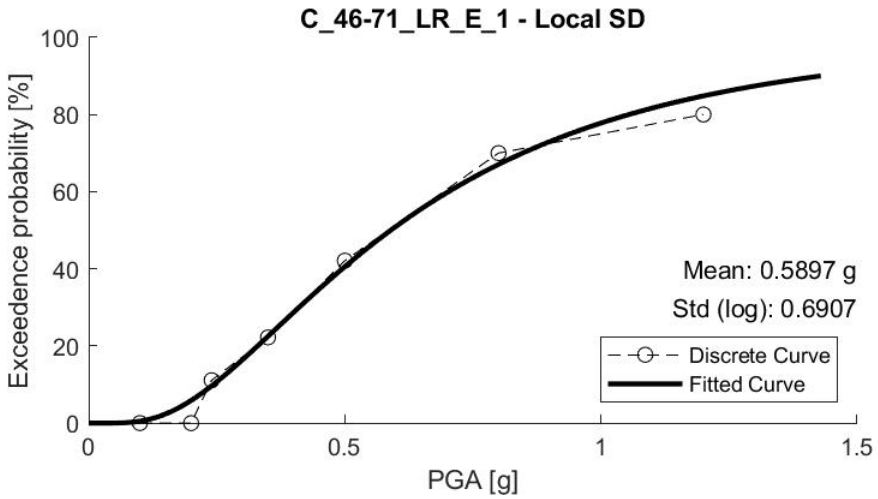

Fig. 13.10 – Fragility curve for C_46-71_LR_E_1 cluster, local SD limit state

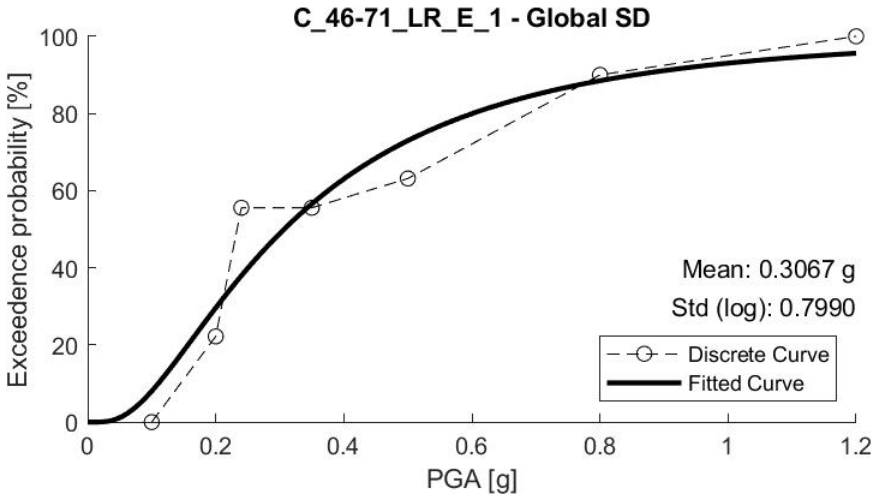

Fig. 13.11 – Fragility curve for C_46-71_LR_E_1 cluster, global SD limit state

In Fig. 13.10 and Fig. 13.11 are depicted respectively the fragility curves for local and global significant damage limit states as defined in Section 11.1. Said figures provide both the discrete representation of the fragility curve deriving from numerical results and the smooth fitted curve as described in Section 12.1.

In Fig. 13.11 a feature of obtained results can be highlighted. A fragility curve is expected to be monotonically increasing, as the percentage of structures exceeding the considered limit state has to be higher for higher values of the Intensity Measure IM. While the *Structural Resurrection* phenomenon described in Vamvatsikos et al. (2002) can partially describe why sometimes this feature fails to be respected, it cannot explain the extent of this behaviour in discrete fragility functions: it is indeed expected that this phenomenon is faded out when several models are analysed for the fragility function definition.

The non-monotonicity of the discrete fragility functions can be explained with the statistical error introduced by the use of a *finite* number of analyses: infinite analyses would bring to an *exact* assessment of the fragility functions, at least in correspondence of the considered stripes. The use of a finite number of analyses gives just an approximation of those values, intrinsically including an error. The amount of this error decreases as the number of analyses increases. However it is hard to *a priori* define the

number of analyses to be run in order to achieve a desired error, given the outstanding number of parameters involved in the response definition and the extreme non-linearity of the response itself.

As a feature of the proposed procedure, resulting fragility curves can be straightforwardly compared: the use of the PGA as intensity measure is in fact independent from the structure (as it would have been the use of the spectral acceleration at the first mode period, as it is usually made from several authors). However, it is worth highlighting that spectral information and in general the whole information on hazard characteristics is not lost, being included in the result.

As an example of this feature, in Fig. 13.12 the fragility curve for the C_46-71_LR_E_0 cluster is depicted.

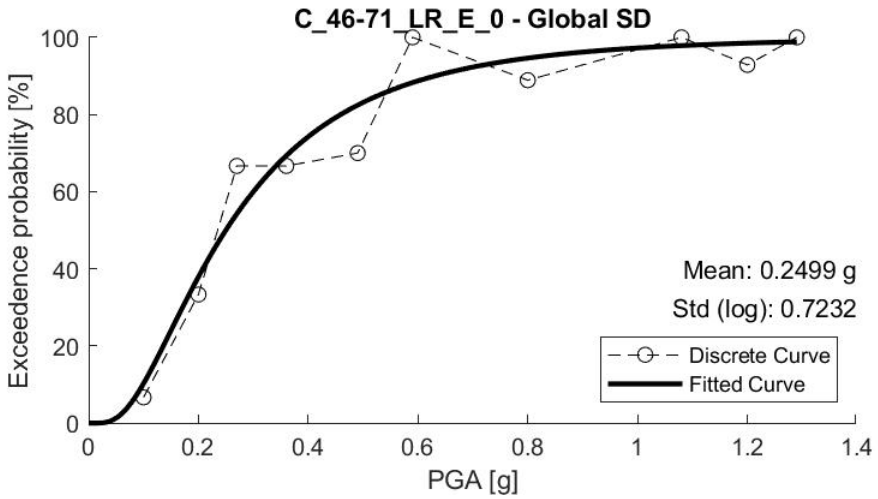

Fig. 13.12 – Fragility curve for C_46-71_LR_E_0 cluster, global SD limit state

It is worth highlighting that Fig. 13.12 and Fig. 13.11 can be used to directly compare the influence of the seismic category over the results in terms of fragility curves. In fact, while the considered limit state is the same (global significant damage limit state), between the two clusters C_46-71_LR_E_1 and C_46-71_LR_E_0 only the seismic category is different (1st category for the first, no seismic category for the latter).

In Fig. 13.13 a comparison between the fragility curves of clusters C_46-71_LR_E_1 and C_46-71_LR_E_0 for the global SD limit state are depicted. In Fig. 13.14 said

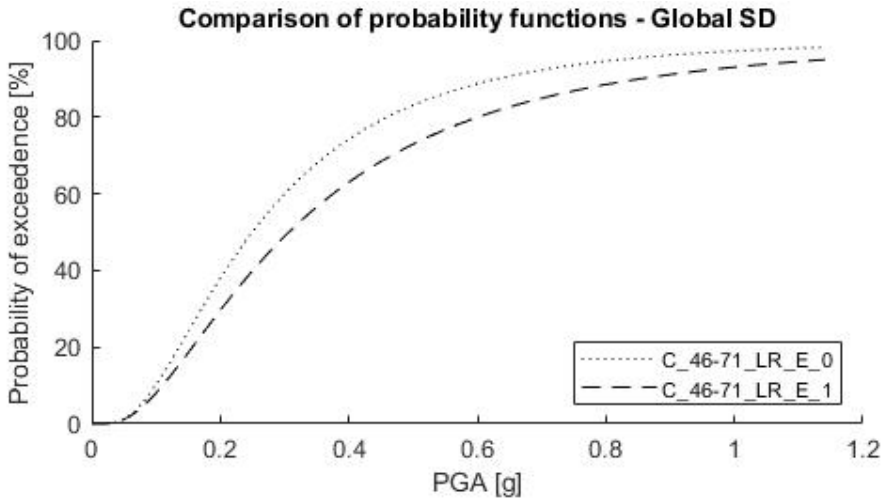

Fig. 13.13 – Fragility functions for the global SD limit state - Comparison between C_46-71_LR_E_1 and C_46-71_LR_E_0 clusters results

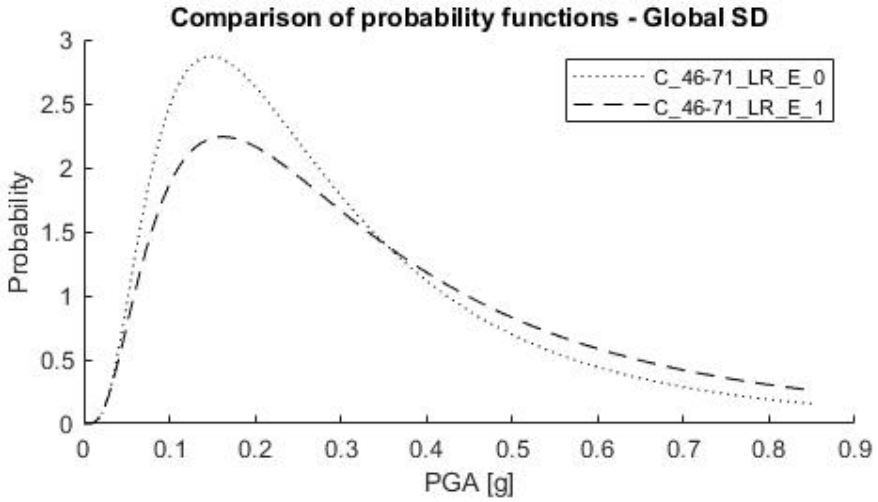

Fig. 13.14 – Probability functions for the global SD limit state threshold - Comparison between C_46-71_LR_E_1 and C_46-71_LR_E_0 clusters results

comparison is depicted directly in terms of probability functions for the threshold of the considered limit state.

14. INSIGHT INTO RESULTS: APPLICATION TO BOVINO MUNICIPALITY

In order to give a further insight into the obtained results, it is interesting applying it to a set of real buildings. For instance, amongst the Puglia region, the municipality of Bovino in the province of Foggia has been selected as example case study.

According to the surveys made in the Bovino municipality, together with the data collected from the CARTIS form of the municipality, the urban area of Bovino can be split into two homogeneous compartments, whose outlines are depicted in Fig. 14.1.

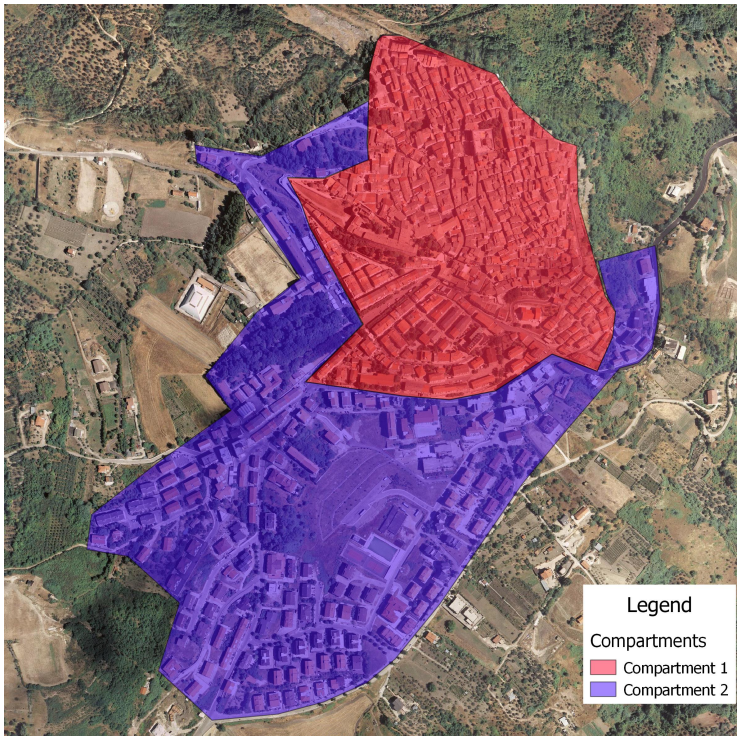

Fig. 14.1 – Outlines of homogeneous compartments in the urban area of Bovino

The first compartment represents the historical center of this town, and buildings here present are mostly masonry buildings.

The second compartment is the expansion area of the town, founded in the second half of the XX century, in which most of the buildings have a reinforced concrete structure. Obviously, given that the proposed procedure has been implemented only for RC buildings until now, analyses have been focused on this compartment.

Regarding the soil conditions, several documents and projects have been consulted, and all seem to be in accordance in defining a soil category *B* as in both NTC2018 and EC8-1:2004.

Moreover, according to Section 13.2.1 and Annex A Bovino is included into the homogeneous municipalities group 2.

14.1 Buildings classification

As a first step, buildings in the municipality have been classified according to clusters defined in Section 13.3. In order to make this classification, information from several sources have been collected as described in Section 7.2 (*e.g.* from census data, direct surveys and interviews, CARTIS form).

For building classification purposes, a neural net has been trained according to Fig. 14.2 in order to organize all of the data collected on the buildings.

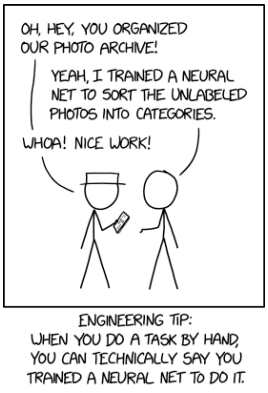

Fig. 14.2 – An unusual description of the neural net trained for building classification

According to the building typologies defined through clusters in Tab. 13.5, information on plan shapes, number of floors and construction years are summarized (only for

RC residential buildings) in Fig. 14.3, Fig. 14.4 and Fig. 14.5 respectively.

In order to discern RC buildings from other structural typologies, data from *15° Censimento Generale della Popolazione e delle Abitazioni* (2011) have been cross-checked with visual inspections.

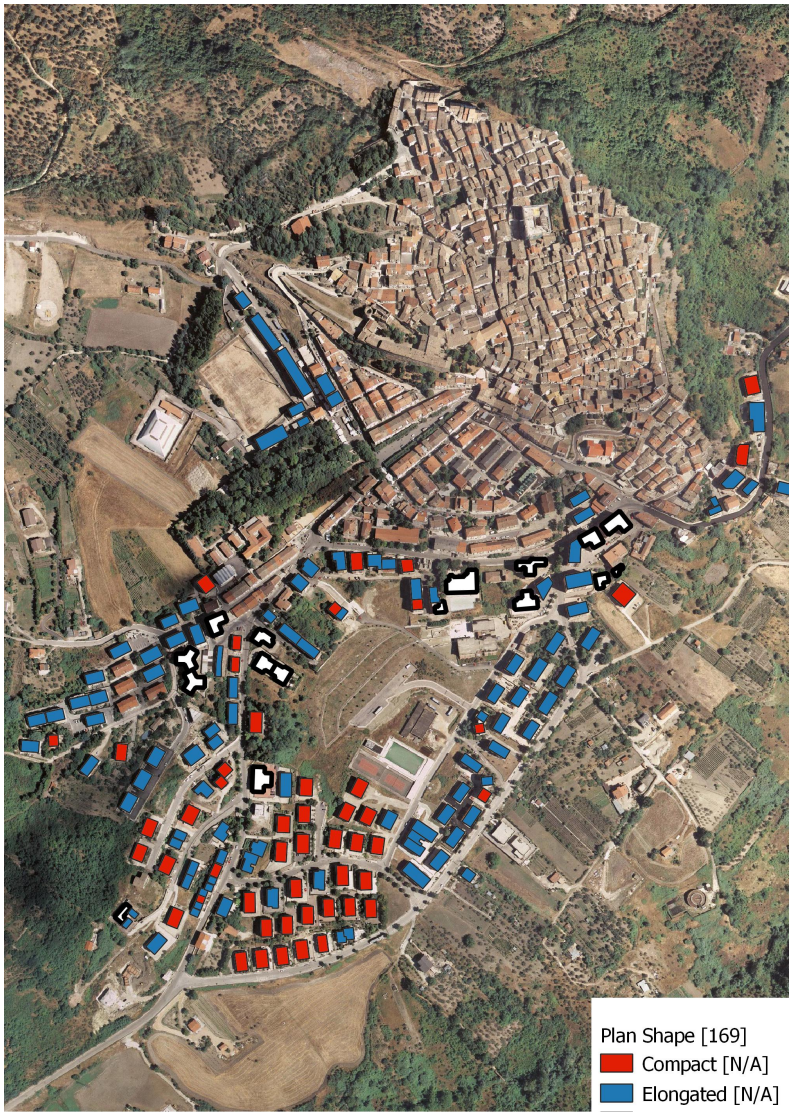

Fig. 14.3 – Plan shapes of RC buildings in Bovino municipality

Regarding plan shapes, buildings are divided into elongated and compact. Those

classes are explicitly defined for rectangular shapes, thus every building having a shape consistently different from the rectangular have been dropped. For rectangular (or almost-rectangular) shapes, the ratio b/h between the main dimensions of the bounding box is defined, and the building is classified as having an *elongated* plan shape if $b/h > 1.5$ and *compact* otherwise.

Fig. 14.4 – Heights of RC buildings in Bovino municipality

About the number of floors, data have been collected from *15° Censimento Generale della Popolazione e delle Abitazioni* (2011) and then cross-checked via visual inspection. For instance, buildings are classified according to the number of floors N in low-rise ($N \leq 3$), mid-rise ($4 \leq N \leq 6$) and high-rise ($N \geq 7$). The latter category, however, has been dropped.

Fig. 14.5 – Construction periods of RC buildings in Bovino municipality

Tab. 14.1 – Number of buildings in each cluster for the Bovino municipality

Cluster	Number of buildings
C_72-81_LR_E_1	27
C_72-81_MR_E_1	22
C_72-81_MR_C_1	18
C_46-71_MR_E_1	12
C_72-81_LR_C_1	9
C_46-71_LR_E_1	6
Others	9
Not classifiable	66

Regarding the construction period, data available from *15° Censimento Generale della Popolazione e delle Abitazioni* (2011) have been integrated with information collected through interviews. Buildings are then classified based on their construction year Y in clusters: 1946-1971, 1972-1981, >1981. It is worth highlighting that, with respect to the clustering in Tab. 13.5, there is not the <1945 cluster, namely because no RC buildings have been found that can be traced back to those years.

About the seismic category of the municipality at the time of the construction, it has been observed that in R.D. 25/03/1935 Bovino was included in the 1st seismic category. Thus, every building in the municipality can be assumed to be designed according to the 1st seismic category requirements.

After this operation, each building that fulfilled any of the requirements in Tab. 13.5 for its inclusion in a cluster has been matched with its relative information on vulnerability. Obviously, not all buildings were classified in a cluster, *e.g.* because of its recent construction, for its irregular plan shape, etc.

As a results, in Tab. 14.1 the number of buildings in the Bovino municipality that belong to clusters defined in Tab. 13.5 are summarized.

14.2 Results

For each of the clusters in Tab. 14.1, fragility functions for each limit state listed in Section 11.1 have been defined.

While in Annex B said fragility curves are depicted in their graphical format, in Tab. 14.2 their distribution parameters are presented.

Tab. 14.2 – Fitted fragility curves parameters

Cluster	Limit state	μ [g]	β
C_72-81_LR_E_1	Global NC	0.3384	0.5364
	Local NC	0.3828	0.3941
	Global SD	0.2004	0.8949
	Local SD	0.3661	0.4268
	Global DL	0.0982	1.1973
	Local DL	0.0923	1.4422
C_72-81_MR_E_1	Global NC	0.2944	0.7785
	Local NC	0.3604	0.4212
	Global SD	0.2383	0.8755
	Local SD	0.3433	0.4949
	Global DL	0.1275	1.3558
	Local DL	0.1522	1.3618
C_72-81_MR_C_1	Global NC	0.2998	0.6075
	Local NC	0.3660	0.4755
	Global SD	0.1988	0.6432
	Local SD	0.3244	0.4399
	Global DL	0.0965	1.0923
	Local DL	0.1076	1.1003
C_46-71_MR_E_1	Global NC	0.3045	0.7747
	Local NC	0.3364	0.6005
	Global SD	0.2347	0.9669
	Local SD	0.2986	0.7703
	Global DL	0.1355	1.5082
	Local DL	0.1502	1.5411
C_72-81_LR_C_1	Global NC	0.4488	0.7261
	Local NC	0.5336	0.5282
	Global SD	0.2335	0.7049
	Local SD	0.4615	0.5817
	Global DL	0.1075	1.0463
	Local DL	0.1599	0.7087
C_46-71_LR_E_1	Global NC	0.3887	1.1943
	Local NC	0.4786	0.7899
	Global SD	0.1447	1.0864
	Local SD	0.3592	0.9402
	Global DL	0.0874	1.0603
	Local DL	0.0864	1.0323

Tab. 14.3 – Hazard characteristics for Bovino

T **[years]**	30	50	72	101	140	201	475	975	2475
p **(probability in 1yr)**	0.0333	0.0200	0.0139	0.0099	0.0071	0.0050	0.0021	0.0010	0.0004
PGA **[g]**	0.0498	0.0625	0.0741	0.0894	0.1036	0.1216	0.1836	0.2526	0.3808

Hazard characteristics for Bovino have been also defined starting from the values of PGA given in NTC2018 for a fixed set of return periods T as depicted in Tab. 14.3. Starting from said values, a probability distribution is fitted in order to effectively represent hazard continuously.

For instance, values of PGA in Tab. 14.3 are assumed to be the expected maximum value in the return period T. Thus, probabilities p represent the *non-exceeding probabilities* over a 1 year period range. In Fig. 14.6 couples $PGA - p$ from Tab. 14.3 are used to fit the ones' complement of a log-normal cumulative distribution function, resulting in a distribution having mean $\mu = 0.0058g$ and standard deviation of logarithm $\beta = 1.1680$.

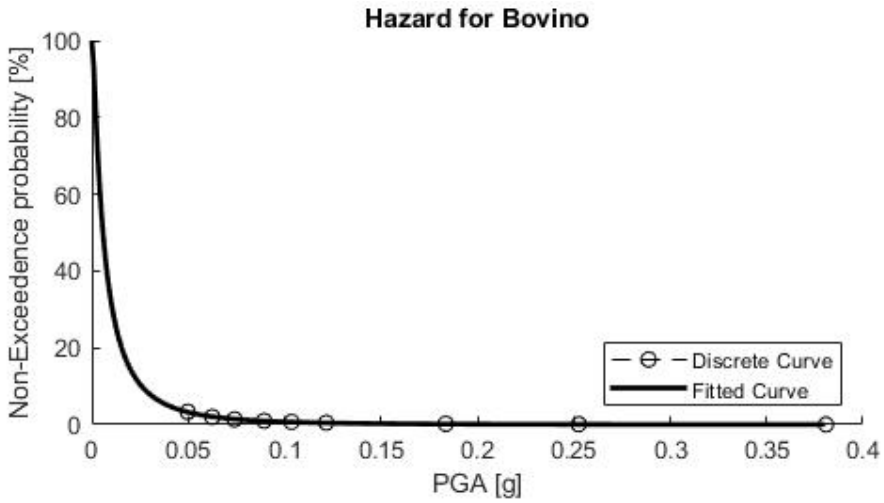

Fig. 14.6 – Fitting of probability distribution for maximum expected PGA

14.2.1 Vulnerability maps

Fragility curves as defined in Tab. 14.2 and hazard characteristics according to Fig. 14.6 can be combined in order to assess the exceedence probability for each considered limit

state. For instance, accoding to the ***PBEE*** (Performance-Based Earthquake Engineering) principles, the annual exceeding probability can be computed through Eq. 14.1 (as given for example in CNR DT 212:2013).

$$\lambda_{LS} = \int_0^{\infty} FF_{LS}(PGA) \cdot \left| \frac{d\,\lambda_{PGA}}{d\,PGA}(PGA) \right| \, d\,PGA \tag{14.1}$$

where: $FF_{LS}(PGA) =$ value of the fragility function at the PGA level, *i.e.* the probability that the considered limit state LS is exceeded at the intensity level PGA

$\lambda_{PGA}(PGA) =$ value of the hazard function in Fig. 14.6 at the PGA level, so that its derivative represents the probability that the intensity level PGA is observed in a 1 year interval

For instance, Eq. 14.1 is approximated through a discrete formulation for practical purposes according to Eq. 14.2.

$$\lambda_{LS} = \sum_{a_g=0}^{\infty} FF_{LS}(a_g) \cdot \left| \Delta\lambda_{PGA}(a_g) \right| \tag{14.2}$$

Starting from the annual exceedence probability of each considered limit state λ_{LS}, the exceedence probability over a generic time interval of Y years can be computed through Eq. 14.3. Results of this computation for a 50 years time interval are presented in Tab. 14.4 for each building cluster and limit state.

$$\lambda_{LS,Y} = 1 - (1 - \lambda_{LS})^{Y} \tag{14.3}$$

Results in Tab. 14.4 are presented as vulnerability maps from Fig. 14.7 to Fig. 14.12 in order to give an immediate representation of the vulnerability in the municipality. In said figures, full green colour is reserved to buildings that fulfil requirements for new buildings according to NTC2018 (*i.e.* 5% for NC, 10% for SD and 63% for DL), being assumed the equivalence between limit states (NC-SLC SD-SLV DL-SLD).

From presented vulnerability maps, some observations can be made. In general, local limit states appear to be less severe than their global counterparts: *e.g.* for local

Tab. 14.4 – 50 years exceedence probabilities for considered limit states

Cluster	Limit state	$\lambda_{LS,50}$ [%]
C_72-81_LR_E_1	Global NC	3.7031
	Local NC	1.5357
	Global SD	33.0368
	Local SD	1.9803
	Global DL	90.1282
	Local DL	97.0228
C_72-81_MR_E_1	Global NC	12.0121
	Local NC	2.0254
	Global SD	23.8333
	Local SD	3.0541
	Global DL	88.3250
	Local DL	82.5034
C_72-81_MR_C_1	Global NC	6.4677
	Local NC	2.3870
	Global SD	17.8220
	Local SD	2.9032
	Global DL	86.4499
	Local DL	82.4880
C_46-71_MR_E_1	Global NC	11.0580
	Local NC	4.7632
	Global SD	30.7052
	Local SD	11.3528
	Global DL	91.9846
	Local DL	90.5946
C_72-81_LR_C_1	Global NC	3.8195
	Local NC	1.0200
	Global SD	15.3633
	Local SD	1.9379
	Global DL	79.4484
	Local DL	31.1727
C_46-71_LR_E_1	Global NC	25.6281
	Local NC	4.2638
	Global SD	66.7747
	Local SD	13.7566
	Global DL	88.5923
	Local DL	87.8287

Fig. 14.7 – Vulnerability map for Global NC limit state

Fig. 14.8 – Vulnerability map for Local NC limit state

Fig. 14.9 – Vulnerability map for Global SD limit state

Fig. 14.10 – Vulnerability map for Local SD limit state

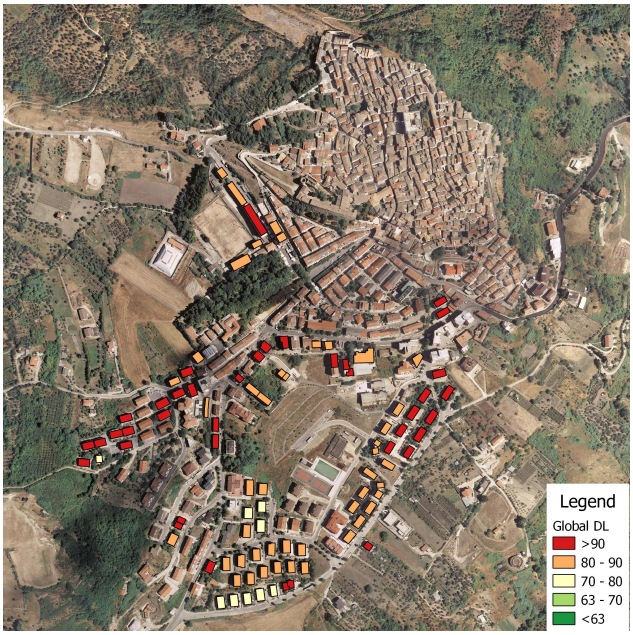

Fig. 14.11 – Vulnerability map for Global DL limit state

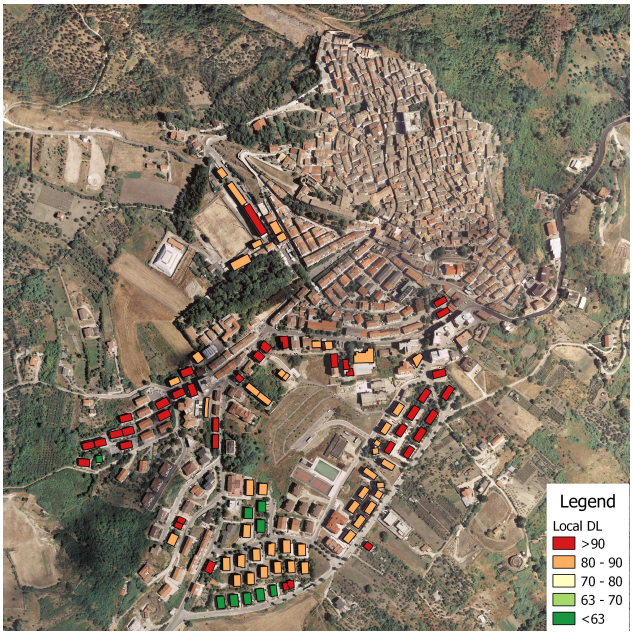

Fig. 14.12 – Vulnerability map for Local DL limit state

NC limit state in Fig. 14.8 all of the buildings are classified as compliant to the code prescription, while for its global counterpart in Fig. 14.7 the situation is clearly worse. Moreover, while a direct comparison between different limit states makes no sense, it appears that the seismic vulnerability decreases with the increase of the limit state severity, *i.e.* the vulnerability decreases from DL limit state to SD and then NC limit states.

14.2.2 Risk maps

Starting from collected informations about the vulnerability of the existing buildings, seismic risk can be assessed.

According to the definition of risk in Eq. 1.1, exposure is to be defined. From *15° Censimento Generale della Popolazione e delle Abitazioni* (2011) the average value of housing area per inhabitant is defined to be $\alpha = 36mq$. Thus, for each building it is possible to define the expected number of inhabitants as in Eq. 14.4

$$I = \frac{n \cdot A}{\alpha} \tag{14.4}$$

where: $n =$ number of floors
$A =$ plan area in mq
$\alpha =$ average value of housing area per inhabitant

In the present work it is assumed that human life is threatened when SD limit state is exceeded, and for instance global SD limit state is considered. Thus, exceedence probabilities of global SD limit state over a period of 50 years as presented in Tab. 14.4 can be multiplied with the expected number of inhabitants of each building in order to assess the expected number of human lives threatened from seismic events in the next 50 years.

In Fig. 14.13 a risk map in terms of expected threatened human lives for the next 50 years is depicted. As a result, at least 1021 human lives are expected to be threatened by seismic events in the next 50 years. Moreover, it is worth highlighting that this esteem

only considers *some* buildings, thus the true value of this parameter is expected to be significantly higher if all the buildings stock is taken into account.

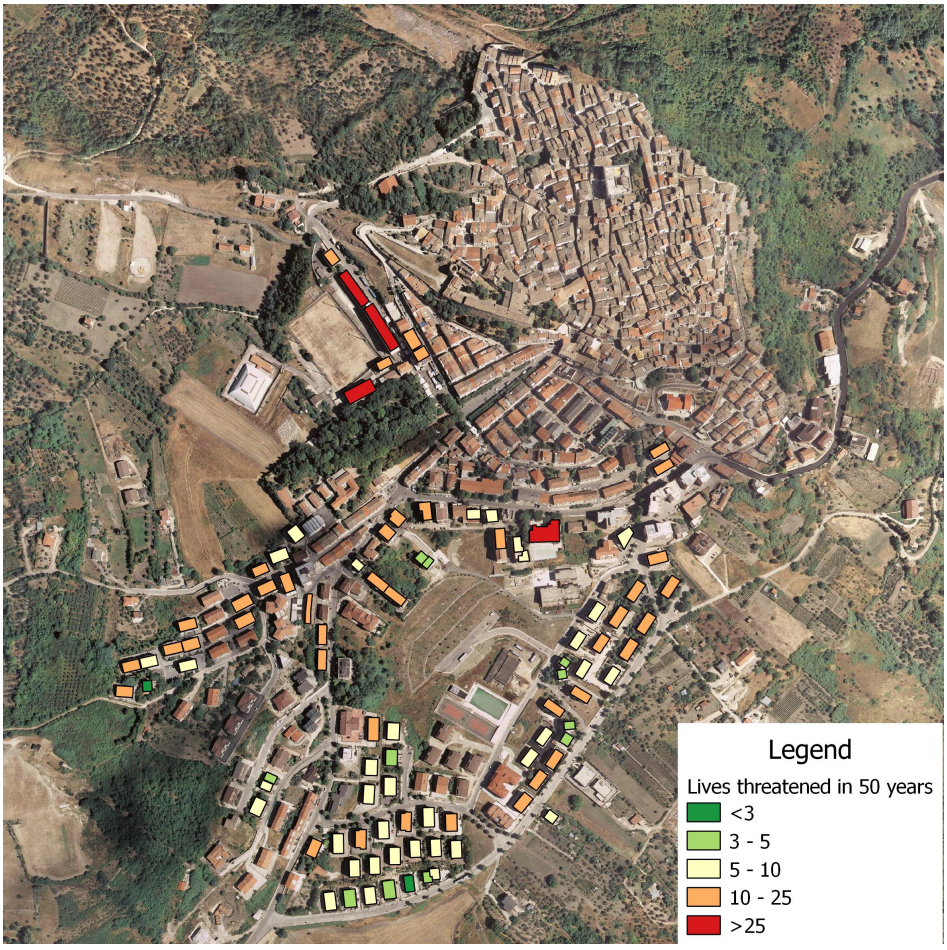

Fig. 14.13 – Risk map in terms of expected human lives threatened by seismic events in the next 50 years

Part IV

Conclusions and future developments

15. CONCLUSIONS

In the present work a novel framework for the solution of the seismic vulnerability of RC buildings at regional scale has been proposed, and an implementation through an automatic tool has been developed.

The proposed framework represents an attempt in the struggle of deepening the knowledge of the seismic vulnerability of the built environment, with the explicit goal of tighten the gap between existing procedures for individual buildings (that assure an outstanding reliability of the results) and available methods for regional scale assessment (that are usually extremely simplified or results are hardly expendable).

In the developing of the procedure, a paramount importance have been given to the reliability of the results, thus trying to minimize simplifications. For instance, several simplifications have been still introduced in the procedure, but each can be overcome with some effort in coding.

In order to enhance the reliability of results, improvements in some crucial elements have been proposed.

In Section 9.1 a novel beam model has been proposed. This proposal represents the attempt of overcoming some mathematical incongruities of existing beam models, so that results in terms of structural elements response are subjected to tinier errors, in accordance to the general objective of the search of more precise results.

In Chapter 10 a new strategy for the solution of the time integration problem has been developed. For instance, the solution given by the proposed approach has been demonstrate to be *exact*, and hence to be *unique*. Those features are obviously coherent with the search of reliable and precise results.

In order to test both the framework and its implementation, two applications have been presented in Part III.

The first application has been made in the regional territory of Puglia. Within this ex-

ample application fragility curves for a set of 36 homogeneous building typologies have been defined, which were determined on the basis of CARTIS form, thus representing what is expected to be a wide percentage of the existing building. For all of the buildings that fall in any of those defined 36 typologies, vulnerability is statistically determined, and hence important assessments can be made.

A second application has been made in the municipality of Bovino, in the province of Foggia, in Puglia. This application has a totally different meaning than the first, as it can be considered the *extension* of that one: starting from those results, the assessment of seismic vulnerability of individual buildings have been made. As a result, a spatial representation of the vulnerability condition of the town has been presented. The simplicity and thus reliability of the output is considered an outstanding positive feature of the procedure in its whole.

16. FUTURE DEVELOPMENTS

While the present work is mainly focused on the presentation of the procedure, some example applications have been presented. However, those applications have to be considered as a proof of the feasibility of the procedure, being clear that not all of its potential has been fully revealed.

A future development that can be straightforwardly achieved is the application of the procedure to a wider group of municipalities, right after needed data are collected: one of the most powerful potential of the procedure is that once analyses are run outcomes can be directly applied to all of the structures that belong to the same homogeneous area and to the same building cluster.

Regarding the procedure itself, some improvements can be scheduled mainly according to the availability of data for their implementation. Namely, some of said improvements are the following:

- If the **SOCRATES** form (described in Section 7.2.1) is extensively used to collect data, further insights in building clustering can be made, and the statistical assessment of several parameters can be achieved (*e.g.* balcony incidence, spans length distribution). Moreover, the **SOCRATES** form itself can be directly linked to the present procedure outcomes, in order to directly categorize each existing structure into one of the defined clusters and then link its results in terms of vulnerability and/or risk. As a further development, the same approach can be thought without the clustering step, thus thinking at a single-building level: this approach, however, would need an extremely high number of analyses, reliability of data would be needed to be assessed, so that the entire approach could be not feasible.
- Some simplifying hypothesis of the procedure can be overcome in future developments. As an example, hypothesis 1 at page 63 about the shear-type behaviour

of the structures can be easily overcome opportunely modifying the procedure. While outcomes are not expected to vary a lot, a modification of this type goes in the same direction of the whole procedure main goal: increasing the reliability of the outcomes.

- Regarding the non-linear modelling of elements, some improvements can be included. About structural elements modelling described in Section 9.2, the effect of the axial load variation can be included, other hysteresis models can be implemented, different assessments of degradation can be considered. With reference to the infills modelling described in Section 9.3, any other model can be implemented in the procedure, *e.g.* introducing several struts for the infill behaviour assessment in order to capture also its influence over the surrounding structural elements. For both elements, any different model can be used for the assessment of their backbone curves.
- The need of additional data is clear looking at the statistical assessment of materials in Section 13.4. Regarding concrete, further insights are needed in order to assess the eventual variation of concrete characteristics over time, both due to the different usage of concrete strength classes over time and due to ageing-related concrete degradation. With reference to infills, almost no data are available about the characteristics of those elements in the existing building stock. Collecting said data would significantly improve the accuracy of the outcomes.
- While the procedure is derived from a strict theoretical approach, its results need to be validated through empirical data. One of the most important future developments of the procedure is exactly its validation using real-world data from past earthquakes. In order to make this step possible, however, further insights are needed about the definition of limit states (see Section 11.1), especially with regard to their correlation with damage information collected from past events.
- In order to make all of those improvements quickly implemented, together with the possibility of finding new unnoticed problems and/or capabilities of the procedure, the developed tool **EX:MIRIAM** should have to be made available as

soon as possible to different users.

While significant improvements are possible, the presented procedure can be considered the beginning of a long journey toward significantly more reliable and accurate results in seismic vulnerability analyses at regional scale.

ACKNOWLEDGEMENTS

I will spend only few words for thanking some important persons: every extent of this section would be inadequate for the amount of help and support that I received from many individuals.

First of all, I want to express my gratitude to prof. ***Giuseppina Uva***: your guidance has been fundamental in my whole path, and your indications have been determinant for its direction.

I also owe so much to profs. ***Maddalena***, ***Coclite*** (both), ***Puglisi***, ***Florio***, ***Devillanova***: mostly for the time spent with me, but I will be always grateful for the way you challenged me.

Special thanks to my reviewers, profs. ***Vukobratovic***, ***Bagassi*** and ***Perrone***: your precious suggestions have been crucial for the enhancement of this thesis.

A sincere appreciation to my colleagues ***Sergio***, ***Valeria***, ***Andrea***: it has been an honour to share this path with you.

My most heartfelt gratitude goes to ing. ***Andrea Fiore***: no words can describe how helpful has been your support and example. You have all of my esteem.

To my wife, my parents, my brother, my family: your unconditional support has been fundamental in my whole life.

To ***Christian***: your light shines bright, leading our paths. I still consider myself your *favourite uncle*.

Miriam, my darling, my heart, my whole. In Latin, *e*/*ex* + name translates to *"moving from"*, with the idea of a movement with direction inside-outside. My whole work is for you, my whole work is *from* you, the source of my motivation and inspiration.

Pier Luigi

REFERENCES

> We are like dwarfs on the shoulders of giants, so that we can see more than they, and things at a greater distance, not by virtue of any sharpness of sight on our part, or any physical distinction, but because we are carried high and raised up by their giant size
>
> *Bernard De Chartres*

ISTAT. *15° Censimento Generale della Popolazione e delle Abitazioni*. in italian (data available at http://dati-censimentopopolazione.istat.it).

Abassy, Tamer A (2012). "Piecewise analytic method." In: *International Journal of Applied Mathematical Research* 1.1, pp. 77–107.

Aiello, Maria Antonietta, Pier Luigi Ciampoli, Andrea Fiore, Daniele Perrone, and Giuseppina Uva (2017a). "Appraisal of the contribution of infill panels in regional vulnerability analyses of existing RC buildings in Puglia." In: *XVII ANIDIS Conference on 'Ingegneria Sismica in Italia'*, pp. 158–168.

– (Dec. 2017b). "Influence of Infilled Frames on Seismic Vulnerability Assessment of Recurrent Building Typologies." In: *Ingegneria Sismica* 34.4, pp. 58–80.

Ambartsumian, SA (1958). "On the theory of bending plates." In: *Izv Otd Tech Nauk AN SSSR* 5.5, pp. 69–77.

Ancheta, Timothy D., Robert B. Darragh, Jonathan P. Stewart, Emel Seyhan, Walter J. Silva, et al. (May 2013). *PEER NGA-West2 Database*. PEER 2013/03. PEER - Pacific Earthquake Engineering Research Center.

Andersen, Lars and Johan Clausen (2008). "Impedance of surface footings on layered ground." In: *Computers & structures* 86.1-2, pp. 72–87.

Antofie, T.E., B. Doherty, and M. Marin-Ferrer (2018). *Mapping of risk web-platforms and risk data: collection of good practices*. Technical Report EUR 29086 EN. JRC (Joint Research Center).

Arnold, C., R. Reitherman, and Inc Building Systems Development (1981). *Building Configuration and Seismic Design: The Architecture of Earthquake Resistance*. Building Systems Development. URL: https://books.google.it/books?id=U9FRAAAAMAAJ.

Asteris, Panagiotis G., C.Z. Chrysostomoy, I.P. Giannopoulos, and E. Smyrou (May 2011). "Masonry infilled reinforced concrete frames with openings." In: *COMPDYN 2011 - III ECCOMAS Thematic Conference on computational methods in structural dynamics and earthquake engineering*.

Aydogdu, Metin (2009). "A new shear deformation theory for laminated composite plates." In: *Composite structures* 89.1, pp. 94–101.

Baker, Jack W and C Allin Cornell (2006). "Spectral shape, epsilon and record selection." In: *Earthquake Engineering & Structural Dynamics* 35.9, pp. 1077–1095.

Baker, Jack W and Cynthia Lee (2018). "An improved algorithm for selecting ground motions to match a conditional spectrum." In: *Journal of Earthquake Engineering* 22.4, pp. 708–723.

Baker, JW (2013). "Trade-offs in ground motion selection techniques for collapse assessment of structures." In: *Vienna Congress on Recent Advances in Earthquake Engineering and Structural Dynamics*, pp. 28–30.

Ballarini, Roberto (2003). "The Da Vinci-Euler-Bernoulli Beam Theory." In: *Mechanical Engineering Magazine Online* 7.

Barro, Enrico (1934). *L'ingegnere sul posto di lavoro*.

Bathe, KJ and EL Wilson (1972). "Stability and accuracy analysis of direct integration methods." In: *Earthquake Engineering & Structural Dynamics* 1.3, pp. 283–291.

Bathe, Klaus-Jürgen (2007). "Conserving energy and momentum in nonlinear dynamics: a simple implicit time integration scheme." In: *Computers & structures* 85.7-8, pp. 437–445.

Bathe, Klaus-Jürgen and Mirza M Irfan Baig (2005). "On a composite implicit time integration procedure for nonlinear dynamics." In: *Computers & Structures* 83.31-32, pp. 2513–2524.

Bathe, Klaus-Jürgen and Gunwoo Noh (2012). "Insight into an implicit time integration scheme for structural dynamics." In: *Computers & Structures* 98, pp. 1–6.

Bazzi, G and E Anderheggen (1982). "The ρ-family of algorithms for time-step integration with improved numerical dissipation." In: *Earthquake Engineering & Structural Dynamics* 10.4, pp. 537–550.

Benedetti, D and Petrini V Sulla (1984). "Vulnerabilità di Edifici in Muratura: Proposta di un Metodo di Valutazione." In: *L'industria delle Costruzioni* 149.1, pp. 66–74.

El-Betar, Sameh A (2018). “Seismic vulnerability evaluation of existing RC buildings.” In: *HBRC journal* 14.2, pp. 189–197.

Borzi, Barbara, Helen Crowley, and Rui Pinho (2008). “The influence of infill panels on vulnerability curves for RC buildings.” In: *Proceedings of the 14th world conference on earthquake engineering, Beijing, China*.

Borzi, Barbara, Rui Pinho, and Helen Crowley (2008). “Simplified pushover-based vulnerability analysis for large-scale assessment of RC buildings.” In: *Engineering Structures* 30.3, pp. 804–820.

Bouc, R (1971). “A mathematical model for hysteresis.” In: *Acta Acustica united with Acustica* 24.1, pp. 16–25.

Bradley, Brendon A (2010). “A generalized conditional intensity measure approach and holistic ground-motion selection.” In: *Earthquake Engineering & Structural Dynamics* 39.12, pp. 1321–1342.

– (2013). “A critical examination of seismic response uncertainty analysis in earthquake engineering.” In: *Earthquake Engineering & Structural Dynamics* 42.11, pp. 1717–1729.

Braga, F, M Dolce, and D Liberatore (1982). “A statistical study on damaged buildings and an ensuing review of the MSK-76 scale.” In: *Proceedings of the seventh European conference on earthquake engineering, Athens, Greece*, pp. 431–450.

Brent, R (1976). “A new algorithm for minimizing a function of several variables without calculating derivatives.” In: *Algorithms for minimization without derivatives*, pp. 200–248.

Bucinskas, Paulius and Lars Vabbersgaard Andersen (2017). “Semi-analytical approach to modelling the dynamic behaviour of soil excited by embedded foundations.” In: *Procedia engineering* 199, pp. 2621–2626.

Calvi, G Michele, Rui Pinho, Guido Magenes, Julian J Bommer, L Fernando Restrepo-Vélez, and Helen Crowley (2006). “Development of seismic vulnerability assessment methodologies over the past 30 years.” In: *ISET journal of Earthquake Technology* 43.3, pp. 75–104.

Calvi, Gian Michele (1999). “A displacement-based approach for vulnerability evaluation of classes of buildings.” In: *Journal of Earthquake Engineering* 3.03, pp. 411–438.

Cardona, Omar D and Luis E Yamín (1997). “Seismic microzonation and estimation of earthquake loss scenarios: integrated risk mitigation project of Bogotá, Colombia.” In: *Earthquake Spectra* 13.4, pp. 795–814.

Carniel, R, C Cecotti, A Chiarandini, S Grimaz, E Picco, and M Riuscetti (2001). “A definition of seismic vulnerability on a regional scale: the structural typology as a significant parameter.” In: *Bollettino di Geofisica Teorica e Applicata* 42, pp. 139–157.

Cetisli, Fatih (2015). “Effect of openings on infilled frame stiffness.” In: *GRAĐEVINAR* 67, pp. 787–798.

Al-Chaar, Ghassan (2002). *Evaluating strength and stiffness of unreinforced masonry infill structures*. ERDC CERL TR-02-1. US Army Corps of Engineers, Construction Engineering Research Laboratory.

Chang, Shuenn-Yih (2017). “Unusual overshooting in steady-state response for structure-dependent integration methods.” In: *Journal of Earthquake Engineering* 21.8, pp. 1220–1233.

– (2018a). “Elimination of overshoot in forced vibration responses for Chang explicit family methods.” In: *Journal of Engineering Mechanics* 144.2, p. 04017177.

– (2018b). “Improved formulations of the CR and KR methods for structural dynamics.” In: *Earthquake Engineering and Engineering Vibration* 17.2, pp. 343–353.

Chang, Shuenn-yih (1999). *An unconditionally stable explicit algorithm in time history analysis*. National Center for Research on Earthquake Engineering.

Chang, Shuenn-Yih and Wen-I Liao (2005). “An unconditionally stable explicit method for structural dynamics.” In: *Journal of earthquake engineering* 9.03, pp. 349–370.

Chen, Cheng and James M Ricles (2008). “Development of direct integration algorithms for structural dynamics using discrete control theory.” In: *Journal of Engineering Mechanics* 134.8, pp. 676–683.

Chung, Jintai and GM1223971 Hulbert (1993). “A time integration algorithm for structural dynamics with improved numerical dissipation: the generalized-α method.” In.

Chung, Jintai and Gregory M Hulbert (1994). “A family of single-step Houbolt time integration algorithms for structural dynamics.” In: *Computer methods in applied mechanics and engineering* 118.1-2, pp. 1–11.

Ciampoli, Pier Luigi, Andrea Fiore, and Giuseppina Uva (2020). “To a new kinematic model aimed at the computational analysis of reinforced concrete beams.” (in press).

Cimellaro, Gian Paolo and Sebastiano Marasco (2015). “A computer-based environment for processing and selection of seismic ground motion records: OPENSIGNAL.” In: *Frontiers in Built Environment* 1, p. 17.

Clough, Ray W (1966). “Effect of stiffness degradation on earthquake ductility requirements.” In: *Proceedings of Japan earthquake engineering symposium*.

Colombo, Giuseppe (1890). *Manuale dell’Ingegnere civile e industriale*. Ed. by Ulrico Hoepli. XI.

– (1895). *Manuale dell’Ingegnere*. Ed. by Ulrico Hoepli. XIV.

Conte, Myriam (2018). “Classi Tipologico-Strutturali di Edifici Esistenti in c.a. ed Elementi Caratteristici di Vulnerabilitá Strutturale e Sismica: Ricognizione ed Analisi nel Contesto Pugliese.” Master Degree Thesis.

Cosenza, Edoardo, Gaetano Manfredi, Maria Polese, and Gerardo M Verderame (2005). “A multilevel approach to the capacity assessment of existing RC buildings.” In: *Journal of Earthquake Engineering* 9.01, pp. 1–22.

Cowper, GR (1966). “The shear coefficient in Timoshenko’s beam theory.” In: *ASME Journal of Applied Mechanics* 3, pp. 335–340.

Crowley, H, R Pinho, JJ Bommer, and JF Bird (2006). “Development of a displacement-based method for earthquake loss assessment.” In: *European School for Advanced Studies in Reduction of Seismic Risk, Pavia, Research Report No. ROSE-2006* 1.

Crowley, Helen, Rui Pinho, and Julian J Bommer (2004). “A probabilistic displacement-based vulnerability assessment procedure for earthquake loss estimation.” In: *Bulletin of Earthquake Engineering* 2.2, pp. 173–219.

Dekker, TJ (1969). *Finding a zero by means of successive linear interpolation, Constructive Aspects of the Fundamental Theorem of Algebra (B. Dejon and P. Henrici, eds.)*

Del Gaudio, Carlo (2015). “Seismic Fragility Assessment of RC Buildings at Large Scale.” XXVII Cycle. PhD Thesis. University of Naples Federico II.

Del Gaudio, Carlo, Marco Di Ludovico, Maria Polese, Gaetano Manfredi, Andrea Prota, Paolo Ricci, and Gerardo M Verderame (2020). “Seismic fragility for Italian RC buildings based on damage data of the last 50 years.” In: *Bulletin of Earthquake Engineering* 18.5, pp. 2023–2059.

Del Zoppo, M, C Del Vecchio, M Di Ludovico, A Prota, and G Manfredi (2016). “Shear failure of existing RC columns under seismic actions.” In: *Proc., Italian Concrete Days, GWMAX Editore, Erba, Italy*.

Di Pasquale, Giacomo, Giampiero Orsini, and Roberto W Romeo (2005). “New developments in seismic risk assessment in Italy.” In: *Bulletin of Earthquake Engineering* 3.1, pp. 101–128.

Dolce, Mauro, Angelo Masi, Maria Marino, and Marco Vona (2003). “Earthquake damage scenarios of the building stock of Potenza (Southern Italy) including site effects.” In: *Bulletin of Earthquake Engineering* 1.1, pp. 115–140.

Dolsek, Matjaz (2009). “Incremental dynamic analysis with consideration of modeling uncertainties.” In: *Earthquake Engineering & Structural Dynamics* 38.6, pp. 805–825.

Du, Wenqi, Chao-Lie Ning, and Gang Wang (2019). “The effect of amplitude scaling limits on conditional spectrum-based ground motion selection.” In: *Earthquake Engineering & Structural Dynamics* 48.9, pp. 1030–1044.

Dumova-Jovanoska, E (2004). “Fragility curves for RC structures in Skopje region.” In: *Proceedings of the 13th World Conference on Earthquake Engineering*. 3.

ATC-13:1985: *Earthquake damage evaluation data for California*. ATC - Applied Technology Council.

Eisenberger, Moshe (2003). “An exact high order beam element.” In: *Computers & structures* 81.3, pp. 147–152.

EC6-1-1: *EN 1996-1-1:2005 - Eurocode 6: Design of masonry structures - Part 1-1: General rules for reinforced and unreinforced masonry structures*. CEN - European Committee for Standardization. European Standard.

EC8-1:2004: *EN 1998-1:2004 - Eurocode 8: Design of structures for earthquake resistance – Part 1: General Rules, seismic actions and rules for buildings*. CEN - European Committee for Standardization. European Standard.

EC8-3:2005: *EN 1998-3:2005 - Eurocode 8: Design of structures for earthquake resistance – Part 3: Assessment and retrofitting of buildings*. CEN - European Committee for Standardization. European Standard.

Faccioli, Ezio, Roberto Paolucci, and Manuela Vanini (Oct. 2015). “Evaluation of Probabilistic Site-Specific Seismic-Hazard Methods and Associated Uncertainties, with Applications in the Po Plain, Northern Italy.” In: *Bulletin of the Seismological Society of America* 105.5.

Fäh, D, F Kind, K Lang, and D Giardini (2001). “Earthquake scenarios for the city of Basel.” In: *Soil Dynamics and Earthquake Engineering* 21.5, pp. 405–413.

Fajfar, Peter (1999). “Capacity spectrum method based on inelastic demand spectra.” In: *Earthquake Engineering & Structural Dynamics* 28.9, pp. 979–993.

Fuller, Samuel H and Lynette I Millett (2011). *The Future of Computing Performance: Game Over or Next Level?* National Academy Press.

Ghassemieh, M and M Karimi-rad (2008). “A Quadratic Acceleration Time Integration Method for Problems in Structural Dynamics.” In: *8th International Congress on Advances in Civil Engineering, Famagusta, North Cyprus*.

Ghugal, Yuwaraj Marotrao and Rajneesh Sharma (2009). “A hyperbolic shear deformation theory for flexure and vibration of thick isotropic beams.” In: *International Journal of Computational Methods* 6.04, pp. 585–604.

Giovinazzi, Sonia and Sergio Lagomarsino (2004). “A macroseismic method for the vulnerability assessment of buildings.” In: *13th World Conference on Earthquake Engineering*. Vol. 896, pp. 1–6.

GNDT (1993). *Rischio sismico di edifici pubblici–Parte I: aspetti metodologici*.

Google LLC. *Google Maps*. URL: https://www.google.com/maps.

Goudreau, Gerald Lee and Robert L Taylor (1973). “Evaluation of numerical integration methods in elastodynamics.” In: *Computer Methods in Applied Mechanics and Engineering* 2.1, pp. 69–97.

Goudreau, GL and RL Taylor (1972). “Evaluation of Numerical Integration Methods in Elastodynamics, Computor Meth.” In: *Appl. Mech. and Engin* 2.

Grant, Damian, Julian J Bommer, Rui Pinho, and Gian Michele Calvi (2006). “Defining priorities and timescales for seismic intervention in school buildings in Italy.” In: *IUSS Monograph*.

Grünthal, G (1998). “Cahiers du Centre Européen de Géodynamique et de Séismologie: Volume 15–European Macroseismic Scale 1998.” In: *European Center for Geodynamics and Seismology, Luxembourg*.

Gruttmann, F and W Wagner (2001). “Shear correction factors in Timoshenko’s beam theory for arbitrary shaped cross-sections.” In: *Computational mechanics* 27.3, pp. 199–207.

Guagenti, E and V Petrini (1989). “The case of old buildings: towards a damage-intensity relationship.” In: *Proceedings of the Fourth Italian National Conference on Earthquake Engineering, Milan, Italy*, pp. 145–153.

Gui, Yao, Jin-Ting Wang, Feng Jin, Cheng Chen, and Meng-Xia Zhou (2014). “Development of a family of explicit algorithms for structural dynamics with unconditional stability.” In: *Nonlinear Dynamics* 77.4, pp. 1157–1170.

Hassan, Ahmed F and Mete A Sozen (1997). “Seismic vulnerability assessment of low-rise buildings in regions with infrequent earthquakes.” In: *ACI Structural Journal* 94.1, pp. 31–39.

Heyliger, PR and JN Reddy (1988). "A higher order beam finite element for bending and vibration problems." In: *Journal of sound and vibration* 126.2, pp. 309–326.

Hilber, Hans M and Thomas JR Hughes (1978). "Collocation, dissipation and [overshoot] for time integration schemes in structural dynamics." In: *Earthquake Engineering & Structural Dynamics* 6.1, pp. 99–117.

Hilber, Hans M, Thomas JR Hughes, and Robert L Taylor (1977). "Improved numerical dissipation for time integration algorithms in structural dynamics." In: *Earthquake Engineering & Structural Dynamics* 5.3, pp. 283–292.

Hoff, C and PJ Pahl (1988). "Development of an implicit method with numerical dissipation from a generalized single-step algorithm for structural dynamics." In: *Computer Methods in Applied Mechanics and Engineering* 67.3, pp. 367–385.

Hopper, Michael W. (2009). "Analytical Models for the Nonlinear Seismic Response of Reinforced Concrete Frames." PhD Thesis. Pennsylvania State University.

Ibarra, Luis F, Ricardo A Medina, and Helmut Krawinkler (2005). "Hysteretic models that incorporate strength and stiffness deterioration." In: *Earthquake engineering & structural dynamics* 34.12, pp. 1489–1511.

Iervolino, Iunio and Gaetano Manfredi (2008). "A review of ground motion record selection strategies for dynamic structural analysis." In: *Modern Testing Techniques for Structural Systems*. Springer, pp. 131–163.

Iervolino, Iunio, Gaetano Manfredi, Maria Polese, Gerardo Mario Verderame, and Giovanni Fabbrocino (2007). "Seismic risk of RC building classes." In: *Engineering Structures* 29.5, pp. 813–820.

INGV - Istituto Nazionale di Geofisica e Vulcanologia. *Interactive Seismic Hazard Maps*. URL: http://esse1-gis.mi.ingv.it/.

Iovino, Renato, Emanuele La Mantia, and Salvatore Simonetti (2014). "La corrosione delle armature per carbonatazione del calcestruzzo." In: *CONCRETE 2014: Progetto e tecnologia per il costruito - Tra XX e XXI secolo*.

CNR10024:1986: *Analisi di strutture mediante elaboratore: impostazione e redazione delle relazioni di calcolo*. CNR - Consiglio Nazionale delle Ricerche. CNR indications.

C.M. 23/05/1957: *Circolare Ministeriale n.1472 23/05/1957 'Armatura delle strutture in cemento armato'*. Ministero dei Lavori Pubblici - Consiglio Superiore. Operative Indications from Italian Government.

C.M. 21/01/2019: *Circolare Ministeriale n.7 21/01/2019 'Istruzioni per l'applicazione dell'aggiornamento delle Norme Tecniche per le Costruzioni di cui al Decreto Ministeriale 17/01/2018'*. C.S.LL.PP. - Consiglio Superiore dei Lavori Pubblici. Operative Indications from Italian Government.

CNR - Consiglio Nazionale delle Ricerche (1953). *Manuale dell'architetto*.

D.L. 05/11/1916: *Decreto Luogotenenziale n.1526 05/11/1916 'Testo unico delle disposizioni legislative emanate in dipendenza del terremoto del 28 dicembre 1908'*. Governo Italiano. Italian Standard.

D.M. 01/04/1983: *Decreto Ministeriale 01/04/1983 'Norme tecniche per l'esecuzione delle opere in cemento armato normale, precompresso e per le strutture metalliche'*. Ministero dei Lavori Pubblici. Italian Standard.

D.M. 03/03/1975: *Decreto Ministeriale 03/03/1975 'Approvazione delle norme tecniche per le costruzioni in zone sismiche'*. Ministero dei Lavori Pubblici. Italian Standard.

D.M. 09/01/1996: *Decreto Ministeriale 09/01/1996 'Norme tecniche per il calcolo, l'esecuzione ed il collaudo delle opere in cemento armato, normale e precompresso e per le strutture metalliche'*. Ministero dei Lavori Pubblici. Italian Standard.

D.M. 10/01/1907: *Decreto Ministeriale 10/01/1907*. Ministero dei Lavori Pubblici. Italian Standard.

D.M. 14/02/1992: *Decreto Ministeriale 14/02/1992 'Norme tecniche per l'esecuzione delle opere in cemento armato normale e precompresso e per le strutture metalliche'*. Ministero dei Lavori Pubblici. Italian Standard.

D.M. 16/01/1996: *Decreto Ministeriale 16/01/1996 'Norme tecniche per le costruzioni in zone sismiche'*. Ministero dei Lavori Pubblici. Italian Standard.

D.M. 16/06/1976: *Decreto Ministeriale 16/06/1976 'Norme tecniche per la esecuzione delle opere in cemento armato normale e precompresso e per le strutture metalliche'*. Ministero dei Lavori Pubblici. Italian Standard.

D.M. 19/06/1984: *Decreto Ministeriale 19/06/1984 'Norme tecniche per le costruzioni in zone sismiche'*. Ministero dei Lavori Pubblici. Italian Standard.

D.M. 24/01/1986: *Decreto Ministeriale 24/01/1986 'Norme tecniche relative alle costruzioni sismiche'*. Ministero dei Lavori Pubblici. Italian Standard.

D.M. 26/03/1980: *Decreto Ministeriale 26/03/1980 'Norme tecniche per l'esecuzione delle opere in cemento armato normale, precompresso e per le strutture metalliche'*. Ministero dei

Lavori Pubblici. Italian Standard.

D.M. 27/07/1985: *Decreto Ministeriale 27/07/1985 'Norme tecniche per l'esecuzione delle opere in cemento armato normale e precompresso e per le strutture metalliche'*. Ministero dei Lavori Pubblici. Italian Standard.

D.M. 30/05/1972: *Decreto Ministeriale 30/05/1972 'Norme tecniche alle quali devono uniformarsi le costruzioni in conglomerato cementizio, normale e precompresso ed a struttura metallica'*. Ministero dei Lavori Pubblici. Italian Standard.

NTC2008: *DM 14/01/2008 Approvazione delle Nuove Norme Tecniche per le costruzioni*. Ministero dei Lavori Pubblici. Italian Standard.

NTC2018: *DM 17/01/2018 Aggiornamento delle 'Norme Tecniche per le costruzioni'*. Ministero dei Lavori Pubblici. Italian Standard.

CNR DT 212:2013: *Istruzioni per la Valutazione Affidabilistica della Sicurezza Sismica di Edifici Esistenti*. CNR - Consiglio Nazionale delle Ricerche. CNR indications.

L. 25/11/1962: *Legge n.1684 25/11/1962 'Provvedimenti per l'edilizia, con particolari prescrizioni per le zone sismiche'*. Governo Italiano. Italian Standard.

R.D. 29/07/1933: *Regio Decreto n.1213 29/07/1933 'Norme per l'accettazione dei leganti idraulici e per la esecuzione delle opere in conglomerato cementizio'*. Governo Italiano. Italian Standard.

R.D. 18/04/1909: *Regio Decreto n.193 18/04/1909*. Governo Italiano. Italian Standard.

R.D. 23/10/1924: *Regio Decreto n.2089 23/10/1924 'Norme tecniche ed igieniche di edilizia per le località colpite dal terremoto'*. Governo Italiano. Italian Standard.

R.D. 22/11/1937: *Regio Decreto n.2105 22/11/1937 'Norme tecniche di edilizia con speciali prescrizioni per le località colpite dai terremoti'*. Governo Italiano. Italian Standard.

R.D. 16/11/1939 n.2228: *Regio Decreto n.2228 16/11/1939 'Norme per l'accettazione dei leganti idraulici'*. Governo Italiano. Italian Standard.

R.D. 16/11/1939 n.2229: *Regio Decreto n.2229 16/11/1939 'Norme per l'esecuzione delle opere in conglomerato cementizio semplice od armato'*. Governo Italiano. Italian Standard.

R.D. 13/03/1927: *Regio Decreto n.431 13/03/1927 'Norme tecniche ed igieniche per le località colpite dai terremoti'*. Governo Italiano. Italian Standard.

R.D. 25/03/1935: *Regio Decreto n.640 25/03/1935 'Nuovo testo delle norme tecniche di edilizia con speciali prescrizioni per le località colpite dai terremoti'*. Governo Italiano. Italian Standard.

R.D. 03/04/1930: *Regio Decreto n.682 03/04/1930 'Norme tecniche ed igieniche di edilizia per le località sismiche'*. Governo Italiano. Italian Standard.

Jalayer, Fatemeh and CA Cornell (2009). "Alternative non-linear demand estimation methods for probability-based seismic assessments." In: *Earthquake Engineering & Structural Dynamics* 38.8, pp. 951–972.

Jalayer, Fatemeh, Hossein Ebrahimian, Andrea Miano, Gaetano Manfredi, and Halil Sezen (2017). "Analytical fragility assessment using unscaled ground motion records." In: *Earthquake Engineering & Structural Dynamics* 46.15, pp. 2639–2663.

Jayaram, Nirmal, Ting Lin, and Jack W Baker (2011). "A computationally efficient ground-motion selection algorithm for matching a target response spectrum mean and variance." In: *Earthquake Spectra* 27.3, pp. 797–815.

JBDPA (1990). *Standard for Evaluation of Seismic Capacity of Existing Reinforced Concrete Buildings*.

Kaczkowski, Z (1968). "Plates." In: *Statical calculations. Arkady, Warsaw*.

Kaneko, T (1975). "On Timoshenko's correction for shear in vibrating beams." In: *Journal of Physics D: Applied Physics* 8.16, p. 1927.

Kant, T and A Gupta (1988). "A finite element model for a higher-order shear-deformable beam theory." In: *Journal of sound and vibration* 125.2, pp. 193–202.

Kant, Tarun, DRJ Owen, and OC Zienkiewicz (1982). "A refined higher-order C plate bending element." In: *Computers & structures* 15.2, pp. 177–183.

Kappos, AJ, KC Stylianidis, and Kyriazis Pitilakis (1998). "Development of seismic risk scenarios based on a hybrid method of vulnerability assessment." In: *Natural Hazards* 17.2, pp. 177–192.

Karama, M, KS Afaq, and S Mistou (2003). "Mechanical behaviour of laminated composite beam by the new multi-layered laminated composite structures model with transverse shear stress continuity." In: *International Journal of solids and structures* 40.6, pp. 1525–1546.

Kato, Daisuke and Tetsuo Nagahashi (2011). "Failure Mode of Columns of Existing R/C Building Damaged During the 2007 Niigata Chuetsu-Oki Earthquake." In: *Procedia Engineering* 14, pp. 204–211.

Katsanos, Evangelos I, Anastasios G Sextos, and George D Manolis (2010). "Selection of earthquake ground motion records: A state-of-the-art review from a structural engineering perspective." In: *Soil Dynamics and Earthquake Engineering* 30.4, pp. 157–169.

Katsikadelis, John T (2013). “A new direct time integration scheme for the nonlinear equations of motion in structural dynamics.” In: *Proceedings of the 10th HSTAM International Congress on Mechanics*, pp. 1–14.

Kim, Jung J. (Dec. 2018). “Development of Empirical Fragility Curves in Earthquake Engineering considering Nonspecific Damage Information.” In: *Advances in Civil Engineering*, pp. 1–13.

Kircher, Charles A, Robert V Whitman, and William T Holmes (2006). “HAZUS earthquake loss estimation methods.” In: *Natural Hazards Review* 7.2, pp. 45–59.

Kolay, Chinmoy and James M Ricles (2014). “Development of a family of unconditionally stable explicit direct integration algorithms with controllable numerical energy dissipation.” In: *Earthquake engineering & structural dynamics* 43.9, pp. 1361–1380.

Kunnath, SK, RE Valles-Mattox, and AM Reinhorn (1996). “Evaluation of seismic damageability of a typical r/c building in midwest united states.” In: *11th World Conference on Earthquake Engineering*.

Kwon, Sun-Beom, Klaus-Jürgen Bathe, and Gunwoo Noh (2020). “An analysis of implicit time integration schemes for wave propagations.” In: *Computers & Structures* 230, p. 106188.

Kwon, Sun-Beom and Jae-Myung Lee (2018). “Development of Non-Dissipative Direct Time Integration Method for Structural Dynamics Application.” In: *Computer Modeling in Engineering & Sciences* 118.1, pp. 41–89.

Lanzano, Giovanni, Sara Sgobba, Lucia Luzi, Rodolfo Puglia, Francesca Pacor, Chiara Felicetta, Maria D’Amico, Fabrice Cotton, and Dino Bindi (2019). “The pan-European Engineering Strong Motion (ESM) flatfile: compilation criteria and data statistics.” In: *Bulletin of Earthquake Engineering* 17.2, pp. 561–582.

LECA (Jan. 2014). *Consolidamento e rinforzo dei solai*.

Levinson, MARK (1981). “A new rectangular beam theory.” In: *Journal of Sound and vibration* 74.1, pp. 81–87.

Levy, Maurice (1877). “Mémoire sur la théorie des plaques élastiques planes.” In: *Journal de mathématiques pures et appliquées*, pp. 219–306.

Lima, Carmine, Gaetano De Stefano, and Enzo Martinelli (2014). “Seismic response of masonry infilled RC frames: practice-oriented models and open issues.” In: *Earthquakes and Structures* 6.4, pp. 409–436.

Liu, Pengfei, Qinyan Xing, Dawei Wang, and Markus Oeser (2017). “Application of dynamic analysis in semi-analytical finite element method.” In: *Materials* 10.9, p. 1010.

INGV - Istituto Nazionale di Geofisica e Vulcanologia. *Engineering Strong Motion Database (ESM) (Version 2.0)*. https://doi.org/10.13127/ESM.2. URL: https://esm-db.eu/.

Magritte, René and Harry Torczyner (1977). *Magritte, ideas and images*. HN Abrams.

Mainstone, Rowland J (1974). *Supplementary note on the stiffnesses and strengths of infilled frames*. Building Research Establishment, Building Research Station.

Mander, John Barrie (1983). "Seismic design of bridge piers." PhD Thesis. University of Canterbury. Civil Engineering.

Mansouri, Ali, Mohammad S. Marefat, and Mohammad Khanmohammadi (2013). "Experimental evaluation of seismic performance of low-shear strength masonry infills with openings in reinforced concrete frames with deficient seismic details." In: *The Structural design of Tall and Special Buildings* 23.15, pp. 1190–1210.

Mantari, JL, AS Oktem, and C Guedes Soares (2012). "A new trigonometric shear deformation theory for isotropic, laminated composite and sandwich plates." In: *International Journal of Solids and Structures* 49.1, pp. 43–53.

Masi, Angelo (2003). "Seismic vulnerability assessment of gravity load designed R/C frames." In: *Bulletin of Earthquake Engineering* 1.3, pp. 371–395.

– (2005). "La stima della resistenza del calcestruzzo in situ mediante prove distruttive e non distruttive." In: *Il Giornale delle Prove non Distruttive Monitoraggio Diagnostica* 1, p. 2005.

Masi, Angelo, Andrea Digrisolo, and Giuseppe Santarsiero (2019). "Analysis of a large database of concrete core tests with emphasis on within-structure variability." In: *Materials* 12.12, p. 1985.

Medvedev, SV and W Sponheuer (1969). "Scale of seismic intensity." In: *Proc. IV World Conference of the Earthquake Engineering, Santiago, Chile, A-2*, pp. 143–153.

Meletti, C. and V. Montaldo (July 2007). *Stime di pericolositá sismica per diverse probabilità di superamento in 50 anni: valori di* a_g. Progetto DPC-INGV S1, Deliverable D2. INGV - Istituto Nazionale di Geofisica e Vulcanologia. URL: http://esse1.mi.ingv.it/data/D2.pdf.

Michels, Dominik L and Mathieu Desbrun (2015). "A semi-analytical approach to molecular dynamics." In: *Journal of Computational Physics* 303, pp. 336–354.

Monaco, Paola, Gianfranco Totani, Giovanni Barla, Antonio Cavallaro, Antonio Costanzo, et al. (Oct. 2009). "Geotechnical Aspects of the L'Aquila Earthquake." In: *XVIIth Conference on Soil Mechanics & Geotechnical Engineering*.

Mondal, Goutam and Sudhir K Jain (2008). “Lateral stiffness of masonry infilled reinforced concrete (RC) frames with central opening.” In: *Earthquake spectra* 24.3, pp. 701–723.

Mpampatsikos, V., Roberto Nascimbene, and Lorenza Petrini (2008). “A Critical Review of the R.C. Frame Existing Building Assessment Procedure According to Eurocode 8 and Italian Seismic Code.” In: *Journal of Earthquake Engineering* 12.sup1, pp. 52–82. DOI: 10.1080/13632460801925020.

Murty, AV Krishna (1984). “Toward a consistent beam theory.” In: *AIAA journal* 22.6, pp. 811–816.

Murty, CVR and Sudhir K Jain (2000). “Beneficial influence of masonry infill walls on seismic performance of RC frame buildings.” In: *12th world conference on earthquake engineering*.

FEMA 273: *NEHRP Guidelines for the seismic rehabilitation of buildings*. Applied Technology Council. US Standard.

Neves, AMA, AJM Ferreira, E Carrera, M Cinefra, CMC Roque, RMN Jorge, and CM Mota Soares (2013). “Static, free vibration and buckling analysis of isotropic and sandwich functionally graded plates using a quasi-3D higher-order shear deformation theory and a meshless technique.” In: *Composites Part B: Engineering* 44.1, pp. 657–674.

Newmark, Nathan M (1959). “A method of computation for structural dynamics.” In: *Journal of the engineering mechanics division* 85.3, pp. 67–94.

Newmark, Nathan Mortimore (1952). *Computation of dynamic structural response in the range approaching failure*. Department of Civil Engineering, University of Illinois.

Noh, Gunwoo and Klaus-Jürgen Bathe (2018). “Further insights into an implicit time integration scheme for structural dynamics.” In: *Computers & Structures* 202, pp. 15–24.

– (2019). “The Bathe time integration method with controllable spectral radius: The ρ_∞-Bathe method.” In: *Computers & Structures* 212, pp. 299–310.

Olivito, Renato S, Saverio Porzio, Carmelo Scuro, Domenico L Carnì, and Francesco Lamonaca (2019). “SHM systems applied to the built heritage inventory at the territorial scale. A preliminary study based on CARTIS approach.” In: *2019 IMEKO TC4 International Conference on Metrology for Archaeology and Cultural Heritage, MetroArchaeo 2019*. IMEKO-International Measurement Federation Secretariat, pp. 53–58.

On a Union Civil Protection Mechanism (Dec. 2013). Decision. European Parliament and the Council of the European Union.

Ordaz, Mario, Eduardo Miranda, Eduardo Reinoso, and Luis E Pérez-Rocha (1998). "Seismic loss estimation model for Mexico City." In: *Universidad Nacional Autónoma de México, México DF*.

Orsini, Giampiero (1999). "A model for buildings' vulnerability assessment using the parameterless scale of seismic intensity (PSI)." In: *Earthquake Spectra* 15.3, pp. 463–483.

Otani, Shunsuke (1974). *SAKE: A computer program for inelastic response of R/C frames to earthquakes*. Tech. rep. University of Illinois Engineering Experiment Station. College of …

Ozcebe, Guney, Haluk Sucuoglu, M Semih Yucemen, Ahmet Yakut, and Joseph Kubin (2006). "Seismic risk assessment of existing building stock in istanbul a pilot application in zeytinburnu district." In: *Proceedings of 8th US national conference on earthquake engineering, San Fransisco*. Citeseer.

Ozdemir, P, MH Boduroglu, and A Ilki (2005). "Seismic safety screening method." In: *International Workshop*, p. 19.

Panagiotakos, TB and MN Fardis (1996). "Seismic response of infilled RC frames structures." In: *11th world conference on earthquake engineering*. 225.

Panc, V (1975). *Theories of elastic plates (Vol. 2)*.

Park, Young-Ji, AH-S Ang, and Yi-Kwei Wen (1984). *Seismic damage analysis and damage-limiting design of RC buildings*. Tech. rep. University of Illinois Engineering Experiment Station. College of …

Perrone, Daniele, Marianovella Leone, and Maria Antonietta Aiello (2016). "Evaluation of the infill influence on the elastic period of existing RC frames." In: vol. 123. Elsevier, pp. 419–433.

Pesaresi, Martino, Daniele Ehrlich, Thomas Kemper, Alice Siragusa, Aneta J. Florczyk, Sergio Freire, and Christina Corbane (2017). *Atlas of Human Planet - Global Exposure to Natural Hazards*. Science for Policy Report EUR 28556 EN. JRC (Joint Research Center).

Pinho, R, JJ Bommer, and S Glaister (2002). "A simplified approach to displacement-based earthquake loss estimation analysis." In: *Proceedings of the 12th European conference on earthquake engineering*, pp. 9–13.

Pischiutta, Marta, Giovanna Cultrera, Arrigo Caserta, and Lucia Luzi (2010). "Topographic effects on the hill of Nocera Umbra, central Italy." In: *Geophysical Journal International* 182, pp. 977–987.

Polese, Maria, Marco Gaetani d'Aragona, and Andrea Prota (2019). "Simplified approach for building inventory and seismic damage assessment at the territorial scale: An application for

a town in southern Italy." In: *Soil dynamics and earthquake engineering* 121, pp. 405–420.

Polese, Maria, Marco Di Ludovico, Marco Gaetani d'Aragona, Andrea Prota, and Gaetano Manfredi (2020). "Regional vulnerability and risk assessment accounting for local building typologies." In: *International journal of disaster risk reduction* 43, p. 101400.

Polyakov, SV (1956). "Masonry in framed buildings: An investigation into the strength and stiffness of masonry infilling, Translation into English by GL Cairns." In: *Gosdarstvenoeizdatel'stvoliteraturypostroitel'stvuiarkhitekture: Moscow*.

FEMA 356: *Prestandard and commentary for the seismic rehabilitation of buildings*. ASCE American Society of Civil Engineers. US Standard.

Protti, Edmondo (1934). *Solai, soffitti, coperti nella moderna edilizia*. Tecniche Utilitarie.

FEMA P-154: *Rapid Visual Screening of Buildings for Potential Seismic Hazard: a Handbook*. ATC Applied Technology Council. US Standard.

RDB (1956). *Manualetto ERREDIBI*.

– (1958). *Manualetto ERREDIBI*.

– (1968). *Manualetto ERREDIBI*.

Reddy, Junuthula N (1984). "A simple higher-order theory for laminated composite plates." In: *Journal of Applied Mechanics* 51.4, pp. 745–752.

Reissner, E (1975). "On tranverse bending of plates, including the effect of transverse shear deformation." In: *International Journal of Solids and Structures* 11.5, pp. 569–573.

Ricci, Paolo, Mariano Di Domenico, and Gerardo M Verderame (2018). "Experimental investigation of the influence of slenderness ratio and of the in-plane/out-of-plane interaction on the out-of-plane strength of URM infill walls." In: *Construction and Building Materials* 191, pp. 507–522.

Rodrigues, Hugo, Humberto Varum, and Aníbal Costa (2010). "Simplified macro-model for infill masonry panels." In: *Journal of Earthquake Engineering* 14.3, pp. 390–416.

Rossetto, Tiziana and Amr Elnashai (2005). "A new analytical procedure for the derivation of displacement-based vulnerability curves for populations of RC structures." In: *Engineering structures* 27.3, pp. 397–409.

Rossi, Guido (1982). "Resistenza a compressione delle murature in laterizio . proposta di una formula su basi sperimentali valida anche per elementi a "foratura non uniforme" e/o giunti di malta interrotti." In: *6th International Brick and Block Masonry Conference*.

Rota, M, A Penna, C Strobbia, and G Magenes (Oct. 2008). “Direct derivation of fragility curves from Italian post-earthquake survey data.” In: *Proceedings of the 14th world conference on earthquake engineering, Beijing, China, October*, pp. 12–17.

Ruggieri, Sergio, Francesco Porco, Giuseppina Uva, and Dimitrios Vamvatsikos (2020). “Two frugal options to assess class fragility and seismic safety for low-rise reinforced concrete school buildings in Southern Italy.” In: *Bulletin of Earthquake Engineering*. Manuscript submitted for publication.

Sabetta, Fabio, Agostino Goretti, and Antonio Lucantoni (Jan. 1998). “Empirical fragility curves from damage surveys and estimated strong ground motion.” In: *Eleventh European Conference on Earthquake Engineering*.

Sayyad, Atteshamuddin S and Yuwaraj M Ghugal (2017a). “A unified shear deformation theory for the bending of isotropic, functionally graded, laminated and sandwich beams and plates.” In: *International Journal of Applied Mechanics* 9.01, p. 1750007.

Sayyad, Atteshamuddin Shamshuddin (2011). “Comparison of various refined beam theories for the bending and free vibration analysis of thick beams.” In: *Applied and Computational Mechanics* 5, pp. 217–230.

Sayyad, Atteshamuddin Shamshuddin and Yuwaraj M Ghugal (2017b). “Single variable refined beam theories for the bending, buckling and free vibration of homogenous beams.” In: *Applied and Computational Mechanics* 10.2.

Scawthorn, C, H Iemura, and Y Yamada (1981). “Seismic damage estimation for low-and mid-rise buildings in japan.” In: *Earthquake Engineering & Structural Dynamics* 9.2, pp. 93–115.

Sgobba, Sara, Rodolfo Puglia, Francesca Pacor, Lucia Luzi, Emiliano Russo, Chiara Felicetta, Giovanni Lanzano, Maria D’Amico, Roberto Baraschino, Georgios Baltzopoulos, et al. (2019). “REXELweb: A tool for selection of ground-motion records from the Engineering Strong Motion database (ESM).” In: *7th International Conference on Earthquake Geotechnical Engineering (ICEGE)*.

Shi, G, KY Lam, and TE Tay (1998). “On efficient finite element modeling of composite beams and plates using higher-order theories and an accurate composite beam element.” In: *Composite Structures* 41.2, pp. 159–165.

Shimpi, Rameshchandra P and Yuwaraj M Ghugal (2001). “A new layerwise trigonometric shear deformation theory for two-layered cross-ply beams.” In: *Composites Science and Technology* 61.9, pp. 1271–1283.

Shome, Nilesh, C Allin Cornell, Paolo Bazzurro, and J Eduardo Carballo (1998). “Earthquakes, records, and nonlinear responses.” In: *Earthquake Spectra* 14.3, pp. 469–500.

Singhal, Ajay and Anne S Kiremidjian (1996). “Method for probabilistic evaluation of seismic structural damage.” In: *Journal of Structural Engineering* 122.12, pp. 1459–1467.

– (1998). “Bayesian updating of fragilities with application to RC frames.” In: *Journal of structural Engineering* 124.8, pp. 922–929.

Regione Puglia. *SIT Puglia*. URL: http://www.sit.puglia.it.

Smith, B Stafford (1962). “Lateral stiffness of infilled frames.” In: *Journal of the Structural Division* 88.6, pp. 183–226.

Soldatos, KP (1992). “A transverse shear deformation theory for homogeneous monoclinic plates.” In: *Acta Mechanica* 94.3-4, pp. 195–220.

Spence, RJS, AW Coburn, S Sakai, and A Pomonis (1991). “A parameterless scale of seismic intensity for use in seismic risk analysis and vulnerability assessment.” In: *Earthquake, Blast and Impact*, p. 19.

Stephen, Neil Gordon (1980). “Timoshenko’s shear coefficient from a beam subjected to gravity loading.” In: *Journal of Applied Mechanics* 47.

Takeda, Toshikazu, Mete Avni Sozen, and N Norby Nielsen (1970). “Reinforced concrete response to simulated earthquakes.” In: *Journal of the Structural Division* 96.12, pp. 2557–2573.

Tasnimi, A.A. and A. Mohebkhah (2011). “Investigation on the behavior of brick-infilled steel frames with openings, experimental and analytical approaches.” In: *Engineering Structures* 33, pp. 968–980.

Thai, Chien H, Loc V Tran, Dung T Tran, T Nguyen-Thoi, and H Nguyen-Xuan (2012). “Analysis of laminated composite plates using higher-order shear deformation plate theory and node-based smoothed discrete shear gap method.” In: *Applied Mathematical Modelling* 36.11, pp. 5657–5677.

Thywissen, Katharina (2006). *Components of Risk - A comparative glossary*. Technical Report 2/2006. UNU Institute for Environment and Human Security (UNU-EHS).

Timoshenko, SP (1921). “On the correction factor for shear of the differential equation for transverse vibrations of bars of uniform cross-section.” In: *Philosophical Magazine*, p. 744.

Touratier, M (1991). “An efficient standard plate theory.” In: *International journal of engineering science* 29.8, pp. 901–916.

Uva, G, F Porco, and A Fiore (2012). “Appraisal of masonry infill walls effect in the seismic response of RC framed buildings: A case study.” In: *Engineering Structures* 34, pp. 514–526.

Uva, Giuseppina, Valeria Leggieri, and Mirco Morrone (2019). “Use of data derived by different sources for the seismic vulnerability assessment of current building stock in GIS environment: an application to the municipality of Bisceglie, Italy.” In: *3rd International Conference on International Conference on Recent Advances in Nonlinear Design, Resilience and Rehabilitation of Structures, CoRASS 2019*.

Vaiana, Nicolò, Salvatore Sessa, Francesco Marmo, and Luciano Rosati (2019). “Nonlinear dynamic analysis of hysteretic mechanical systems by combining a novel rate-independent model and an explicit time integration method.” In: *Nonlinear Dynamics* 98.4, pp. 2879–2901.

Vamvatsikos, Dimitrios and C Allin Cornell (2002). “Incremental dynamic analysis.” In: *Earthquake engineering & structural dynamics* 31.3, pp. 491–514.

Vasil’Ev, VV and SA Lur’e (1992). “On refined theories of beams, plates, and shells.” In: *Journal of composite materials* 26.4, pp. 546–557.

Veneziano, D, JM Sussman, U Gupta, and SM Kunnumkal (2002). “Earthquake loss under limited transportation capacity: Assessment, sensitivity and remediation.” In: *Proceedings of the Seventh US National Conference on Earthquake Engineering, Boston, USA (on CD)*.

Verderame, Gerardo M, Paolo Ricci, Carlo Del Gaudio, and Gaetano Manfredi (2013). “A simplified method for seismic vulnerability assessment of infilled RC buildings: Methodology.” In: *Atti del XV congresso nazionale ANIDIS ‘‘L’ingegneria Sismica in Italia”, Padova, Italy, June*.

Verderame, Gerardo Mario, Paolo Ricci, Marilena Esposito, and Filippo Carlo Sansiviero (2011). “Le Caratteristiche Meccaniche degli Acciai Impiegati nelle Strutture in ca realizzate dal 1950 al 1980.” In: *XXVI Convegno Nazionale AICAP*.

Vlasov, Vasilii Zakharovich (1966). “Beams, plates and shells on elastic foundation.” In: *Israel Program for Scientific Translation*.

Wen, Wei-Bin, Kai-Lin Jian, and Shao-Ming Luo (2014). “An explicit time integration method for structural dynamics using septuple B-spline functions.” In: *International Journal for Numerical Methods in Engineering* 97.9, pp. 629–657.

Whitman, Robert V (Oct. 1973). “Damage probability matrices for prototype buildings.” In: *Structures Publication* 380.

Wilson, Edward L (1965). “Structural analysis of axisymmetric solids.” In: *Aiaa Journal* 3.12, pp. 2269–2274.

Wilson, EL, I Farhoomand, and KJ Bathe (1972). “Nonlinear dynamic analysis of complex structures.” In: *Earthquake Engineering & Structural Dynamics* 1.3, pp. 241–252.

Wong, Christopher (2019). *Newmark-beta Method for Nonlinear Single DOF Systems*. MATLAB Central File - url: https://mathworks.com/ matlabcentral/ fileexchange/ 71007-newmark-beta-method-for-nonlinear-single-dof-systems.

Wood, WL, M Bossak, and OC Zienkiewicz (1980). “An alpha modification of Newmark’s method.” In: *International Journal for numerical methods in Engineering* 15.10, pp. 1562–1566.

Yakut, Ahmet (2004). “Preliminary seismic performance assessment procedure for existing RC buildings.” In: *Engineering Structures* 26.10, pp. 1447–1461.

YANG, B (2007). “A closed-form approach to modeling and dynamic analysis of beams, plates and shell.” In: *Analysis and Design of Plated Structures*. Elsevier, pp. 219–253.

Yang, B and CD Mote Jr (1991). “Frequency-domain vibration control of distributed gyroscopic systems.” In.

Yina, SH (2011). “An unconditionally stable explicit method for structural dynamics.” In: *Procedia engineering* 14, pp. 2519–2526.

Youngs, Robert, M Power, G Wang, F Makdisi, and CC Chin (2007). “Design ground motion library (DGML)–tool for selecting time history records for specific engineering applications.” In: *SMIP07 Seminar on Utilization of Strong-Motion Data*. California Geological Survey Sacramento, CA, pp. 109–110.

Zenkour, Ashraf M (2013). “Bending of FGM plates by a simplified four-unknown shear and normal deformations theory.” In: *International Journal of Applied Mechanics* 5.02, p. 1350020.

ZHAI, W-M (1996). “Two simple fast integration methods for large-scale dynamic problems in engineering.” In: *International journal for numerical methods in engineering* 39.24, pp. 4199–4214.

Zhang, Lihong, Tianyun Liu, and Qingbin Li (2015). “A robust and efficient composite time integration algorithm for nonlinear structural dynamic analysis.” In: *Mathematical Problems in Engineering* 2015.

Zuccaro, G, M Dolce, D De Gregorio, E Speranza, and C Moroni (2015). “La scheda CARTIS per la caratterizzazione tipologico-strutturale dei comparti urbani costituiti da edifici ordinari. Valutazione dell’esposizione in analisi di rischio sismico.” In: *Proceedings of the GNGTS*.

A. MUNICIPALITIES CLUSTERING FROM HOMOGENEOUS HAZARD ASSESSMENT (PUGLIA REGION)

Tab. A.1 – Homogeneous groups of municipalities (split by provinces)

Group	Municipalities
Group I	**FOGGIA:** Apricena, Cagnano Varano, Carlantino, Carpino, Casalnuovo Monterotaro, Casalvecchio di Puglia, Castelnuovo della Daunia, Celenza Valfortore, Chieuti, Ischitella, Lesina, Manfredonia, Mattinata, Monte Sant'Angelo, Peschici, Poggio Imperiale, Rignano Garganico, Rodi Garganico, San Giovanni Rotondo, San Marco in Lamis, San Nicandro Garganico, San Paolo di Civitate, San Severo, Serracapriola, Torremaggiore, Vico del Gargano, Vieste **TARANTO:** Castellaneta, Crispiano, Ginosa, Laterza, Massafra, Mottola, Palagianello, Palagiano, Statte
Group II	**FOGGIA:** Accadia, Alberona, Anzano di Puglia, Ascoli Satriano, Biccari, Bovino, Candela, Carapelle, Castelluccio Valmaggiore, Castelluccio dei Sauri, Celle di San Vito, Cerignola, Deliceto, Faeto, Foggia, Lucera, Monteleone di Puglia, Motta Montecorvino, Ordona, Orsara di Puglia, Orta Nova, Panni, Pietramontecorvino, Rocchetta Sant'Antonio, Roseto Valfortore, San Marco la Catola, Sant'Agata di Puglia, Stornara, Stornarella, Troia, Volturara Appula, Volturino, Zapponeta **BAT:** Andria, Barletta, Bisceglie, Canosa di Puglia, Margherita di Savoia, Minervino Murge, San Ferdinando di Puglia, Spinazzola, Trani, Trinitapoli **BARI:** Corato, Molfetta, Poggiorsini, Ruvo di Puglia, Terlizzi
Group III	**BARI:** Acquaviva delle Fonti, Adelfia, Alberobello, Altamura, Bari, Binetto, Bitetto, Bitonto, Bitritto, Capurso, Casamassima, Cassano delle Murge, Cellammare, Gioia del Colle, Giovinazzo, Gravina in Puglia, Grumo Appula, Locorotondo, Modugno, Noci, Palo del Colle, Putignano, Sammichele di Bari, Sannicandro di Bari, Santeramo in Colle, Toritto, Turi, Valenzano **BRINDISI:** Ceglie Messapica, Cisternino, Fasano, Francavilla Fontana, Ostuni, Villa Castelli **TARANTO:** Carosino, Faggiano, Fragagnano, Grottaglie, Leporano, Lizzano, Martina Franca, Monteiasi, Montemesola, Monteparano, Pulsano, Roccaforzata, San Giorgio Ionico, San Marzano di San Giuseppe, Taranto, Torricella **LECCE:** Alessano, Andrano, Aradeo, Bagnolo del Salento, Botrugno, Calimera, Cannole, Caprarica di Lecce, Carpignano Salentino, Casarano, Castri di Lecce, Castrignano de' Greci, Castrignano del Capo, Castro, Cavallino, Collepasso, Corigliano d'Otranto, Corsano, Cursi, Cutrofiano, Diso, Gagliano del Capo, Galatina, Giuggianello, Giurdignano, Lizzanello, Maglie, Martano, Martignano, Matino, Melendugno, Melissano, Melpignano, Miggiano, Minervino di Lecce, Montesano Salentino, Morciano di Leuca, Neviano, Nociglia, Ortelle, Otranto, Palmariggi, Parabita, Patú, Poggiardo, Presicce-Acquarica, Ruffano, Salve, San Cassiano, San Donato di Lecce, Sanarica, Santa Cesarea Terme, Scorrano, Seclí, Sogliano Cavour, Soleto, Specchia, Spongano, Sternatia, Supersano, Surano, Taurisano, Tiggiano, Tricase, Tuglie, Ugento, Uggiano la Chiesa, Vernole, Zollino
Group IV	**BARI:** Castellana Grotte, Conversano, Mola di Bari, Monopoli, Noicattaro, Polignano a Mare, Rutigliano, Triggiano **BRINDISI:** Brindisi, Carovigno, Cellino San Marco, Erchie, Latiano, Mesagne, Oria, San Donaci, San Michele Salentino, San Pancrazio Salentino, San Pietro Vernotico, San Vito dei Normanni, Torchiarolo, Torre Santa Susanna **TARANTO:** Avetrana, Manduria, Maruggio, Sava **LECCE:** Alezio, Alliste, Arnesano, Campi Salentina, Carmiano, Copertino, Galatone, Gallipoli, Guagnano, Lecce, Lequile, Leverano, Monteroni di Lecce, Nardó, Novoli, Porto Cesareo, Racale, Salice Salentino, San Cesario di Lecce, San Pietro in Lama, Sannicola, Squinzano, Surbo, Taviano, Trepuzzi, Veglie

B. FRAGILITY FUNCTIONS FOR THE BUILDING CLUSTERS IN THE BOVINO MUNICIPALITY

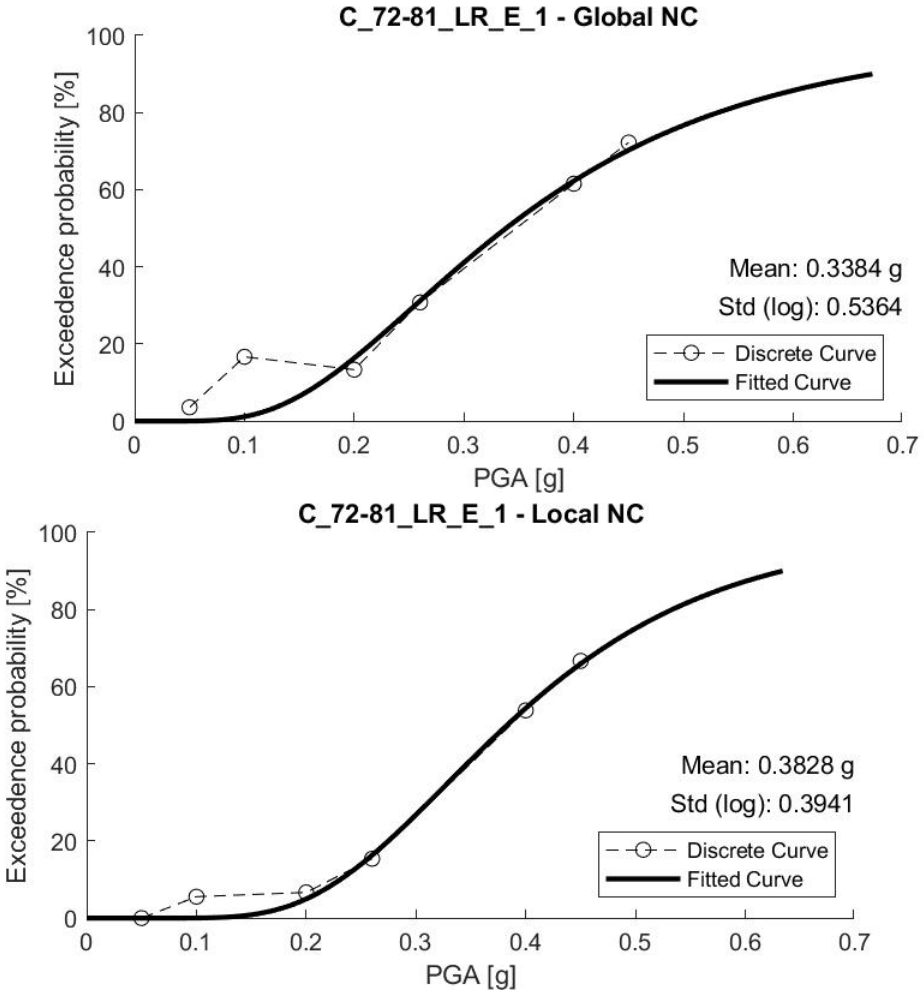

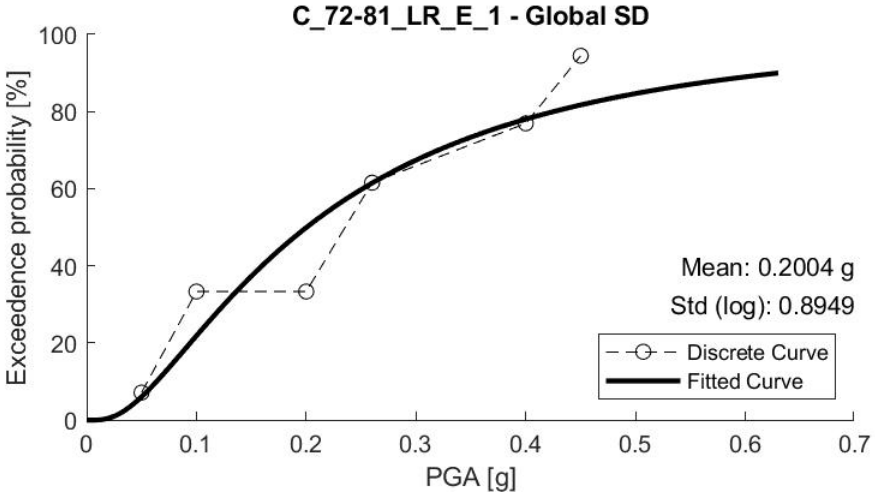
C_72-81_LR_E_1 - Global SD
Exceedence probability [%]
PGA [g]
Mean: 0.2004 g
Std (log): 0.8949
Discrete Curve
Fitted Curve

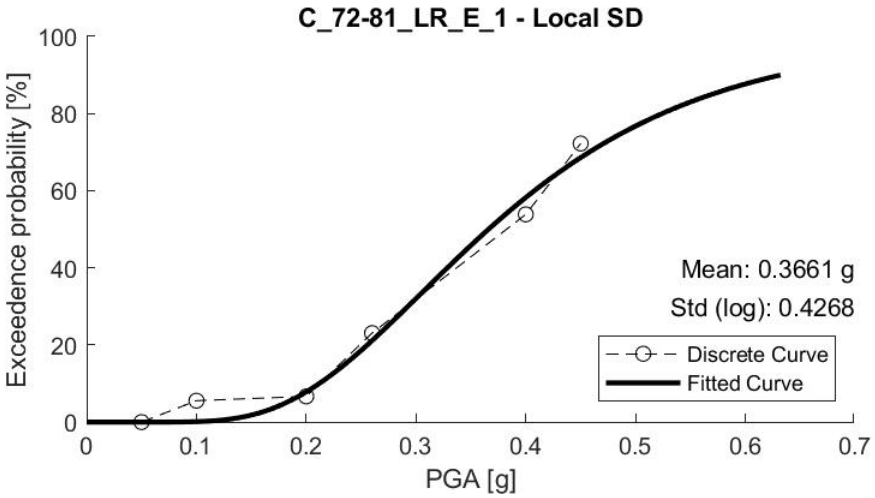
C_72-81_LR_E_1 - Local SD
Exceedence probability [%]
PGA [g]
Mean: 0.3661 g
Std (log): 0.4268
Discrete Curve
Fitted Curve

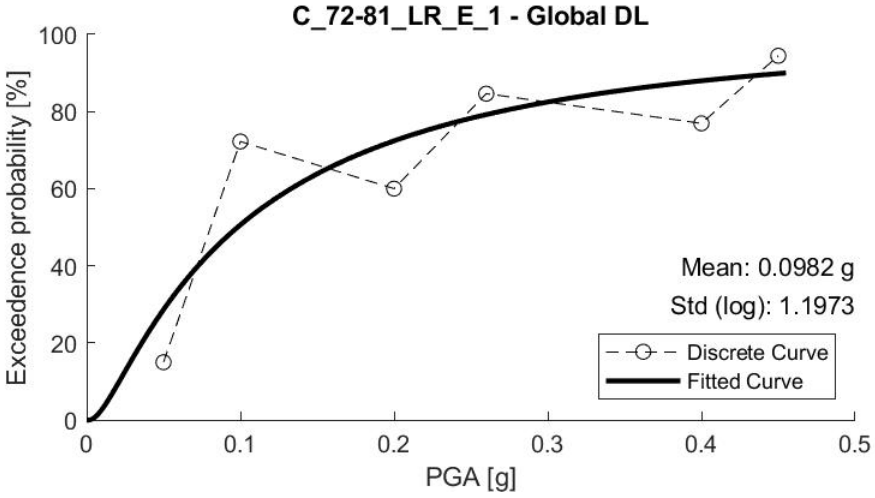
C_72-81_LR_E_1 - Global DL
Exceedence probability [%]
PGA [g]
Mean: 0.0982 g
Std (log): 1.1973
Discrete Curve
Fitted Curve

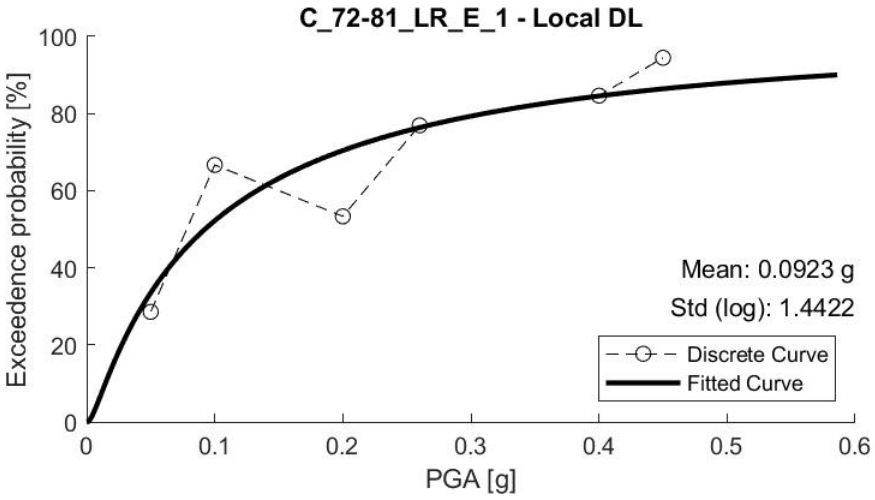
C_72-81_LR_E_1 - Local DL
Exceedence probability [%]
PGA [g]
Mean: 0.0923 g
Std (log): 1.4422
Discrete Curve
Fitted Curve

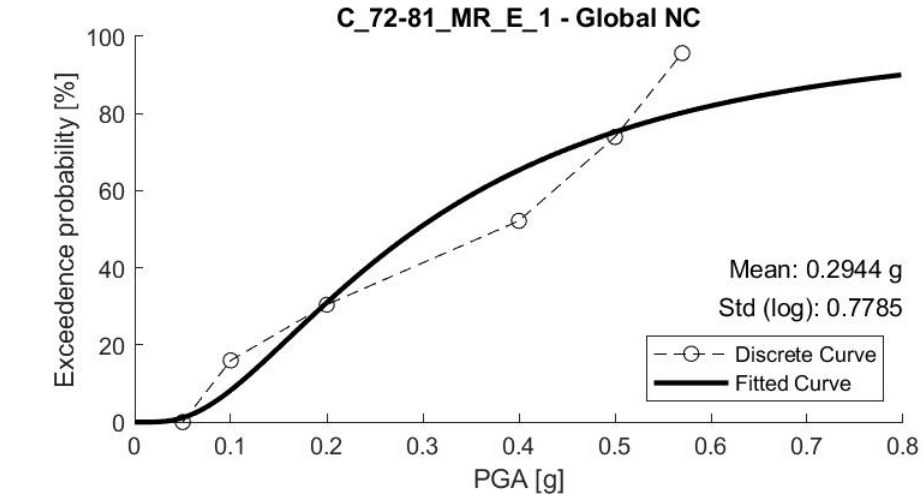
C_72-81_MR_E_1 - Global NC
Exceedence probability [%]
PGA [g]
Mean: 0.2944 g
Std (log): 0.7785
Discrete Curve
Fitted Curve

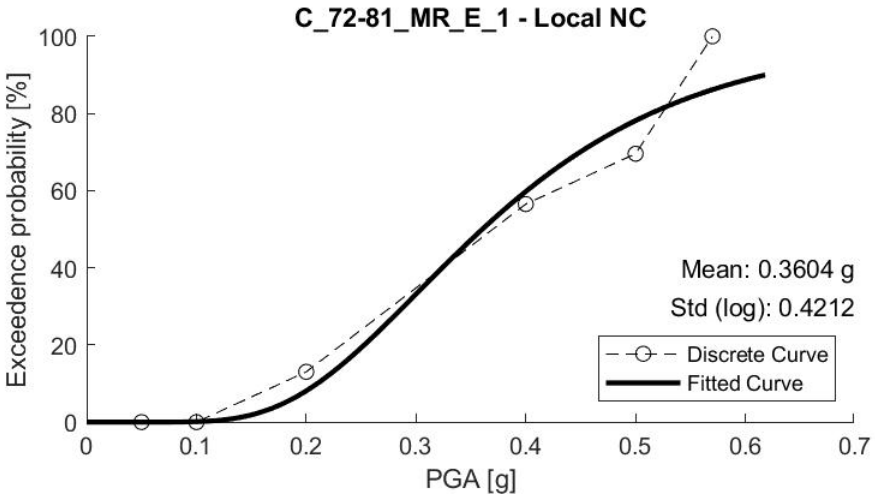
C_72-81_MR_E_1 - Local NC
Exceedence probability [%]
PGA [g]
Mean: 0.3604 g
Std (log): 0.4212
Discrete Curve
Fitted Curve

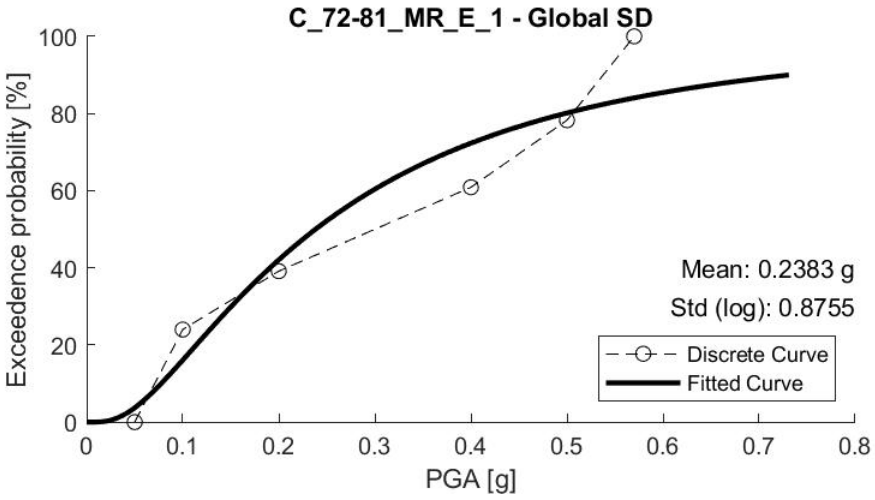
C_72-81_MR_E_1 - Global SD
Exceedence probability [%]
PGA [g]
Mean: 0.2383 g
Std (log): 0.8755
Discrete Curve
Fitted Curve

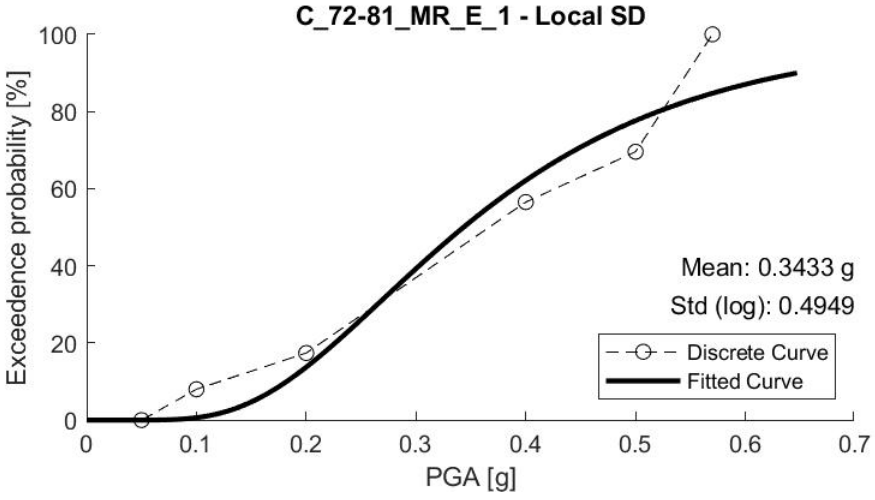
C_72-81_MR_E_1 - Local SD
Exceedence probability [%]
PGA [g]
Mean: 0.3433 g
Std (log): 0.4949
Discrete Curve
Fitted Curve

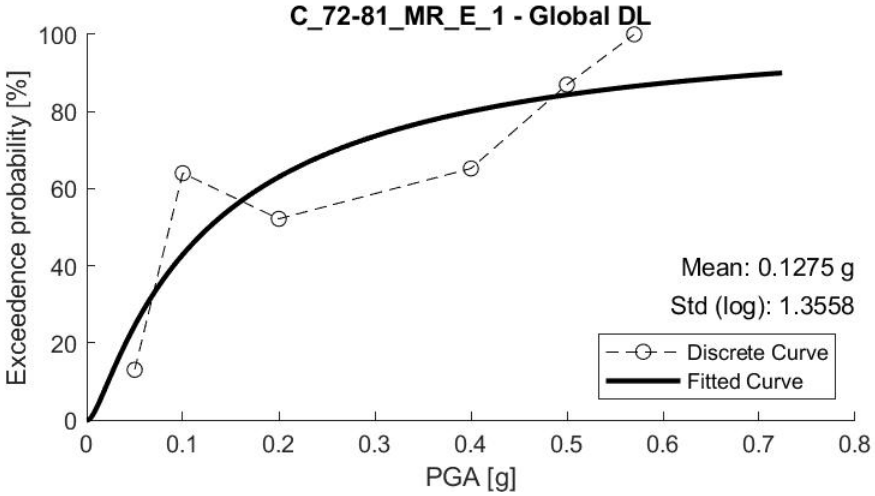
C_72-81_MR_E_1 - Global DL
Exceedence probability [%]
PGA [g]
Mean: 0.1275 g
Std (log): 1.3558
Discrete Curve
Fitted Curve

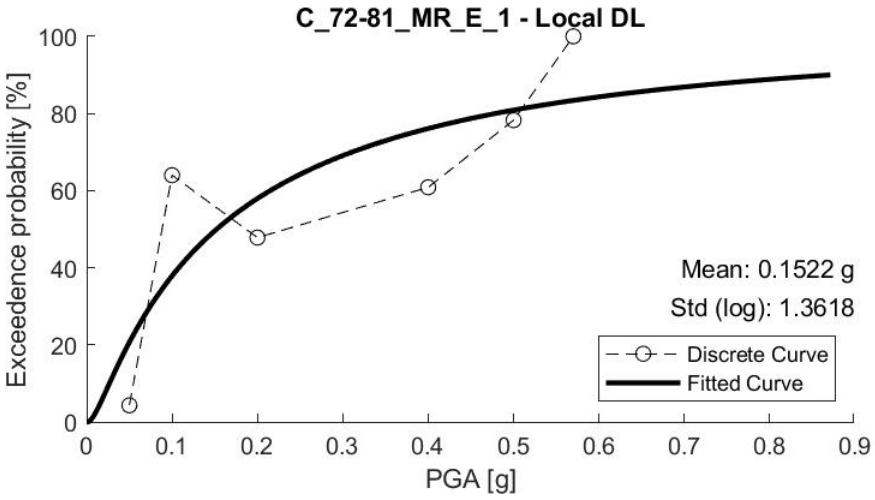
C_72-81_MR_E_1 - Local DL
Exceedence probability [%]
PGA [g]
Mean: 0.1522 g
Std (log): 1.3618
Discrete Curve
Fitted Curve

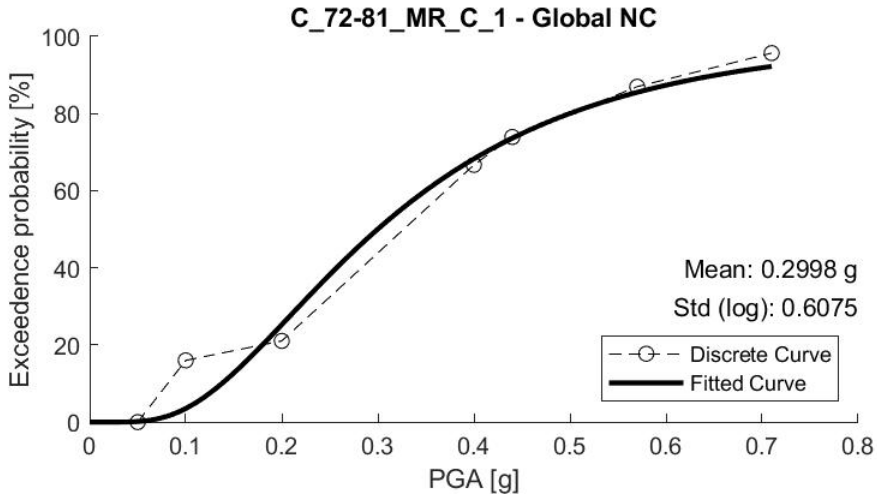
C_72-81_MR_C_1 - Global NC
Exceedence probability [%]
PGA [g]
Mean: 0.2998 g
Std (log): 0.6075
Discrete Curve
Fitted Curve

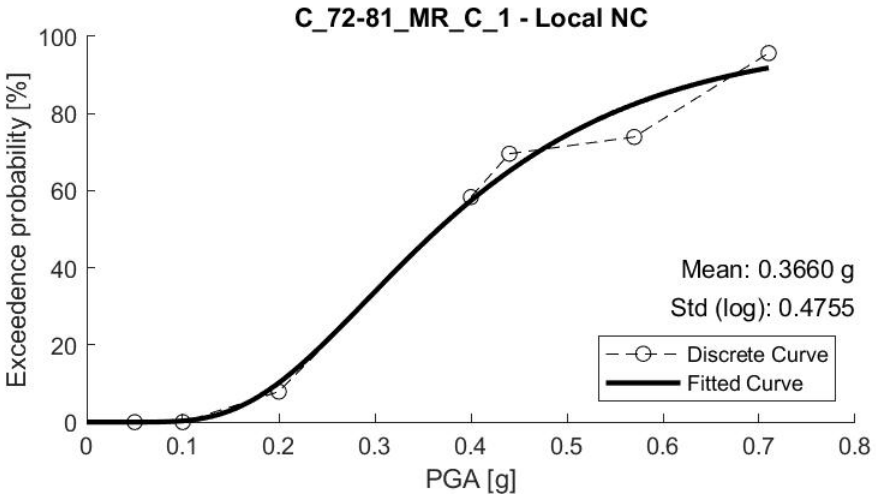
C_72-81_MR_C_1 - Local NC
Exceedence probability [%]
PGA [g]
Mean: 0.3660 g
Std (log): 0.4755
Discrete Curve
Fitted Curve

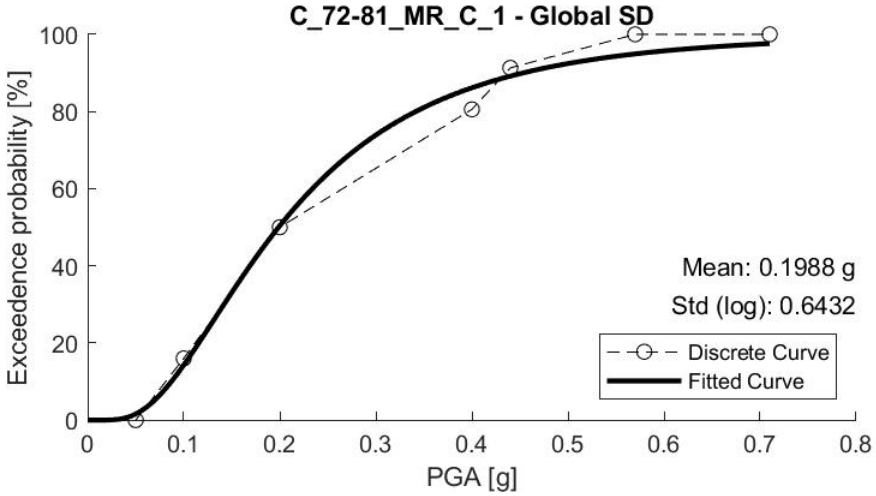
C_72-81_MR_C_1 - Global SD
Exceedence probability [%]
PGA [g]
Mean: 0.1988 g
Std (log): 0.6432
Discrete Curve
Fitted Curve

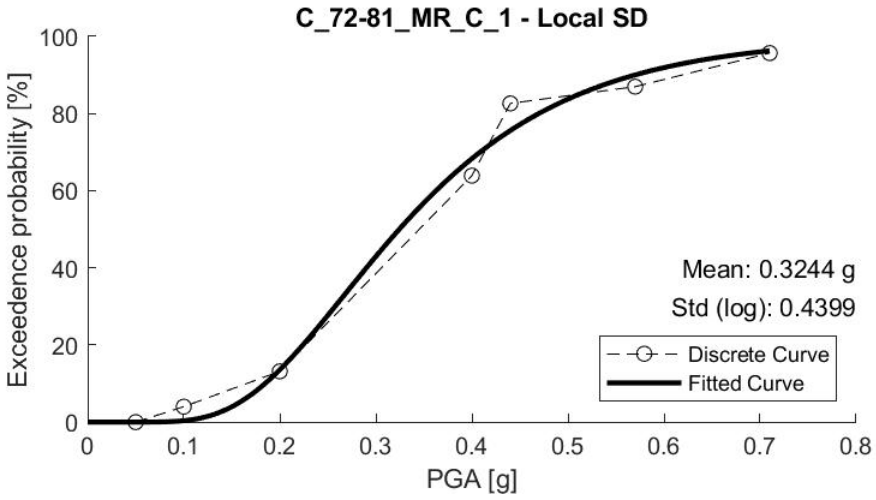
C_72-81_MR_C_1 - Local SD
Exceedence probability [%]
PGA [g]
Mean: 0.3244 g
Std (log): 0.4399
Discrete Curve
Fitted Curve

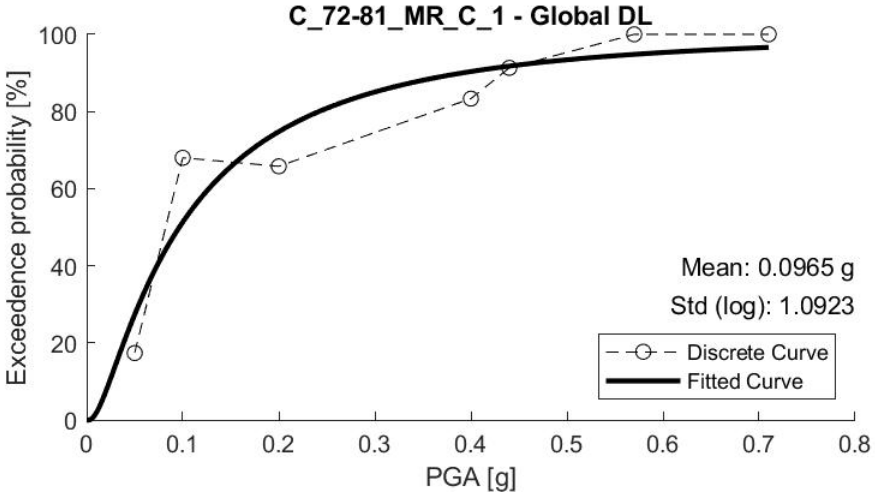
C_72-81_MR_C_1 - Global DL
Exceedence probability [%]
PGA [g]
Mean: 0.0965 g
Std (log): 1.0923
Discrete Curve
Fitted Curve

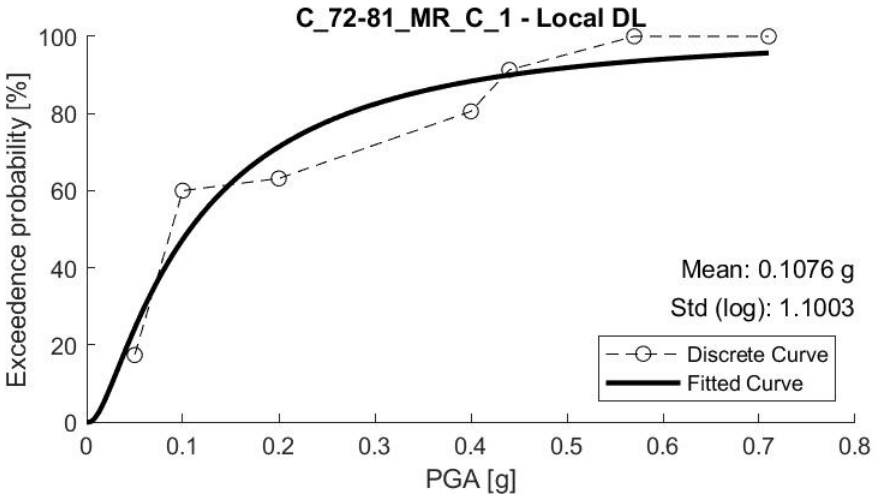
C_72-81_MR_C_1 - Local DL
Exceedence probability [%]
PGA [g]
Mean: 0.1076 g
Std (log): 1.1003
Discrete Curve
Fitted Curve

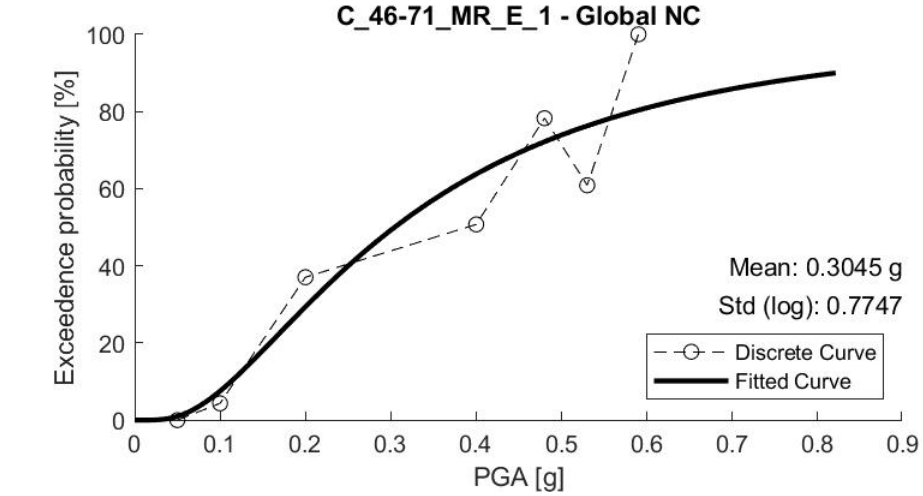
C_46-71_MR_E_1 - Global NC
Exceedence probability [%]
PGA [g]
Mean: 0.3045 g
Std (log): 0.7747
Discrete Curve
Fitted Curve

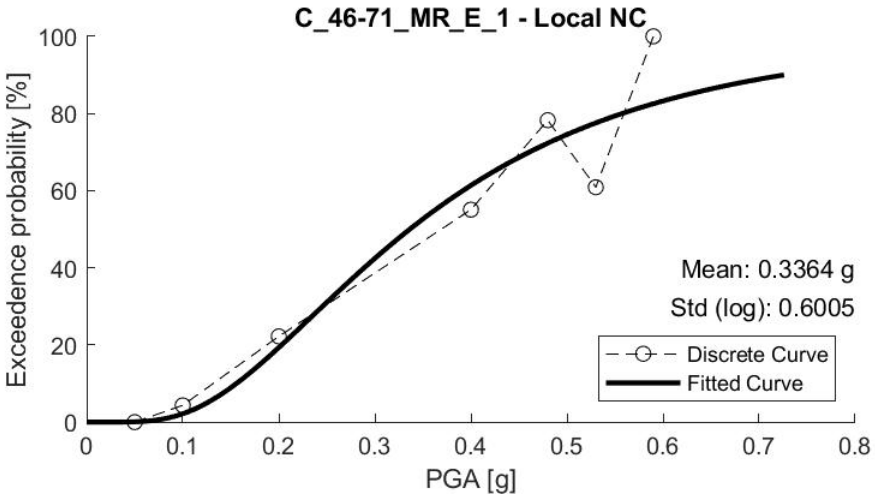
C_46-71_MR_E_1 - Local NC
Exceedence probability [%]
PGA [g]
Mean: 0.3364 g
Std (log): 0.6005
Discrete Curve
Fitted Curve

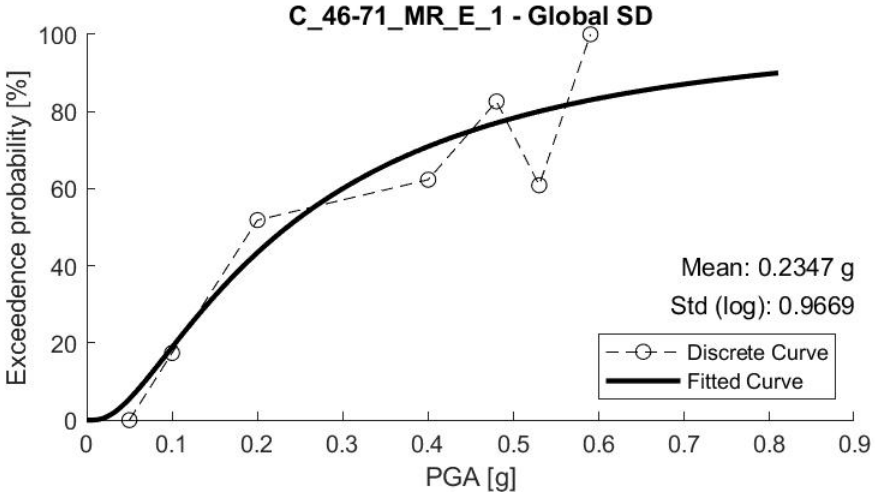
C_46-71_MR_E_1 - Global SD
Exceedence probability [%]
PGA [g]
Mean: 0.2347 g
Std (log): 0.9669
Discrete Curve
Fitted Curve

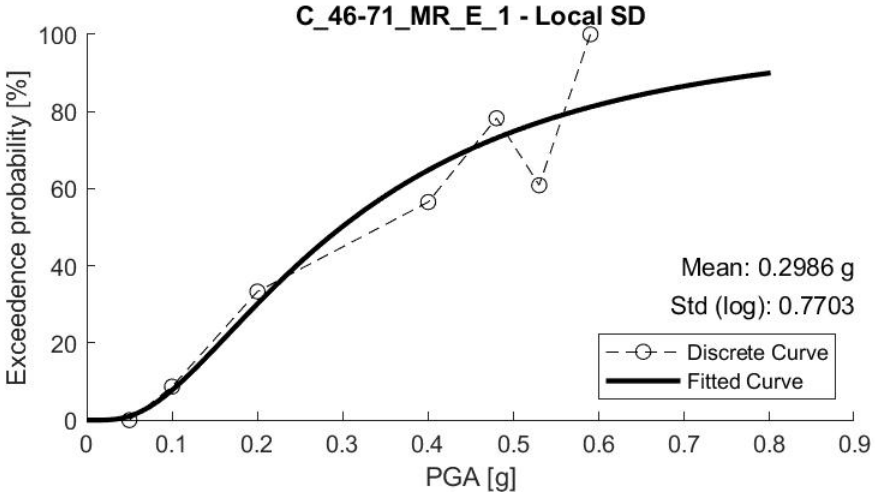
C_46-71_MR_E_1 - Local SD
Exceedence probability [%]
PGA [g]
Mean: 0.2986 g
Std (log): 0.7703
Discrete Curve
Fitted Curve

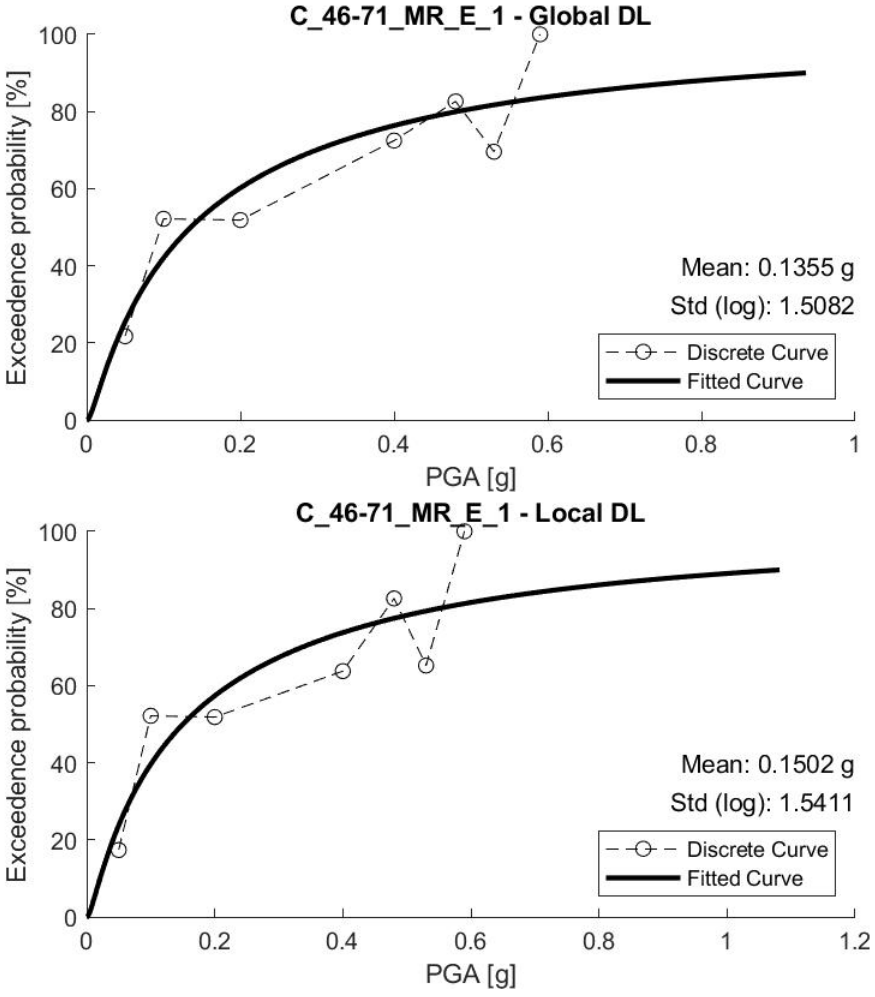
C_46-71_MR_E_1 - Global DL
Exceedence probability [%]
PGA [g]
Mean: 0.1355 g
Std (log): 1.5082
Discrete Curve
Fitted Curve
C_46-71_MR_E_1 - Local DL
Exceedence probability [%]
PGA [g]
Mean: 0.1502 g
Std (log): 1.5411
Discrete Curve
Fitted Curve

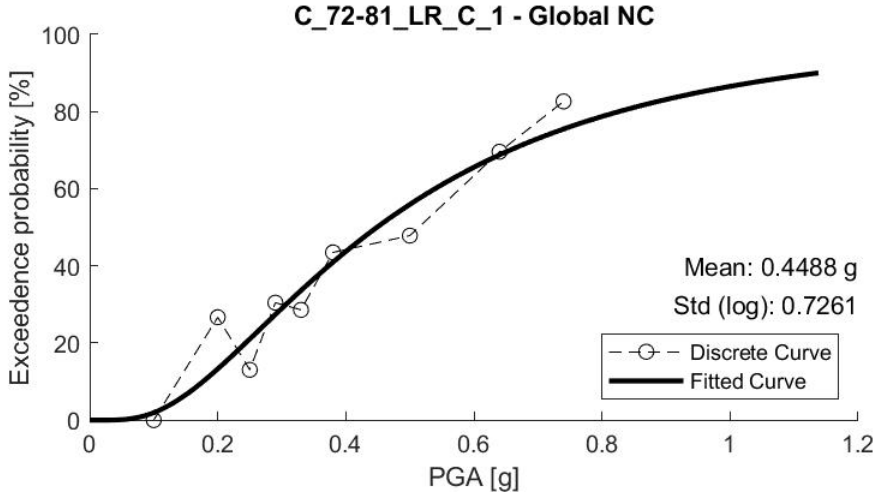
C_72-81_LR_C_1 - Global NC
Exceedence probability [%]
PGA [g]
Mean: 0.4488 g
Std (log): 0.7261
Discrete Curve
Fitted Curve

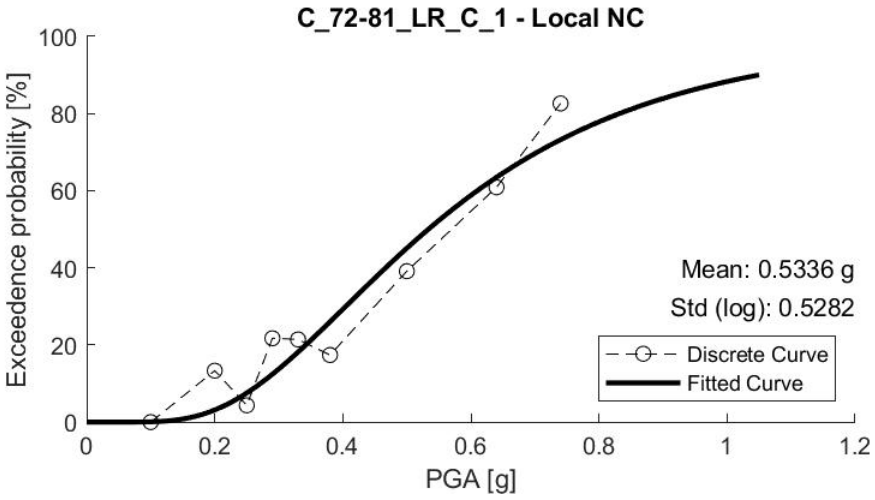
C_72-81_LR_C_1 - Local NC
Exceedence probability [%]
PGA [g]
Mean: 0.5336 g
Std (log): 0.5282
Discrete Curve
Fitted Curve

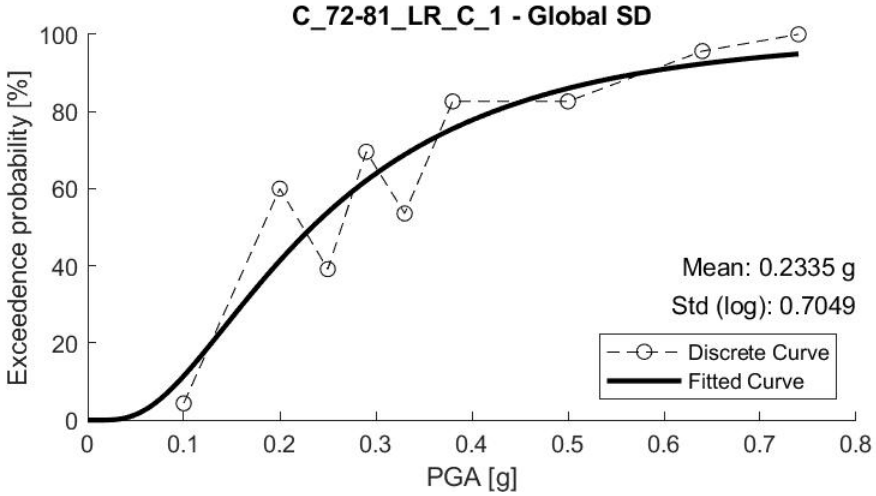
C_72-81_LR_C_1 - Global SD
Exceedence probability [%]
PGA [g]
Mean: 0.2335 g
Std (log): 0.7049
Discrete Curve
Fitted Curve

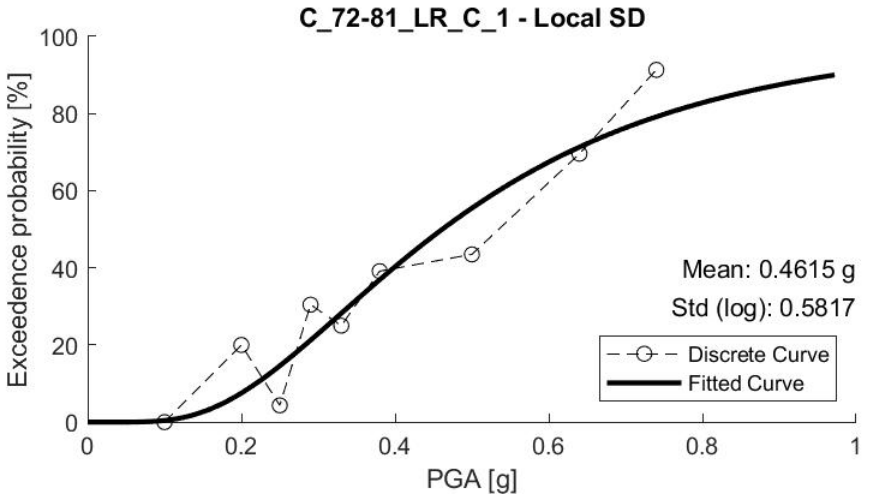
C_72-81_LR_C_1 - Local SD
Exceedence probability [%]
PGA [g]
Mean: 0.4615 g
Std (log): 0.5817
Discrete Curve
Fitted Curve

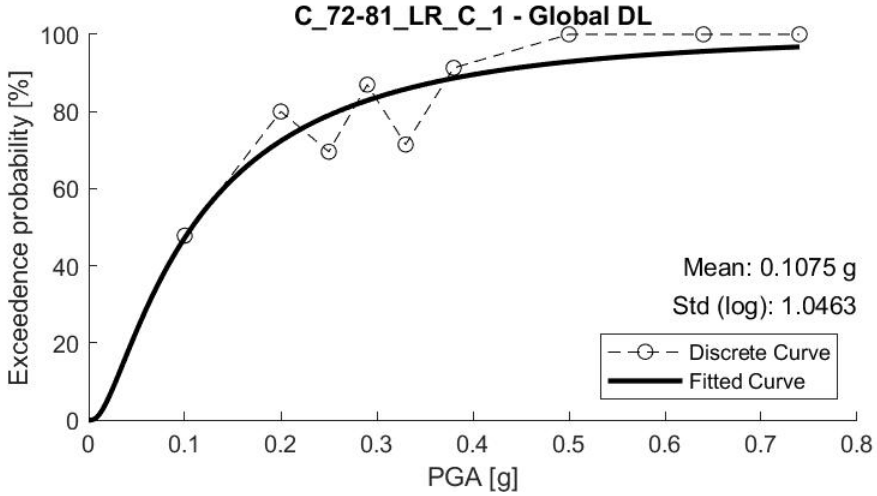
C_72-81_LR_C_1 - Global DL
Exceedence probability [%]
PGA [g]
Mean: 0.1075 g
Std (log): 1.0463
Discrete Curve
Fitted Curve

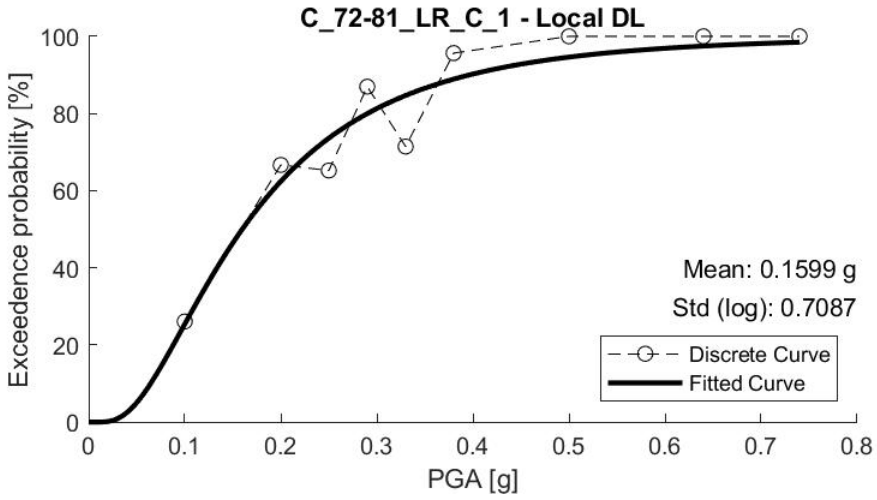
C_72-81_LR_C_1 - Local DL
Exceedence probability [%]
PGA [g]
Mean: 0.1599 g
Std (log): 0.7087
Discrete Curve
Fitted Curve

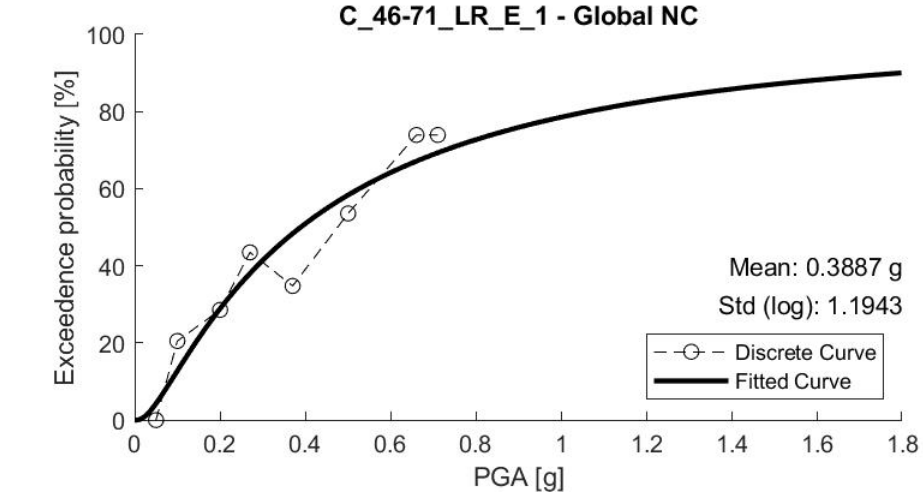
C_46-71_LR_E_1 - Global NC
Exceedence probability [%]
PGA [g]
Mean: 0.3887 g
Std (log): 1.1943
Discrete Curve
Fitted Curve

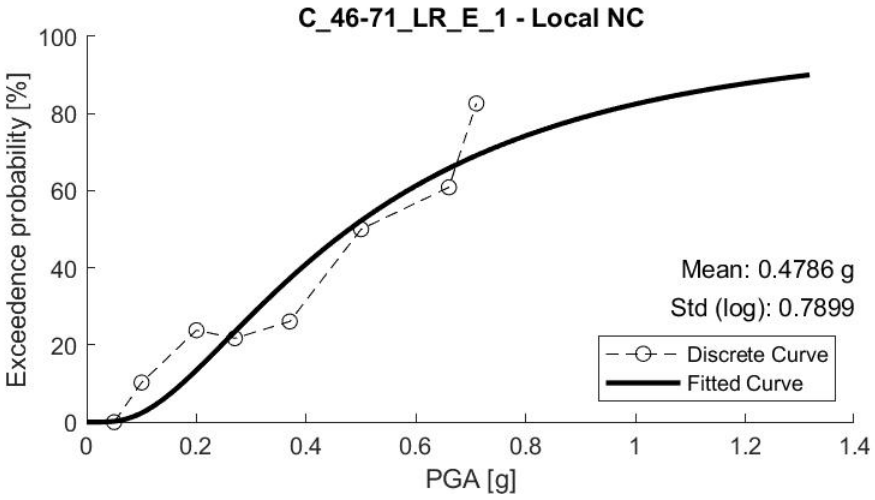
C_46-71_LR_E_1 - Local NC
Exceedence probability [%]
PGA [g]
Mean: 0.4786 g
Std (log): 0.7899
Discrete Curve
Fitted Curve

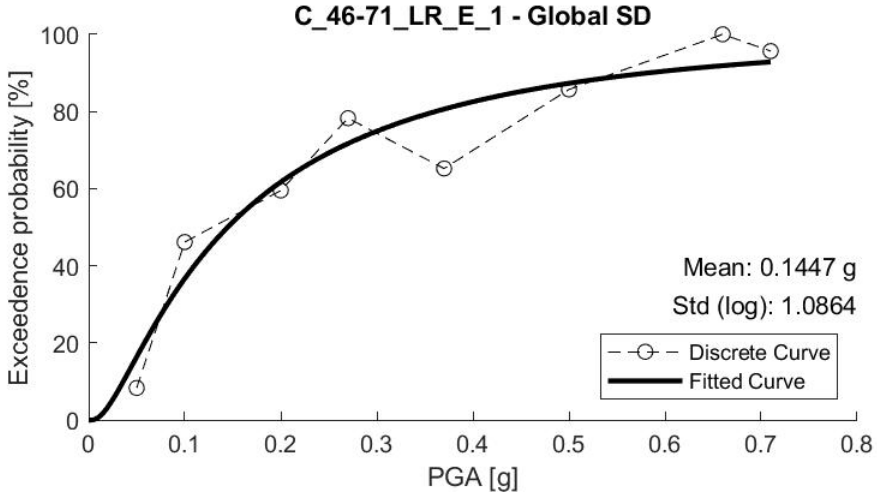
C_46-71_LR_E_1 - Global SD
Exceedence probability [%]
PGA [g]
Mean: 0.1447 g
Std (log): 1.0864
Discrete Curve
Fitted Curve

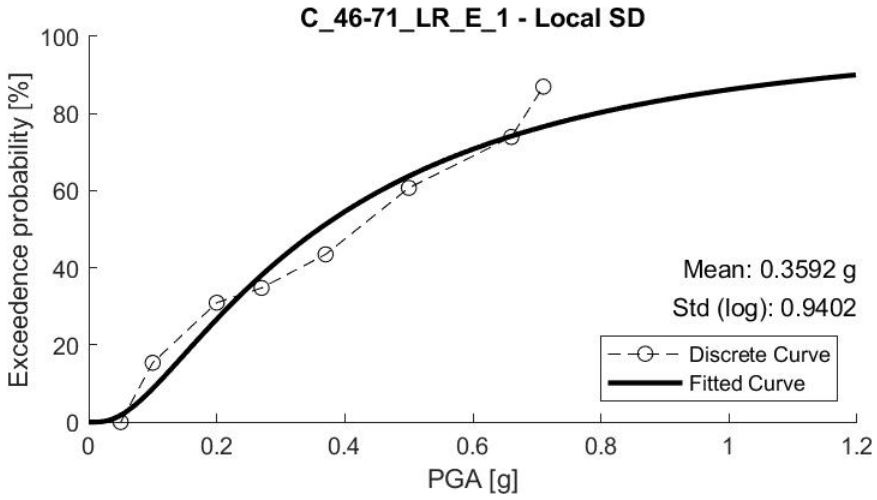
C_46-71_LR_E_1 - Local SD
Exceedence probability [%]
PGA [g]
Mean: 0.3592 g
Std (log): 0.9402
Discrete Curve
Fitted Curve

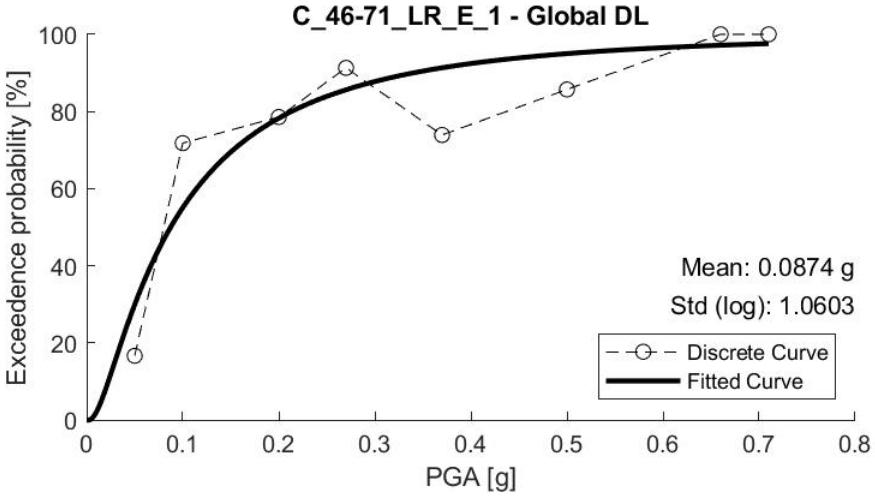
C_46-71_LR_E_1 - Global DL
Exceedence probability [%]
PGA [g]
Mean: 0.0874 g
Std (log): 1.0603
Discrete Curve
Fitted Curve

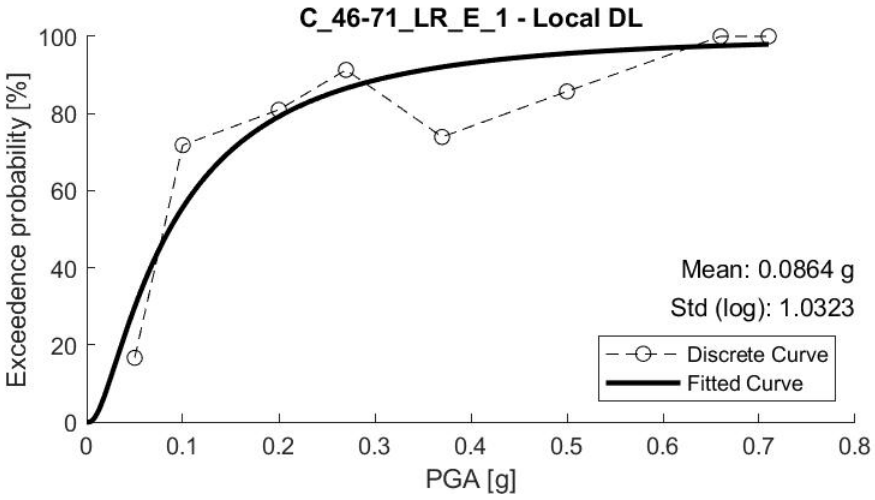
C_46-71_LR_E_1 - Local DL
Exceedence probability [%]
PGA [g]
Mean: 0.0864 g
Std (log): 1.0323
Discrete Curve
Fitted Curve

CURRICULUM VITAE

CIAMPOLI PIER LUIGI

Polytechnic University of Bari – via Orabona, 4 – 70126 Bari, Italy

+39 327 6115091

pierluigi.ciampoli@poliba.it
ing.ciampoli.fg@gmail.com

EDUCATION

16/02/2017 **Masters Degree in Civil Engineering (LM-23)** QEQ Level 7

Polytechnic University of Bari

Grade 105/110 – Thesis in "Seismic Design": "**Variabilità delle verifiche di sicurezza per effetto delle differenti valutazioni riguardanti i materiali e gli elementi non strutturali**". Tutor prof. Uva, Co-Tutor ing. Fiore

18/11/2010 **Bachelor Degree in Civil Engineering (L-07)** QEQ Level 6

Polytechnic University of Bari

Grade 98/110 – Thesis in "Applied Geology": "**Aspetti Geologici e Idrogeologici della Capitanata**". Tutor prof. Monterisi

Main attended courses

- "III One Day Workshop on Applied Mathematics" prof. Coclite - Politecnico di Bari
- "Calcolo scientifico in Python – Ottimizzazione ed equazioni differenziali per la modellistica" prof. Marcuzzi - Università di Padova
- "Advanced research in concrete technology: Innovation and Sustainability" prof. Uva – Politecnico di Bari
- "Advanced numerical modelling and nonlinear analysis of existing buildings under seismic actions" prof. Porco - Politecnico di Bari
- "Modelling of concrete members and systems for seismic response analysis" prof. Fardis - Università Federico II di Napoli
- "Modelling the mechanics of masonry structures" proff. Casolo Milani - Politecnico di Milano
- "Introduction to Statistical Mechanics and Applications" prof. Florio – Politecnico di Bari
- "Research Methodology" prof. Carnimeo - Politecnico di Bari
- "Elements of probability for engineering science" prof. Camarda - Politecnico di Bari